2013

Microfluidics for the Analysis of Integral Membrane Proteins: A Top-down Approach

Katrina Nychole Battle
Louisiana State University and Agricultural and Mechanical College, battlek.lsu08@gmail.com

MICROFLUIDICS FOR THE ANALYSIS OF INTEGRAL MEMBRANE PROTEINS: A TOP-DOWN APPROACH

A Dissertation

Submitted to the Graduate Faculty of the
Louisiana State University and
Agricultural and Mechanical College
in partial fulfillment of the
requirements for the degree of
Doctor of Philosophy

in

The Department of Chemistry

by
Katrina Nychole Battle
B.S., Jackson State University, 2008
December 2013

This work is dedicated to my aunt Felicia Gilliland, my paternal grandmother Pearlene Battle, my brother Lenard Battle, my parents Leonard and Sherrye Battle, and last but certainly not least my advisor Professor Steven A. Soper. Each of them gave me the inspiration I needed during my pursuit of my Ph.D., and for that I am forever grateful.

Acknowledgements

First and foremost I would like to thank God for the many blessings he has bestowed upon me throughout this journey called life. He has given me both wisdom and courage to step out on faith and allow him to use me to do his will in every way possible and for that I am so grateful and thankful. I would like to thank my spiritual advisors and church families from both the Piney Grove Baptist Church and the New Pilgrim Baptist Church for their guidance, words of prayer and encouragement, and support.

I want to be sure to thank my parents Leonard and Sherrye Battle for every ounce of support and love that they have given me. They have supported me financially, emotionally, and mentally from day one and words cannot express the amount of love, admiration, and gratitude I have for them. I am truly thankful to have them in my life. I thank my brother, Davion, for his support and phone calls, as well my other immediate and extended family members. I want to give a special "thank you" to my friends who have provided me with a support system outside of chemistry that has been so instrumental in keeping me sane (Lainette, Shayla, Chyree, MeKella, and 37 T.P.E.) I love you all for everything you have done.

I thank my advisor, Professor Steven A. Soper, for his mentorship, guidance, expert advice, the opportunity to work in his research laboratory, and most of all his patience. His guidance is and has been invaluable and I cannot say enough about how much his help and support has meant to me personally and for my career. I have learned so much about writing, presenting, and being prepared for what is to come in the future in this field of work. Dr. Soper you have truly been instrumental in seeing me through this process and I cannot say thank you enough for the support you have provided. I definitely cannot forget about the

wonderful people from the Soper research group who have also been very influential in my success. A special thanks goes to Dr. Małgorzata Witek for her help and guidance on the SPE work and Dr. Mateusz Hupert for his assistance with fabrication and hot-embossing instruction during my tenure at Louisiana State University and my time in North Carolina. I thank Franklin Uba for his assistance with the instrumentation I used and for allowing me to talk to him about ideas for my work no matter what time of day or night it was, Joyce Kamande for teaching me cell culturing, and Matt Jackson for his help as well with the COMSOL software and the physics calculations. A huge thank you to the Soper Group members Nyoté, Colleen, Maria, Brandon, Swathi, Kumu, and Mira for keeping my spirits up and talking with me and allowing me to bounce ideas and suggestions off of them and all of the encouragement they gave me to help me push through. You guys don't know how much that meant to me so I thank you. I also would like to express words of gratitude to former group members Drs. Samuel K. Njoroge and John K. Osiri for their help and advice with the 2D microcapillary electrophoresis work. A special thanks to Dr. Sally Hunsucker and Dr. Paul Armistead for their advice and guidance with the Western blotting analysis.

I thank everyone that I have met in the Chemistry departments both at Louisiana State University and the University of North Carolina Chapel Hill for their support, including all students that have offered suggestions and advice. I would also like to thank the staff at LSU CAMD for their assistance with the polymer devices that were used in my work. I thank my dissertation committee members and the many LSU professors that taught, inspired and/or encouraged me, including Professors John Pojman, Jane Garno, Isiah Warner, Patrick DiMario, and Robin McCarley and also a special thank you to the Chemistry Department at Jackson State University, Dr. Ashton Hamme and Dr. Jacqueline Stevens as well as Ms.

Sandra Hall and Ms. Maxine Simpson for their help and support throughout the years. I am very grateful to the Bridges to Doctorate Program at LSU and the National Science Foundation Graduate Research Fellowship for their funding support throughout my graduate matriculation. There is not nearly enough space and time to say thank you to every single person that has helped me along the way and I surely did not intend to leave anyone out so I give a great big “thank you” to everyone who has played a special part in my life, you know who you are and without a doubt I am grateful for you and for everything that you have done. I thank you all for your love, prayers, and continued support. Thank You!

Table of Contents

List of Tables

List of Figures

List of Schemes

List of Abbreviations and Acronyms

1D	One-dimensional
2D	Two-dimensional
2DE	Two-dimensional Electrophoresis
CE	Capillary Electrophoresis
CHAPS	[(3-Cholamidopropyl)dimethylammonio]-1-propanesulfonate
CID	Collision Induced Dissociation
CTC	Circulating Tumor Cell
Da	Dalton
ddH_2O	Double-distilled Water
DMF	Digital Microfluidics
DNA	Deoxyribonucleic acid
DTE	Dithioerythritol
DTT	Dithiothreitol
ECD	Electron Capture Dissociation
ECL	Enhanced chemiluminescence
EDC	ethyl-3-(3Dimethylaminopropyl)carbodiimide)
EDTA	Ethylenediaminetetraacetic acid
EGTA	Ethylene glycol-bis(2-aminoethylether)-*N,N,N,N'*-tetraacetic acid
EOF	Electroosmotic Flow
EpCAM	Epithelial Cell Adhesion Molecule
ESI	Electrospray Ionization
FCS	Fetal Calf Serum
FITC	Fluorescein isothiocyanate
FSE	Free-solution Zone Electrophoresis
FT-ICR	Fourier Transform Ion Cyclotron Resonance
GPI	Glycosylphosphatidylinositol
H	Plate height
HABA	2-(4'-hydroxyazobenzene)-2-carboxylic acid
H_D	Height equivalent of a theoretical plate for longitudinal diffusion
HeLa cells	Cervical cancer cell line from Henrietta Lacks
hMSC	Human Mesenchymal Stem Cell
HPLC	High-Performance Liquid Chromatography
HRP	Horseradish peroxidase
H_{TOT}	Total plate height
IEF-PAGE	Isoelectric Focusing Polyacrylamide Gel Electrophoresis
IEX	Ion Exchange Chromatography
IMAC	Immobilized Metal Affinity Chromatography
IPG	Immobilized pH Gradient
KCl	Potassium Chloride
kD/kDa	Kilodalton
kV	Kilovolt
LC	Liquid Chromatography
LC-MS/MS	Liquid Chromatography Tandem Mass Spectrometry
L_{eff}	Effective Separation Length

LIF	Laser-induced Fluorescence
L_{inj}	Injection Length
LOD	Limit of Detection
L_{tot}	Total Separation Length
M	Molar
MALDI	Matrix-assisted Laser Desorption Ionization
MCF-7	Michigan Cancer Foundation-7 (invasive breast ductal carcinoma)
MEKC	Micellar Electrokinetic Chromatography
MES buffer	(1M), 2-(N-morpholino) ethanesulfonic acid
MHEC	Methyl hydroxyl ethyl cellulose
mL	Milliliter
MS	Mass Spectrometry
MS/MS	Tandem Mass Spectrometry
MT	Migration time
MudPIT	Multidimensional Protein Identification Technology
MW	Molecular Weight
MWCO	Molecular Weight Cutoff
N	Separation efficiency or Plate Number
Na_2CO_3	Sodium Carbonate
NALDI	Nanostructure-assisted Laser Desorption Ionization
NHS	*N*-hydroxysucinimide
nM	Nanomolar
NMR	Nuclear Magnetic Resonance
O	Orthogonality
P	Peak capacity
PBS	Phosphate Buffered Saline
PCR	Polymerase Chain Reaction
PDMS	Poly(dimethylsiloxane)
PDVF	Polyvinylidene difluoride
pI	Isoelectric point
pIEF	Peptide Isoelectric Focusing
PMMA	Poly(methyl methacrylate)
Pt	Platinum (platinum wire)
PTM	Post translational modification
Q-TOF	Quadrupole Time-of-Flight
RP	Reversed-phase
RP-IPOCCEC	Reverse-phase Ion Pair Open Channel Capillary Electrochromatograpy
RPLC	Reversed-phase Liquid Chromatography
RSD	Relative Standard Deviation
S-NHS-LC-biotin	Sulfosuccinimidyl-6-(biotinamido)hexanoate
S-NHS-SS-biotin	Sulfosuccinimidyl-2-(biotinamido)-ethyl-1,3'- dithiopropionate
SCX	Strong Cation Exchange
SCX-RPLC	Strong Cation Exchange Reversed-phase Liquid Chromatography
SDS	Sodium Dodecyl Sulfate
SDS μ-CGE	Sodium Dodecyl Sulfate micro-Capillary Gel Electrophoresis

SDS-PAGE	Sodium Dodecyl Sulfate Polyacrylamide Gel Electrophoresis
SELDI	Surface-enhanced Laser Desorption Ionization
SEM	Scanning Electron Microscope
SPAD	Single Photon Avalanche Diode
SPE	Solid-phase Extraction
TBS	Tris-buffered saline
TBST	Tris-buffered saline, Tween-20
TCEP	Tris(2-carboxyethyl)phosphine
T_g	Glass transition temperature
TMD	Transmembrane Domains
TOF	Time-of-Flight
UV	Ultraviolet
µ-CE	Micro-Capillary Electrophoresis
µ-CGE	Micro-Capillary Gel Electrophoresis
μ_{eof}	Electroosmotic Mobility
μ_{ep}	Electrophoretic Mobility
µM	Micromolar

Abstract

The development of fully automated and high-throughput systems for proteomics is now in demand because of the need to generate new protein-based disease biomarkers. Unfortunately, it is difficult to identify protein biomarkers that are low abundant when in the presence of highly abundant proteins, especially in complex biological samples like serum, cell lysates, and other biological fluids. Membrane proteins, which are in many cases of low abundance compared to cytosolic proteins, have various functions and can provide insight into the state of disease and serve as targets for new drugs making them attractive biomarker candidates. Traditionally, proteins are identified through the use of gel electrophoretic techniques and two-dimensional protein profile patterns have been used as potential diagnostic tools for biomarker discovery and the profiles from protein content of body fluids or cells are available in databases.

However, gel electrophoretic methods are not always suitable for particular protein samples. Microfluidics offers the potential as a fully automated platform for the efficient analysis of complex samples, such as membrane proteins and do so with performance metrics that exceed their bench top counterparts. In recent years, there have been various applications and improvements to microfluidics and their use for proteomic analysis reported in the literature. In addition, microfluidics offers the potential of a disposable, low cost, and easily fabricated method to perform analysis on complex samples. In this work through the use of microfluidic devices, we demonstrate the ability to effectively extract and purify biotinylated cell surface membrane proteins from the cell lysate of MCF-7 human breast carcinoma. In addition, we also attempt to separate membrane proteins from MCF-7 cells.

Our on-chip assay (μ-solid-phase extraction, μSPE) allows us to extract membrane proteins and rid the sample of contaminating cytosolic proteins (purification) in order to do further analysis on the membrane proteins. We also attempted to separate a complex biological sample using a microchip that is suitable for multidimensional techniques that employed sodium dodecyl sulfate micro-capillary gel electrophoresis (SDS μ-CGE) in the 1st dimension and micro-micellar electrokinetic capillary chromatography (μ-MEKC) in the 2nd dimension. Proteins were detected by laser-induced fluorescence following their labeling with dyes. Because our overall goal of this work is the development of a completely integrated system for the analysis of complex protein samples, we also discuss the integration of the extraction module with the separation module along with fabrication steps toward the integration of modules for the digestion of proteins on chip and interfacing the device with MALDI-MS.

1 Microfluidics for the Analysis of Integral Membrane Proteins: A Top-down Approach

1.1 The Study of Proteins

1.1.1 The Proteome and Proteomics

The field of proteomics is focused on the determination of structures, expressions, interactions, and functions, which includes activities, roles and localizations of the proteome - a catalogue of the proteins in a specific organism coded by the genome. The original definition of the proteome views it as the protein complement of the genome, thereby not accounting for the numerous post-translational modifications and the varying state of proteins.[1,2] Proteomics involves a comprehensive analysis, including the determination of structure, modifications, expression levels, localization and protein-protein interactions, within a given organism, cell, biological fluid, or tissue. Schramm *et al.*[3], reported that proteomics involves the functional analysis of the full set of proteins by high-throughput technologies in a given system. This definition suggests that proteomics goes beyond identification and that protein analysis requires advanced technologies, such as high-throughput processing techniques. Proteomics attempts to tackle three main areas of interest: (1) protein expression; (2) protein structure; and (3) protein function.[4]

1.1.2 Challenges in Proteomics

Various populations of proteins perform the higher biological functions in the cellular network making proteomics an attractive tool for research and scientists alike.[5] In cancer research, particularly in identifying biomarkers for new drugs and drug discovery, proteomics is vital because proteins have been selected for investigation as biomarkers because of their past performance as biomarkers for other disease states or other cancers or because of their

function or family relationships.[6] Throughout the past twenty years, there has been a growing interest in approaches toward discovering new biomarkers that may allow early diagnosis, prognosis, classification of disease subtypes, prediction of treatment response, and identification of potential targets for drug therapy. For most of these applications, a single marker is likely insufficient for stratification, and a panel of markers, *i.e*. molecular profiles or biosignatures can be more useful. Such biomarker profiles can be identified at different molecular levels, such as DNA, RNA, microRNA, and protein. A significant portion of the biomarker discovery efforts using -*omics* approaches has been in the area of cancer, and several markers are already in routine clinical practice, such as K-Ras mutation and HER-2 amplification. A particular area of interest is the cell surface proteome due to its ease of accessibility and the possibility to serve as an ideal target for novel protein drugs. Most acknowledge the importance of proteomics as procuring extensive information required for the entire supplement of proteins comprising the proteome.

Traditionally, proteomic analyses of complex protein samples involve the resolution of proteins using two-dimensional (2D) gel electrophoresis that includes isoelectric focusing (IEF) coupled with sodium dodecyl sulfate-polyacrylamide gel electrophoresis (SDS-PAGE) and followed by the identification of resolved proteins by mass spectrometry.[7,8] The idea of building protein databases was proposed using subtractive pattern analysis of these gels.[9-11] Over time, with the advances in analytical protein technologies and advancements in mass spectrometry, it became possible for many proteins to be resolved by 2D-PAGE. However, the disadvantages of 2D-PAGE include a large amount of sample handling, a limited dynamic range, and difficulties resolving low abundance proteins[12-14] with extreme pI and molecular weights,[15,16] and hydrophobic proteins such as membrane proteins.[7] The solubility of

hydrophobic proteins (membrane proteins) is problematic due to incompatibility with the IEF buffers, and if the proteins are solubilized, they are prone to precipitation at their isoelectric point (pI). To alleviate the issue of solubility with IEF buffers, many investigators have used 1D gel coupled with mass spectrometry for identification of the proteins.[17-19] Yet, the limitation of this approach is the increased protein complexity in each 1D gel band.

Shotgun methods provide a powerful alternative to 2D gels. Shotgun proteomics is analogous to shotgun sequencing where DNA is broken into small fragments; these fragments are sequenced, and recombined *in silico* to determine the DNA sequence of an organism. In a general shotgun proteomic pipeline, a mixture of proteins is digested into peptides (using proteases such as trypsin), the peptides are loaded onto at least a two-dimensional chromatography based separation system, peptides are eluted into a tandem mass spectrometer in an automated fashion, and the resulting tandem mass spectrometry data is analyzed by powerful computational systems. Proteins are first digested with proteases into a more complex peptide mixture that is then analyzed directly by LC/MS and protein identifications are determined by database searching software.

This general approach is rapid and readily automated, but requires significant computing resources for data analysis. Moreover, as with gel-based methods, the solubility of membrane proteins is also a major challenge for non-gel shotgun approaches. Large scale shotgun proteomics effectively began with the introduction of multidimensional protein identification technology (MudPIT) in which a microcapillary column is packed with reversed phase (RP) and strong cation exchange (SCX) packing material, loaded with a complex peptide mixture and placed in line between an HPLC and a tandem mass spectrometry system.[20-22] In addition to 2D gel and shotgun proteomic techniques, industrial-scale (liters)

approaches have also been reported for sample pooling of smaller proteins < 40,000 Da and fragments of large proteins. Using over 12,000 plasma fractions, Rose *et al.*[23] reported thousands of peptide identifications, which permitted the identification of 502 different proteins and polypeptides from a single pool.

Given the cost (liter-scale amounts of protein) and labor intensiveness (2D gel techniques) of such methods, they are clearly not applicable to routine clinical tests and are of marginal use in confirming candidate biomarkers where thousands of individual samples must be analyzed separately to placate statistical criteria for diagnostic specificity and sensitivity. Regrettably, proteomics is still burdened with numerous challenges that hinder its goals. These challenges can be categorized as; (a) the sample type; (b) limitations of bench-top approaches; and (c) analysis of data.

1.1.3 Complexity of Protein Sample

The proteome is very complex. The human genome is composed of approximately 3 x 10^4 genes.[24,25] Proteins sizes can range from a few amino acids to several thousands making them a very diverse and distinct class of molecules. They possess wide pI ranges and can be hydrophilic or extremely hydrophobic to the point where they are almost irretrievable from aqueous media.[26] For example, proteins associated with the cell membrane contain hydrophobic domains that make them particularly difficult to analyze using traditional methods such as isoelectric focusing (IEF). Because of their hydrophobic and basic (as in charge) nature, and frequently large size, their isolation is not easy.

A primary difficulty encountered in the study of membrane proteins is that of obtaining the protein of interest. Membrane proteins are usually present at low levels in biological membranes, and it is rare that a single protein species is a major peptidic

constituent of the membrane.[27] In addition most membrane proteins cannot be readily obtained in sufficient amounts from their native environments and thus attempts are made to overexpress them. A second difficulty is that membrane proteins are naturally embedded in a lipid bilayer, which in even the simplest organism is a complex, heterogeneous and dynamic environment. This limits (but does not exclude) the use of many standard biophysical techniques to determine structure and function such as X-ray crystallography, circular dichroism, NMR, ligand-binding studies, classical kinetic characterization, the identification of structure–function relationships and also restricts applications since they require the protein to be extracted from its native membrane and studied in a detergent or lipid environment *in vitro*.[27] This necessity leads to difficulties in sample preparation and spectral contributions from lipids. Finally, membrane proteins are not generally soluble in aqueous media.

The need for membrane proteins to inhabit surroundings that satisfy their hydrophobicity therefore requires special synthetic systems for *in vitro* work. Unfortunately, reconstituting purified proteins into such systems has proven to be very difficult. Despite the problems of working with membrane proteins, they remain an important area for study due to their role in the control of fundamental biochemical processes and their importance as pharmaceutical targets. Conventional methods for membrane isolation such as gradient separation,[28] polymer partitioning,[29] and chemical treatment[30] typically result in high purity but are often cumbersome and protein yields are poor. The dynamic range (*i.e.* abundance, size, function) of proteins within a single cell can span close to six orders of magnitude.[31] It has been estimated that between 100,000 to 250,000 proteins are encoded by roughly 25,000 human genes through post-translational modifications and differential splicing, which can produce an additional 5 to 10 different proteins from each gene.[32,33]

1.1.4 Limitations of Bench-top Approaches for Proteomic Analyses

Proteomics attempts to simultaneously determine the identities, functions, and quantities of proteins.[34] The need for large sample volumes, poor performance and labor-intensive demands are all challenges associated with available bench-top techniques used in proteomics.

For example, IEF-PAGE coupled with SDS-PAGE is a common strategy used to form 2D electrophoresis platforms, providing a dynamic range of $10^2 – 10^4$ and a limit-of-detection (LOD) ~10^{-6} M. This technique can routinely resolve >2,000 spots per gel, which is well below the amount of proteins present in a proteomic sample. Moreover, it requires well-trained personnel, has limited automation potential, and can be time consuming.[35] Mass spectrometry (MS), on the other hand, provides better LOD (~10^{-15} mole for peptides) and high specificity, however, 2D-PAGE cannot be coupled on-line with MS to achieve a fast multidimensional protein separation and identification.[36] As a result, multi-dimensional liquid phase-based separation methods using different electrophoretic and chromatographic techniques have been greatly developed as complementary methodologies because they can be coupled on-line with mass spectrometers for protein identification. The feasibility of multi-modular combinations of high-performance liquid chromatography (HPLC), isoelectric focusing (IEF), chromatofocusing (CF), capillary electrophoresis (CE) as well as combinations of different HPLC modes provides numerous options for the separation of protein complexes and peptides.[37] Ion-exchange chromatography (IEX) together with reversed-phase (RP) liquid chromatography (RPLC) is one example of orthogonal 2D-LC analysis.[38] The total peak capacity in this 2D separation can be greater than 5000 and high-

sensitivity peptide identification may therefore be achieved because of increased resolution and the resultant decrease in peptide overlap.[39]

Among various kinds of 2D-LC techniques, the combination of strong cation exchange (SCX) mode separation in the first dimension and RP separation in the second dimension has become a dominant separation technology. As a classical proteome research strategy, this SCX–RPLC approach provides a large amount of biological information as a complement to traditional 2D-PAGE approach. Fujij *et al.*[40] described an on-line SCX–RPLC workflow involving stepwise salt elution using ammonium formate that was employed for SCX separations and the resulting fractions were subjected to RPLC-MS analysis after concentration and desalting. Vitali and co-workers[41] also employed SCX–RPLC with tandem MS (MS/MS) strategy to identify proteins from *Bifidobacterium infantis*. Digested proteins were first separated through a SCX column and the fractions were collected every minute. After drying and resuspension, protein fractions were further separated and identified through a homemade RPLC coupling with a quadrupole time-of-flight (Q-TOF) mass spectrometer.

However, there is no amplification technique in proteomics similar to PCR in genomics and therefore, proteins must be analyzed in their native concentrations. Also, because of the inability to amplify protein targets using techniques employed in genomics, proteome analysis can be much more challenging. This can be compounded by the high complexity of proteome samples. No single chromatographic or electrophoretic procedure to-date possesses the peak capacity required to resolve a complex mixture, such as that found in a single proteome, to resolve all of its individual components.

1.1.5 Complications of Protein Data Analysis

Measurable parameters in proteomics are large in number, and require many biological and methodological replicates, which may not be so easy to attain. Bias in protein data analysis is widespread and can be viewed as a threat to the validity of protein biomarkers where results have been unclear or irreproducible.[42,43] This issue is apparent when handling large data sets, such as those presented in proteomic analyses. It is intrinsically easier to find a correlation irrespective of real cause and effect due to false positive probably outnumbering true positives.[34] Lay *et al*. [34] pointed out that the failure of many proteomic studies correlates with the failure to consider the analytical need to define quality standards, including method validation and standardization. Also, due to a lack of quality standards, it is difficult to compare results generated from various laboratories.

The analysis of a full proteome presents a formidable task and, in spite of recent technical developments, remains to be achieved for any species. The task is challenging because proteomes have a sizeable and undetermined complexity. What is certain is that the number of proteins in a species proteome exceeds by far the number of genes in the corresponding genome. This diversity arises from the fact that a particular gene can produce numerous distinct proteins as a result of alternative splicing of primary transcripts, the presence of sequence polymorphisms, posttranslational modifications, and other protein processing mechanisms.[44] Moreover, proteins span a concentration range that surpasses the dynamic range of any single analytical method or instrument.

Peripheral membrane proteins do not interact with the hydrophobic core of the phospholipid bilayer; they are usually bound to the membrane indirectly by interactions with integral membrane proteins or directly through ionic interactions with the lipid polar head

groups. Membrane proteins are, in some cases, amphipathic and can contain both hydrophobic and hydrophilic domains. These characteristics render them extremely difficult to analyze.[7] As a result, even though 20-30% of the human genome may encode for membrane proteins,[45] they are underrepresented in most analyses.[46]

A central goal of proteomics has been the complete and, in most instances, quantitative analysis of the proteome of a species or, in multicellular organisms, a particular cell or tissue type. Although this goal has remained tenuous, significant progress has been made in the development of an array of technologies for proteome analysis and their application to biological and clinical research. At the present time, MS is generating the majority of proteomic data, more specifically by tandem MS (MS/MS) with increasing performance.[47] The instrumentation and diverse workflows share a commonality in that they generate hundreds to thousands of fragment ion spectra per hour of data acquisition. However, the assignment of fragment ion spectra to peptide sequences, the interference of the proteins represented by the identified peptides, and the determination of their abundance in the sample being analyzed present complex statistical and computational challenges. Therefore, it is essential that tools and solutions that provide both accurate and reproducible results and can be generally applied to these problems be developed for proteomic studies.[47] The determination of function and abundance of individual proteins is also critical.

The correct assignment of the fragment ion spectrum to a peptide sequence is the first key step in proteomic data processing. A plethora of software tools and computational approaches have been developed to automatically assign peptide sequences to fragment ion spectra and can be classified into three categories: (i) Database searching; (ii) *De novo* sequencing; and (iii) alternative "hybrid" strategies. Database searching involves peptide

sequences being identified by correlating the fragment spectra that are acquired with theoretical spectra predicted for each peptide contained in a protein sequences database. In *de novo* sequencing, peptide sequences are clearly read out directly from fragment ion spectra. In addition, the alternative approaches that combine both database searching and *de novo* sequencing offer the option of performing "error-tolerant" database searching after the extraction of short sequence tags of 3-5 residues in length.

Several MS/MS database search programs have been developed and take the fragment ion spectrum of a peptide as input and score it against theoretical fragmentation patterns constructed for peptides from the searched database. The group of candidate peptides is restricted based on user-specified criteria such as proteolytic enzyme constraint and mass tolerance.[47] The output from the program is a list of fragment ion spectra matched to peptide sequences that have been ranked according to each score and, typically, the best scoring peptide match is considered during the subsequent statistical analysis step. The search score measures the degree of similarity between the experimental spectrum and the theoretical spectrum, and therefore serves as the primary discriminating parameter for separating correct from incorrect identifications.

There are numerous scoring schemes available including spectral correlation functions (SEQUEST) or related concepts such as shared fragment counts and dot product (TANDEM, OMSSA, MASCOT).[47] Scoring functions can also be based on empirically observed rules or statistically derived fragmentation frequencies. The score actually reported by the tool can be based on an arbitrary scale or converted to a statistical measure known as the expectation value, *E*, which refers to the expected number of peptides with scores equal to or better than the observed score under the assumption that peptides are matching the experimental

spectrum by random chance. The *E* value is computed by assuming that the database search score follows a particular distribution, *i.e.* Poisson, or by empirical fitting of the observed distribution of scores.[48-50] This score is largely unchanged under different scoring methods and gives a clearer interpretation of quality of the match across different instrument platforms and search algorithms. However, it should be noted that neither the best match nor a high search score (or low *E* value) are reliable indicators for a true match. Discriminating true from false matches is therefore a critical next step in proteomic data analysis.

Spectral identification can be done using spectral matching with a library of spectra representing the peptide sequences contained in the proteome map.[51-53] The spectral library is compiled from a large collection of experimentally observed mass spectra of correctly identified peptides. An unknown spectrum can then be identified by comparison to candidates in the spectral library to determine the match with the highest spectral similarity.[54] Although the method of spectral matching outperforms database searching in speed, error rate, and sensitivity characteristics of the results, no peptides will be identified that were not previously entered into the respective spectral library. In the *de novo* sequencing approach, the amino acid sequence of a peptide is read from a fragment ion spectrum with the main advantage over database searching being that it allows identification of spectra for which the exact peptide sequence is not present in the searched sequence database, such as those peptides that contain sequences with modified peptides or polymorphisms.

Yet, *de novo* analysis is computationally intensive and requires high quality fragment ion spectra. Furthermore, peptide sequences extracted using *de novo* algorithms need to be matched against sequences of known proteins present in the sequence databases because researchers are more interested in knowing the proteins present in the sample. Hybrid

strategies that combine both database searching and *de novo* sequencing start with the interference of short sequence tags (partial sequences) from MS/MS spectra, followed by an error-tolerant database search, which will allow for one or more mismatches between sequence of the peptide that produced the spectrum and the database sequence.[55-57] By limiting the search to only those database peptides that contain the sequence tag extracted from the spectrum, the database search time can be reduced significantly.

Although proteome analysis has seen various improvements over the last decade with respect to sample processing, data analysis, and data acquisition, many challenges remain. And are primarily associated with the complexity of the proteome itself. There are also challenges related to the analysis of the information contained in proteomic datasets. Inferring the identities of proteins, protein isoforms, and differentially modified proteins in a sample from confidently identified proteins is also a challenge. Two alternatives that are being utilized more frequently is top-down proteomics, which is focused on the analysis of intact proteins rather than the peptides and has the potential to resolve populations of proteins into their components,[58-60] and the targeted analysis of specific peptides of high information content (proteolytic peptides) that collectively represent the proteome, thus eliminating the redundancy of current methods that are available now.[47,61,62] Although substantial progress has been made in the effort to improve the analysis of proteomic data, the development of new algorithms and analysis tools still remain before these technologies can be implemented routinely.

1.2 Membrane Proteins: Organelle-specific Sub-population of the Proteome

A strategy to overcome the challenges associated with full proteome analysis is to target proteomes of certain organelles, for example membrane proteins. Conventional

proteome analysis can include fractionation of biological cell components and performing the analysis on individual organelles[63] such that only a sub-population of the full proteome is analyzed. Organelle pre-fractionation normally involves cell homogenization, density gradient separation of organelles, detergent extraction of membrane proteins, and two-phase partitioning with high-salt and high-pH washes. These processes can be lengthy, labor-intensive, and may result in poor yields.[63-65]

A principal sub-population of the proteome is membrane proteins, which provide important cellular functions such as controlling transport into and out of the cell and communication and regulating responses to external stimuli. Membrane proteins are normally classified into one of two categories, integral and peripheral and are based on the nature of their association with the cell membrane (see Figure 1.1).

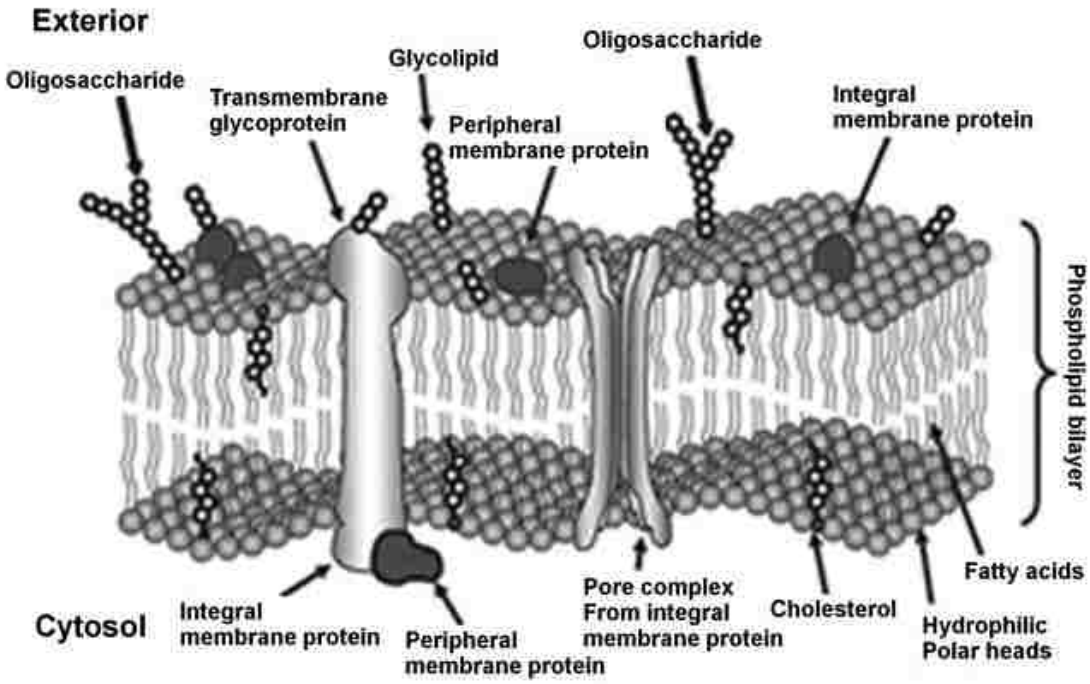

Figure 1.1 Various membrane proteins and their associations with the biological membrane (Reproduced from Cordwell, S. J.; Thingholm, T. E. *Proteomics* **2010**, *10*, 611[66] with permission, Copyright 2013, John Wiley & Sons).

Integral membrane proteins have domains embedded in the phospholipid bilayer and contain hydrophobic amino acid side-chain residues that interact with fatty acyl groups of the phospholipids, anchoring the protein to the membrane. They function primarily in signal transduction. Proteins that have domains that span the entire phospholipid bilayer are called transmembrane proteins. These molecules can possess several hundred amino acid residues that extend both into the aqueous medium on either side of the bilayer and multiple transmembrane domains (TMDs) within the membrane.[67] Integral membrane proteins are, in most cases, amphipathic and can contain both hydrophobic and hydrophilic domains. These characteristics render them extremely difficult to analyze,[7] and as a result, they are underrepresented in most analyses.[46] Peripheral membrane proteins do not interact with the hydrophobic core of the phospholipid bilayer; they are usually bound to the membrane indirectly by interactions with integral membrane proteins or directly through ionic interactions with the lipid polar head groups.

The isolation of sub-populations of the proteome can be combined with specific protein tagging strategies to reduce cross-contamination. For example, immobilized antibodies against membrane proteins were utilized for the purification of a membrane fraction using magnetic beads, but were limited to proteins for which a specific antibody was available.[68] Protein radioactive labeling has been employed in different protein studies for the isolation of membrane proteins [69] and quantitative analysis of proteins by MS is often performed with isotope-coded affinity tags.[14] Surface-protein biotinylation strategies with affinity purification using avidin or streptavidin columns, avidin-modified magnetic beads or visualized by hybridization with streptavidin-HRP complexes have been reported and new surface membrane proteins identified.[70-76]

1.2.1 Importance of Integral Membrane Proteins

Integral (or peripheral) membrane proteins act as major gateways into the intracellular environment. All cells and most intracellular organelles are enclosed in an impermeable lipid bilayer and the integral membrane proteins are embedded in these membranes. They are the entry and exit routes for many ions, nutrients, waste products, hormones, drugs and large molecules such as proteins and DNA. They are also responsible for much of the communication between cells and their environment. Additionally, these proteins provide responses to external stimuli. Cells can make a huge variety of membrane proteins. Approximately, 38% of all proteins encoded by the mammalian genome and more than one-third of the current list of potential biomarkers are classified as membrane proteins.[77-79]

The medical importance of this enormous family of proteins cannot be undervalued. Integral membrane proteins have been reported to play key roles in host-pathogen interactions[77,80-82] and cell regeneration after injury.[83] Cardiovascular diseases, cancer, and diseases caused by degeneration of cells within the central nervous system are major health problems in the United States.[77,84-86] Proteomic investigations into Integral membrane proteins have the potential to identify new biomarkers that ensure early disease diagnosis, offer targets for new therapeutics, and provide an indication of response to therapy.

Integral membrane proteins are localized on the cell surface and are the first to be impacted by pathological changes in the cellular microenvironment. As part of the cellular response to a pathological insult, Integral membrane proteins may be secreted or shed from the cell surface into biological fluids (plasma, cerebrospinal fluid, or urine). [87] The level of Integral membrane proteins in these fluids can provide valuable diagnostic and/or prognostic information about disease, disease severity, and the progress of the therapy for the disease.[88]

As stated previously, membrane and membrane-associated cell surface proteins represent more than one-third of the proteins encoded by the human genome, however, they also account for more than two-thirds of the targets for existing drugs.[89] They are also an area of special interest because of their accessibility to new drugs for treatment of the above-mentioned diseases.[86,89,90] Therefore, it is critical that advances toward the isolation and identification of Integral membrane proteins continue, especially those with multiple trans-membrane domains (TMDs) and post-translational modifications (PTMs) due to their expansive roles as possible disease biomarkers and target molecules in disease treatment.

1.2.2 Difficulties in Handling Integral Membrane Proteins

Membrane proteins are unique within proteome research due to their diversity and behavior during the process of purification and separation.[66,79] Membrane proteins are embedded in the lipid bilayer and the composition of these lipids varies among the systems. The nature of the lipids can affect the stability of the protein. Several post-translational modifications (PTMs) of membrane proteins can produce extreme micro-heterogeneity that can reduce the efficiency of electrophoretic and chromatographic separations. The PTMs and hydrophobicity of Integral membrane proteins also cause complications with their identification by MS.[79,91] Membrane proteins are extracted from the host cell membrane by the addition of detergents, which cover the hydrophobic surface of the protein, allowing solubilization.

The choice of detergent is a crucial part of the purification process. Often a series of detergents are tested and the detergent that extracts the largest quantity of soluble, active, homogeneous, stable protein is used; however, it should be noted that just because a detergent is successful with extracting membrane proteins, it does not mean that they will be

solubilized. Despite advances in methods to analyze hydrophobic proteins, integral membrane proteins are still under-represented in most membrane proteomes.[79,92] Contamination of the membrane protein fraction by other organelles and non-membrane proteins, which interact with the plasma membranes during the purification process, is a serious issue. It is paramount that problems such as these be alleviated or eliminated to guarantee the purest membrane protein fraction for further downstream analysis.

1.3 Current Methodologies in Integral Membrane Protein Analysis

The study of membrane proteins using high resolution and throughput proteomics remains challenging. While membrane proteins are generally low in abundance, the foremost impediment in their analysis is poor solubility. Integral membrane proteins, in particular, contain both hydrophobic and hydrophilic domains, which makes them difficult to purify and characterize on a proteomic scale. In order to undertake a comprehensive analysis of membrane proteins, several areas need to be considered. The analysis can be divided into four main experimental steps: (i) enrichment and purification of membrane proteins; (ii) solubilization of membrane proteins; (iii) separation; and (iv) identification and characterization (analytical techniques). Each of these steps provides experimental challenges and influences the success of the experimental design and the interpretation of the results.

1.3.1 Enriching and Purifying Integral Membrane Proteins

There are several strategies available to probe targets that are in low abundance, including detection methods with single-molecule sensitivity that utilize fluorescence and/or electrochemistry. Mutch *et al*. developed a technique to count low-copy-number membrane proteins in synaptic vesicles.[125,126] They used this approach to quantify proteins in isolated, single synaptic vesicles and they were able to quantify seven major membrane proteins of rat

brain synaptic vesicles. The method combined organelle purification with immunolabeling, microfluidics, and total-internal-reflection fluorescence (TIRF) microscopy. The enrichment and purification of integral membrane proteins is one of the most critical components of the experimental approach, with the major challenge being the presence of contaminating, higher abundance cytosolic proteins in the final protein extract prior to solubilization and analysis. Some of the strategies for the enrichment of membrane proteins are summarized in Table 1.1 and will be discussed in the next few sections.

Table 1.1 Strategies for Membrane Protein Enrichment

Membrane Protein Enrichment Strategy	**Principle**	**Sample Origin**	**Results**	**Drawbacks**	**Ref.**
Two-phase purification	Isolation of membrane proteins from soluble proteins according to hydrophobicity	Rat liver	67% were integral membrane proteins	Actin contamination in membrane protein fraction, laborious	94
Enrichment using a solution of cationic colloidal silica particles	Electrostatic cross-linking to silica particles	Rat lung, microvascular endothelial cells	81% were classified as membrane proteins	High detergent conc. affects protein stability & further analysis	95
Wash with high salt or high pH conditions	Removal of loosely bound cytosolic proteins	Rat Liver	Efficiently removed peripheral membrane proteins	Only loosely bound cytosolic proteins removed, protein cleavage	96
Differential centrifugation or density sedimentation	Isolation of membrane proteins from sub-cellular organelles based on difference in organelle densities	Mouse liver	50% of the proteins were integral membrane proteins	Contamination of cytosolic proteins, sample handling, laborious	97

Table 1.1 Strategies for Membrane Protein Enrichment (continued)

Membrane Protein Enrichment Strategy	Principle	Sample Origin	Results	Drawbacks	Ref.
Enrichment using secondary antibody super-paramagnetic beads	Beads coated with antibodies against known membrane proteins	Mouse liver	67% were membrane proteins or proteins associated with plasma membrane	Antibodies must be specific for membrane proteins	98
Combination of sucrose centrifugation and sodium carbonate extraction	Purification of membrane proteins and removal of cytosolic proteins loosely bound to membrane	hMSC	57.3% were integral membrane proteins	Time consuming, pH conditions have negative effects on proteins	99

Many of the membrane protein fractions are obtained from tissue samples or cells that have been lysed by physical or chemical means.[66] Membrane protein fractions with high purity and stringency are also hard to obtain from samples where little material exists to begin with.[66,93] In studies with membrane proteins in which cell culture systems are utilized, often only Integral membrane proteins of the highest abundance are identified; and of those identified, many have poor reproducibility due to the presence of contaminating proteins from other organelles.[66] Listed below are some the bench top techniques used for the enrichment and isolation of membrane proteins along with a short description as to their implementation.

1.3.1.1 Precipitation and/or Density Gradient Centrifugation of Integral Membrane Proteins

Sub-fractionation is a means for reducing the complexity of an initially complex sample, improving the dynamic range, and consequently enhancing the identification of low abundance proteins or those specific to a research problem of interest.[96,97,100-104] Traditionally,

the purification of membrane proteins involves density gradient ultra-centrifugation and/or chemical precipitation. Using chemical precipitation requires aqueous two-phase purification, where membrane and membrane proteins are separated from cytosolic (soluble) proteins according to their hydrophobicity, such as PEG 3350 or dextran T-500.[105,106] Aqueous two-phase purification has also been utilized for the fractionation of membrane proteins prior to MS analysis, resulting in the identification of 42% and 67% of integral membrane proteins of rat brain and liver proteins, respectively, as an example.[105,107]

Density sedimentation or differential centrifugation of whole cell lysates, tissue lysates, or microsomes can be employed to separate membrane proteins from other sub-cellular organelles due to their difference in density.[108-112] Zhang *et al.* applied sucrose density gradient centrifugation to isolate membrane protein fractions from mouse liver, identifying 50% of integral membrane proteins from a total of 175 proteins.[112] Washing steps using high salt and high pH can improve the removal of cytosolic proteins, especially those that are loosely bound to the cell membrane.[113] The combination of sodium carbonate extraction with sucrose gradient centrifugation has also been used to enrich for membrane proteins. With this combination, a total of 463 proteins were identified in which 122 (26.3%) were predicted membrane proteins.[110]

Triton X-114 and other strong non-ionic detergents may also be used for the separation of extracted hydrophobic and hydrophilic proteins. The solution is homogenous at 0°C, but separates into an aqueous phase and detergent phase when heated above 20°C with the separation becoming more apparent at increasing temperatures, and is also affected by the presence of other surfactants.[95] The hydrophilic proteins separate to the aqueous phase and the hydrophobic membrane proteins are found in the detergent phase.[95] This method has been

shown to be very efficient and has also been used for the separation of glycosylphosphatidylinositol (GPI)-anchored proteins.[115] Thingholm and co-workers investigated the efficiency and reproducibility of combining sodium carbonate extraction with sucrose centrifugation for the enrichment of membrane proteins tested in the preparation for phosphorproteomic studies of human mesenchymal stem cell (hMSC) membrane proteins.[116] There are also commercially available methods such as the Mem-PER™ Plus Membrane Protein Extraction Kit (Pierce Biotechnology, Rockford, IL) that use detergents to release cytosolic proteins into an aqueous phase and solubilize membrane proteins using detergents.

However, it should be noted that although these studies employing two-phase purification, density sedimentation, or conventional differential centrifugation were successful in the confirmation of the enrichment of the integral membrane proteins, they have also been known to be contaminated with significant amounts of cytoplasmic organelles, making it difficult to compare protein expression profiles between two preparation methods.[75,114]

1.3.1.2 Cross-linking of Integral Membrane Protein Complexes

Exposed integral membrane proteins can be purified using protein cross-linking reagents to maintain the membrane protein complexes as close to their native state as possible. After cell lysis, the non-complexed proteins can be removed by immunoprecipitation using antibodies directed against the membrane proteins of interest, size-exclusion chromatography, or through the use of a cross-linker that enables affinity purification.[66] Several groups have employed this technique to get a better understanding of surface protein topology with protein complexes.[117] A variation of this approach was introduced by Freed *et al.*[118] that allowed for biotinylation and surface protein cross-linking. In turn, the strategy provided a robust means of affinity purifying the complexes that resulted from the cross-linking. Recently,

photocrosslinking strategies have been utilized to improve the purification of membrane proteins.[119] The study by Gubbens and co-workers employed cross-linking mitochondrial membrane proteins to phospholipids and led to the identification of several membrane proteins from the sub-sub cellular fraction.[119] Their studies indicated that this approach could be an extremely effective way to further improve the identification of genuine membrane proteins.

1.3.1.3 Cell-surface Shaving to Improve Identification of Integral Membrane Proteins

The concept of cell-surface shaving for the improvement in identifying and quantifying proteins exposed on the cell surface has been discussed for quite some time.[120,121] The idea is formulated around using a protease in free solution around intact cells. Peptides that are exposed on the surface are cleaved by the protease into the surrounding solution. They are then collected and analyzed using tandem mass spectrometry for identification (see Figure 1.2).[66]

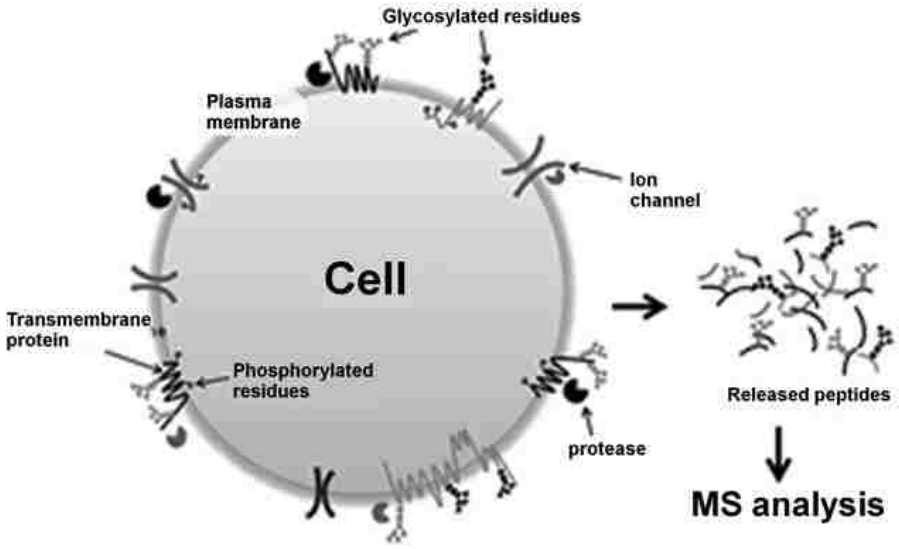

Figure 1.2 Cell ‘‘shaving.’’ Surface-exposed peptides are released by protease digestion into the surrounding solution. The peptides are then collected and analyzed by MS/ MS for their identification (Reproduced from Cordwell, S. J.; Thingholm, T. E. *Proteomics* **2010**, *10*, 611[66] with permission, Copyright 2013, John Wiley & Sons).

In theory, this method could prove to be very advantageous. First, it provides information about the surface topology of the cell (*i.e*. for those epitopes that are exposed on the surface, which are capable of interacting with other surface molecules, foreign particles, *etc.*). Furthermore, if proven successful, there would be no need for the solubilization of highly hydrophobic proteins because those peptides exposed on the surface would be soluble even from integral membrane proteins that are insoluble. Unfortunately, cells have been unstable during the protease treatment when using this method. In addition, removal of cell debris is difficult when using centrifugation, and there has been significant contamination of cytoplasmic proteins after cell lysis. Yet, there has been some success when investigating bacterial systems (mainly Gram positive containing bacteria due the sturdy cell wall);[121,122] nevertheless, there are still a large amount of cytoplasmic proteins remaining on the identified protein lists, which reduces the confidence in the assignment of those epitopes exposed on the surface.

There has been work by Speers and co-workers[123] on *HeLa* cells using proteinase-K and high pH treatment combined with micro-LC-MS/MS performed at high temperatures. The authors reported a significant improvement in the identification of integral membrane proteins, with ~87% of those having transmembrane domains. Elortza *et al*.[124] further modified the strategy and coined the term "shave and conquer" to describe phospholipase D treatment to remove GPI-anchored proteins from the cell surfaces of both plant and human cells. While there has been some success with this technique, it should be noted that problems still exist with cell lysis and that they have yet to be fully realized or overcome.

1.3.1.4 Fractionation of Sub-cellular Organelles for Enrichment

The current approach to proteomics is to assess fractions of organelles rather than cell homogenates by MS. As a result, the complex human proteome can be broken into simpler components. However, the quality of the data received relies heavily on the purity of the organelle fraction. There have been reports of more recently developed methods to generate high purity fractions of organelles that sediment at the same rate as other organelles or contaminants.[127,128]

For example, fluorescence-activated organelle sorting (FAOS), in which fluorescently tagged antibodies interact with highly expressed surface proteins that are specific to the organelle of interest, has been used to generate highly pure fractions.[127] Gauthier *et al*. performed the proteomic analysis of the endocrine secretory granules of corticotropes-derived cells (AtT-20 cells) using FAOS.[128] The authors circumvented the density gradient centrifugation steps. In order to purify the secretory granules, endocrine cells were transfected with a construct encompassing part of a secretory granule specific protein fused in frame with green fluorescent protein (GFP). Once sorted, the enriched secretory granules were lysed and their content was found to be closely related to that derived from other endocrine granules isolated through conventional density gradient protocols.[129] Furthermore, MS analysis of the ensuing complex protein mixture was performed without resorting to gel electrophoresis, which, if deemed necessary, could add a further refinement step.

1.3.1.5 Immunoaffinity Techniques for Enriching Integral Membrane Proteins

Affinity enrichment has also been used for the isolation of membrane proteins. In this case, enrichment was achieved through the use of silica or magnetic beads that have been coated with specific antibodies, a method that can be applied to both tissue samples and cells

grown in culture. Several groups have been successful in using immobilized monoclonal antibodies against known membrane proteins for enrichment.[130,131] Moreover, the method is both an efficient and specific technique for additional purification of previously enriched fractions of membrane proteins.

In 2004, Chang *et al.*[114] developed a protocol for the isolation of neutrophil plasma membranes utilizing a plasma membrane marker antibody, anti-CD15, attached to superparamagnetic beads. Cells were initially disrupted by nitrogen cavitation and then incubated with anti-CD15 antibody-conjugated superparamagnetic beads. The beads were then washed to remove unbound cellular debris. These methods were coupled with immunodetection methods (Western blots) and an adenosine 5′-diphosphate-ribosylation assay to measure the amount of membrane-associated $G_{i\alpha}$ proteins. Lawson *et al.*[101] used the same technique in 2006 for the enrichment of membrane proteins from rat liver and two different hepatic carcinoma cell lines. Zhang and co-workers[132] optimized an immunoaffinity protocol by using secondary antibody super-paramagnetic beads to enrich membrane proteins from mouse liver and compared the method to sucrose density centrifugation. Their optimized method showed a threefold increase in the amount of identified membrane proteins, and contamination of abundant, mitochondrial proteins was decreased. There has been a variation of this approach using cells that have been coated with antibody-conjugated magnetic beads with the authors reporting achieving ~98% purity in the isolation of membrane protein sheets.[133]

1.3.2 Solubilizing Integral Membrane Proteins

After successful enrichment of the membrane protein fractions, there still remains the issue of solubilizing the membrane proteins for further downstream analysis. Membrane

proteins are distributed in the lipid bilayers of cell membrane making them hydrophobic, but they also have hydrophilic regions that extend into the cytoplasm of the cellular region. They are very difficult to solubilize in water-based environments, because they easily form aggregates and precipitates in aqueous media;[134] however, water-based environments are vital for IEF. Therefore, many other detergents, including Triton X-114, octylglucoside, CHAPS, C8Ø, sulfobetaines (SB 3-10, SB 3-12, *etc*.), and ASB-14,[8,135,136] among others, have been employed to aid in the solubility of membrane proteins in aqueous solutions.

Unfortunately, none of the detergents that are currently in place are satisfactory for all the membrane proteins.[135,136] For example, C8Ø is good for isolating more abundant and hydrophobic membrane proteins, but not for a variety of critical membrane-associated proteins,[8] which suffer loses after being processed with C8Ø. Secondly, proteins may precipitate at or close to their pI during IEF, where their solubility is lowest.[137] Interactions between proteins with the acrylamide buffering groups resulting in adsorption of proteins in the immobilized pH gradient (IPG) matrix cause severe quantitative losses of membrane proteins.

Rabilloud and co-workers[138-140] utilized thiourea to alleviate this issue with hydrophobic membrane proteins. Nonetheless, protein loses still occurred due to thiourea inhibiting the SDS-protein binding, and, most importantly, increasing the solubility of lipids, which interfere with the isolation and separation of the membrane proteins in 2DE.[141,142] Additionally, there is a limitation on the use of reducing agents. Detergents can interfere with downstream processing (*i.e.* mass spectrometry) because they can have negative effects on the enzymes used for digestion. Some of the main methods for membrane protein solubilization discussed throughout this section are summarized in Table 1.2.

Table 1.2 Membrane Protein Solubilization Methods

Membrane Solubilization Techniques	**Principle**	**Sample Origin**	**Results**	**Drawbacks**	**Ref.**
Carbonate extraction and solubilization using organic solvent free of surfactant	Avoid interference with subsequent MS analysis	Membrane proteins in *D. radiodurans* strain R1 cells	Extensive coverage of the *D. radiodurans* membrane sub-proteome	Use of organic solvents & high pH affect downstream analysis	143
Detergent solubilization w/chaotropic reagents or strong ionic detergent	Extraction of detergent-resistant proteins	Rat liver	Identification of members of the annexin family in the detergent-insoluble fraction	High conc. of detergents, laborious	144
Phase separation of extracted hydrophobic and hydrophilic proteins using detergent	Triton X-114 is homogenous at 0°, but forms detergent phase at 20° containing membrane proteins and aqueous phase with hydrophilic proteins	Method tested the efficiency of solubilizing both hydrophilic and hydrophobic proteins in two different phases	Hydrophilic proteins were solely identified in the aqueous phase and hydrophobic proteins were identified in the detergent phase	High conc. of detergents in membrane protein fraction	104
Repeated freezing and thawing	Solubilize proteins that are loosely associated with the membrane	Rat liver and hepatocellular carcinoma Morris hepatoma 7777	Shown to be reproducible and reliable	Repeated freezing and thawing of protein reduces stability	145

Many reducing agents have been employed for IEF, and each has its own drawbacks. Dithiothreitol (DTT), dithioerythritol (DTE), and tris(2-carboxyethyl) phosphine (TCEP) are weakly acidic and are charged at alkaline pH, migrating towards the anode. Consequently,

there will be a deficiency at the basic end of the IPG strip during IEF and, in turn, will cause re-oxidation of reduced S-S bonds of the proteins and contribute to the horizontal streak.[143]

Repeated freezing and thawing is a technique that has been used to solubilize those proteins only loosely associated with the plasma membrane and not those with many transmembrane domains.[144] Following extraction, various detergents must be used to solubilize those integral membrane proteins that are highly hydrophobic, but what detergent is used is dependent upon the downstream separation/fractionation techniques employed.[104,113,145,146] It is vital that the known biochemistry of the system being investigated is taken into account. For example, the use of chaotropic reagents such as urea or guanidine hydrochloride, or strong ionic detergents such as SDS, may not be compatible with some separation protocols, or may inhibit the optimal functionality of certain proteases like trypsin.[145,147]

Many groups have used liver tissue from rats as a model for membrane protein studies. One study combined sodium cholate and polidocanol to solubilize rat liver membrane proteins in order to study (Ca^{2+}-Mg^{2+})-ATPase.[146] Studies by Josic and co-workers[144,145] have employed different solubilizing agents and Triton X-100. After the solubilization of the membrane proteins, they used an ethanol/acetone wash to remove lipids and precipitate the detergent-resistant proteins. The proteins were then subsequently solubilized with urea and the zwitterionic detergent CHAPS. Unfortunately, membrane proteins with several transmembrane domains were not solubilized.[148] Prior to separation with SDS-PAGE and LC-MS/MS, Clifton *et al*. utilized EGTA with octyl-glucopyranoside for the extraction of detergent resistant proteins.[149] In a consequent study, the same group used a sequential extraction method by repeated freezing and thawing as the first step, followed by washes with

different salt solutions and/or high pH. Thirdly, the integral membrane proteins were solubilized with different detergents and finally, the proteins that were insoluble in detergent were extracted with calcium chelation using EDTA or EGTA in combination with octylglucoside or CHAPS.[149]

As previously stated, there are still many challenges with solubilization of integral membrane proteins because several suitable detergents and chaotropes used interfere with the downstream separations, particularly liquid chromatography (LC). In addition, if mass spectrometry is to be used (*i.e*. electrospray ionization, ESI-MS), the use of detergents can introduce noise into the analytical technique due to the chemicals there within, and thus, must be removed prior to analysis.[153] Although methods exist to achieve detergent removal, they usually result in loss of analyte and are not necessarily compatible with studies that wish to examine samples with low yield or sample targets low in abundance.

Detergent removal is typically done by precipitation of the proteins using trichloroacetic acid (TCA), a combination of chloroform and methanol, or with organic solvents such as acetone. Furthermore, in addition to the overall loss of proteins from the sample following precipitation, it is likely possible that hydrophobic proteins of interest are also lost during this step.[101,149] Blonder *et al*.[153] employed the combination of carbonate extraction and solubilization using organic solvent that was free of surfactants to avoid the loss of the hydrophobic proteins. They then followed with tryptic digestion prior to MS analysis. Moreover, thiourea has specifically been shown to improve the solubilization of membrane proteins.[149]

1.3.3 Separating Complex Fractions of Integral Membrane Proteins

After successful purification/enrichment of the membrane proteins and their solubilization, the sample is still complex and further fractionation is necessary in order to increase the eventual protein/peptide identification coverage, which is how many proteins are identified with the subsequent MS analysis. Methods of fractionation are typically focused on either separation at the peptide or protein level.[66] There are various techniques available to perform protein separation including: two-dimensional electrophoresis utilizing IEF and SDS-PAGE; SDS-PAGE coupled to liquid chromatography and tandem MS (LC/MS/MS) known as "slice and dice;" and methods for peptide separation after proteolytic digestion such as multidimensional peptide LC coupled to tandem MS and peptide isoelectric focusing (pIEF).

1.3.3.1 Two-dimensional Electrophoresis (2DE) with Isoelectric Focusing (IEF) and SDS-PAGE for the Separation of Integral Membrane Proteins

For a number of years, the most popular method used for fractionation has been SDS-PAGE,[155-157] either as the sole method of separation, or in combination with IEF to produce a 2DE technique (*i.e.* IEF in the first dimension coupled with SDS-PAGE in the second dimension) that can offer high peak capacities compared to a 1DE approach. While 2DE remains one of the core separation technologies of proteomic analysis, proteins that are extremely basic (positively charged), hydrophobic, or of large mass present significant challenges for 2DE separation due to aggregation, oxidation, precipitation, and the physical limitations of the 1D immobilized pH gradient (IPG) strip.[158] Since the introduction of commercially available immobilized pH gradient strips, several groups have experimented with IEF conditions using various detergents alone or in combination,[159] thiol oxidants,[160] and alternative detergents.[141]

McDonough and co-workers utilized modified equilibrium conditions between the IPG strip and the second dimension to get better focus and quantification of a positively charged integral membrane protein and also improved migration into the second dimension.[158] Techniques using IEF have enabled fractionation of proteins and peptides to be performed in solution, and new protocols have been developed using several detergents, thiol oxidation reagents, and different denaturants in order to make improvements to the isoelectric focusing.[141,159] In order to provide enhanced sensitivity and improved reproducibility for peptide separations, IEF in IPG strips, free-flow electrophoresis, or in liquid isoelectric focusing has been used.[161,162]

Chick *et al*. used an IPG-pIEF to identify 626 membrane proteins from rat liver, however, this only represented 42% of the identified proteins suggesting that there is a need for further investigation into enriched membrane proteomes in order to increase the identification rate of protein contamination from other sub-cellular fractions.[163] Free flow electrophoresis has been used as a suitable approach for the separation of organelles, peptides, and proteins[164,165] and has been shown to be highly reproducible, with excellent separation collecting up to 96 fractions.[162]

There have been variations of the gel-based separation technique reported, such as the "slice and dice" method in which complex mixtures are separated by SDS-PAGE and the resulting gel is "sliced" into equal bands throughout the lane. Each band is then "diced" into smaller pieces and subjected to proteolytic digestion to release peptides that can be identified using reversed-phase (RP) LC-MS/MS.[66] By utilizing this technique, hydrophobic proteins can be solubilized efficiently. Yet, 2DE employing IEF and SDS-PAGE have significant limitations at the protein level that minimize their effectiveness for membrane protein

separation and 2DE usually offers poor resolution of hydrophobic or basic proteins especially those with > 3 transmembrane domains.

In work published by Xu *et al.*,[166] the authors used IEF with SDS-PAGE to separate outer membrane proteins from *E. coli*. With this 2DE technique, they were able to obtain ~50 spots that were representative of membrane proteins. The 2DE gel (IEF/SDS-PAGE) from the separation is shown in Figure 1.3. The spots that are more darkly stained are most likely representative of membrane proteins that are more abundant and the faint spots are those of membrane proteins that are lower in abundance. Several groups have attempted direct analysis of intact membrane proteins and identification of their covalent modifications. In this approach, the protein mixtures are first solubilized and then chromatographically resolved. Intact membrane proteins of up to 61 kDa[167-170] have been analyzed directly by LC/MS.

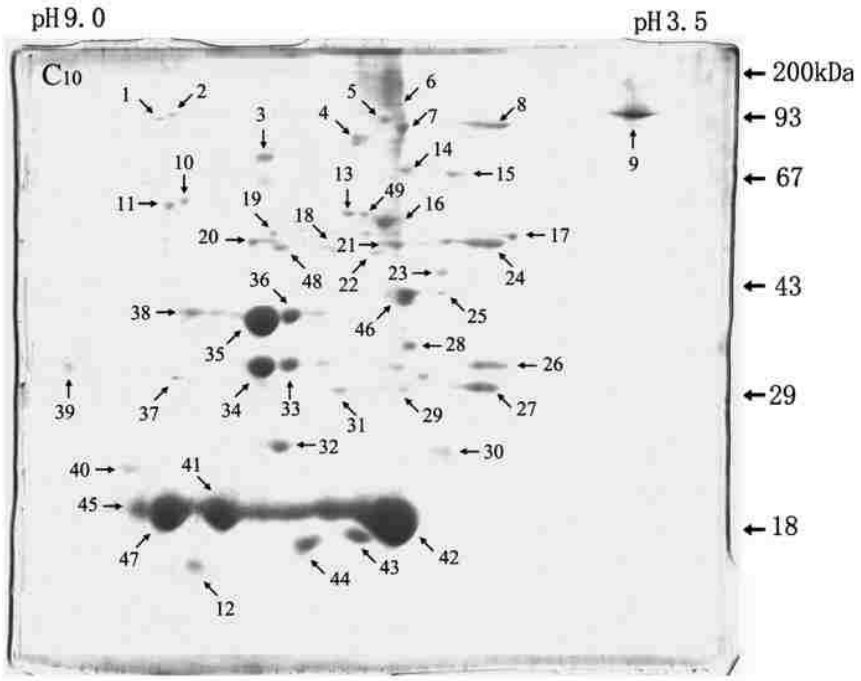

Figure 1.3 A 2DE profile of outer membrane proteins from *E. coli* employing IEF in the first dimension and SDS-PAGE in the second dimension (Reproduced from Xu, C.; Lin, X.; Ren, H.; Zhang, Y.; Wang, S.; Peng, X. *Proteomics* **2006**, *6*, 462[166] with permission, Copyright 2013, John Wiley & Sons).

le Coutre and co-workers[167] employed high performance liquid chromatography (HPLC) coupled to electrospray ionization MS (ESI-MS) to separate and identify solubilized membrane proteins from *E. coli*. As the authors demonstrated (see Figure 1.4), chromatography combined with ESI-MS can separate an individual membrane protein from a crude mixture and measure its molecular mass, which can be used subsequently to identify the protein with a database search, provided the database sequence is correct and the isolated protein has not been post-translationally modified.

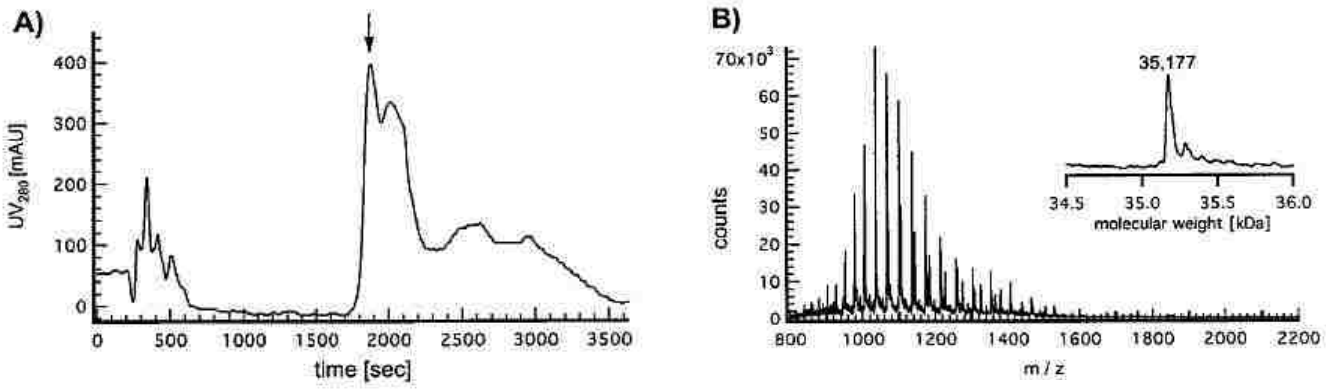

Figure 1.4 (A) The elution profile of solubilized *E. coli* membrane proteins with HPLC. (B) ESI-MS spectrum of the peak indicated in panel A (Reproduced from le Coutre, J.; Whitelegge, J. P.; Gross, A.; Turk, E.; Wright, E. M.; Kaback, H. R.; Faull, K. F. *Biochemistry* **2000**, *39*, 4237.[167] with permission, Copyright 2013, American Chemical Society).

However, both methods have limited sensitivity making it difficult to detect lower abundance proteins, and the dynamic range is limited meaning that peptide-focused, liquid-based strategies are more often used.[171]

1.3.3.2 Separating Integral Membrane Proteins Utilizing Liquid Chromatography

To date, the most common method employed for the separation of integral membrane proteins or peptides from the proteolytic digestion of integral membrane proteins is high performance liquid chromatography (HPLC). Because of the complexity of biological

samples, a multi-dimensional separation approach is required in which various methods are combined.[22,172,173] Strong cation exchange chromatography can be combined with reversed-phase liquid chromatography (on- or off-line) for multi-dimensional protein identification technology (MudPIT), which can be directly coupled to a mass spectrometer for tandem MS (MS/MS) analysis.[22] Wolters *et al*.[22] utilized HPLC with MudPIT analysis to detect and identify proteins of the *S. cerevisiae* proteome. Integral membrane proteins are difficult to identify with 2D-PAGE, mainly due to solubility problems.[174] Yet, unlike most other approaches, in the MudPIT scheme, protein digestion takes place first and thus overcomes protein solubility in solution or gel. In the analysis of the *S. cerevisiae* proteome via MudPIT, 131 proteins with three or more predicted transmembrane domains were detected and identified.[22] In addition, a highly efficient separation can be achieved due to the high loading capacity provided by strong cation exchange combined with the high resolving power of reversed-phase LC.[171,175] This 2D LC strategy is routinely used for the analysis of integral membrane proteins since hydrophilic peptides from insoluble proteins are adaptable to rapid analysis.

1.4 Analysis Strategies for Membrane Proteins

1.4.1 Two Main Strategies for Mass Spectrometry Analysis of Proteins

It would be preferable for a proteomic platform to quantitatively analyze the entire proteome in a high-throughput fashion, and do it with high sensitivity.[176] There are two widely used approaches to protein analysis and identification: Bottom-up and top-down strategies. In the bottom-up approach, the intact protein mixture is directly subjected to proteolytic digestion (usually with trypsin) without first separating the proteins. In addition, proteins in complex mixtures can be separated before enzymatic (or chemical) digestion

followed by direct peptide mass fingerprinting-based acquisition or further peptide separation on-line coupled to tandem MS, which is then followed by the separation of the peptides, typically with liquid chromatography, with the isolated peptides being submitted for tandem mass analysis.

A variation of the bottom-up approach is called "shotgun proteomics" because it is typically centered on early digestion of a protein mixture followed by a multidimensional chromatographic separation of the peptides and then coupled to a mass spectrometer for peptide mass determination. The essential difference in shotgun proteomics from the traditional bottom-up technique is that a non-separated protein mixture is digested instead of an isolated individual protein (see Figure 1.5).

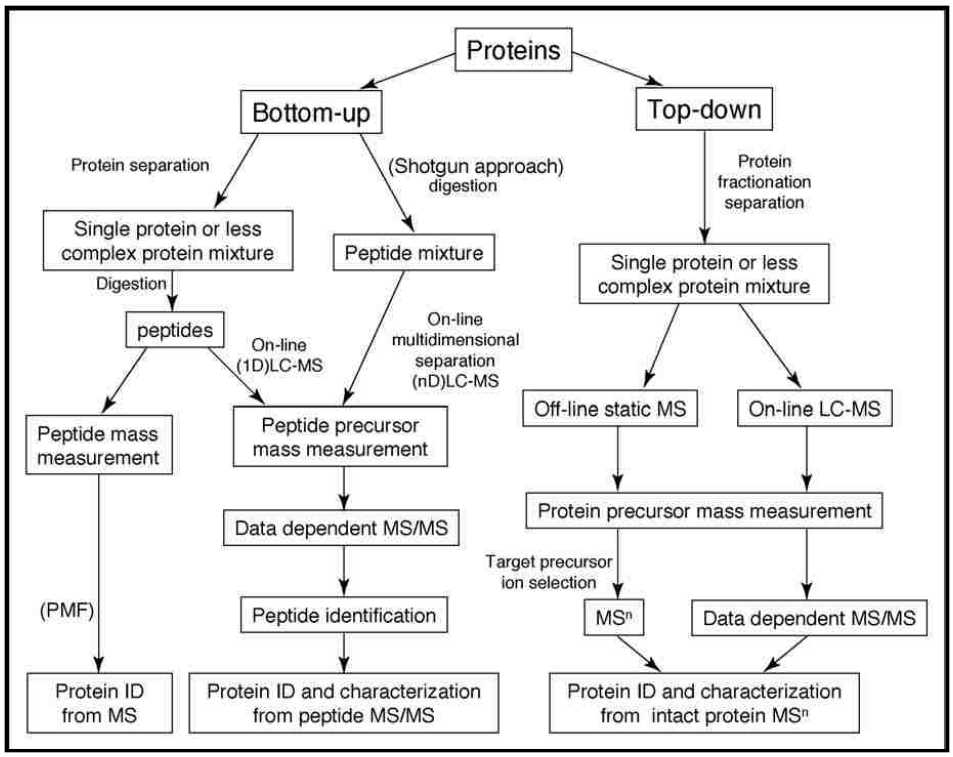

Figure 1.5 Overview of strategies for MS-based protein characterization and identification. Proteins extracted from biological samples can be analyzed by bottom-up or top-down methods. An on-line LC–MS strategy can also be used for large-scale protein interrogation (Reproduced from Han, X.; Aslanian, A.; Yates, J. R., 3rd *Current opinion in chemical biology* **2008**, *12*, 483.[177] with permission, Copyright 2013, Elsevier).

In the top-down approach, proteins in complex mixtures are fractionated and separated into pure single proteins or less complex protein mixtures, followed by off-line static infusion of sample into the mass spectrometer for intact protein mass measurement and intact protein fragmentation.

1.4.1.1 The "Top-Down" Approach

In the "top-down" approach, an individual protein mixture, or an individual protein, is digested. This digestion generates peptides, which are more uniform and easier to analyze as opposed to a complex protein sample that contains a mixture of small, large, hydrophobic, and acidic/basic proteins and these extreme properties tend to yield poor 2D IEF/SDS-PAGE results[4]. Top-down MS is becoming a powerful technology for comprehensive analysis of protein modifications.[59,178-188] In contrast to bottom-up MS, top-down MS analyzes intact proteins without proteolytic digestion as shown in Figure 1.6. This strategy preserves the labile structural characteristics that are mostly destroyed in bottom-up MS.[187] It can universally detect all the existing modifications, including PTMs (*i.e.*, phosphorylation, methylation, and acetylation) and sequence variants (*i.e.*, mutants, alternatively spliced isoforms, and amino acid polymorphisms) concurrently in one spectrum (a "bird's-eye" view) without a prior knowledge.[187]

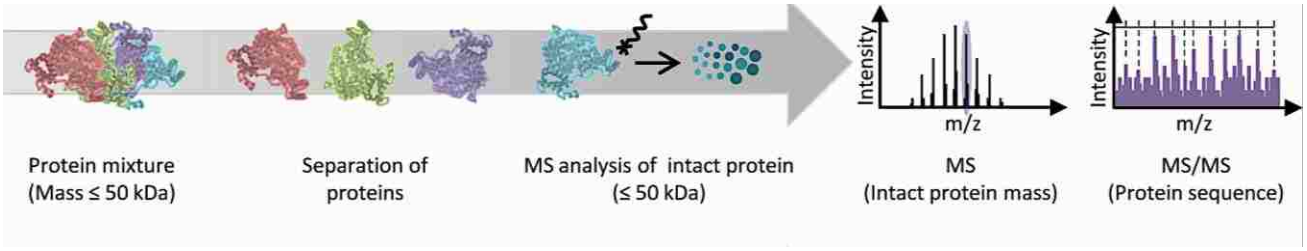

Figure 1.6 Overview of the top-down proteomic strategy (Reproduced from Switzar, L.; Giera, M.; Niessen, W. M. *Journal of proteome research* **2013**, *12*, 1067[189] with permission, Copyright 2013, American Chemical Society).

Top-down MS first measures the molecular weight of an intact protein and compares it with the calculated value based on the DNA-predicted protein sequence, which can easily reveal any changes/modifications in the protein sequence globally (the "top" part). Then, a specific modified form of interest can be directly isolated in the mass spectrometer ("a gas-phase purification") and subsequently fragmented in the mass spectrometer by tandem MS (MS/MS), such as collision-induced dissociation (CID) and electron-capture dissociation (ECD), for highly reliable mapping of the modification sites (the "down" part).[187,190] The incorporation of the novel MS/MS technique, ECD,[191] has greatly enhanced the capability of top-down MS in structural analysis of biomolecules.[192] As a non-ergodic fragmentation method,[191] ECD preserves labile PTMs during the fragmentation process; thus, it is particularly suitable for the localization of labile PTMs.[178,180] In terms of an ionization source, electrospray ionization (ESI) is commonly used for top-down strategies, particularly because liquid chromatography (LC), used in the separation of the peptides, couples naturally to ESI due to the ability of continuous sample infusion into the ESI source.[193] However, this continuous infusion of sample can overwhelm the mass spectrometer and cause a more complex peptide mass spectra to be generated. The top-down approach has the benefit of giving closer to full sequence coverage.[194] Top-down approaches have been used to better understand the link between the observed changes and biological states of proteins.

These links usually become clearer when studying the regulation of a protein's function/activity achieved through changes in abundance, PTMs, balances in protein isoforms (different forms of the same protein that can arise from the same gene by alternative splicing or single nucleotide polymorphisms), cleavage of the proteins, and relocalization. In many instances, different isoforms are present and can lead to different activities or functions. It

should be noted that this approach requires high-resolution instrumentation such as FT-ICR MS, electron capture dissociation or electron transfer dissociation capabilities and reports have suggested that even quadrupole time-of-flight (Q-TOF) instrumentation can be modified to successfully undertake top-down approaches.[195]

High-resolution instrumentation is needed because of the need to resolve the high molecular weights of intact proteins and protein mixtures with high complexity. The top-down strategy has been successful in identifying post-translational modifications in individual proteins, including myosin-binding protein C,[180] and histones.[196] The sequencing of polymorphisms has also been done using this technique.[198] Typically, intact proteins need to be extracted from cell/tissue lysate, solubilized, and separated/purified before MS analysis. Protein samples then need to be introduced to a mass spectrometer in buffer conditions compatible with MS analysis.

The buffers employed to extract/solubilize proteins usually involve a high salt concentration, with the addition of detergents, such as SDS, Triton X-100, *etc*. to increase the solubility of the protein. These salts and detergents interfere with MS detection of proteins because they are present in large excess relative to proteins and have much higher ionization efficiency, which will, therefore, suppress protein signals. Standard procedures for detergent removal typically involve precipitation and resolubilization of proteins in detergent-free buffers, which may result in sample loss because some portion of protein may become insoluble in detergent-free buffers. Recently, there are efforts allocated in designing MS-compatible acid labile detergents with the hope of replacing these traditional detergents.[198,199] Alternatively, proteins can also be selectively solubilized based on their inherent chemical properties, such as biospecificity, hydrophobicity, and charge without the use of a

detergent.[200] Moreover, these techniques can also be used to fractionate a specific sub-proteome before chromatographic separation.

Gel-based separation is widely used in bottom-up proteomics because trypsin-digested peptides can be effectively retrieved from gels.[201,202] However, it is technically challenging to extract the intact proteins from gel matrices with a high recovery rate.[203] Thus, gel-based separation is not applicable in top-down MS. Solution-based isoelectric focusing, coupled with a multiplex tube gel electrophoresis separation device, referred to as gel-eluted liquid fraction entrapment electrophoresis,[204] has been developed for intact protein separation based on their MWs and applied to proteins (10–250 kDa) with a high resolution and a high recovery rate.[183,201,205] Nevertheless, the surfactant SDS is still present in the sample so the proteins need to be precipitated in organic solvent and resolubilized in MS-compatible buffers. LC is ideally suited for proteomics because it can be conveniently interfaced with MS.[206-208] The major LC techniques utilized for intact protein separation include affinity chromatography, ion-exchange chromatography, size-exclusion chromatography, and RP chromatography.[48] Affinity chromatography has been one of the most effective and specific protein purification methods.[50] For example, immunoaffinity methods have been used to effectively purify cardiac troponin I (cTnI) from animal and human myocardium.[178,185,186,209,210]

Nonetheless, most of the affinity methods have been performed off-line, requiring an additional separation/desalting procedure using RPLC. Ion-exchange chromatography and SCX chromatography have also been used for intact protein separation.[206,211-213] In addition, these separation techniques are used to perform the first-dimension separation, followed by RP chromatography in the second dimension. RP chromatography enhances the separation

from the previous step and performs desalting as the last sample preparation step before MS analysis.[212,213] The 2-dimensional LC approach has the advantage of preconcentrating and desalting the species of interest simultaneously, yielding a higher peak capacity and better separation and, if connected on-line, minimizing sample loss. In contrast to the well-established bottom-up proteomics, the top-down proteomics is still in its early developmental stage and has yet to fully overcome its technical challenges in sample preparation, instrument sensitivity/detection limit, and throughput/automation.[187,214-216]

However, new technological developments are needed to advance top-down proteomics for the analysis of complex samples of cell/tissue lysate and biological fluid. Although the top-down approach is powerful in protein modification analysis, it is primarily performed with direct infusion of a single protein or simple protein mixture (separated off-line), therefore, the analytical throughput and efficiency for large-scale proteome analysis is still a major challenge. To address these limitations, increasing efforts have been made to improve the front-end separation of complex protein mixtures and automated database searching informatics.

1.4.1.2 The "Bottom-Up" Approach

The vast majority of proteomic studies are performed using the 'bottom-up" approach. In this particular workflow (see Figure 1.7), after separation, intact proteins are cleaved using proteases such as Lysine C or enzymes such as trypsin, proteinase-K, or pepsin. Trypsin is most commonly used due to the fact that it is highly specific when cleaving the *C*-terminal side of lysine and arginine residues except when a proline is positioned directly on the *C*-terminal side of the cleavage site.[66] Furthermore, trypsin digestion for most proteins creates a series of peptides in a mass range that is compatible with nearly all MS instruments. However,

although trypsin is the ideal choice for a protease in most of these analyses, other enzymes have also been used as alternatives for digestion or used in parallel with one another to increase the overall proteome coverage.[218] Proteins can also be cleaved utilizing enzyme-free approaches or by combinations of non-enzymatic hydrolysis.

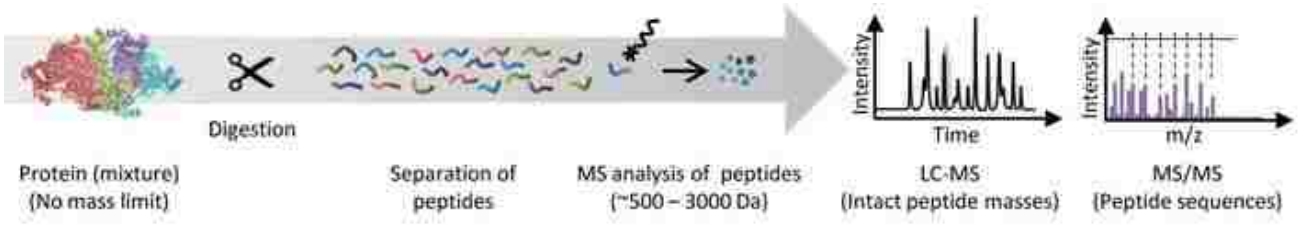

Figure 1.7 Overview of the bottom-up proteomic strategy (Reproduced from Switzar, L.; Giera, M.; Niessen, W. M. *Journal of proteome research* **2013**, *12*, 1067[189] with permission, Copyright 2013, American Chemical Society)

Bottom-up strategies are the standard for large-scale or high-throughput analysis of highly complex samples. There are usually two workflows associated with the bottom-up approach: "sort-then-break" and "break-then-sort."[219] The latter workflow involves protein digestion being conducted first without any prefractionation/separation step and then, the peptides are separated by multidimensional chromatography followed by tandem MS. In the "sort-then-break" approach, off-line protein fractionation and separation is performed first before protein digestion, followed by direct peptide analysis.

When bottom-up analysis is performed on a mixture of proteins it is called "shotgun" proteomics, a term coined by the Yates lab[21,22] because it is analogous to shotgun genomic sequencing. Shotgun proteomics provides an indirect measurement of proteins through peptides derived from proteolytic digestion of intact proteins. In a typical shotgun proteomics experiment, the peptide mixture is fractionated and subjected to LC-MS/MS analysis. Peptide identification is achieved by comparing the tandem MS spectra derived from peptide fragmentation with theoretical tandem MS spectra generated from searching a database of

protein spectra. Protein interface is accomplished by assigning peptide sequences to proteins. Because peptides can be either uniquely assigned to a single protein or shared by more than one protein, the identified proteins may be further scored and grouped based on their peptides.

Bottom-up strategies are suitable for automation, and high sample throughput can be achieved.[220-222] These procedures typically identify a very limited number of peptides per protein, but still enough to identify the gene from which the protein was encoded. They work well in the study of microorganisms where the assumption that one gene codes for only one protein. However, when higher eukaryotes are investigated, processes including alternative splicing, RNA editing and post-translational modification can lead to several different protein species from a single gene. Peptide-based identification strategies enable the identification of the genes from which these proteins are derived. The bottom-up approaches generally do not provide information on the entire protein sequence, and similarly suffer from the fact that peptides from many possible forms of the parent gene products (arising from partial degradation and various covalent modifications) are generally indistinguishable in the absence of additional information (*e.g.*, the MW of the parent protein).

Multidimensional protein identification technology (MudPIT) is an automated bottom-up approach in which the complexity problem is addressed at the peptide level.[22,221] Following enzymatic digestion of a total protein mixture, peptides are separated on a biphasic liquid chromatography column using a strong-cation exchange support as the initial phase, and subsequently reversed-phase material. The peptides are then delivered online to a tandem mass spectrometer, and MS/MS spectra are automatically detected for as many peptides as possible and those spectra used to search protein sequence databases. With this LC/LC/MS/MS procedure, a high-separation of peptides is achieved. The complex

deconvolution takes place mainly in the chromatography step, but the ability of the mass spectrometer to handle several peptides at a time also contributes to the multiple dimensions.[223]

Two generally applicable bottom-up approaches for protein identification include one based upon mass measurements for a set of peptide digestion products from the parent protein and the other based on MS fragmentation (MS/MS) of one or more of these peptides. The first approach is referred to as peptide mass fingerprinting. A set of peptide fragments unique to each protein is created and their masses used as a ‘‘fingerprint’’ to identify the original protein. The peptide mass fingerprinting approach has been broadly applied with conventional MS instrumentation, but its throughput is limited because it requires prior isolation of a single protein (or a simple mixture). The second approach to protein identification is based on the information from dissociation (e.g., using collisional activation or some other energy deposition process) of one or more polypeptides that have typically been isolated by the first stage of the MS analysis.[224-225] Furthermore, the entire bottom-up process can be laborious, time consuming, and limited to adopting automated processes.

1.5 Advantages of Using Microfluidics for Proteomic Analysis

To minimize the disadvantages associated with bench-top strategies (*i.e.* time consumption, sample loss, automation, sample volume, *etc.*), researchers have been and are continuing to explore the use of microchips for proteomic analysis. There are several advantages toward the use of microfluidic platforms for proteomic analysis. Some of the key advantages of microfluidics are the miniaturization and integration of multiple process operations in a single device enabling (a) distinct processing steps without sample transfer, (b) shorter analysis times afforded by decreasing length scales without loss of efficiency and

reducing analyte diffusion, (c) handling of nanoliter volumes, (d) high-throughput processing, (e) a high degree of parallelization, and (f) automation of processing steps.[230]

Devices like these offer the potential of enabling highly efficient, reproducible, and standardized proteomic workflows coupled with low sample consumption. Furthermore, process automation can diminish the need for highly trained analytical personnel, which is a vital attribute in clinical settings. Moreover, limiting manual input reduces the risk of contaminations, which has a major impact on the reliability of proteome analyses.[231] In a 2011 critical review, Liu and Fan discussed the attractiveness of thermoplastic microfluidic devices for both DNA and protein studies including immunoassays and protein separations.[232] This is especially beneficial when the sample contains low abundant proteins such as integral membrane proteins. A high surface-to-volume ratio is afforded when miniaturized platforms are used, which is preferable in the case of protein extraction where the analyte-wall interaction is required especially for extraction onto a solid support. The mass transport is also improved for microfluidics due to smaller diffusional dimensions, which is advantageous for protein digestion or extraction.

1.5.1 Survey of Reported Microfluidic Platforms for Protein Analysis

Several microchip-based proteomic strategies have been demonstrated in the past decade, especially for integrating multiple processing steps onto a single platform for proteomic analysis. Summaries of microfluidic systems that have been used for the analysis of proteins prior to mass spectrometry analysis are listed in Table 1.3 and described within this section.

Table 1.3 Microfluidic Systems for Protein Analysis with processing devices combined prior to MS analysis

Devices or Units Combined	Chip Material	Sample Analyzed	Efficiency/Comments	Ref.
Porous silica pre-concentration unit and μ-CGE separation	Glass	Mixture of up to 7 purified proteins	Pre-concentration factors of ~600 fold	230
Proteolytic reactor and IMAC affinity unit for peptide enrichment	Glass	Model proteins were analyzed individually	Capture bias on IMAC; system required further optimization due to non-specific binding	231
Polystyrene beads for SPE desalting and a CE unit with ESI-interface	PDMS	Six-peptide mixtures dissolved in physiological salt solution	LOD is in the femtomole range	232
SPE enrichment column and a reversed phase separation channel with a nanoelectrospray emitter	Glass	Protein digests spiked into rat plasma samples	LOD of 1–5 fmol.	234

For example, Li *et al.*[227] identified proteins from membrane-bound protein extracts of *Haemophilus influenzae* by separation of the proteome fraction first using 1D SDS-PAGE, then digesting the excised protein spots, and finally introducing the peptides into an integrated microchip consisting of capillary electrophoresis (CE) and nanoelectrospray. The use of surface coatings and a gold-coated nanoelectrospray tip allowed the microchip performance to be similar to a conventional nanoelectrospray CE in terms of LOD and the resolution per meter, yet faster due to the ease of creating shorter capillaries.

The application of the device enabled the identification of peptides in tryptic digests of glycoproteins and further demonstrated that chip-based electrospray devices can be used with

quadrupole time-of-flight mass spectrometry. The authors reported a concentration LOD of 3.2-43.5 nM for different peptides and migration time and peak area reproducibility (*i.e.*, RSD) of 3.1% and 6-13%, respectively. Musiyimi and co-workers[228] developed a poly(methyl methacrylate), PMMA, CE chip that was directly coupled to a rotating ball for a MALDI-TOF MS analysis of protein digests. Mellors and Ramsey[229] demonstrated electrospray MS directly from the corner of a glass chip without a nozzle (external tip) after CE. The CE-MS analysis of peptides and proteins using this device resulted in efficiencies of over 2 $x10^5$ theoretical plates (or 10^6 plates/m).

In the work performed by Foote and co-workers,[230] a microfabricated device with the ability to electrophoretically concentrate fluorescently labeled proteins prior to separation was developed (see Figure 1.8). The proteins were concentrated using a porous silica membrane between adjacent microchannels that allowed for the passage of buffer ions, but excluded larger migrating molecules. The concentrated proteins were then injected into a separation column for electrophoretic analysis. Pre-concentration factors of ~600-fold were achieved using this on-chip format, which was followed by a SDS μ-CGE separation of the proteins. The channels were filled with CE-SDS protein run buffer that was purchased from BioRad and allowed a current of ~1.2 μA when a voltage of 1 kV was applied between preconcentration reservoir 1 and the sample reservoir. Individual microchips were used for up to >200 preconcentration cycles using an applied voltage of 1 kV and an average preconcentration time of ~1 min.

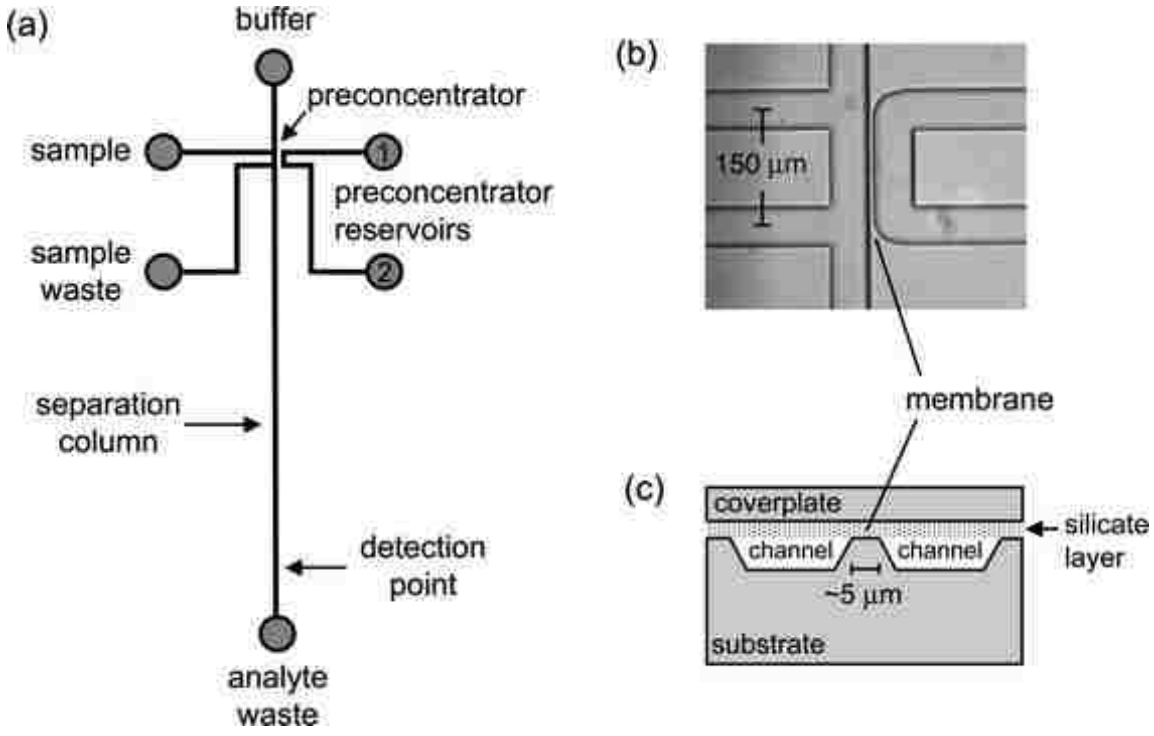

Figure 1.8 (A) Schematic of microchip layout used for peptide preconcentration. (B) Microscopic image of preconcentrator-injector channels. (C) Schematic cross section through injector and preconcentrator channels (Reproduced from Foote, R. S.; Khandurina, J.; Jacobson, S. C.; Ramsey, J. M. *Anal Chem.* Preconcentration of Proteins on Microfluidic Devices Using Porous Silica Membranes. **2005**, *77*, 57.[230] with permission, Copyright 2013, American Chemical Society).

Yue *et al*.[231] described a glass microfluidic system for proteomics that included proteolysis directly coupled to affinity selection (see Figure 1.9). Their initial results using standard phosphopeptide fragments from β-casein in peptide mixtures showed selective capture of the phosphorylated fragments using immobilized metal affinity chromatography (IMAC) beads packed into a microchannel. The results showed selective capture of only phosphopeptide fragments, but digestion of protein was incomplete as indicated from multiple peaks in the CE separations. Application to digestion and capture of a serum fraction showed capture of material; however, non-specific binding was evident.

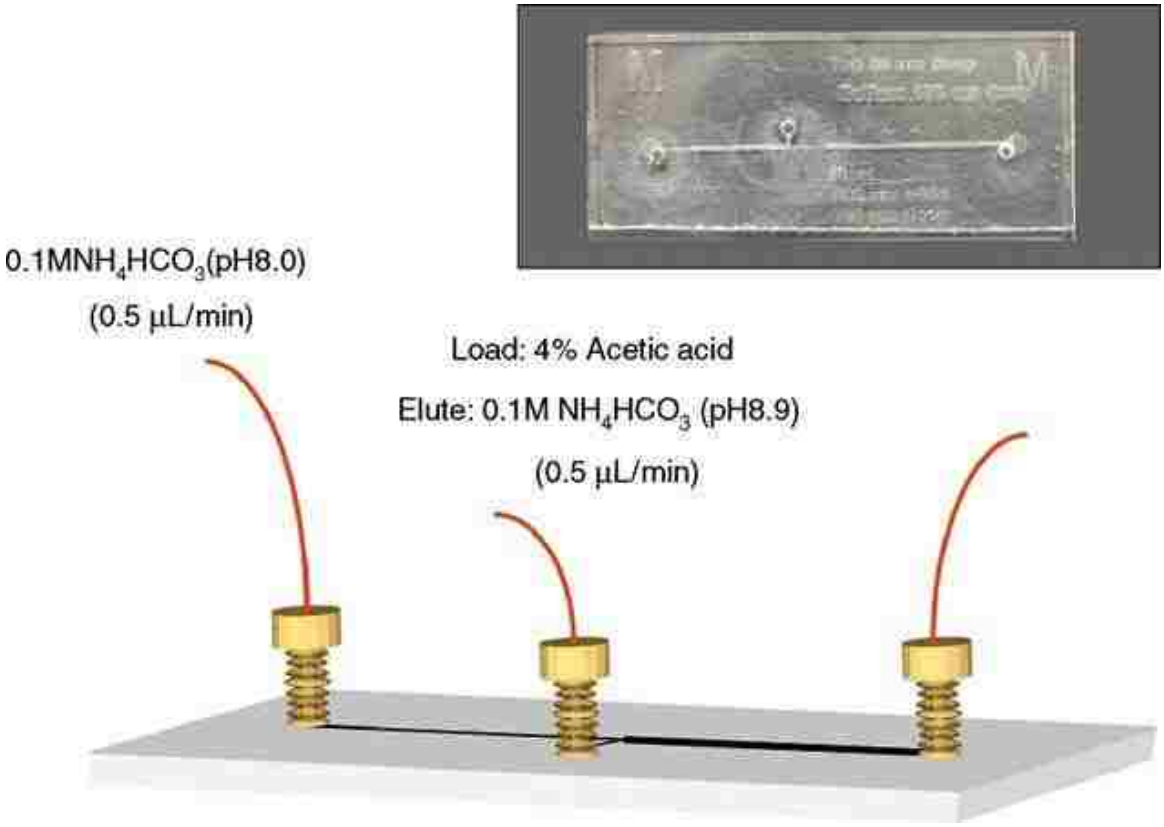

Figure 1.9 Diagram of an integrated trypsin digestion and affinity capture process along with a picture of the actual microdevice (Reproduced from Yue, G. E.; Roper, M. G.; Balchunas, C.; Pulsipher, A.; Coon, J. J.; Shabanowitz, J.; Hunt, D. F.; Landers, J. P.; Ferrance, J. P. *Analytica chimica acta*, Protein digestion and phosphopeptide enrichment on a glass microchip. **2006**, *564*, 116.[231] with permission from Elsevier, Copyright 2013).

An integrated poly(dimethylsiloxane) (PDMS) microchip for SPE and CE followed by ESI/TOF MS has been developed and evaluated by Dahlin and co-workers.[232] The microchip (see Figure 1.10) was fabricated in a novel one-step procedure where PDMS was cast over steel wires in a mold. Once the wires were removed, they defined 50 μm cylindrical channels. Fused-silica capillaries were then successfully inserted into the structure in a tight fit connection. The inner walls of the inserted fused-silica capillaries and the PDMS microchip channels were modified with PolyE-323 (a positively charged polymer) that is used to reduce protein and peptide adsorption on capillary walls during electrophoresis. In this approach, the chip was fabricated in a two-level cross design. The channel at the lower level was packed

with 5 µm hyper-cross-linked polystyrene beads acting as a SPE medium used for desalting. The upper level channel acted as a CE channel and ended in an integrated emitter tip coated with conducting graphite powder to facilitate the electrical contact for ESI.

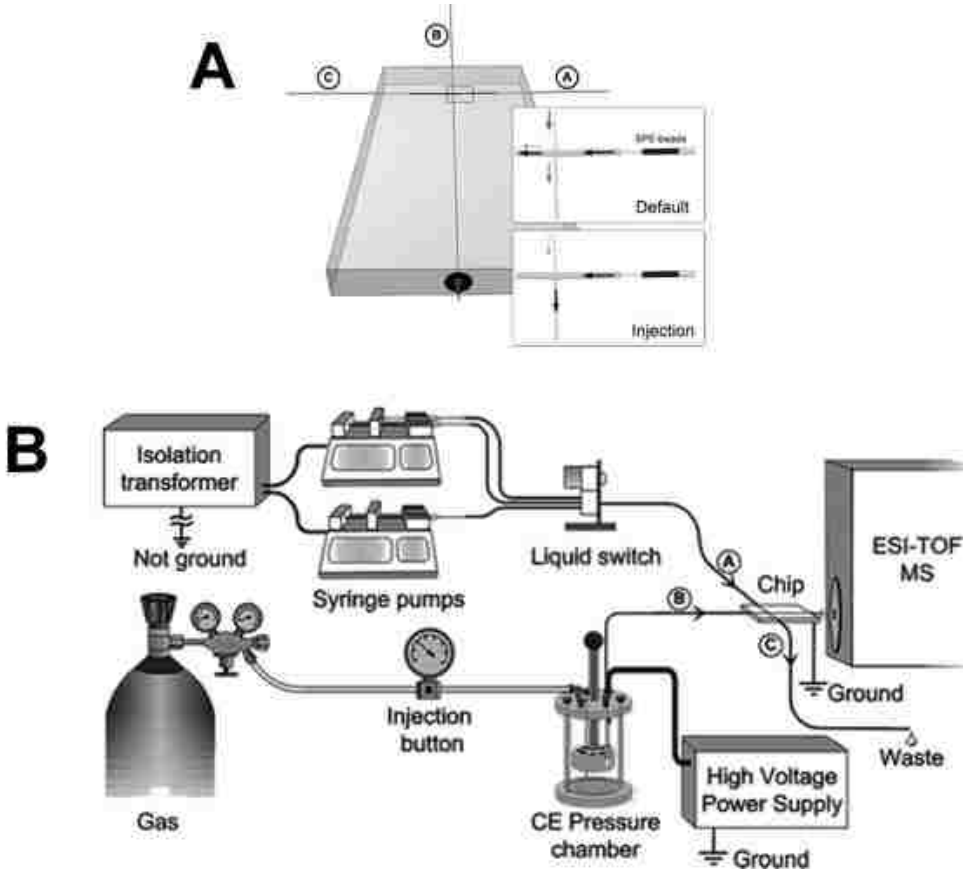

Figure 1.10 (A) Schematic of a PDMS microchip device. Channel A: sample inlet; Channel B: CE; Channel C: waste channel. (B) Schematic showing the instrumental setup and the connection of the microchip to the ESI/TOF MS (Reproduced from Dahlin, A. P.; Bergstrom, S. K.; Andren, P. E.; Markides, K. E.; Bergquist, J. *Anal Chem*. Poly(dimethylsiloxane)-Based Microchip for Two-Dimensional Solid-phase Extraction-Capillary Electrophoresis with an Integrated Electrospray Emitter Tip. **2005**, *77*, 5356.[232] with permission, Copyright 2013, American Chemical Society).

To evaluate the microchip, six-peptide mixtures were dissolved in physiological salt solution, injected, desalted, separated, and sprayed into a MS for analysis with a limit-of-detection in the femtomolar range. The applied CE voltage was varied from -6 to -16 kV with an increment of -2 kV for every injection, giving an electric field of -193 to -516 V/cm. An

integrated microfabricated system composed of a proteolytic reactor and chromatographic column with direct interface to ESI-MS was reported by Carlier *et al.*[233] The system was fabricated from SU-8 and used to perform protein digestion, sample purification, salt removal, and chromatography followed by MS analysis. The chromatographic end of the chip was terminated with a nano-ESI interface. The digestion module was composed of trypsin covalently attached to a monolithic polymer, which was also used to prepare a hydrophobic stationary phase for the desalting or separation of peptides prior to MS analysis

In a similar effort to combine preconcentration with electrophoretic separations, Fortier *et al.*[234] investigated the analytical performances of a fabricated microfluidic device, which included an enrichment column, a reversed phase separation channel, and a nanoelectrospray emitter embedded together in polyimide layers. This configuration minimized transfer lines and connections and reduced post-column peak broadening and dead volume. The compact microchip was interfaced to both ion trap and TOF MS, and its analytical potentials were evaluated in the context of proteomic applications. Sensitivity measurements were performed on a dilution series of protein digests spiked into rat plasma samples and provided a detection limit of 1–5 fmol.

Huft *et al.*[235] fabricated a column geometry that allowed both robust and low-pressure packing of liquid chromatography columns in PDMS devices (see Figure 1.11). They combined the use of high-performance chromatography and valve-based microfluidics. The packing was achieved in minutes and enabled the integration of multiple parallel columns on a single device with high yield and without defects. The approach works by using microvalve control to reconfigure the columns for operation in either the packing or separation mode. The authors utilized pulse tests to show that the columns fabricated in this manner can achieve

high efficiency and reproducibility. They also reported plate heights (for the separation of dye-labeled ssDNA) that were comparable to conventional high-performance capillary columns and plate numbers that exceeded 1,000,000 plates.

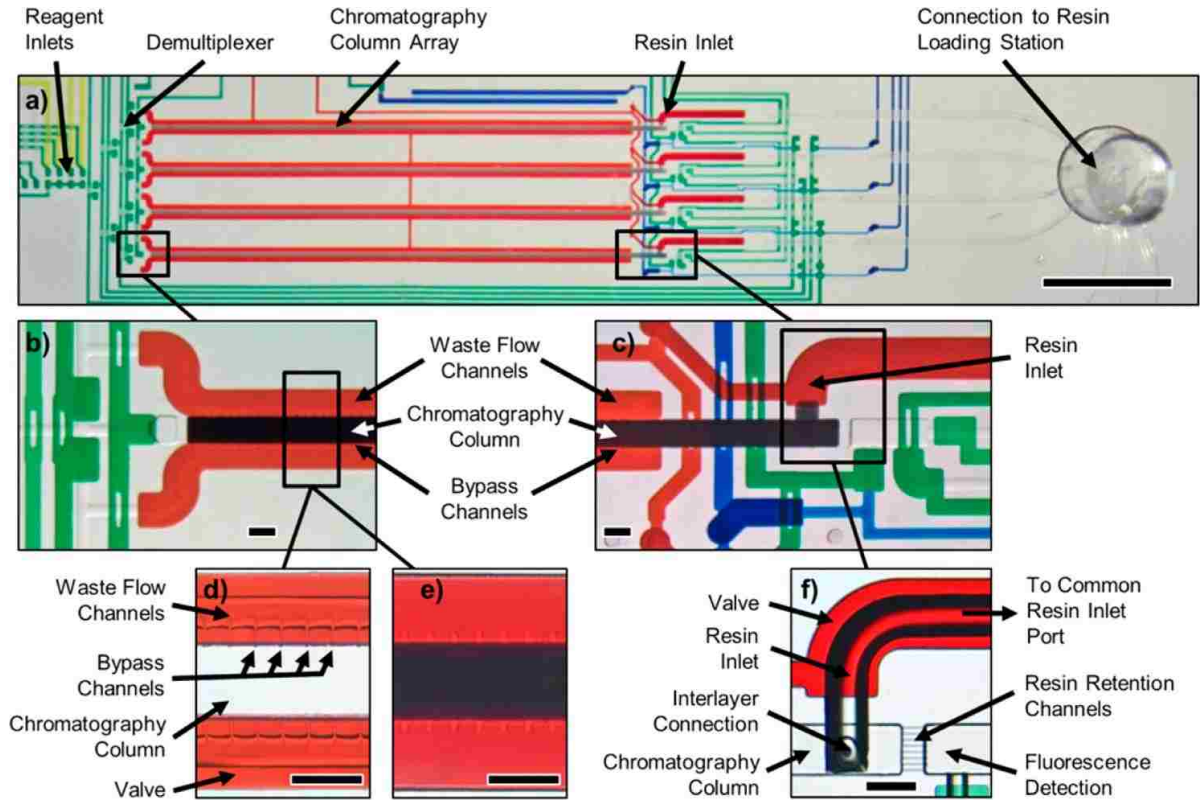

Figure 1.11 Micrographs of solid-phase chromatography columns fabricated in PDMS. (a) before packing of the columns, (b) front of one column after packing, (c) back of same column from *b* with resin inlet closed, (d) bypass channels along a section of unpacked column, (e) section in panel *d* after packing, (f) resin inlet from *c*. (Reproduced from Huft, J., Haynes, C. A., and Hansen, C. L. *Anal Chem* **2013**, *85*, 1797.[235] with permission, Copyright 2013, American Chemical Society).

Gottschlich[236] and Liu[237] both reported lab-on-chip techniques for separating and detecting protein mixtures. Gottschlich and co-workers integrated a microreactor, injector and electrophoretic separator and a second reactor for derivatization on a monolithic substrate followed by fluorescence detection. Liu integrated capillary electrophoresis, postcolumn labeling and fluorescence detection on a microfabricated system. Wang and *et al*.[239] described

a microfluidic device that integrated an electrospray ionization source for MS with a protein digestion bed, a capillary electrophoresis channel, and an injector on a monolithic substrate. The protein digestion bed had trypsin immobilized onto microbeads to permit faster digestion and to eliminate autodigestion products that might hinder sample characterization.

1.5.2.1 Digital Microfluidics for Proteomic Analysis

Microfluidic devices that can handle droplets can also perform a variety of functions (*i.e.* sorting, storage, and splitting) and can be integrated to MS or CE instrumentation.[240,241] Digital microfluidics (DMF) is characterized by the manipulation of discrete droplets on hydrophobic, insulated electrode arrays that have no channels. When successive potentials are applied to the electrodes, droplet manipulations such as merging, mixing, splitting, and dispensing from reservoirs are facilitated.[242] Because droplets are individually addressable and have individual boundaries, they can act as discrete microreactors. A DMF method was developed for the extraction and purification of protein from a complex biological sample by precipitation, rinsing, and resolubilization, with protein recoveries of roughly 80%.[243] Applications involving MS can also be used with DMF, which has increased its popularity in recent years. In-line coupling with DMF is a likely fit because both techniques require liquid samples and compatible volumes. Jebrail and co-workers reported the first in-line interface for DMF and nanoESI-MS.[244] The device consisted of a DMF platform and a microchannel nanoESI emitter that was used for the quantification of amino acids from samples of dried blood spots.

Another way to integrate (in-line) DMF and MS is to use a specialized ionization technique. Surface acoustic wave nebulization (SAWN) exploits the acceleration of acoustic waves that have propagated on the surface of a piezoelectric substrate and produces an aerosol

that contains solvated ions from a liquid droplet on the surface.[245] Dennison *et al*. coupled SAWN to MS for top-down protein fragmentation studies.[246] Luk and Wheeler reported an integrated DMF device (see Figure 1.12) for multistep proteomic processing.[247]

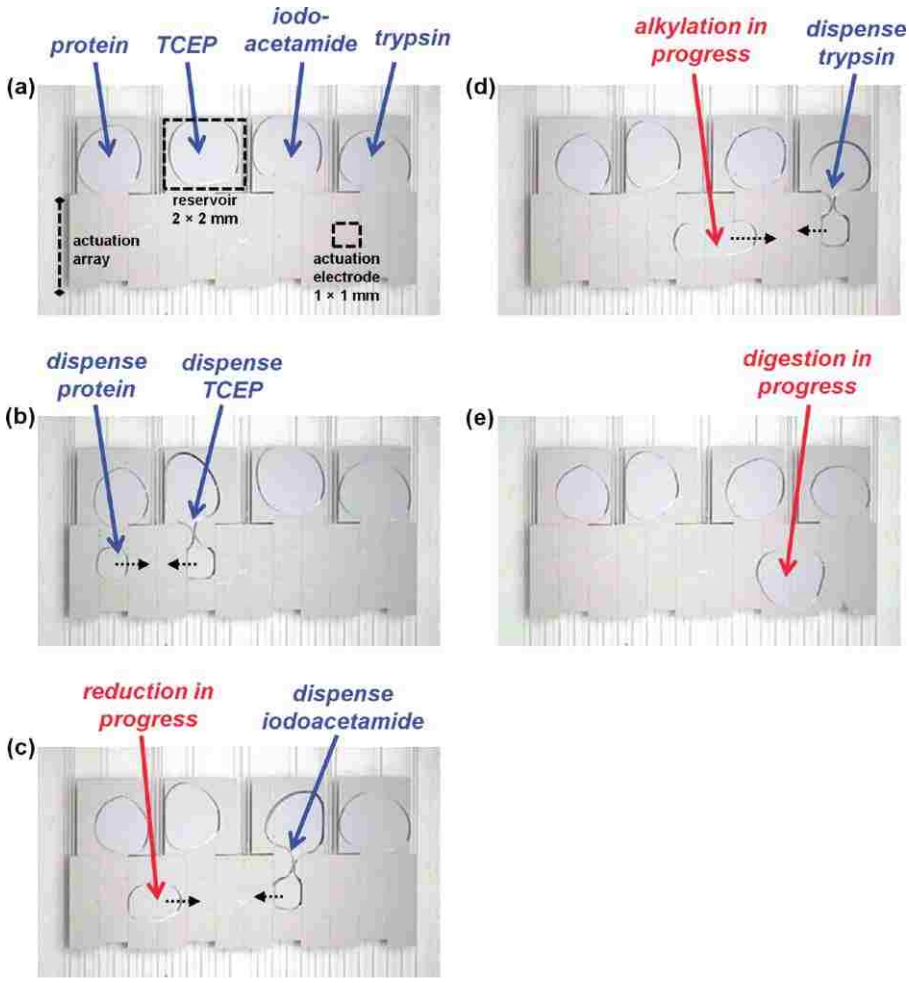

Figure 1.12 A sequence of images depicting the proteomic sample workup of the protein sample going through reduction, alkylation, and digestion on the DMF device. (a,b) Droplets containing insulin and TCEP merged are dispensed from reservoirs, merged and mixed. (c) A droplet of iodoacetamide being dispensed and merged with the sample droplet and mixed. After incubation (d) the sample droplet is merged with a droplet of trypsin for digestion and (e) final incubation. (Reproduced from Luk, V. N. and Wheeler, A. R. *Anal Chem* **2009**, *15*, 4524.[247] with permission, Copyright 2013, American Chemical Society).

The device performed sample reduction, alkylation, and enzymatic digestion on a single platform and interfaced with MALDI-MS to qualitatively confirm the protein products from the reaction steps. This device is an excellent example of integrating multiple processing

steps in proteomics on a single platform for analysis. Luk and Wheeler have also used DMF to fabricate hydrogel microreactors for proteolytic digestion (see Figure 1.13).[248]

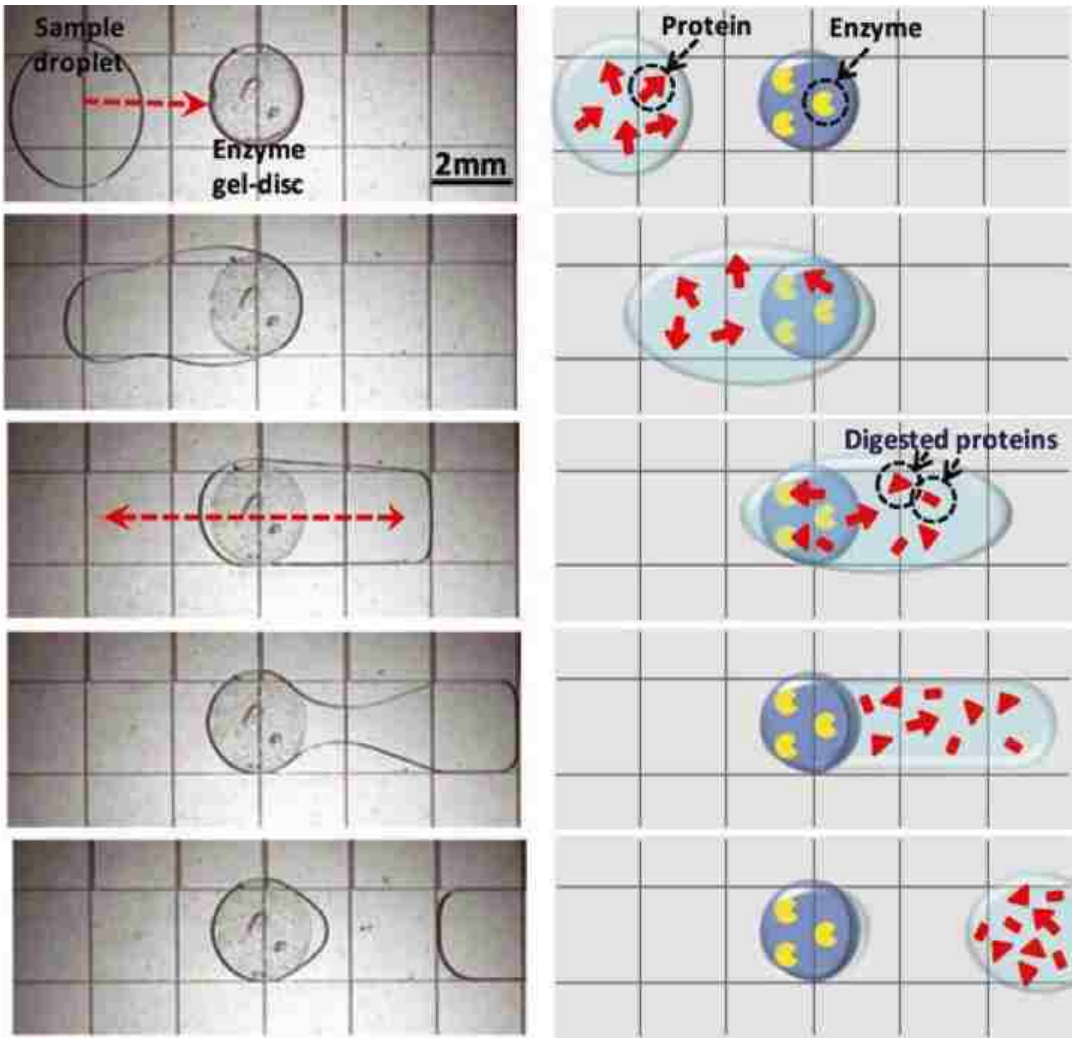

Figure 1.13 Series of images from a movie and a schematic displaying the hydrogel proteolytic enzymes microreactors performing digestion in a 2-mm-diameter gel disc on a DMF device. (Reproduced and adapted from Luk, V. N.; Fiddes, L. K.; Luk, V. M.; Kumacheva, E.; Wheeler, A. R. Digital Microfluidic Hydrogel Microreactors for proteomics. *Proteomics* **2012**, *12*, 1310.[248] with permission, Copyright 2013, American Chemical Society).

The authors employed cylindrical agarose discs with immobilized trypsin or pepsin and integrated them into DMF devices. The 1 mg/mL BSA or lysozyme protein samples were sequentially reduced, alkylated, and digested with all sample and reagent handling controlled

by droplet operation. The MALDI-MS analysis of the products showed that by performing digestion in this manner, they were able to obtain higher sequence coverage.

Digital microfluidics is not a cure-all for all MS applications, and there are still some challenges and limitations that need to be addressed before DMF becomes a widespread technique. Biofouling, which is a negative side effect of using high surface-to-volume ratios due to the increased rate of adsorption of analytes from solution to the solid surface, is problematic for DMF and can lead to cross-contamination. However, the drawbacks of biofouling have lead to significant improvements such as the use of oils to encapsulate droplets,[249,250] the use of nanostructured super-hydrophobic surfaces or amphiphilic additives to limit adsorption,[251,252] and films that are removable to prevent cross-contamination between steps. In spite of these challenges, DMF is still an emerging powerful tool for upstream sample processing in proteomic analysis. The 'hands-off' approach augments the ability to fully automate sample processing steps and analysis on a single platform, which makes DMF extremely attractive.

1.6 More Efforts Toward On-chip Proteomic Processing

The uses of spotted array-based tools have also garnered attention for proteomic analysis.[253] In array-based methods, small spots of proteins are immobilized onto silicon-based substrates (usually glass). The array can then be used to screen complex protein mixtures for particular binding affinities or other interactions. These arrays potentially address several concerns associated with the 2DE-MS (IEF/SDS-PAGE): the arrays can be used at little cost, provide consistently reliable and rapid results and are simple to use. Haab and colleagues[254] utilized printed protein arrays to measure protein–protein interactions based on a fluorescence assay. Spotted arrays can also be used to probe protein–small molecule

interactions. Immobilized proteins are patterned onto a microscope slide using high-precision contact printing to deliver small quantities of protein to an aldehyde-coated glass surface.[255] Using this system, spot densities of >1600 spots cm^{-2} can be achieved with spot diameters of 150–200 μm. This technology has been applied to the identification of protein kinase substrates and for screening protein–protein interactions.

Surface-enhanced affinity capture, a promising version of surface-enhanced laser and ionization (SELDI) technology,[256] uses probe surfaces to extract or structurally modify a particular protein. After the addition of a matrix solution to enhance laser energy transfer and sample ionization, samples are analyzed using TOF-MS. Advantages of this approach include a reduced amount of sample preparation before MS and the ability to capture trace amounts of proteins directly from biological fluids.

Although these devices hold tremendous promise to address some of the limitations facing approaches for proteome analysis, they too have their own limits (*i.e.* fabrication, material compatibility, *etc.*). Much of the work mentioned here thus far deals with the analysis of known protein mixtures or peptides and not complex biological samples that contain membrane proteins.

1.7 Concluding Remarks

It should be noted that the majority of the aforementioned microfluidic systems analyzed peptides, model proteins, nucleic acids, or purified protein samples. Therefore, there is still a need for a proteomic platform that can analyze complex biological samples such as those containing integral membrane proteins or whole cell lysates. As previously stated, membrane proteins offer an abundance of possibilities for biomarker discovery, drug development, and treatment of various diseases such as cancer.

The need to understand the biological mechanisms involved in cancer and infectious and inflammatory diseases at the clinical levels implies not only comprehensive protein identification but also expression profiling of proteins across healthy and disease patient samples. In this context, the challenge of proteomics lies in the complexity of protein mixtures, the number of samples, and the reproducibility of analysis. Kotz and co-workers[257] developed a microfluidic device to isolate neutrophils directly from whole blood in order to process proteins for proteomic (mass spectrometry) studies (see Figure 1.14).

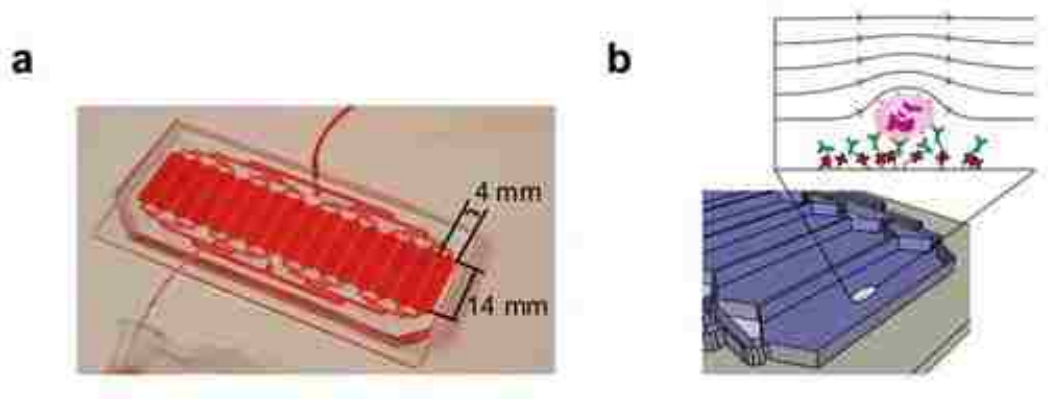

Figure 1.14 Microfluidic device used for clinical genomic and proteomic studies. (a) microfluidic chip design and (b) schematic of the surface functionalization of antibodies to the device. (Reprinted and adapted from Kotz, K. T.; Xiao, W.; Miller-Graziano, C.; Qian, W. J.; Russom, A.; Warner, E. A.; Moldawer, L. L.; De, A.; Bankey, P. E.; Petritis, B. O.; Camp, D. G., 2nd; Rosenbach, A. E.; Goverman, J.; Fagan, S. P.; Brownstein, B. H.; Irimia, D.; Xu, W.; Wilhelmy, J.; Mindrinos, M. N.; Smith, R. D.; Davis, R. W.; Tompkins, R. G.; Toner, M. *Nat Med* **2010**, *16*, 1042.[257] with permission, Copyright 2013).

The authors demonstrated the scalability of the device as well as its application in a clinical setting. The microfluidic device was able to capture highly enriched (>95%) neutrophils directly from whole blood in ~5 min and in sufficient quantity and purity for mass spectrometry-based proteomic analysis. The proteomic samples were of high enough quality to discriminate between small differences in neutrophil activation states. Furthermore, the authors implemented the utility of the device in a clinical program and observed the changes in gene expression of neutrophils that are highly regulated after traumatic injury.

To date, there is still a need for a microfluidic system that can perform a complete proteomic analysis of a complex protein sample, especially those containing membrane proteins. When considering an integrated system such as those listed in the sections above, it is very important that the processes there within are compatible one another. It is critical that each step can operate independently, but there also cannot be interference between steps. For example, reagents used for extracting or isolating proteins in a sample must be compatible with subsequent separation and mass analysis steps. In addition, when investigating the use of a microfluidic system, it may be beneficial to take a step-by-step approach to ensure that the downstream processes are not negatively affected by those upstream. Improvements still need to be made in the area of protein enrichment and purification, which is a critical aspect of the work because as much material as possible is needed for the separation and the further downstream processes of protein digestion and subsequent peptide mass analysis since there is no procedure in place to amplify protein such as PCR for DNA. Much of the work mentioned previously involves off-chip protein enrichment strategies, which could result in loss of sample when moving on to subsequent analysis (*i.e.* separation, MS analysis, *etc.*).

1.8 Research Objective

The objective of this work was to design, fabricate, and characterize the operation of a fully integrated fluidic system that will serve as a foundation for a novel method to analyze proteins from complex biological samples based upon a top-down proteomic strategy. However, before integration is done, we must optimize each entity separately. Because enrichment is so critical in the case of low abundant proteins (*i.e.* integral membrane proteins), a module for the enrichment and purification of integral membrane proteins will be fabricated and will employ affinity techniques and microposts to extract membrane proteins

from whole cell lysate. This platform will be particularly useful for extracting only integral membrane proteins of interest through the use of a bioaffinity reactor based on the avidin-biotin interaction. The use of this platform is two-fold as it will extract the integral membrane proteins and also purify the membrane protein fraction by excluding cytosolic proteins and nucleic acid material.

The next step is the 2-dimensional CE separation of intact integral membrane proteins with μ-capillary gel electrophoresis (μ-CGE) in the first dimension coupled with micellar electrokinetic chromatography (MEKC) in the second dimension. This module is based upon previous work performed in our group.[258,259] The separation in the first dimension will be based on the molecular weights of the individual proteins and the second dimension will separate the proteins based upon their hydrophobicity and interaction with SDS micelles. We are taking a top-down approach because we want to separate the proteins intact and then do further analysis with MS. The two modules will be integrated, a module for digestion added, and coupled with MS based upon work previously done by Musyimi and Lee.[228,260] Once completed, the fluidic system will offer researchers a fully integrated microfluidic platform for the complete analysis of integral membrane proteins from complex biological samples. A system of this nature will afford future opportunities for biomarker discovery, drug development, and diagnostics.

1.9 References

(1) de Hoog, C. L.; Mann, M. *Annual review of genomics and human genetics* **2004**, *5*, 267.

(2) Wilkins, M. R.; Pasquali, C.; Appel, R. D.; Ou, K.; Golaz, O.; Sanchez, J. C.; Yan, J. X.; Gooley, A. A.; Hughes, G.; Humphery-Smith, I.; Williams, K. L.; Hochstrasser, D. F. *Biotechnology (N Y)* **1996**, *14*, 61.

(3) Schramm, A.; Apostolov, O.; Sitek, B.; Pfeiffer, K.; Stuhler, K.; Meyer, H. E.; Havers, W.; Eggert, A. *Klinische Padiatrie* **2003**, *215*, 293.

(4) Kussmann, M.; Affolter, M.; Fay, L. B. *Combinatorial chemistry & high throughput screening* **2005**, *8*, 679.

(5) Srinivas, P. R.; Verma, M.; Zhao, Y.; Srivastava, S. *Clinical chemistry* **2002**, *48*, 1160.

(6) Hanash, S. M.; Pitteri, S. J.; Faca, V. M. *Nature* **2008**, *452*, 571.

(7) Santoni, V., Malloy, M. and Rabilloud, T. *Electrophoresis* **2000**, *21*, 1054.

(8) Santoni, V.; Kieffer, S.; Desclaux, D.; Masson, F.; Rabilloud, T. *Electrophoresis* **2000**, *21*, 3329.

(9) Garrels, J. I. *The Journal of biological chemistry* **1989**, *264*, 5269.

(10) Garrels, J. I.; Franza, B. R., Jr. *The Journal of biological chemistry* **1989**, *264*, 5283.

(11) Garrels, J. I.; Franza, B. R., Jr. *The Journal of biological chemistry* **1989**, *264*, 5299.

(12) Fountoulakis, M.; Takacs, M. F.; Berndt, P.; Langen, H.; Takacs, B. *Electrophoresis* **1999**, *20*, 2181.

(13) Fountoulakis, M.; Takacs, M. F.; Takacs, B. *Journal of chromatography. A* **1999**, *833*, 157.

(14) Gygi, S. P., Rist, B., Gerber, S.A., Turecek, F., Gelb, M.H. and Aebersold, R. *Nature Biotechnology* **1999**, *17*, 994.

(15) Corthals, G. L.; Wasinger, V. C.; Hochstrasser, D. F.; Sanchez, J. C. *Electrophoresis* **2000**, *21*, 1104.

(16) Oh-Ishi, M.; Satoh, M.; Maeda, T. *Electrophoresis* **2000**, *21*, 1653.

(17) Ferro, M.; Salvi, D.; Riviere-Rolland, H.; Vermat, T.; Seigneurin-Berny, D.; Grunwald, D.; Garin, J.; Joyard, J.; Rolland, N. *Proc Natl Acad Sci U S A* **2002**, *99*, 11487.

(18) Galeva, N.; Altermann, M. *Proteomics* **2002**, *2*, 713.

(19) Sintegral membrane proteinson, R. J.; Connolly, L. M.; Eddes, J. S.; Pereira, J. J.; Moritz, R. L.; Reid, G. E. *Electrophoresis* **2000**, *21*, 1707.

(20) Link, A. J.; Eng, J.; Schieltz, D. M.; Carmack, E.; Mize, G. J.; Morris, D. R.; Garvik, B. M.; Yates, J. R., 3rd *Nat Biotechnol* **1999**, *17*, 676.

(21) Washburn, M. P.; Wolters, D.; Yates, J. R., 3rd *Nat Biotechnol* **2001**, *19*, 242.

(22) Wolters, D. A.; Washburn, M. P.; Yates, J. R., 3rd *Anal Chem* **2001**, *73*, 5683.

(23) Rose, K.; Bougueleret, L.; Baussant, T.; Bohm, G.; Botti, P.; Colinge, J.; Cusin, I.; Gaertner, H.; Gleizes, A.; Heller, M.; Jimenez, S.; Johnson, A.; Kussmann, M.; Menin, L.; Menzel, C.; Ranno, F.; Rodriguez-Tome, P.; Rogers, J.; Saudrais, C.; Villain, M.; Wetmore, D.; Bairoch, A.; Hochstrasser, D. *Proteomics* **2004**, *4*, 2125.

(24) Lander, E. S. *et a*l. *Nature* **2001**, *409*, 860.

(25) Venter, J. C. *et al*. *Science* **2001**, *291*, 1304.

(26) Lion, N.; Rohner, T. C.; Dayon, L.; Arnaud, I. L.; Damoc, E.; Youhnovski, N.; Wu, Z. Y.; Roussel, C.; Josserand, J.; Jensen, H.; Rossier, J. S.; Przybylski, M.; Girault, H. H. *Electrophoresis* **2003**, *24*, 3533.

(27) Seddon, A. M.; Curnow, P.; Booth, P. J. *Biochimica et biophysica acta* **2004**, *1666*, 105.

(28) Morre, D. In *Molecular Techniques and Approaches in Developmental Biology*; Chrispeels, M. J., Ed.; John Wiley: New York, NY, 1973, p 1.

(29) Morre, D. J.; Morre, D. M. *BioTechniques* **1989**, *7*, 946.

(30) Lenstra, J. A.; Bloemendal, H. *European journal of biochemistry / FEBS* **1983**, *135*, 413.

(31) Anderson, N. L.; Anderson, N. G. *Molecular & cellular proteomics : MCP* **2002**, *1*, 845.

(32) Collins, F. S.; Lander, E. S.; Rogers, J.; Waterston, R. H.; Int Human Genome Sequencing, C. *Nature* **2004**, *431*, 931.

(33) Froehlich, T.; Arnold, G. J. *Journal of Neural Transmission* **2006**, *113*.

(34) Lay, J. O.; Borgmann, S.; Liyanage, R.; Wilkins, C. L. *Trac-Trends Anal. Chem.* **2006**, *25*, 1046.

(35) Ahmed, N.; Rice, G. E. *Journal of chromatography. B, Analytical technologies in the biomedical and life sciences* **2005**, *815*, 39.

(36) Wang, H.; Hanash, S. *Journal of chromatography. B, Analytical technologies in the biomedical and life sciences* **2003**, *787*, 11.

(37) Tang, J.; Gao, M.; Deng, C.; Zhang, X. *Journal of chromatography. B, Analytical technologies in the biomedical and life sciences* **2008**, *866*, 123.

(38) Issaq, H. J.; Chan, K. C.; Janini, G. M.; Conrads, T. P.; Veenstra, T. D. *Journal of chromatography. B, Analytical technologies in the biomedical and life sciences* **2005**, *817*, 35.

(39) Shi, Y.; Xiang, R.; Horvath, C.; Wilkins, J. A. *Journal of chromatography. A* **2004**, *1053*, 27.

(40) Fujii, K.; Nakano, T.; Hike, H.; Usui, F.; Bando, Y.; Tojo, H.; Nishimura, T. *Journal of chromatography. A* **2004**, *1057*, 107.

(41) Vitali, B.; Wasinger, V.; Brigidi, P.; Guilhaus, M. *Proteomics* **2005**, *5*, 1859.

(42) Coombes, K. R.; Morris, J. S.; Hu, J.; Edmonson, S. R.; Baggerly, K. A. *Nat Biotechnol* **2005**, *23*, 291.

(43) Ransohoff, D. F. *Nature reviews. Cancer* **2005**, *5*, 142.

(44) Aebersold, R.; Mann, M. *Nature* **2003**, *422*, 198.

(45) Stevens, T. J.; Arkin, I. T. *Proteins* **2000**, *39*, 417.

(46) Wu, C. C. a. Y., J.R. *Nature Biotechnology* **2003**, *21*, 262.

(47) Domon, B.; Aebersold, R. *Science* **2006**, *312*, 212.

(48) Geer, L. Y.; Markey, S. P.; Kowalak, J. A.; Wagner, L.; Xu, M.; Maynard, D. M.; Yang, X.; Shi, W.; Bryant, S. H. *Journal of proteome research* **2004**, *3*, 958.

(49) Sadygov, R. G.; Yates, J. R., 3rd *Anal Chem* **2003**, *75*, 3792.

(50) Fenyo, D.; Beavis, R. C. *Anal Chem* **2003**, *75*, 768.

(51) Yates, J. R., 3rd; Morgan, S. F.; Gatlin, C. L.; Griffin, P. R.; Eng, J. K. *Anal Chem* **1998**, *70*, 3557.

(52) Craig, R.; Cortens, J. C.; Fenyo, D.; Beavis, R. C. *Journal of proteome research* **2006**, *5*, 1843.

(53) Frewen, B. E.; Merrihew, G. E.; Wu, C. C.; Noble, W. S.; MacCoss, M. J. *Anal Chem* **2006**, *78*, 5678.

(54) Stein, S. E.; Scott, D. R. *J. Am. Soc. Mass Spectrom.* **1994**, *5*, 859.

(55) Mann, M.; Wilm, M. *Anal Chem* **1994**, *66*, 4390.

(56) Tabb, D. L.; Saraf, A.; Yates, J. R., 3rd *Anal Chem* **2003**, *75*, 6415.

(57) Tanner, S.; Shu, H.; Frank, A.; Wang, L. C.; Zandi, E.; Mumby, M.; Pevzner, P. A.; Bafna, V. *Anal Chem* **2005**, *77*, 4626.

(58) Meng, F.; Forbes, A. J.; Miller, L. M.; Kelleher, N. L. *Mass spectrometry reviews* **2005**, *24*, 126.

(59) Han, X.; Jin, M.; Breuker, K.; McLafferty, F. W. *Science* **2006**, *314*, 109.

(60) Chait, B. T. *Science* **2006**, *314*, 65.

(61) Kuster, B.; Schirle, M.; Mallick, P.; Aebersold, R. *Nature reviews. Molecular cell biology* **2005**, *6*, 577.

(62) Mallick, P.; Schirle, M.; Chen, S. S.; Flory, M. R.; Lee, H.; Martin, D.; Ranish, J.; Raught, B.; Schmitt, R.; Werner, T.; Kuster, B.; Aebersold, R. *Nat Biotechnol* **2007**, *25*, 125.

(63) Huber Lukas, A., Pfaller, K. and Vietor, I. *Circulation Research* **2003**, *92*, 962.

(64) Josic, D. a. C., J.G. *Proteomics* **2007**, *7*, 3010.

(65) Yan, W.; Aebersold, R.; Raines, E. W. *Journal of Proteomics* **2009**, *72*, 4.

(66) Cordwell, S. J.; Thingholm, T. E. *Proteomics* **2010**, *10*, 611.

(67) Lodish, H. *Molecular Cell Biology*; 5th ed., 2003.

(68) Kikuchi, M., Hatano, N., Yokota, S., Shimozawa, N., Imanaka, T. and Taniguchi, H. *Journal of Biological Chemistry* **2004**, *279*, 421.

(69) Vuong, G. L., Weiss, S.M., Kammer, W., Priemer, M., Vingron, M., Nordheim, A. and Cahill, M.A. *Electrophoresis* **2000**, *21*, 2594.

(70) Chen, W. N.; Yu, L. R.; Strittmatter, E. F.; Thrall, B. D.; Camp, D. G., 2nd; Smith, R. D. *Proteomics* **2003**, *3*, 1647.

(71) Jang, J. H.; Hanash, S. *Proteomics* **2003**, *3*, 1947.

(72) Sabarth, N.; Lamer, S.; Zimny-Arndt, U.; Jungblut, P. R.; Meyer, T. F.; Bumann, D. *The Journal of biological chemistry* **2002**, *277*, 27896.

(73) Shin, B. K.; Wang, H.; Yim, A. M.; Le Naour, F.; Brichory, F.; Jang, J. H.; Zhao, R.; Puravs, E.; Tra, J.; Michael, C. W.; Misek, D. E.; Hanash, S. M. *The Journal of biological chemistry* **2003**, *278*, 7607.

(74) Tang, X.; Yi, W.; Munske, G. R.; Adhikari, D. P.; Zakharova, N. L.; Bruce, J. E. *Journal of proteome research* **2007**, *6*, 724.

(75) Zhang, W.; Zhou, G.; Zhao, Y.; White, M. A.; Zhao, Y. *Electrophoresis* **2003**, *24*, 2855.

(76) Zhao, Y.; Zhang, W.; Kho, Y.; Zhao, Y. *Anal Chem* **2004**, *76*, 1817.

(77) Josic, D.; Clifton, J. G.; Kovac, S.; Hixson, D. C. *Current opinion in molecular therapeutics* **2008**, *10*, 116.

(78) Polanski, M., Anderson, M. D. *Biomarker Insights* **2006**, *2*, 1.

(79) Josic, D.; Clifton, J. G. *Proteomics* **2007**, *7*, 3010.

(80) Bouzianas, D. G. *Expert Rev Anti-Infe* **2007**, *5*, 665.

(81) Viswanathan, K. a. F., K. *Expert Review of Proteomics* **2007**, *4*, 815.

(82) Wahl, A., Weidanz, J., Hildeband, W. *Expert Review of Proteomics* **2006**, *3*, 641.

(83) Mellgren, R. L.; Zhang, W. L.; Miyake, K.; McNeil, P. L. *Journal of Biological Chemistry* **2007**, *282*, 2567.

(84) Balestrieri, M. L.; Giovane, A.; Mancini, F. P.; Napoli, C. *Current medicinal chemistry* **2008**, *15*, 555.

(85) Lewczuk, P.; Wiltfang, J. *Proteomics* **2008**, *8*, 1292.

(86) Bermudez-Crespo, J.; Lopez, J. L. *Proteomics. Clinical applications* **2007**, *1*, 983.

(87) Rucevic, M.; Hixson, D.; Josic, D. *Electrophoresis* **2011**, *32*, 1549.

(88) Lai, Z. W.; Steer, D. L.; Smith, A. I. *Current opinion in molecular therapeutics* **2009**, *11*, 623.

(89) Landry, Y.; Gies, J. P. *Fund Clin Pharmacol* **2008**, *22*, 1.

(90) Griffin, N. M.; Schnitzer, J. E. *Molecular & cellular proteomics : MCP* **2011**, *10*, R110 000935.

(91) Blonder, J.; Chan, K. C.; Issaq, H. J.; Veenstra, T. D. *Nat Protoc* **2006**, *1*, 2784.

(92) He, J.; Liu, Y.; He, S.; Wang, Q.; Pu, H.; Tong, Y.; Ji, J. *Proteomics. Clinical applications* **2007**, *1*, 231.

(93) Gutstein, H. B.; Morris, J. S.; Annangudi, S. P.; Sweedler, J. V. *Mass spectrometry reviews* **2008**, *27*, 316.

(94) Robinson, J. M.; Ackerman, W. E. t.; Tewari, A. K.; Kniss, D. A.; Vandre, D. D. *Analytical biochemistry* **2009**, *387*, 87.

(95) Bordier, C. *The Journal of biological chemistry* **1981**, *256*, 1604.

(96) Taylor, R. S.; Wu, C. C.; Hays, L. G.; Eng, J. K.; Yates, J. R., 3rd; Howell, K. E. *Electrophoresis* **2000**, *21*, 3441.

(97) Stasyk, T.; Huber, L. A. *Proteomics* **2004**, *4*, 3704.

(98) Gloriam, D. E.; Foord, S. M.; Blaney, F. E.; Garland, S. L. *Journal of medicinal chemistry* **2009**, *52*, 4429.

(99) Lindberg, S.; Banas, A.; Stymne, S. *Plant physiology and biochemistry : PPB / Societe francaise de physiologie vegetale* **2005**, *43*, 261.

(100) Josic, D.; Brown, M. K.; Huang, F.; Callanan, H.; Rucevic, M.; Nicoletti, A.; Clifton, J.; Hixson, D. C. *Electrophoresis* **2005**, *26*, 2809.

(101) Lawson, E. L.; Clifton, J. G.; Huang, F.; Li, X.; Hixson, D. C.; Josic, D. *Electrophoresis* **2006**, *27*, 2747.

(102) Righetti, P. G.; Castagna, A.; Antonioli, P.; Boschetti, E. *Electrophoresis* **2005**, *26*, 297.

(103) Shin, J. H.; Krapfenbauer, K.; Lubec, G. *Electrophoresis* **2006**, *27*, 2799.

(104) Roy, I.; Mondal, K.; Gupta, M. N. *Journal of chromatography. B, Analytical technologies in the biomedical and life sciences* **2007**, *849*, 32.

(105) Cao, R.; Li, X.; Liu, Z.; Peng, X.; Hu, W.; Wang, X.; Chen, P.; Xie, J.; Liang, S. *Journal of proteome research* **2006**, *5*, 634.

(106) Srivastava, R.; Pisareva, T.; Norling, B. *Proteomics* **2005**, *5*, 4905.

(107) Schindler, J.; Lewandrowski, U.; Sickmann, A.; Friauf, E.; Nothwang, H. G. *Molecular & cellular proteomics : MCP* **2006**, *5*, 390.

(108) Adam, P. J.; Boyd, R.; Tyson, K. L.; Fletcher, G. C.; Stamps, A.; Hudson, L.; Poyser, H. R.; Redpath, N.; Griffiths, M.; Steers, G.; Harris, A. L.; Patel, S.; Berry, J.; Loader, J. A.; Townsend, R. R.; Daviet, L.; Legrain, P.; Parekh, R.; Terrett, J. A. *The Journal of biological chemistry* **2003**, *278*, 6482.

(109) Blonder, J.; Terunuma, A.; Conrads, T. P.; Chan, K. C.; Yee, C.; Lucas, D. A.; Schaefer, C. F.; Yu, L. R.; Issaq, H. J.; Veenstra, T. D.; Vogel, J. C. *The Journal of investigative dermatology* **2004**, *123*, 691.

(110) Foster, L. J.; Zeemann, P. A.; Li, C.; Mann, M.; Jensen, O. N.; Kassem, M. *Stem Cells* **2005**, *23*, 1367.

(111) Navarre, C.; Degand, H.; Bennett, K. L.; Crawford, J. S.; Mortz, E.; Boutry, M. *Proteomics* **2002**, *2*, 1706.

(112) Zhang, L.; Xie, J.; Wang, X.; Liu, X.; Tang, X.; Cao, R.; Hu, W.; Nie, S.; Fan, C.; Liang, S. *Proteomics* **2005**, *5*, 4510.

(113) Fujiki, Y.; Hubbard, A. L.; Fowler, S.; Lazarow, P. B. *The Journal of cell biology* **1982**, *93*, 97.

(114) Chang, P. S.; Absood, A.; Linderman, J. J.; Omann, G. M. *Analytical biochemistry* **2004**, *325*, 175.

(115) Elortza, F.; Nuhse, T. S.; Foster, L. J.; Stensballe, A.; Peck, S. C.; Jensen, O. N. *Molecular & cellular proteomics : MCP* **2003**, *2*, 1261.

(116) Thingholm, T. E.; Larsen, M. R.; Ingrell, C. R.; Kassem, M.; Jensen, O. N. *Journal of proteome research* **2008**, *7*, 3304.

(117) Weerasekera, R.; She, Y. M.; Markham, K. A.; Bai, Y.; Opalka, N.; Orlicky, S.; Sicheri, F.; Kislinger, T.; Schmitt-Ulms, G. *Proteomics* **2007**, *7*, 3835.

(118) Freed, J. K.; Smith, J. R.; Li, P.; Greene, A. S. *Proteomics* **2007**, *7*, 2371.

(119) Gubbens, J.; Ruijter, E.; de Fays, L. E.; Damen, J. M.; de Kruijff, B.; Slijper, M.; Rijkers, D. T.; Liskamp, R. M.; de Kroon, A. I. *Chemistry & biology* **2009**, *16*, 3.

(120) Solis, N.; Larsen, M. R.; Cordwell, S. J. *Proteomics* **2010**, *10*, 2037.

(121) Tjalsma, H.; Lambooy, L.; Hermans, P. W.; Swinkels, D. W. *Proteomics* **2008**, *8*, 1415.

(122) Rodriguez-Ortega, M. J.; Norais, N.; Bensi, G.; Liberatori, S.; Capo, S.; Mora, M.; Scarselli, M.; Doro, F.; Ferrari, G.; Garaguso, I.; Maggi, T.; Neumann, A.; Covre, A.; Telford, J. L.; Grandi, G. *Nat Biotechnol* **2006**, *24*, 191.

(123) Speers, A. E.; Blackler, A. R.; Wu, C. C. *Anal Chem* **2007**, *79*, 4613.

(124) Elortza, F.; Mohammed, S.; Bunkenborg, J.; Foster, L. J.; Nuhse, T. S.; Brodbeck, U.; Peck, S. C.; Jensen, O. N. *Journal of proteome research* **2006**, *5*, 935.

(125) Mutch, S. A.; Kensel-Hammes, P.; Gadd, J. C.; Fujimoto, B. S.; Allen, R. W.; Schiro, P. G.; Lorenz, R. M.; Kuyper, C. L.; Kuo, J. S.; Bajjalieh, S. M. *et al*. *Journal of Neuroscience* **2010**, *31*, 1461.

(126) Mutch, S. A.; Kensel-Hammes, P.; Gadd, J. C.; Fujimoto, B. S.; Schiro, P. G; Bajjalieh, S. M.; Chium D. T. *Nature Protocols* **2001**, *6*, 1953.

(127) Gauthier, D. J. and Lazure, C. *Expert Reviews in Proteomics* **2008**, *5*, 603.

(128) Gauthier, D. J.; Sobota, J. A.; Ferraro, F.; Mains, R. E.; Lazure, C. *Proteomics* **2008**, *8*, 3848.

(129) Brunner, Y.; Coute, Y.; Iezzi, M.; Foti, M.; Fukuda, M.; Hochstrasser, D. F.; Wollheim, C. B. *Mol Cell Proteomics* **2007**, *6*, 1007.

(130) Meikle, P. J.; Ng, K. F.; Johnson, E.; Hoogenraad, N. J.; Stone, B. A. *The Journal of biological chemistry* **1991**, *266*, 22569.

(131) Van Hoof, D.; Dormeyer, W.; Braam, S. R.; Passier, R.; Monshouwer-Kloots, J.; Ward-van Oostwaard, D.; Heck, A. J.; Krijgsveld, J.; Mummery, C. L. *Journal of proteome research* **2010**, *9*, 1610.

(132) Zhang, L.; Wang, X.; Peng, X.; Wei, Y.; Cao, R.; Liu, Z.; Xiong, J.; Ying, X.; Chen, P.; Liang, S. *Journal of proteome research* **2007**, *6*, 34.

(133) Watarai, H.; Hinohara, A.; Nagafune, J.; Nakayama, T.; Taniguchi, M.; Yamaguchi, Y. *Proteomics* **2005**, *5*, 4001.

(134) Chevallet, M.; Santoni, V.; Poinas, A.; Rouquie, D.; Fuchs, A.; Kieffer, S.; Rossignol, M.; Lunardi, J.; Garin, J.; Rabilloud, T. *Electrophoresis* **1998**, *19*, 1901.

(135) Babu, G. J.; Wheeler, D.; Alzate, O.; Periasamy, M. *Analytical biochemistry* **2004**, *325*, 121.

(136) Santoni, V.; Rabilloud, T.; Doumas, P.; Rouquie, D.; Mansion, M.; Kieffer, S.; Garin, J.; Rossignol, M. *Electrophoresis* **1999**, *20*, 705.

(137) Esteve-Romero, J.; Simo-Alfonso, E.; Bossi, A.; Bresciani, F.; Righetti, P. G. *Electrophoresis* **1996**, *17*, 704.

(138) Rabilloud, T.; Adessi, C.; Giraudel, A.; Lunardi, J. *Electrophoresis* **1997**, *18*, 307.

(139) Molloy, M. P.; Herbert, B. R.; Walsh, B. J.; Tyler, M. I.; Traini, M.; Sanchez, J. C.; Hochstrasser, D. F.; Williams, K. L.; Gooley, A. A. *Electrophoresis* **1998**, *19*, 837.

(140) Rabilloud, T. *Electrophoresis* **1996**, *17*, 813.

(141) Musante, L.; Candiano, G.; Ghiggeri, G. M. *Journal of chromatography. B, Biomedical sciences and applications* **1998**, *705*, 351.

(142) Wang, S. B., Hu, Q., Sommerfeld, M., Chen, F. *Journal of Applied Phycology* **2003**, *15*, 485.

(143) Thingholm, T. E.; Larsen, M. R. *Methods Mol Biol* **2009**, *527*, 57.

(144) Thingholm, T. E.; Jorgensen, T. J.; Jensen, O. N.; Larsen, M. R. *Nat Protoc* **2006**, *1*, 1929.

(145) Nguyen, V.; Cao, L.; Lin, J. T.; Hung, N.; Ritz, A.; Yu, K.; Jianu, R.; Ulin, S. P.; Raphael, B. J.; Laidlaw, D. H.; Brossay, L.; Salomon, A. R. *Molecular & cellular proteomics : MCP* **2009**, *8*, 2418.

(146) Hoving, S.; Gerrits, B.; Voshol, H.; Muller, D.; Roberts, R. C.; van Oostrum, J. *Proteomics* **2002**, *2*, 127.

(147) Clifton, J. G.; Li, X.; Reutter, W.; Hixson, D. C.; Josic, D. *Journal of chromatography. B, Analytical technologies in the biomedical and life sciences* **2007**, *849*, 293.

(148) Josic, D.; Zeilinger, K. *Methods Enzymol* **1996**, *271*, 113.

(149) Lin, S. H.; Fain, J. N. *The Journal of biological chemistry* **1984**, *259*, 3016.

(150) Josic, D.; Clifton, J. G. *Proteomics* **2007**, *7*, 3010.

(151) Nouwens, A. S.; Cordwell, S. J.; Larsen, M. R.; Molloy, M. P.; Gillings, M.; Willcox, M. D.; Walsh, B. J. *Electrophoresis* **2000**, *21*, 3797.

(152) Clifton, J. G.; Brown, M. K.; Huang, F.; Li, X.; Reutter, W.; Hofmann, W.; Hixson, D. C.; Josic, D. *Journal of chromatography. A* **2006**, *1123*, 205.

(153) Blonder, J.; Goshe, M. B.; Moore, R. J.; Pasa-Tolic, L.; Masselon, C. D.; Lipton, M. S.; Smith, R. D. *Journal of proteome research* **2002**, *1*, 351.

(154) Rabilloud, T. *Electrophoresis* **1998**, *19*, 758.

(155) Anderson, N. G.; Anderson, N. L. *Analytical biochemistry* **1978**, *85*, 331.

(156) Anderson, N. L.; Anderson, N. G. *Electrophoresis* **1991**, *12*, 883.

(157) O'Farrell, P. H. *The Journal of biological chemistry* **1975**, *250*, 4007.

(158) McDonough, J.; Marban, E. *Proteomics* **2005**, *5*, 2892.

(159) Luche, S.; Santoni, V.; Rabilloud, T. *Proteomics* **2003**, *3*, 249.

(160) Olsson, I.; Larsson, K.; Palmgren, R.; Bjellqvist, B. *Proteomics* **2002**, *2*, 1630.

(161) Chick, J. M.; Haynes, P. A.; Bjellqvist, B.; Baker, M. S. *Journal of proteome research* **2008**, *7*, 4974.

(162) Li, R. X.; Zhou, H.; Li, S. J.; Sheng, Q. H.; Xia, Q. C.; Zeng, R. *Journal of proteome research* **2005**, *4*, 1256.

(163) Chick, J. M.; Haynes, P. A.; Molloy, M. P.; Bjellqvist, B.; Baker, M. S.; Len, A. C. *Journal of proteome research* **2008**, *7*, 1036.

(164) Hartwig, S.; Feckler, C.; Lehr, S.; Wallbrecht, K.; Wolgast, H.; Muller-Wieland, D.; Kotzka, J. *Proteomics* **2009**, *9*, 3209.

(165) Islinger, M.; Weber, G. *Methods Mol Biol* **2008**, *432*, 199.

(166) Xu, C.; Lin, X.; Ren, H.; Zhang, Y.; Wang, S.; Peng, X. *Proteomics* **2006**, *6*, 462.

(167) le Coutre, J.; Whitelegge, J. P.; Gross, A.; Turk, E.; Wright, E. M.; Kaback, H. R.; Faull, K. F. *Biochemistry* **2000**, *39*, 4237.

(168) Whitelegge, J. P.; Zhang, H.; Aguilera, R.; Taylor, R. M.; Cramer, W. A. *Molecular & cellular proteomics : MCP* **2002**, *1*, 816.

(169) Gomez, S. M.; Nishio, J. N.; Faull, K. F.; Whitelegge, J. P. *Molecular & cellular proteomics : MCP* **2002**, *1*, 46.

(170) Cadene, M.; Chait, B. T. *Anal Chem* **2000**, *72*, 5655.

(171) Ning, Z. B.; Li, Q. R.; Dai, J.; Li, R. X.; Shieh, C. H.; Zeng, R. *Journal of proteome research* **2008**, *7*, 4525.

(172) Machtejevas, E.; John, H.; Wagner, K.; Standker, L.; Marko-Varga, G.; Forssmann, W. G.; Bischoff, R.; Unger, K. K. *Journal of chromatography. B, Analytical technologies in the biomedical and life sciences* **2004**, *803*, 121.

(173) Peng, J.; Elias, J. E.; Thoreen, C. C.; Licklider, L. J.; Gygi, S. P. *Journal of proteome research* **2003**, *2*, 43.

(174) Santoni, V.; Molloy, M.; Rabilloud, T. *Electrophoresis* **2000**, *21*, 1054.

(175) Barnea, E.; Sorkin, R.; Ziv, T.; Beer, I.; Admon, A. *Proteomics* **2005**, *5*, 3367.

(176) Haynes, P. A.; Yates, J. R., 3rd *Yeast* **2000**, *17*, 81.

(177) Han, X.; Aslanian, A.; Yates, J. R., 3rd *Current opinion in chemical biology* **2008**, *12*, 483.

(178) Ayaz-Guner, S.; Zhang, J.; Li, L.; Walker, J. W.; Ge, Y. *Biochemistry* **2009**, *48*, 8161.

(179) Ge, Y.; Lawhorn, B. G.; ElNaggar, M.; Strauss, E.; Park, J. H.; Begley, T. P.; McLafferty, F. W. *J Am Chem Soc* **2002**, *124*, 672.

(180) Ge, Y.; Rybakova, I. N.; Xu, Q.; Moss, R. L. *Proc Natl Acad Sci U S A* **2009**, *106*, 12658.

(181) Zabrouskov, V.; Ge, Y.; Schwartz, J.; Walker, J. W. *Molecular & cellular proteomics : MCP* **2008**, *7*, 1838.

(182) Zhang, J.; Dong, X.; Hacker, T. A.; Ge, Y. *J Am Soc Mass Spectrom* **2010**, *21*, 940.

(183) Zabrouskov, V.; Han, X.; Welker, E.; Zhai, H.; Lin, C.; van Wijk, K. J.; Scheraga, H. A.; McLafferty, F. W. *Biochemistry* **2006**, *45*, 987.

(184) Kelleher, N. L.; Lin, H. Y.; Valaskovic, G. A.; Aaserud, D. J.; Fridriksson, E. K.; McLafferty, F. W. *J. Am. Chem. Soc.* **1999**, *121*, 806.

(185) Solis, R. S.; Ge, Y.; Walker, J. W. *J Muscle Res Cell M* **2008**, *29*, 203.

(186) Xu, F. M.; Xu, Q. G.; Dong, X. T.; Guy, M.; Guner, H.; Hacker, T. A.; Ge, Y. *International journal of mass spectrometry* **2011**, *305*, 95.

(187) Siuti, N.; Kelleher, N. L. *Nature methods* **2007**, *4*, 817.

(188) Ryan, C. M.; Souda, P.; Bassilian, S.; Ujwal, R.; Zhang, J.; Abramson, J.; Ping, P.; Durazo, A.; Bowie, J. U.; Hasan, S. S.; Baniulis, D.; Cramer, W. A.; Faull, K. F.; Whitelegge, J. P. *Molecular & cellular proteomics : MCP* **2010**, *9*, 791.

(189) Switzar, L.; Giera, M.; Niessen, W. M. *Journal of proteome research* **2013**, *12*, 1067.

(190) McLafferty, F. W.; Breuker, K.; Jin, M.; Han, X.; Infusini, G.; Jiang, H.; Kong, X.; Begley, T. P. *The FEBS journal* **2007**, *274*, 6256.

(191) Zubarev, R. A.; Horn, D. M.; Fridriksson, E. K.; Kelleher, N. L.; Kruger, N. A.; Lewis, M. A.; Carpenter, B. K.; McLafferty, F. W. *Anal Chem* **2000**, *72*, 563.

(192) Cooper, H. J.; Hakansson, K.; Marshall, A. G. *Mass spectrometry reviews* **2005**, *24*, 201.

(193) Emmett, M. R.; Caprioli, R. M. *J. Am. Soc. Mass Spectrom.* **1994**, *5*, 605.

(194) Whitelegge, J.; Halgand, F.; Souda, P.; Zabrouskov, V. *Expert Rev Proteomics* **2006**, *3*, 585.

(195) Armirotti, A.; Benatti, U.; Damonte, G. *Rapid communications in mass spectrometry : RCM* **2009**, *23*, 661.

(196) Pesavento, J. J.; Bullock, C. R.; LeDuc, R. D.; Mizzen, C. A.; Kelleher, N. L. *The Journal of biological chemistry* **2008**, *283*, 14927.

(197) Whitelegge, J. P.; Zabrouskov, V.; Halgand, F.; Souda, P.; Bassilian, S.; Yan, W.; Wolinsky, L.; Loo, J. A.; Wong, D. T.; Faull, K. F. *International journal of mass spectrometry* **2007**, *268*, 190.

(198) Meng, F. Y.; Cargile, B. J.; Patrie, S. M.; Johnson, J. R.; McLoughlin, S. M.; Kelleher, N. L. *Analytical Chemistry* **2002**, *74*, 2923.

(199) Chen, E. I.; McClatchy, D.; Park, S. K.; Yates, J. R. *Analytical Chemistry* **2008**, *80*, 8694.

(200) Arrell, D. K.; Neverova, I.; Van Eyk, J. E. *Circulation Research* **2001**, *88*, 763.

(201) Kellie, J. F.; Tran, J. C.; Lee, J. E.; Ahlf, D. R.; Thomas, H. M.; Ntai, I.; Catherman, A. D.; Durbin, K. R.; Zamdborg, L.; Vellaichamy, A.; Thomas, P. M.; Kelleher, N. L. *Molecular bioSystems* **2010**, *6*, 1532.

(202) Armirotti, A.; Damonte, G. *Proteomics* **2010**, *10*, 3566.

(203) Fridriksson, E. K.; Baird, B.; McLafferty, F. W. *J. Am. Soc. Mass Spectrom.* **1999**, *10*, 453.

(204) Tran, J. C.; Doucette, A. A. *Analytical Chemistry* **2008**, *80*, 1568.

(205) Vellaichamy, A.; Tran, J. C.; Catherman, A. D.; Lee, J. E.; Kellie, J. F.; Sweet, S. M. M.; Zamdborg, L.; Thomas, P. M.; Ahlf, D. R.; Durbin, K. R.; Valaskovic, G. A.; Kelleher, N. L. *Analytical Chemistry* **2010**, *82*, 1234.

(206) Neverova, I.; Van Eyk, J. E. *J Chromatogr B* **2005**, *815*, 51.

(207) Yates, J. R.; Ruse, C. I.; Nakorchevsky, A. *Annual Review of Biomedical Engineering* **2009**, *11*, 49.

(208) Qian, W. J.; Jacobs, J. M.; Liu, T.; Camp, D. G., 2nd; Smith, R. D. *Molecular & cellular proteomics : MCP* **2006**, *5*, 1727.

(209) Messer, A. E.; Jacques, A. M.; Marston, S. B. *J Mol Cell Cardiol* **2007**, *42*, 247.

(210) Zong, C.; Young, G. W.; Wang, Y.; Lu, H.; Deng, N.; Drews, O.; Ping, P. *Proteomics* **2008**, *8*, 5025.

(211) Gundry, R. L.; Fu, Q.; Jelinek, C. A.; Van Eyk, J. E.; Cotter, R. J. *Proteomics. Clinical applications* **2007**, *1*, 73.

(212) Sintegral membrane proteinson, D. C.; Ahn, S.; Pasa-Tolic, L.; Bogdanov, B.; Mottaz, H. M.; Vilkov, A. N.; Anderson, G. A.; Lipton, M. S.; Smith, R. D. *Electrophoresis* **2006**, *27*, 2722.

(213) Sharma, S.; Sintegral membrane proteinson, D. C.; Tolic, N.; Jaitly, N.; Mayampurath, A. M.; Smith, R. D.; Pasa-Tolic, L. *Journal of proteome research* **2007**, *6*, 602.

(214) Garcia, B. A. *J Am Soc Mass Spectrom* **2010**, *21*, 193.

(215) Armirotti, A.; Damonte, G. *Proteomics* **2010**, *10*, 3566.

(216) Kelleher, N. L. *Anal Chem* **2004**, *76*, 197A.

(217) Kellie, J. F.; Tran, J. C.; Lee, J. E.; Ahlf, D. R.; Thomas, H. M.; Ntai, I.; Catherman, A. D.; Durbin, K. R.; Zamdborg, L.; Vellaichamy, A.; Thomas, P. M.; Kelleher, N. L. *Molecular bioSystems* **2010**, *6*, 1532.

(218) Chen, R.; Jiang, X.; Sun, D.; Han, G.; Wang, F.; Ye, M.; Wang, L.; Zou, H. *Journal of proteome research* **2009**, *8*, 651.

(219) Zhang, Y.; Fonslow, B. R.; Shan, B.; Baek, M. C.; Yates, J. R., 3rd *Chemical reviews* **2013**, *113*, 2343.

(220) Guerrera, I. C.; Kleiner, O. *Bioscience reports* **2005**, *25*, 71.

(221) Link, A. J. *Trends in biotechnology* **2002**, *20*, S8.

(222) Godovac-Zimmermann, J.; Kleiner, O.; Brown, L. R.; Drukier, A. K. *Proteomics* **2005**, *5*, 699.

(223) Lin, D., Alpert, A. J., and Yates, J. R. *Am Genom. Proteomic Technol.* **2001**, *1*, 38.

(224) Yates, J. R., 3rd; McCormack, A. L.; Eng, J. *Anal Chem* **1996**, *68*, 534A.

(225) McCormack, A. L.; Schieltz, D. M.; Goode, B.; Yang, S.; Barnes, G.; Drubin, D.; Yates, J. R., 3rd *Anal Chem* **1997**, *69*, 767.

(226) Lee, J.; Soper, S. A.; Murray, K. K. *Journal of mass spectrometry : JMS* **2009**, *44*, 579.

(227) Li, J.; Kelly, J. F.; Chernushevich, I.; Harrison, D. J.; Thibault, P. *Anal Chem* **2000**, *72*, 599.

(228) Musyimi, H. K.; Guy, J.; Narcisse, D. A.; Soper, S. A.; Murray, K. K. *Electrophoresis* **2005**, *26*, 4703.

(229) Mellors, J. S.; Gorbounov, V.; Ramsey, R. S.; Ramsey, J. M. *Anal Chem* **2008**, *80*, 6881.

(230) Foote, R. S.; Khandurina, J.; Jacobson, S. C.; Ramsey, J. M. *Analytical Chemistry* **2005**, *77*, 57.

(231) Yue, G. E.; Roper, M. G.; Balchunas, C.; Pulsipher, A.; Coon, J. J.; Shabanowitz, J.; Hunt, D. F.; Landers, J. P.; Ferrance, J. P. *Analytica Chimica Acta* **2006**, *564*, 116.

(232) Dahlin, A. P.; Bergstroem, S. K.; Andren, P. E.; Markides, K. E.; Bergquist, J. *Analytical Chemistry* **2005**, *77*, 5356.

(233) Carlier, J.; Arscott, S.; Thomy, V.; Camart, J. C.; Cren-Olive, C.; Le Gac, S. *Journal of chromatography. A* **2005**, *1071*, 213.

(234) Fortier, M.-H.; Bonneil, E.; Goodley, P.; Thibault, P. *Analytical Chemistry* **2005**, *77*, 1631.

(235) Huft, J.; Haynes, C. A.; Hansen, C. L. *Anal Chem* **2013**, *85*, 1797.

(236) Gottschlich, N.; Culbertson, C. T.; McKnight, T. E.; Jacobson, S. C.; Ramsey, J. M. *Journal of chromatography. B, Biomedical sciences and applications* **2000**, *745*, 243.

(237) Liu, Y.; Foote, R. S.; Jacobson, S. C.; Ramsey, R. S.; Ramsey, J. M. *Anal Chem* **2000**, *72*, 4608.

(238) Wang, C.; Oleschuk, R.; Ouchen, F.; Li, J.; Thibault, P.; Harrison, D. J. *Rapid communications in mass spectrometry : RCM* **2000**, *14*, 1377.

(239) Lorenz, R. M. and Chiu, D. T. *Acc Chem Res* **2008**, *42*, 649.

(240) Pei, J.; Li, Q. and Kennedy, R. T. *J Am Soc Mass Spectrom* **2010**, *21*, 1107.

(241) Kirby, A. E. and Wheeler, A. R. *Anal Chem* **2013**, *85*, 6178

(242) Jebrail, M.J. and Wheeler, A. R. *Anal Chem* **2009**, *81*, 330.

(243) Jebrail, M. J.; Yang, H.; Mudrik, J. M.; Lafreniere, N. M.; Mcroberts, c.; Al-Dirbashi, O. Y.; Fisher, L.; Chakraborty, P. and Wheeler, A. R. *Lab Chip* **2011**, *11*, 3218.

(244) Ho, j.; Tan, M. K.; Go, D. B.; Yeo, L. Y.; Friend, J. R. and Chang, H. C. *Anal Chem* **2011**, *83*, 3260.

(245) Dennison, A.; Edgar, J.; Winters, D.; Yoon, s. H.; Huang, Y.; Li, Y.; Walton, A.; Mackay, L.; Goodlett, D. R. and Landridge-Smith, P. Development and Application of Surface Acoustic Wave Nebulization with Digital Microfluidics for Top-Down Protein Fragmentation. Presented at *60th ASMS Conference on Mass Spectrometry and Applied Topics*, Vancouver, Canada, **2012**, TOC pm 3:30.

(246) Luk, V. N. and Wheeler, A. R. *Anal Chem* **2009**, *81*, 4524.

(247) Luk, V. N.; Fiddes, L. K.; Luk, V. M.; Kumacheva, E. and Wheeler, A. R. *Proteomics*, **2012**, *12*, 1310.

(248) Aijian, A. P.; Chatterjee, D. and Garrell, R. L. *Lab Chip* **2012**, *12*, 2552.

(249) Srinivasan, V.; Pamula, V.; Paik, P. and Fair, R. Protein Stamping for MALDI Mass Spectrometry Using and Electrowetting-based Microfluidic Platform. In *Proceedings of SPIE-The International Society for Optical Engineering 5591*; International Society for Optics and Photonics: Bellingham, WA; **2004**; pp 26-32.

(250) Lapierre, F.; Piret, G.; Drobecq, H.; Melnyk, O. Coffinier, Y.; Thomy, V. and Boukerroub, R. *Lab Chip* **2011**, *11*, 1620.

(251) Luk, V. N.; Mo, G. C. H. and Wheeler, A. R. *Langmuir* **2008**, *24*, 6382.

(252) Yang, H.; Luk, V. N. ;Abdelgawd, M.; Barbulovic-Nad, I. and Wheeler, A. R. *Anal Chem* **2009**, *81*, 1061.

(253) Dorsam, R. T.; Gutkind, J. S. *Nature reviews. Cancer* **2007**, *7*, 79.

(254) Haab, B. B.; Dunham, M. J.; Brown, P. O. *Genome biology* **2001**, *2*, RESEARCH0004.

(255) MacBeath, G.; Schreiber, S. L. *Science* **2000**, *289*, 1760

(256) Merchant, M., Weinberger, S. R., *Electrophoresis* **2000**, *21*, 1164.

(257) Kotz, K. T.; Xiao, W.; Miller-Graziano, C.; Qian, W. J.; Russom, A.; Warner, E. A.; Moldawer, L. L.; De, A.; Bankey, P. E.; Petritis, B. O.; Camp, D. G., 2nd; Rosenbach, A. E.; Goverman, J.; Fagan, S. P.; Brownstein, B. H.; Irimia, D.; Xu, W.; Wilhelmy, J.; Mindrinos, M. N.; Smith, R. D.; Davis, R. W.; Tompkins, R. G.; Toner, M. *Nat Med*, **2010**, *16*, 1042.

(258) Osiri, J. K.; Shadpour, H.; Park, S.; Snowden, B. C.; Chen, Z. Y.; Soper, S. A. *Electrophoresis* **2008**, *29*, 4984.

(259) Shadpour, H.; Soper, S. A. *Anal Chem* **2006**, *78*, 3519.

(260) Lee, J.; Musyimi, H. K.; Soper, S. A.; Murray, K. K. *J Am Soc Mass Spectrom* **2008**, *19*, 964.

2 Solid-phase Extraction/Purification of Membrane Proteins from MCF-7 Breast Cancer Cells Using a UV-modified PMMA Microfluidic Bioaffinity µSPE Device

2.1 Introduction

Membrane proteins play key roles in both the pathology and physiology of biological cells including: regulating the trafficking of ions and solutes in and out of the cell, cell-to-cell interactions, and responses to stimuli through surface receptors.[1] Some specific modifications to membrane proteins have been linked to different pathologic states such as, cancer, neurological disorders, and diabetes.[2] Because of these roles, membrane proteins have received attention as possible targets for the development of new therapeutics.

Membrane proteins represent ~1/3 of proteins that are encoded by the human genome.[3,4] Yet, only a small fraction of the cell surface proteome has been characterized[1,5] due to the difficulty in the handling of membrane proteins making their study challenging. Because of the interest in discovering and validating disease-specific protein signatures of diagnostic value or finding new drug targets discovery of personalized therapeutics, studies aimed at the identification, characterization, and quantification of membrane proteins has increased over the past few years. Most notably, several biopharmaceuticals (mainly antibodies) that target membrane proteins are already being used and studied for the treatment of tumors and lymphomas as well as some autoimmune diseases.[6]

It has been difficult to analyze membrane proteins due to their low abundance, especially compared to the cytosolic proteins, their lower frequency of tryptic cleavage sites in the transmembrane domain,[6] and the heterogeneity of membrane proteins.[7,8] Therefore, a number of different approaches have been developed to address these issues. Methods that have been utilized for the isolation of membrane proteins specifically have exploited such analytical methods as ultracentrifugation,[9,10] affinity selection of modified or non-modified

membrane proteins (antibody- or lectin-based approaches),[11,12] or two-phase partitioning[13,14] and extraction.[15,16] Unfortunately, these methods have failed to produce highly pure isolates of the membrane proteins due in part to the large contamination from the cytosolic fraction. More recently, improved techniques for the enrichment of membrane proteins, both *in vivo* and *in vitro*, have been reported.[17] These include the chemical capture of glycosylated membrane proteins,[18] silica beads with the appropriate membrane protein-specific coatings,[19,20] or cell surface biotinylation followed by solid-phase affinity extraction using surface immobilized avidin.[21-23]

The empirical formula of biotin was determined by du Vigneaud and co-workers[24] in 1941 and the structure was established by the same group in 1942.[25,26] The Merck Research Laboratories confirmed the structure via total synthesis of racemic biotin.[27] In 1966, x-ray crystallographic analysis established the absolute configuration of natural (+)-biotin as shown in Figure 2.1.[28] The biotin-binding proteins avidin (from the egg white of birds, reptiles, and amphibians) and streptavidin (from the bacterium *Streptomyces avidinii*) have been employed for the selection of biotinylated targets due to the complex's high affinity ($K_a = 10^{15}\ M^{-1}$).[29]

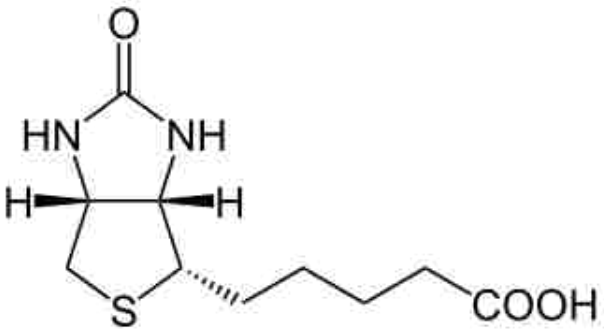

Figure 2.1 Absolute configuration of natural (+)-biotin.

Avidin (pI=10-10.5) has a mass of 67-68 kDa and is formed from four 128 amino acid-subunits with each subunit containing an epitope for biotin (see Figure 2.2) with all binding sites being stable over a wide pH and temperature range. Furthermore, avidin

maintains its high affinity to biotin in spite of the broad range of chemical modifications it can undergo making it useful for the purification of biotinylated molecules from complex sample matrices. Streptavidin (mass = 53 kD) has a lower pI (pI = 6.8-7.5) than avidin and is non-glycosylated allowing a lower degree of nonspecific binding to it compared to avidin.

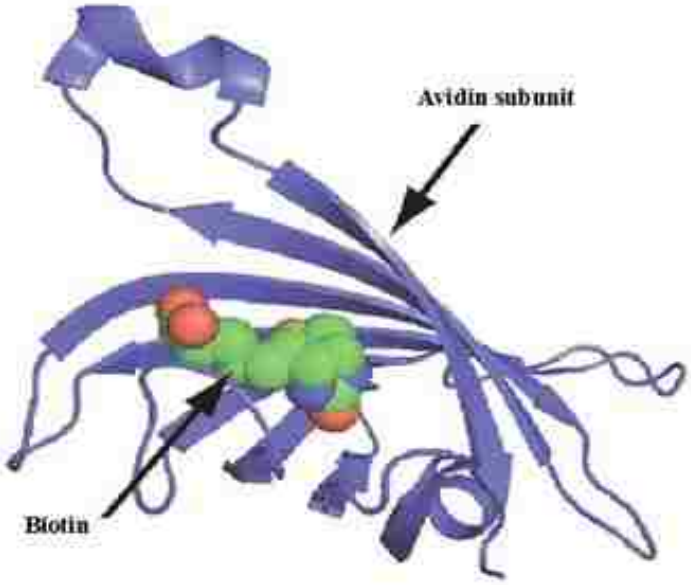

Figure 2.2 Biotin–avidin Interaction: Biotin (green, red, and blue spheres) fits inside a pocket formed by a subunit of avidin protein (blue ribbon). (Reproduced from Weber, P. C.; Ohlendorf, D. H.; Wendoloski, J. J.; Salemme, F. R. *Science* **1989**, *243*, 85.[30] with permission, Copyright 2013, AAAS).

Streptavidin contains a bacterial recognition sequence called the RYD motif (tripeptide Arg-Tyr-Asp) that is similar to the mammalian RGD motif (tripeptide Arg-Gly-Asp) that mediates cell attachment. This RYD motif can bind to cell surface receptors causing high background signals in certain samples. There is a deglycosylated avidin known as NeutrAvidin which has a lower mass (60 kDa) compared to avidin but retains the high biotin-binding affinity. The deglycosylation of NeutrAvidin lowers the pI (pI = 6.3) and reduces the lectin binding to undetectable levels. In addition, lysine residues remain available and the NeutrAvidin can be derivatized or conjugated to a variety of targets at high loads.

NeutrAvidin also lacks the RYD sequence that streptavidin has so there is no risk of nonspecific binding. These advantages make NeutrAvidin attractive as the protein to use for biotin-binding assays.[7,31-35] Table 2.1 summarizes the differences between the various biotin-binding proteins.

Table 2.1 Summary of Biotin-binding Proteins

	Avidin	**Streptavidin**	**NeutrAvidin**
Molecular Weight	67-68 kD	53 kD	60 kD
Biotin Binding Sites	4	4	4
Isoelectric Point (pI)	10-10.5	6.8-7.5	6.3
Affinity for Biotin (K_d)	~10^{-15} M	~10^{-14}-10^{-15} M	~10^{-15} M
Non-specific Binding	Low	High	Lowest

There are three essential components necessary for a reagent to be used for biotinylation: (i) a reactive moiety for the covalent attachment of biotin to a functional group on the chemical target(s). The most commonly used reactive moieties are esters, such as *N*-hydroxysuccinimide (NHS), that can undergo a nucleophilic substitution reaction with primary amines (e.g. ε-amino group in exposed lysine residues present in proteins or peptides). (ii) The biotin moiety itself, which is used for the subsequent interaction of the biotinylated targets with the affinity-based reagent (avidin, streptavidin, or NeutrAvidin). The valeric acid side chain of biotin is important for the avidin association, but the carboxylic acid

group can also present on biotin can be derivatized to incorporate other reactive groups. Utilizing the biotin/avidin association can allow for the use of strong detergents during the purification/extraction steps without loss of material.[36] (iii) A chemical spacer of adequate length to allow for efficient capture of the biotinylated targets with a solid phase in which avidin is covalently attached. The spacer, which is poised between the biotin molecule and the target, can improve biotin accessibility to its association partner by minimizing steric effects induced by the solid surface. The spacer may also contain a functional moiety that can be cleaved chemically or physically to aid in target release after extraction and purification of targets.

In the past decade, several groups have used biotin/avidin affinity interactions to purify membrane proteins. In 2007, Tang and co-workers[33] used three hydrophobic cell-permeable chemical probes, which were designed and synthesized in-house on a modular scaffold for profiling the membrane proteome of *S. oneidensis*. Zhao *et al*.[35] employed biotin/streptavidin to enrich plasma membrane protein fractions. The authors employed a hypotonic buffer and homogenization to lyse biotinylated cells from a human lung carcinoma cell line. After lysis, streptavidin-coated magnetic beads were added to the lysate suspension (see Figure 2.3). The beads were collected using a magnetic plate with the resulting fraction designated as the plasma membrane fraction. The plasma membrane fraction was washed with 1 mL of 1 M KCl (high-salt wash), 0.1 M Na_2CO_3, pH 11.5 (high-pH wash), and finally with a hypotonic buffer. The method resulted in a 400-fold enrichment of plasma membrane proteins relative to the endoplasmic reticulum, which was a major contaminant in the plasma membrane fraction, and also dramatically reduced contamination from other cellular organelles.

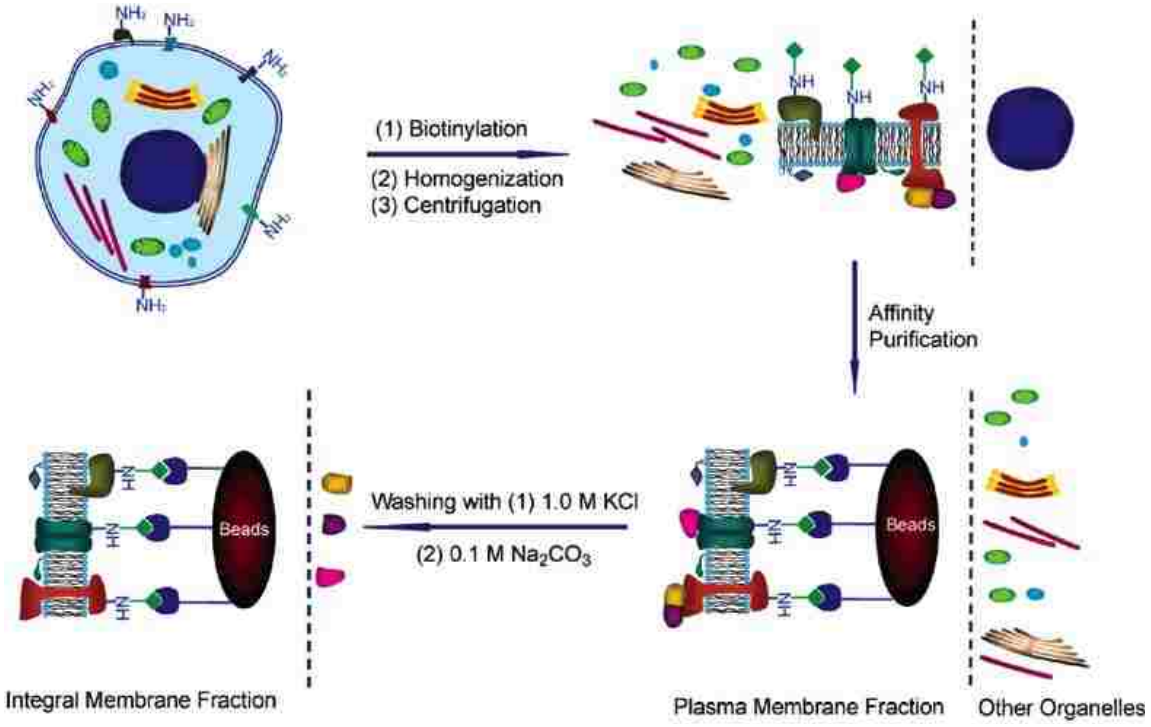

Figure 2.3 Overview of the assay utilized by Zhao *et al*. to enrich plasma membrane proteins from human lung carcinoma cells (Reproduced from Zhao, Y.; Zhang, W.; Kho, Y.; Zhao, Y. *Anal Chem* **2004**, *76*, 1817.[35] with permission, Copyright 2013 American Chemical Society).

In this work, we present a novel method for the affinity enrichment of membrane proteins specifically using a microfluidic device for solid-phase extraction (SPE), which was made via hot embossing using a polymer substrate, in this case poly(methylmethacrylate), PMMA (μSPE device). The extraction bed contained micropillars that were covalently decorated with NeutrAvidin using EDC/NHS coupling chemistry between the NeutrAvidin molecules and the activated polymer surface; UV-activation (254 nm) of the polymer surface. Based on modification procedures of thermoplastics previously outlined in our group,[37] the PMMA enrichment devices were exposed to UV light to generate surface-confined carboxylic acids followed by thermal assembly of the device. Neutravidin could subsequently be covalently strapped to the activated surface and used to select biotinylated proteins following cell lysis.

This device was used for the solid-phase extraction and purification of membrane proteins from a whole cell lysate. The micropillars were used to increase the available surface

area to improve the dynamic range of the assay. As an example of the utility of the μSPE device, MCF-7 breast cancer cells and the extraction of the membrane proteins was evaluated. Intact MCF-7 cells were biotinylated using a reagent that contained a spacer moiety that could be cleaved to quantitatively release the enriched membrane fraction.

Poly(methyl methacrylate), PMMA, was selected as the μSPE device substrate because of its ease of surface modification using UV light (254 nm), its biocompatibility, and the high surface density of functional groups it generates following UV activation. The μSPE device surfaces, including the micropillars, were decorated with NeutrAvidin via EDC/NHS coupling chemistry. We covalently attached biotin to extracellular primary amine groups of membrane proteins with the biotin providing an anchoring group for the affinity enrichment of these biotinylated proteins. The proteins were modified with sulfo-NHS-SS-biotin containing a disulfide-cleavable linker possessing a 24.3 Å spacer to reduce any steric effects. Washes with high salt and high pH solutions were used to remove interfering cytosolic species. Then, the bound membrane proteins could be released from the μSPE device by flooding the bed with a solution of 1,4-dithiothreitol (DTT) in a solubilization buffer. A Bradford assay was used to aid in the evaluation of membrane protein recovery and Western Blotting was performed to evaluate the presence of potential interferences from cytosolic proteins.

2.2 Materials and Methods

2.2.1 Fabrication of PMMA μSPE for Membrane Protein Enrichment

Fabrication of the microfluidic device involved three major steps: (1) Mold insert fabrication using a micro-milling machine (Kern MMP, Kern Micro- and Feinwerktechnik, Murnau-Westried, Germany); (2) hot embossing of the microfluidic structures (HEX02,

JenOptik Mikrotechnik, Jena, Germany) into 3 mm thick PMMA substrates (Goodfellow, United Kingdom); and (3) post-processing of the microfluidic device including drilling of sample reservoirs, UV modification of the immobilization beds and cover plate assembly. The embossed device consisted of six, 24 mm long and 1.4 mm wide channels with microposts serving as the extraction bed. The post dimensions were 100 μm (height) x 100 μm (diameter) with a 50 μm spacing and a total of 3,600 microposts per bed. Each affinity bed had a total surface area of 110 mm^2. Solution reservoirs were created by drilling 1 mm holes into the 3 mm thick PMMA wafers.

Thin PMMA sheets, 0.25 mm thick, were used to enclose the μSPE device by thermal fusion bonding. Prior to enclosure, the PMMA substrate was cleaned using isopropyl alcohol followed by sonication in ddH_2O, then dried in an oven at 70ºC for 30 min. The PMMA substrate and cover plate were sandwiched between two borosilicate glass plates (McMaster, Atlanta, GA, USA) and clamped together prior to insertion into a convection oven. The thermal fusion bonding of the PMMA assembly was done at 100ºC for 20 min.

2.2.2 Design and Operation of the μSPE Device

A variety of methods have been reported to introduce solid extraction phases into microfluidic devices, such as derivatization of microchannel walls with molecular reagents that bear the desired affinity agent, the use of polymeric membranes as sorbents, or the incorporation of magnetic or silica beads.[38] The first demonstration of SPE in a microfluidic format was performed by introducing silica beads into a microchannel and was used for the analysis of amino acids and peptides.[39] We have previously demonstrated a simple and effective method for creating high surface area extraction beds, which incorporate microposts embossed into a fluidic channel. This dramatically simplifies the fabrication process by

eliminating the need for loading silica beads into small channels or the formation of monoliths.[40]

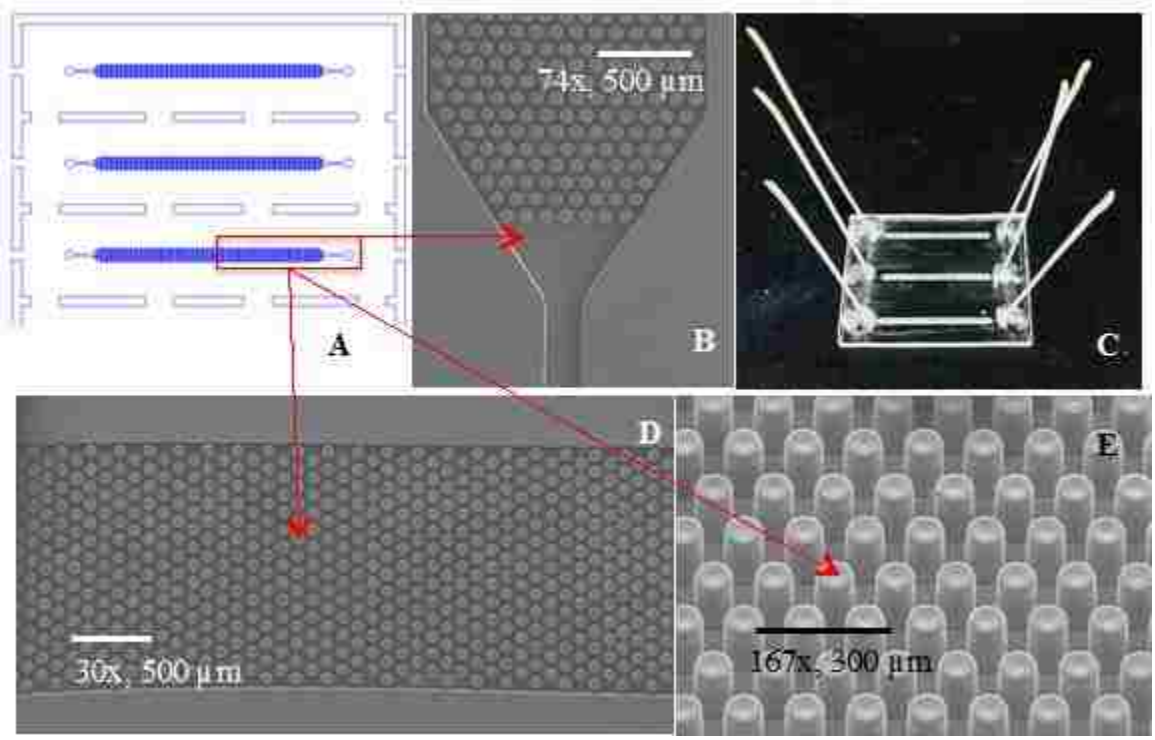

Figure 2.4 (A) Illustration of the topographical layout of the PMMA µSPE device showing the three beds with microposts used for the affinity capture of membrane proteins. (B&D) SEM images of the capture bed and a high magnification SEM (E) of the microposts. (C) A photo of the finished PMMA µSPE device.

A schematic of the fluidic chip is shown in Figure 2.4A. Also shown are SEMs of the microposts poised within the affinity bed (B, D, & E), and a picture of the assembled device (C). Operation of the device involved 3 steps: (i) The sample was loaded into a syringe with the syringe connected via polyetheretherketone (PEEK) tubing (IDEX, Oak Harbor, WA) possessing a length of 9 cm (177 µm ID) to the input and output reservoirs of the µSPE device (see Figure 2.4C); (ii) the sample was dispensed into the reservoirs by loading wit a syringe pump (Harvard Apparatus, Holliston, MA); and (iii) the effluent was collected in microcentrifuge tubes. The affinity bed was washed with buffer solutions by manual loading.

The washing steps were critical in order to remove residual amounts of cellular debris that could potentially interfere with downstream analysis of the membrane proteins.

2.2.3 Surface Modification of the PMMA μSPE Device

The functional scaffold for NeutrAvidin attachment to the PMMA surface was built using a photochemical method (see Scheme 1). In this method, the affinity beds and cover plate were irradiated with a UV light source (22 mW/cm^2; 254 nm) for 15 min using a low pressure Hg lamp (GLF-42, Jelight Company Inc., Irvine, CA). After thermal fusion bonding of the cover slip to the device, the channel was filled with a buffered solution of 0.05 M 2-(N-morpholino) ethanesulfonic acid (MES, pH 5.0) containing 60 mg/mL of 1-ethyly-3-(3-dimethylaminopropyl)carbodiimide (EDC) and 6 mg/mL of N-hydroxysuccinimide (NHS). The solution was allowed to react with the surface at room temperature for 30 min to obtain a succinimidyl ester intermediate.

Scheme 1 shows the photochemical modification of the surface of the μSPE device and the subsequent immobilization of NeutrAvidin via the EDC/NHS coupling reaction. Scheme 1 also describes the surface chemistry for the EDC/NHS coupling and the intermediates that are formed along with the amide bond that is used to immobilize NeutrAvidin to the pendant PMMA surface-confined carboxylic acids that are formed following UV activation. Figure 2.5 shows images of pristine PMMA, UV-modified PMMA, and the PMMA surface with immobilized NeutrAvidin that were taken using brightfield and fluorescence microscopy (for fluorescence microscopy, the excitation wavelength was 488 nm).

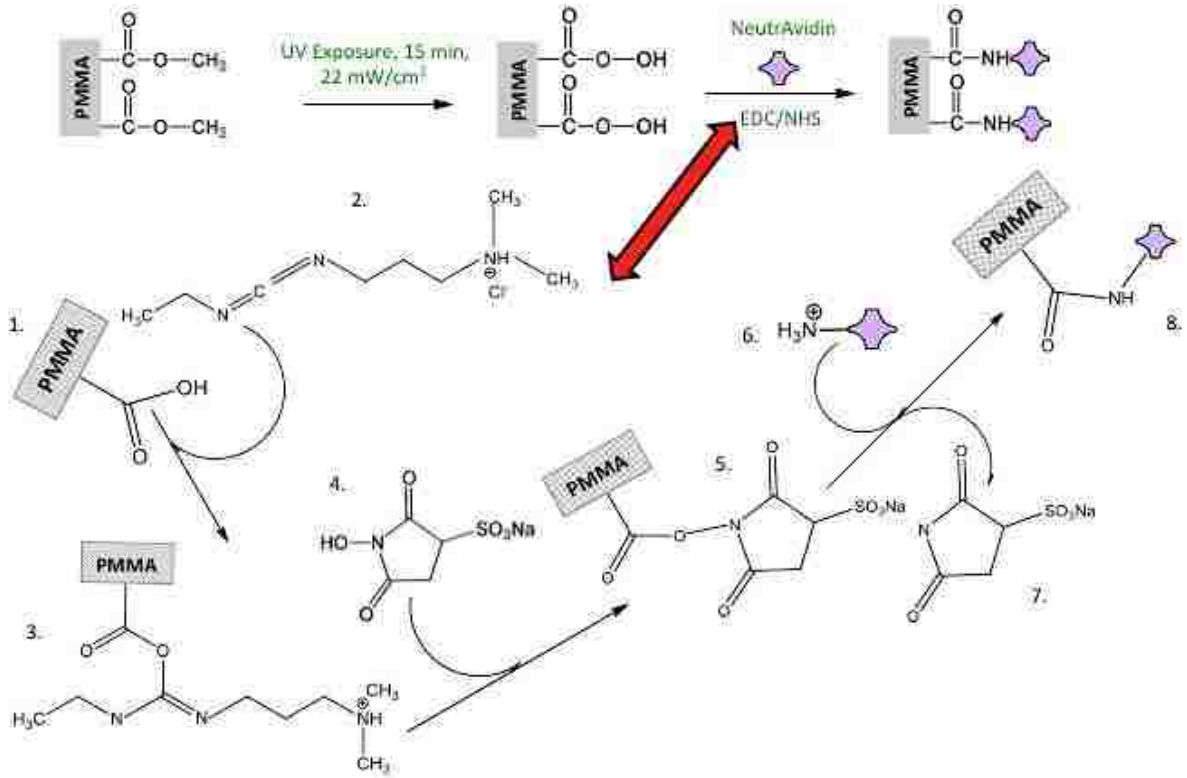

Scheme 1 Reaction processes and intermediates formed on the PMMA surface during the EDC/NHS coupling reaction and NeutrAvidin immobilization. 1. Carboxylic acid; 2. EDC; 3. O-Acylisourea active intermediate; 4. NHS; 5. NHS-Ester intermediate; 6. Primary Amine-containing molecule (i.e. NeutrAvidin); 7. NHS; 8. Amide bond formation.

After the EDC/NHS reaction had incubated with the activated affinity bed surface for 30 min, the surface was rinsed with 1x PBS (pH 8.0) to remove excess EDC/NHS. Next, a 100 μL aliquot of 8 μM NeutrAvidin (in PBS, pH 8.0) was introduced into the extraction bed using manual loading with a syringe. The reaction was allowed to proceed overnight at 4ºC, after which the affinity bed was rinsed with 1x PBS (pH 8.0) to remove any unbound NeutrAvidin.

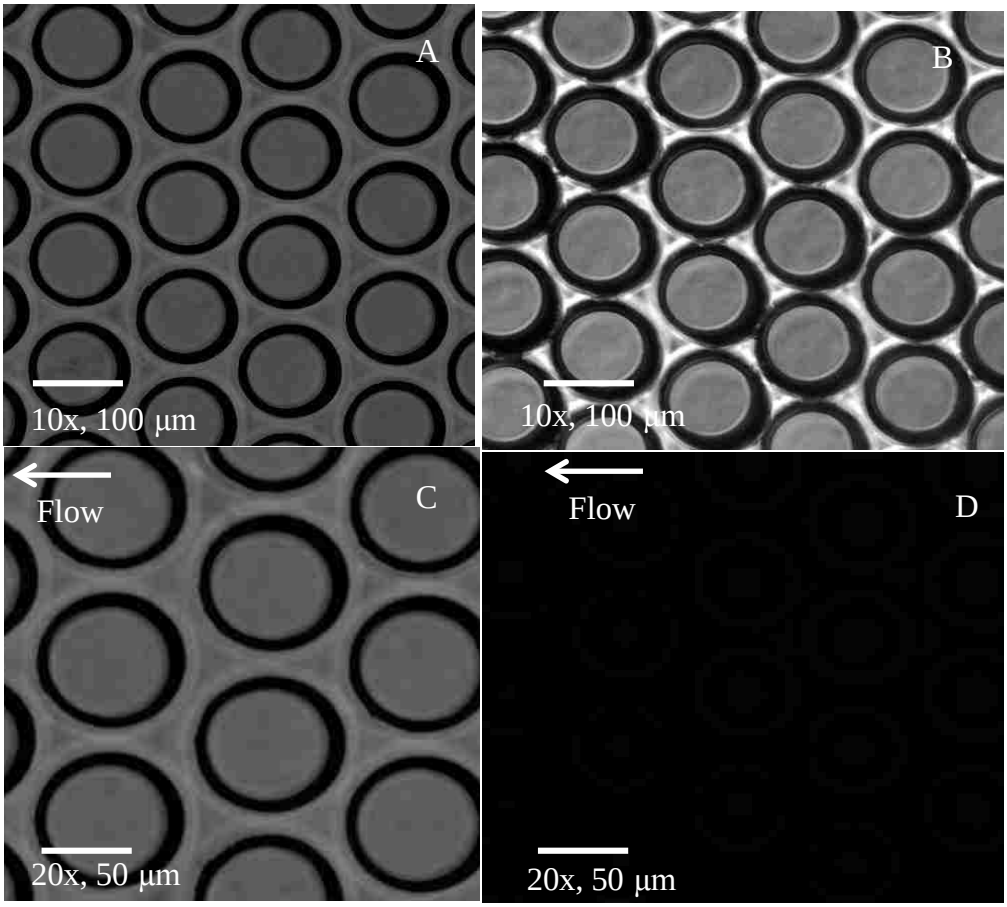

Figure 2.5. Images of the affinity surface: A) Before UV modification (10x, brightfield); B) after UV modification (10x, brightfield); C) after NeutrAvidin immobilization (20x, brightfield); and D) after NeutrAvidin immobilization (20x, fluorescence at 488 nm). All images had an exposure time of 300 ms.

Using a calculation from Lahiri and co-workers,[41] we were able to determine the theoretical estimate of the maximal amount of immobilization for NeutrAvidin corresponding to the maximum number of molecules of NeutrAvidin $(0.9)(10^{14}/\pi r^2)$ per square millimeter that can be close packed in a hexagonal arrangement. We assume that the NeutrAvidin molecules are hard spheres with a radius of 2.6 nm. From the calculation, we found that 6.85 pmol/cm^2 was the theoretical maximum density of NeutrAvidin that could be immobilized given the total surface area of the bed (1.1 cm^2).

2.2.4 Mem-PER™ Plus Membrane Protein Extraction Reagent Kit

In order to provide a direct comparison of the μSPE device and the associated assay to a currently available method for membrane protein extraction, a protein extraction kit available through Pierce Biotechnology (Rockford, IL) was utilized to extract membrane proteins from MCF-7 cells. The kit was used for the enrichment of integral membrane proteins and membrane-associated proteins from cultured mammalian cells or tissue and employs a detergent-based extraction protocol, which eliminates the use of phase separation based solely on hydrophobicity. The cells were permeabilized with a detergent to allow release of soluble cytosolic proteins from the membrane proteins. A second detergent was then used to solubilize the membrane proteins.

Approximately 5×10^6 cells were harvested from the culture dish and were centrifuged at 300× g for 5 min. Then, the pellet was washed with 3 mL of a cell wash solution and the resultant solution centrifuged at 300× g for 5 min. The supernatant was removed and discarded and the cell pellet was resuspended in 1.5 mL of Cell Wash Solution and transferred to a centrifuge tube and centrifuged at 300× g for 5 min with the supernatant discarded. Next, 750 μL of Permeabilization Buffer was added to the cell pellet and briefly vortexed to obtain a homogeneous solution. The pellet was then incubated at 4ºC for 10 min with constant mixing. After incubation, the cells were centrifuged at 16,000× g for 15 min with the supernatant discarded, which contained the cytosolic proteins. Once the cytosolic proteins were removed, 500 μL of the Solubilization Buffer was added to the remaining cell pellet and the cells were resuspended. The cell pellet was then incubated at 4ºC for 30 min with constant mixing. Lastly, centrifugation was done at 16,000x g for 15 min at 4ºC. The

remaining supernatant contained the solubilized membrane and membrane-associated proteins.

2.2.5 Sample Preparation

2.2.5.1 Cell Biotinylation and Lysis

The biotinylation of the membrane proteins was performed on the intact MCF-7cells using a membrane impermeable reagent. As a result, only membrane proteins should be biotinylated, reducing the contamination of cytosolic proteins and other cellular material. The MCF-7 cells, an invasive breast ductal carcinoma, were utilized as a model in these studies. The biotinylation reagent Sulfo-NHS-SS-Biotin (molecular weight of 606.69 g/mol), Sulfosuccinimidyl-2-(biotinamido)-ethyl-1,3'- dithiopropionate, (Pierce Biotechnology, Rockford, IL) is membrane impenetrable and also contains a disulfide-cleavable linker possessing a 24.3 Å spacer to reduce any steric effects caused by the NeutrAvidin support and the biotinylated membrane proteins.

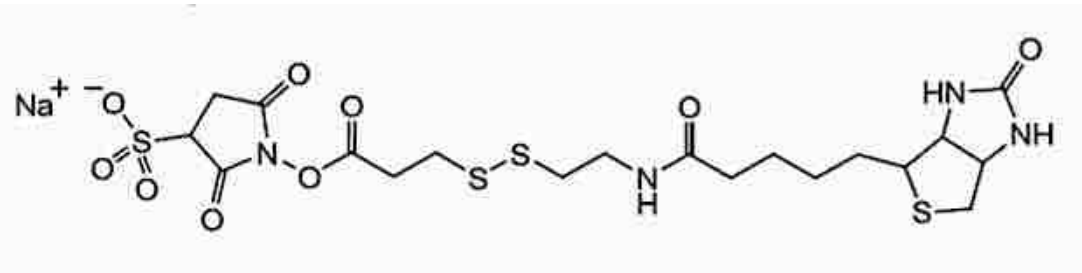

Figure 2.6 Structure of NHS-SS-Biotin with the 24.3 Å spacer.

The MCF-7 adherent cells were first washed with ice-cold 1x PBS (pH 8.0) three times to remove any amine contaminants and culture media from the cells. The cells were then suspended at a concentration of 5 x 10^6 cells/mL in 1x PBS (pH 8.0). Immediately before use, a 10 mM solution of Sulfo-NHS-SS-Biotin was prepared by adding 164 µL of ultrapure water to 1 mg of the biotinylation reagent. Approximately 80 µL of the biotinylation reagent

was added per milliliter of reaction volume (volume added = 160 μL). The reaction was incubated at room temperature for 30 min with constant mixing. After incubation, the cells were washed with 1 mg/mL of lysine (pH 8.0) to quench the reaction by coupling to any non-reacted biotinylation reagent and then washed two times with ice-cold 1x PBS (pH 8.0) to remove any remaining contaminants. The cells were then centrifuged at 300× g for 10 min (4ºC) to obtain a pellet. A fluorescence image (taken at 488 nm) of intact and biotinylated MCF-7 cells is shown in Figure 2.7.

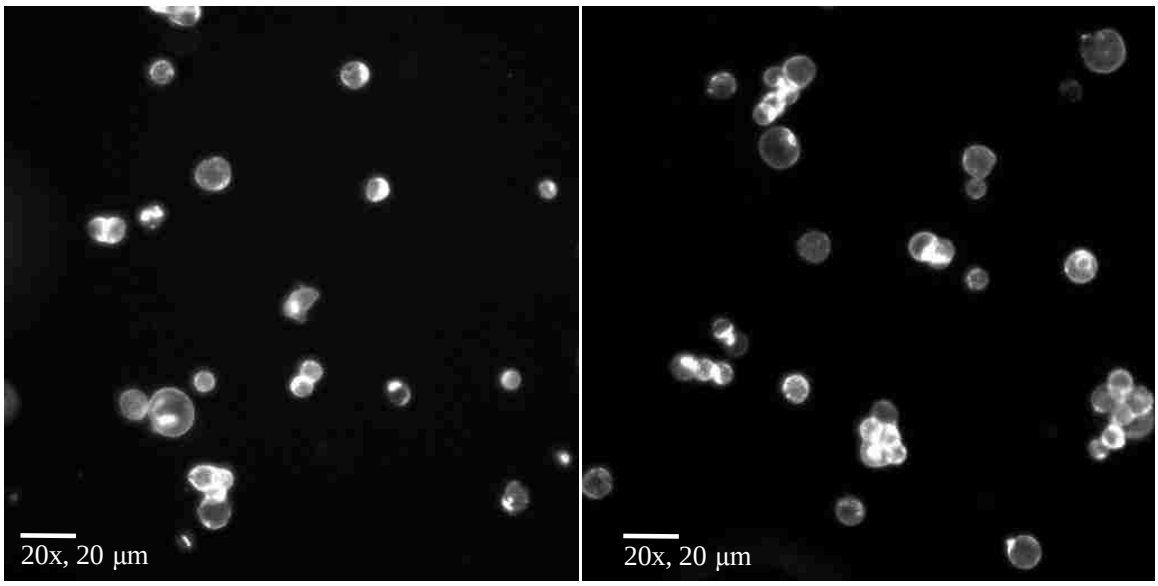

Figure 2.7 Fluorescence images taken at 488 nm (200 ms exposure time) of biotinylated MCF-7 cells that have been stained with FITC- conjugated avidin to show that the cells were biotinylated.

After washing, a 4% CHAPS buffer, 7M urea, 2M thiourea, 30 mM Tris and 5 mM magnesium acetate (pH 8.5) were added to the pellet to lyse the cells. Dialysis was performed overnight with two buffer changes of 4% CHAPS (4ºC) to further remove excess biotin. Biotin incorporation was estimated using HABA, 2-(4'-hydroxyazobenzene)-2-carboxylic acid. The method is based on the ability of HABA to bind to avidin to form a complex with a maximum absorption at 500 nm. A sample containing biotinylated targets is added to the

HABA-avidin solution and because of biotin's higher affinity for avidin, it displaces HABA and the absorption at 500 nm decreases proportionately.[42] The absorbance of the HABA-avidin solution is measured before and after adding the biotinylated sample with the change in absorbance related to the amount of biotin present in the sample. Based on the absorbance measurements from the cells that were biotinylated, it was determined that there were between 2-3 biotin molecules per protein molecule.

2.2.5.2 Western Blotting Analysis

We determined the concentrations of both the membrane proteins and cytosolic proteins from the extraction procedure using a Bradford assay which used 8.2 μg of each protein fraction (membrane, cytosolic, and total lysate). Gel runs for the blotting assay employed the BioRad Mini-PROTEAN System (BioRad, Hercules, CA, USA). The procedure we followed is summarized below.

A 3x Laemmli sample buffer (6% SDS, 30% glycerol, 187.5 mM Tris, 15% β-mercaptoethanol, 0.006% bromophenol blue) with a 5 mL total volume was added to each protein fraction in order to prepare them for gel electrophoresis. The fractions were heated at 95°C for 5 min, cooled on ice and briefly vortexed before being placed on the gel. A 4-15% BioRad precast gel was used along with a PageRuler Prestained Protein Ladder (Pierce Biotechnology, Rockford, IL, USA) that had a molecular weight range of 10-250 kDa. The running buffer (Tris/Glycine/SDS) was used to rinse the wells of the gel and the gel was placed in the gel box along with the running buffer. Five μL of the PageRuler was added to the well and 50 μL of each protein sample was added to the remaining wells. The gel was run for ~35 min at 200 V until the dye front could no longer be seen.

While the gel was running, a PVDF membrane was prepared by incubating in methanol for 30 s, rinsed briefly in ddH_2O and then incubated in ice-cold transfer buffer (20% methanol, 10x Western Transfer Buffer, ddH_2O) for 5 min. The gel was removed from the cassette case and placed on the PVDF membrane and both were sandwiched together with a transfer cassette. The PVDF/gel was placed back into the gel box along with the transfer buffer and run again for 70 min at 250 mA. When the run was completed, the membrane was removed from the cassette and rinsed briefly with a Tris-buffered saline and Tween-20 buffer (0.1% TBST, Tris-buffered saline, Tween-20, ddH_2O). The membrane was blocked in 5% milk (dry milk, 0.1% TBST) for 1 h. The membrane was then incubated overnight at 4°C with the primary antibody (Anti-beta-actin antibody) in 5% dry milk and 0.1% TBST.

After incubation, the antibody solution was decanted from the membrane. The membrane was washed 5 times for 5 min with the 0.1% TBST buffer and blocked for 5 min in 5% milk. The membrane was incubated for 1 h at room temperature with the secondary antibody in 5% milk. The stock secondary antibody solution was diluted 1:5000 with a milk solution (1 μL anti-actin secondary antibody + 5 mL 5% milk). The membrane was washed again with 0.1% TBST (5 times, 5 min) and once for 5 min with 1x Tris-buffered saline (TBS).

Enhanced chemiluminescence (ECL) was employed for detection of the resultant bands. The method works by detecting horseradish peroxidase (HRP) tethered to the secondary antibody forming an enzyme complex. The complex catalyzes the conversion of the chemiluminescent substrate into a sensitized reagent in the vicinity of the antibody, which on further oxidation by hydrogen peroxide produces a triplet (excited) carbonyl that emits light when it decays to the singlet carbonyl. ECL allows detection of minute quantities of a

biomolecule; proteins can be detected down to femtomole quantities. Once the ECL solution was prepared, the membrane was placed side up on a piece of plastic wrap and 2.5 mL of the ECL solution was pipetted over the membrane and incubated for 5 min making sure that no part of the membrane dried out. The membrane was removed from the ECL solution and excess solution was carefully blotted away. The membrane was placed in a plastic sleeve and lightly taped in place. The blot was exposed to film in a darkroom for 30 s and visualized.

2.3 Results and Discussion

2.3.1 Solid-phase Extraction/Purification of Biotinylated MCF-7 Cell Surface Membrane Proteins with Microfluidic Bioaffinity μSPE Device

Previously reported methods for purifying membrane proteins from complex samples have combined the isolation of membrane proteins with specific protein tagging strategies to minimize cross-contamination. For example, antibodies directed against certain membrane proteins were immobilized onto magnetic beads and used for the purification of specific membrane proteins. Unfortunately, this method was limited to proteins for which a specific antibody was available.[43] Protein radioactive labeling has also been employed in different protein studies,[44] and quantitative analysis of proteins by MS was often performed with isotope-coded affinity tags.[45] In 2002, Sabarth *et al*. used the hydrophilic reagent, S-NHS-LC-biotin (sulfosuccinimidyl-6-(biotinamido)hexanoate), to biotinylate surface proteins of *E. coli* with enrichment via avidin-affinity chromatography.[31] As previously mentioned, commercial kits for the extraction of membrane proteins with the use of detergents exist, however, they can potentially possess a high degree of cytosolic contamination that can complicate identification of the membrane proteins due to the relatively higher abundance of the cytosolic components.

The steps employed in our µSPE device and assay of membrane proteins from whole cell lysates are shown in Scheme 2. In the first step, modification of the PMMA surface followed by immobilization of NeutrAvidin is undertaken. Once the surface has been decorated with NeutrAvidin, the affinity bed is ready for infusion of the biotinylated proteins.

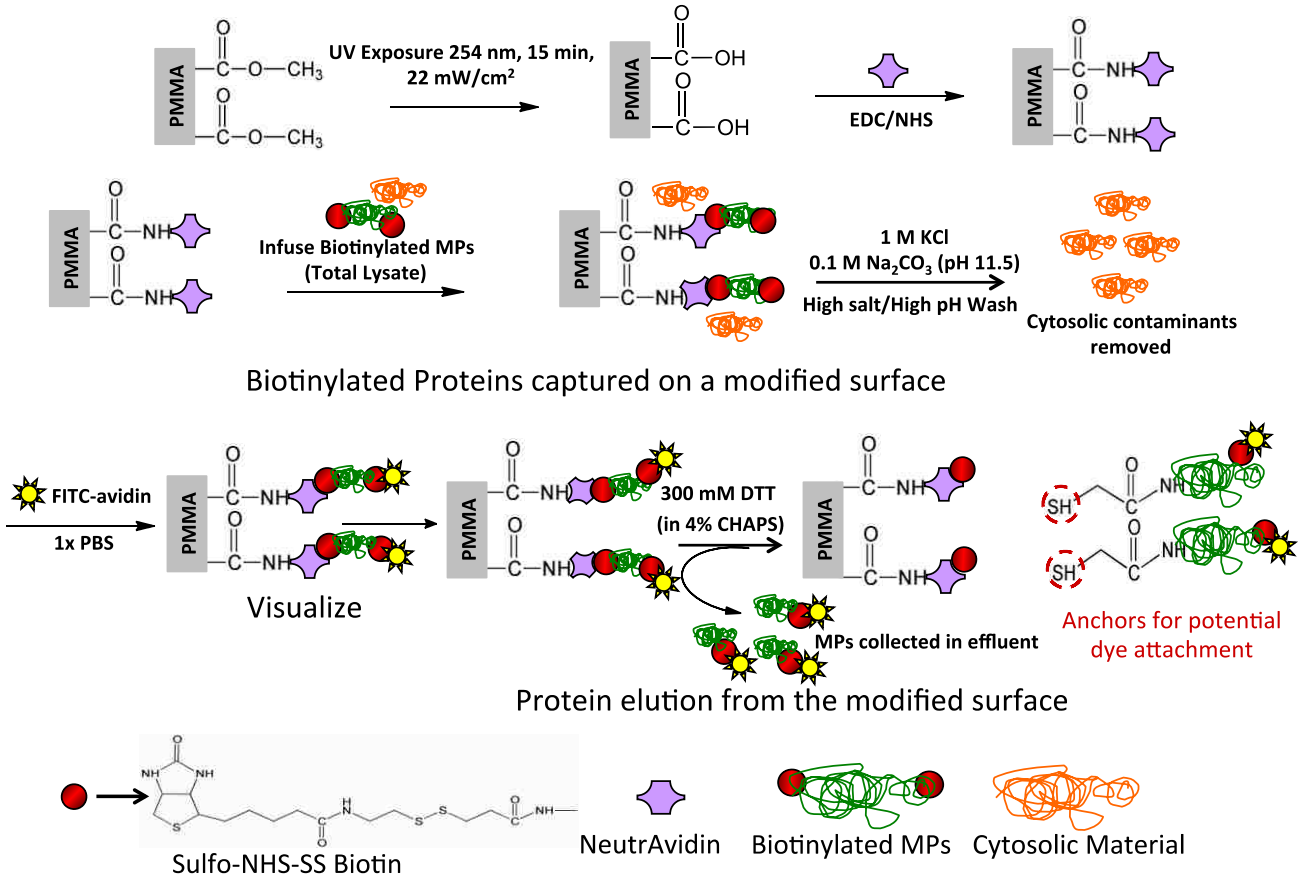

Scheme 2 Overview of the on-chip extraction/purification assay for membrane proteins from cell lysates. Prior to cell lysis, the intact cells were biotinylated.

For the present set of experiments, the cell lysate was infused into the affinity bed at a flow rate of 5.0 µL/min to allow sufficient time for the biotinylated proteins to interact with the surface-confined NeutrAvidin. The surface was then rinsed with a high salt/high pH wash to remove any loosely-bound cytosolic proteins. Following the wash, 300 mM DTT (in 4% CHAPS) was infused continuously for 2 h through the µSPE bed. The surface was finally

rinsed with 1x PBS (pH 8.0) and the effluent containing the released membrane proteins collected for further analysis. The cell lysate originating from 5 x 10^6 MCF-7 biotinylated cells in 4% CHAPS buffer was infused through the affinity bed of the μSPE device. To determine if the biotinylated proteins had indeed been captured by the surface-immobilized NeutrAvidin, we employed avidin labeled with FITC to visualize the affinity surface after infusion of the cell lysate through the device. The FITC-labeled avidin could bind to any available sites remaining on the biotinylated proteins that were not complexed to the surface-confined NeutrAvidin molecules. Figure 2.8 shows fluorescence images of membrane proteins captured on the surface of the bioaffinity device after flooding the bed with FITC-labeled avidin.

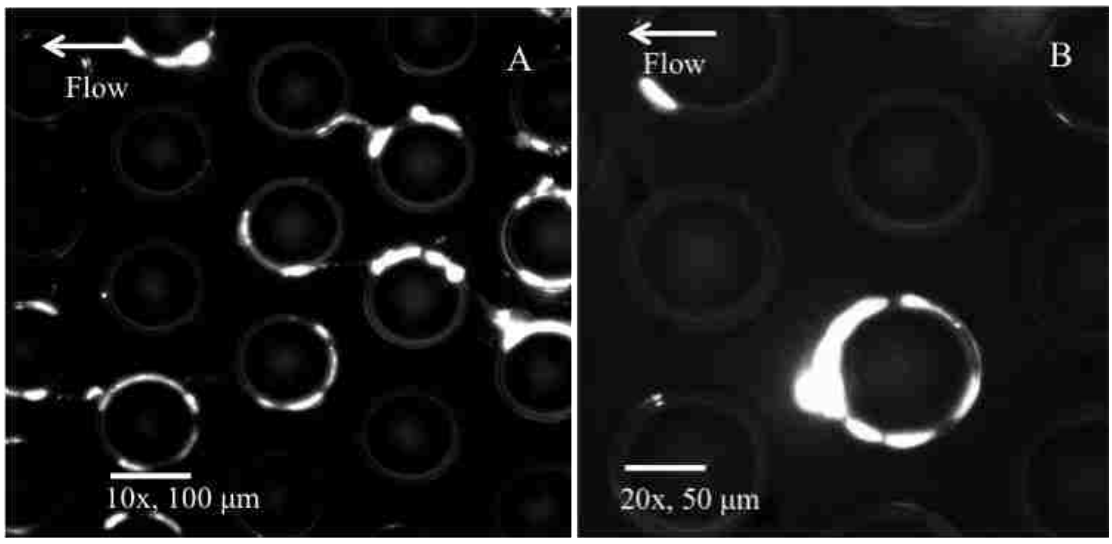

Figure 2.8 Images A and B showing captured membrane proteins on the UV/NeutrAvidin-modified PMMA capture surface. All images were done at a 300 ms exposure time with fluorescence done at 488 nm with FITC-labeled avidin

Figure 2.8A & B show the immobilized membrane proteins at two different magnifications. As shown in Figure 2.8, fluorescence did appear within the affinity beds that were infused with the MCF-7 lysate. However, the resultant fluorescence appeared to be

globular and patchy on the surface of the micropillars. This data suggested that the membrane proteins were not well solubilized using only the 4% CHAPS buffer system before infusion into the affinity bed as well as possibly being partially associated with the cell membrane. Thus, it appears that the 4% CHAPS buffer was not sufficient for both cell lysis and solubilization.

To further aid with the solubilization process, a proprietary solubilization buffer (Pierce Biotechnology, Rockford, IL) was added to the cell lysate after biotinylation and lysis with 4% CHAPS. The addition of this solubilization buffer proved helpful in solubilizing the membrane protein fraction. The results of this new solubilization procedure are shown in Figure 2.9. As shown in the fluorescence image, the resulting fluorescence was more homogeneous around the surface of the pillars containing NeutrAvidin instead of "patchy-like," and globular as noted in Figure 2.8.

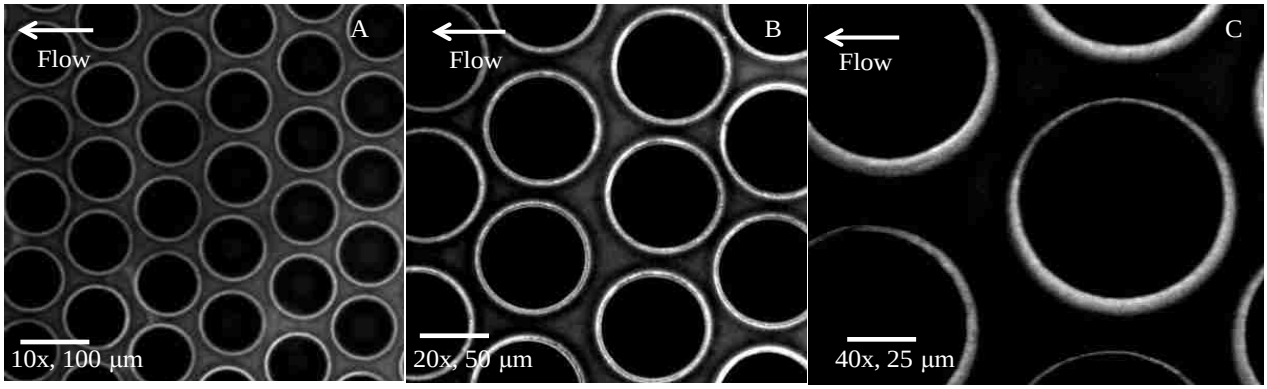

Figure 2.9 Images of the UV/NeutrAvidin-modified PMMA capture surface after the addition of solubilization buffer to the MCF-7 cell lysate. Images A, B, and C were taken at 10x, 20x, and 40x magnification, respectively and all images were done at a 300 ms exposure time. Fluorescence was done at 488 nm with FITC-labeled avidin.

This result indicated that this lysis and solubilization procedure was much more effective than the case of using 4% CHAPS only. Also, as can be seen from these images, the fluorescence was visible from all of the pillars in the microscope field-of-view with all sides

of the pillar showing fluorescence. Therefore, we are operating with a load of protein (originating from 5 x 10^6 MCF-7 cells) that saturates the affinity surface.

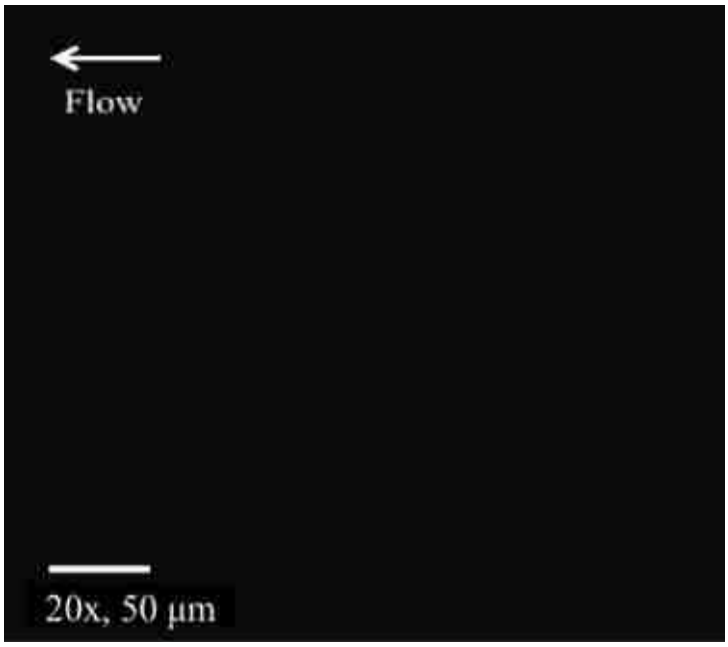

Figure 2.10 Fluorescence at 488 nm (300 ms exposure time) of the μ-SPE surface after NeutrAvidin immobilization and flooding the bed with avidin-FITC to check for non-specific adsorption of the FITC-labeled avidin on the surface.

To make sure that the resulting fluorescence shown in Figure 2.9 did not result from non-specific adsorption of the fluorescently labeled avidin to the PMMA micropillars, we subjected the NeutrAvidin-immobilized affinity bed to a solution containing the FITC-labeled avidin without the bed being subjected to the biotinylated proteins. No fluorescence from the FITC-labeled avidin was observed (see Figure 2.10) indicating that there was no non-specific adsorption.

2.3.2 Release of Captured Biotinylated Membrane Proteins from the μSPE Surface

After affinity selection of the biotinylated membrane proteins by the μSPE device, a 300 mM solution of DTT (in 4% CHAPS) was continuously infused into the SPE bed at a flow rate of 5.0 μL/min for 2 h to release the selected membrane proteins by reducing the

disulfide bond carried in the Sulfo-NHS-biotin reagent. Infusion was done in the dark to prevent photobleaching of the FITC on the surface. A total of 100 μL of a rinsing effluent (1x PBS, pH 8.0) was infused. The chip was then imaged at a 20x magnification using a fluorescence microscope with excitation at 488 nm and a 300 ms exposure time. The resulting image is shown in Figure 2.11. As shown, there was no visible fluorescence from the μSPE surfaces suggesting that the biotinylated membrane proteins were in fact released from the surface.

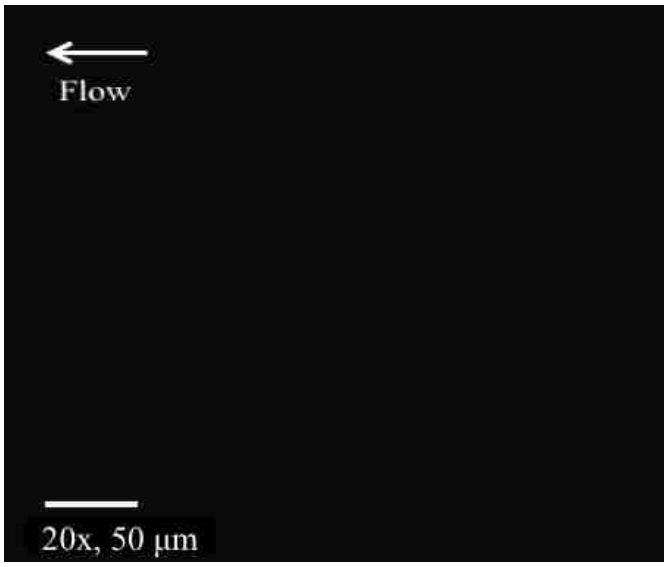

Figure 2.11 Fluorescence image of the μ-SPE surface when excited at 488 nm (300 ms exposure time) following DTT release of the biotinylated membrane proteins.

We further verified that the selected proteins were indeed released from the affinity bed by measuring the fluorescence of the resulting effluent that was collected during the DTT infusion/rinse. Figure 2.12 shows a calibration plot of the fluorescence signal that was generated by the avidin-FITC (in DTT).

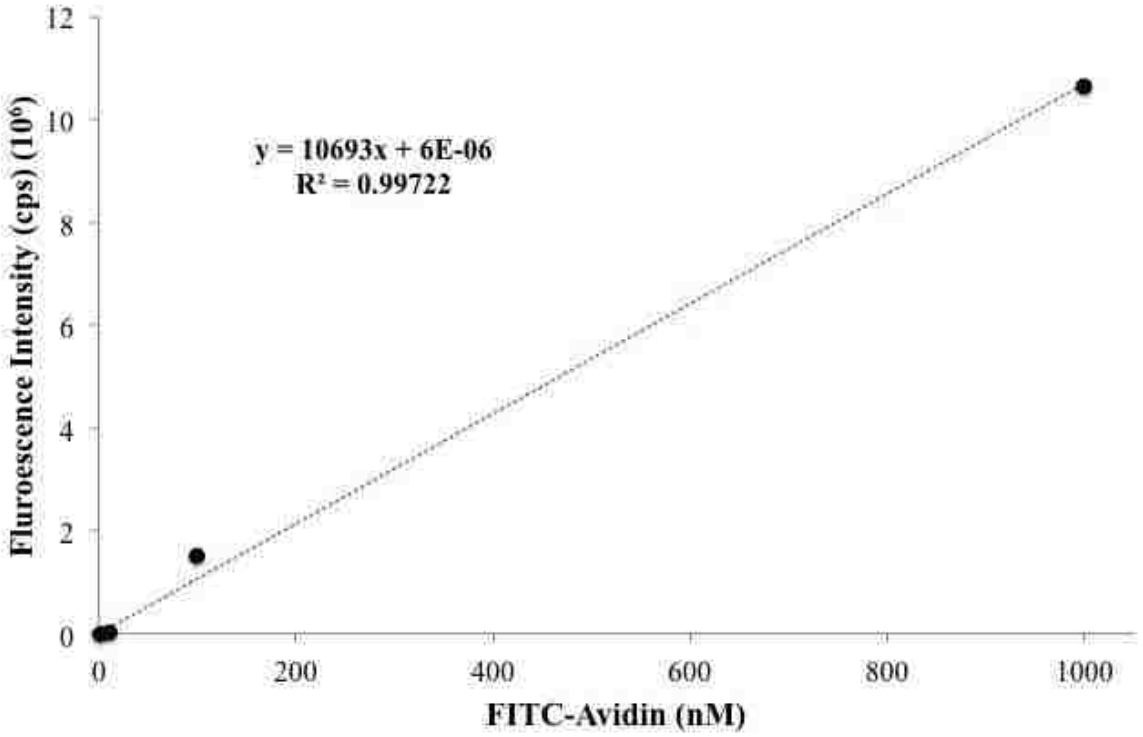

Figure 2.12 Calibration curve of varying concentrations of avidin-FITC.

The fluorescence signal from the effluent not only indicated that there were membrane proteins released from the μSPE bed. A sample of biotinylated MCF-7 membrane proteins that had been labeled with avidin-FITC was also measured in a fluorimeter so that we could determine the initial amount of membrane protein material being used. The concentration of biotinylated protein in a 1 mL sample was found to be 1.71 ± 0.25 pmol. We ran MCF-7 whole cell lysate (5×10^6 cells) volumes of 500, 100, 50, 10, 5, and 1 μL, respectively through the μSPE bed. Recovery of biotinylated protein was calculated by examining the mass of the protein sample before and after purification on the μSPE device. For a 0.374 ± 0.03 pmol sample of biotinylated membrane protein input, a capture efficiency of biotinylated membrane proteins was estimated to be 34.92 ± 3.27%, while it increased to 83 ± 2.14% when the membrane protein concentration was set below 0.019 ± 0.00051 pmol (Figure 2.13).

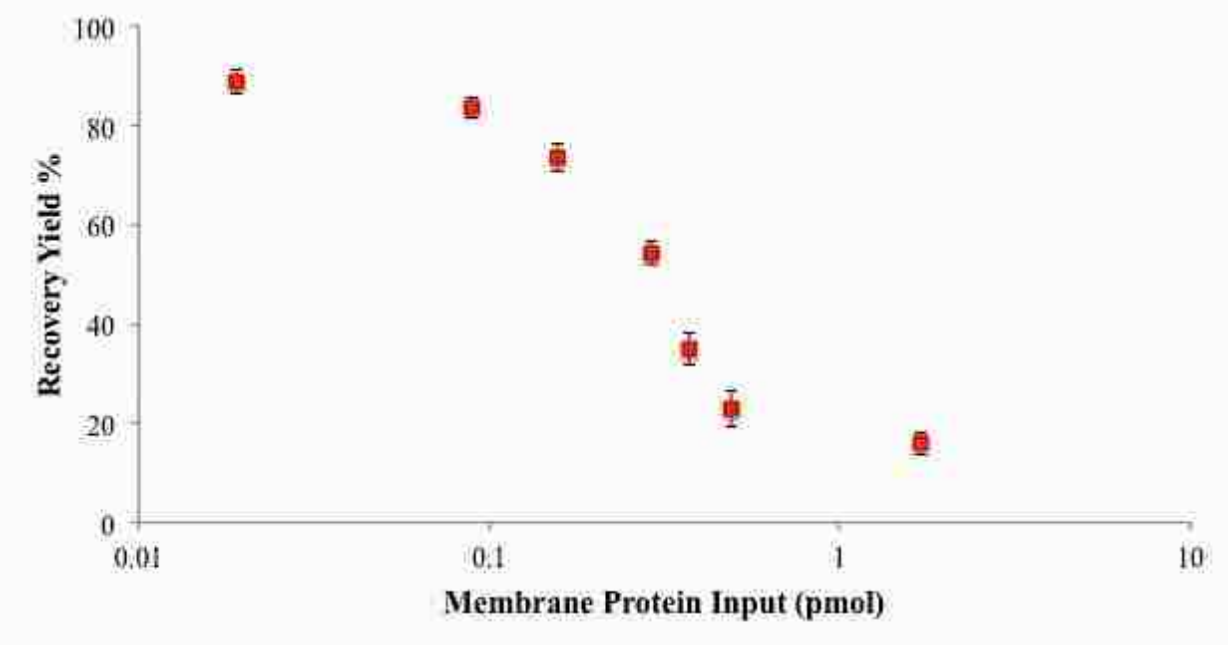

Figure 2.13 The recovery of biotinylated MCF-7 membrane proteins loaded onto the µSPE device using the extraction/purification assay. The total concentration (pmol) before and after µSPE purification was estimated from fluorescence data, which only measured proteins that were biotinylated. Error bars in the graph represent standard deviations from three replicate runs.

The lower recoveries that are observed with higher concentrations of biotinylated protein suggest that the amount of protein that was introduced exceeded the load capacity of the µSPE capture bed (*i.e.* available NeutrAvidin sites). The protein saturation point of 1.71 pmol calculated from Figure 2.13 corresponds well with the theoretical surface density of 6.85 pmol/cm^2.

2.3.3 Western Blotting Analysis to Evaluate the Purity of Extracted MCF-7 Membrane Proteins

To determine the purity of the µSPE fractions free from cytosolic contamination, Western blotting was performed using actin as a marker for cytosolic contamination because it is highly abundant in the cytosol. Western blotting using EpCAM (epithelial cell adhesion molecule) was also used to check for the presence of membrane proteins in µSPE effluent

because it is a membrane protein highly expressed in MCF-7 cells (~200,000-300,000 per cell).[46,47]

The results for the actin Western blot of the protein fractions extracted using the detergent-based technique are shown in Figure 2.14. The Western blot clearly showed the presence of actin with intense bands in the total cell lysate (T) and the cytosolic (C) fractions. In addition, there was also an actin band in the lane where the membrane protein band was, suggesting contamination by cytosolic proteins using the detergent-based isolation technique. This indicated that the detergent-based method is not efficient in removing highly abundant cytosolic proteins from the membrane fraction.

The same Western blot analysis was also carried out after processing the MCF-7 cell lysate (biotinylated) on the µSPE chip to check the purity of the membrane protein fraction. In this case, 25 ng of DTT-released biotinylated membrane protein was loaded onto the gel. Figure 2.14 B & C shows the blots of a biotinylated membrane protein sample that was eluted from the µSPE device. There is clear evidence of the actin band for the total lysate prior to processing using the µSPE device. Lane M of the actin Western blot consisted of the sample that was run through the µSPE affinity bed, subjected to DTT release with the effluent collected following release. In this case, no actin band was evident indicating that the µSPE/DTT release effluent was free from cytosolic contamination.

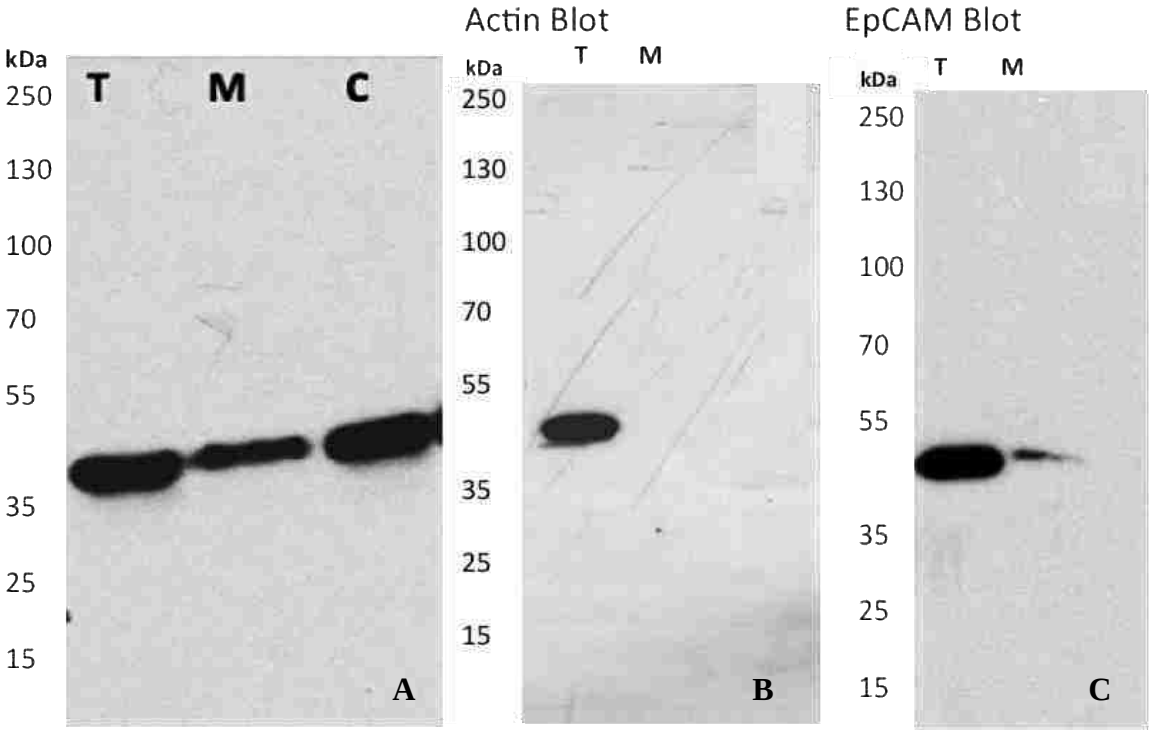

Figure 2.14 **(**A**)** Actin Western blot of MCF-7 protein fractions that were extracted using a detergent-based extraction method (Section 2.2.4). The total lysate (T), membrane protein fraction (M), and the cytosolic protein fraction (C) were all analyzed. The blot shows that there is cytosolic protein contamination in the membrane protein fraction (presence of actin). (B) Actin Western blot of the µSPE extracted membrane proteins (M) and total cell lysate (T) (before on-chip analysis) and (C) EpCAM blot of total cell lysate and µSPE extracted membrane protein sample. The band indicates the presence of actin in the sample. The EpCAM blot confirms that there are membrane proteins present in the effluent from the SPE bed.

We also ran an EpCAM Western blot to make sure that we did in fact have membrane proteins present in the µSPE/DTT release effluent. The blot confirmed the presence of EpCAM in the lane where the µSPE/DTT release effluent was loaded indicating that we were able to detect biotinylated membrane proteins using this Western blot procedure.

2.3.4 Computational Modeling to Understand the Effects of the Chip Geometry on Protein Capture

The µSPE bed consisted of a series of staggered microposts onto which NeutrAvidin was immobilized to serve as the material for enrichment and purification of the biotinylated membrane proteins introduced into the device via hydrodynamic flow. Within this section, we

were interested in understanding how the μSPE bed's geometry, in terms of micropost shape and spacing, affects the capture efficiency of proteins. These studies were carried out using computational fluid dynamics (CFD) conducted with COMSOL Multiphysics 4.3a as well as mathematical derivations using the principles of diffusion.

2.3.4.1 CFD Modeling of Velocity Fields, Protein Flux, and Protein Capture in Several μSPE Bed Configurations

For the CFD simulations, three model geometries composed of staggered rows of micropillars were tested: (I) Circular posts with radii of 50 μm and center-to-center spacing of 150 μm; (II) circular posts with radii of 10.0 μm and center-to-center spacing of 40.0 μm; and (III) diamond posts with side length of 20.0 μm (fileted by 5 μm to reflect the fabrication limits of micro-milling) and center-to-center spacing of 40.0 μm. Geometries I and III were used to understand scaling effects (post size and post spacing), and geometry II was used to understand the effects of post shape (circular versus diamond). Note that in all of these model geometries, the number of posts was restricted to only a few staggered rows (relative to the hundreds occupying a physical μSPE bed) to ensure numerical tractability of the computations.

Using these geometries, we conducted fluid dynamic simulations of steady-state (time independent) laminar flow through the μSPE beds. For this, COMSOL solves the Navier-Stokes equations to provide velocity fields. For comparison, all μSPE beds were designed within COMSOL to have the same fluidic inlet with the fluid (modeled with the properties of water) entering the beds assigned a linear velocity of 0.83 mm s^{-1} to reflect a physical volumetric flow rate of 1 μL min^{-1}. After solving for the steady-state velocity fields, the time-dependent transport of a dilute protein (herein utilizing BSA as a model protein with a

diffusion coefficient[48] of 60 μm^2 s^{-1} and without adjusting for the effects of biotinylation) was calculated.

We first simulated the steady-state (time independent) laminar flow profiles of water traveling through the μSPE beds. The CFD solutions for geometries I-III are shown in Figure 2.15. It is clear that for all geometries, flow around the posts positioned nearest the bed walls is slightly reduced compared to the bulk flow likely resulting from viscous drag along the walls, an artifact of the Poiseuille flow, and the no-slip condition.

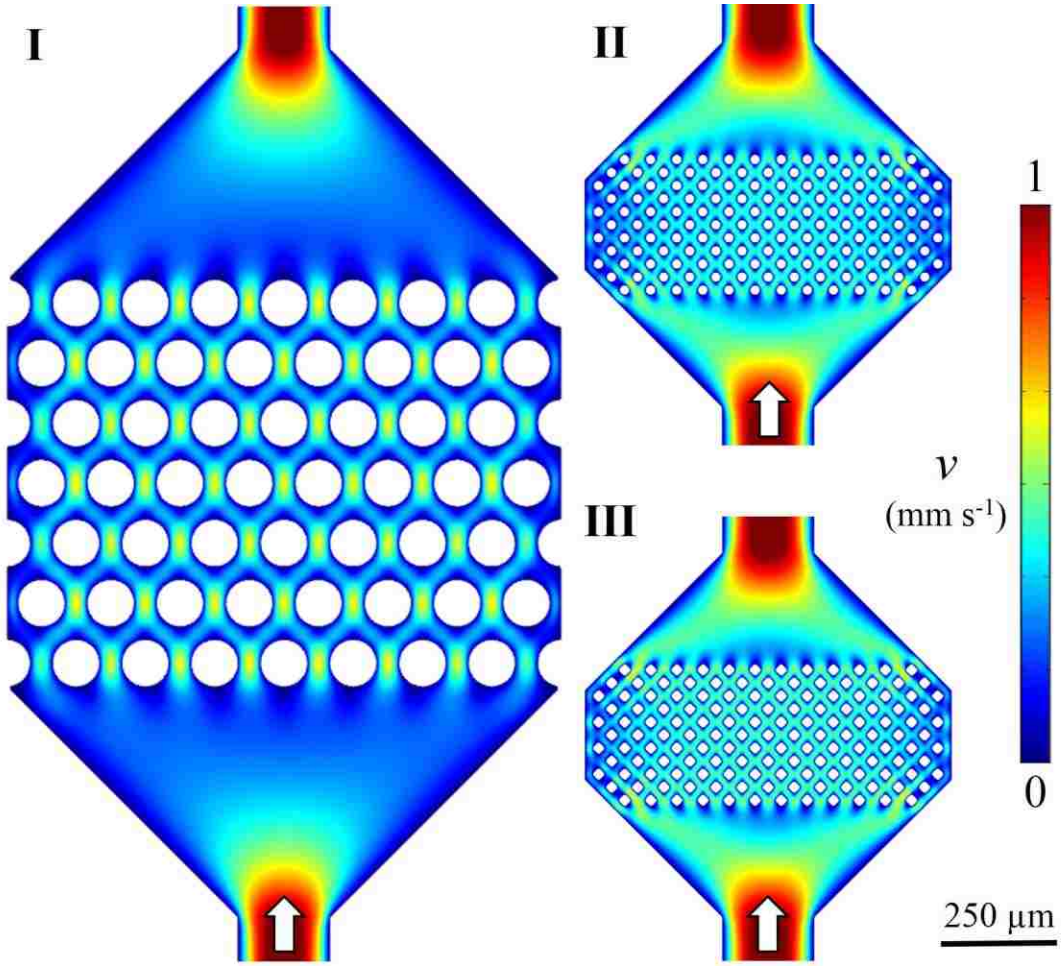

Figure 2.15 Velocity profiles of SPE bed geometries 1-III. Flow fields are scaled in both size and magnitude. Solid, white arrows indicate the direction of flow.

It was also evident that the flow's linear velocity is more homogenous throughout the μSPE beds for geometries II and III, an important point considering flow rate directly translates to protein mass flux. Thus, the beds with smaller posts may provide more uniform flow in addition to a higher surface area. Using these steady-state velocity fields, we conducted time-dependent simulations for the transport of a dilute protein (BSA) solution. These models were simulated for 17.5-25 s with a maximum time step of 0.01 s.

Additionally, the BSA protein was permitted to react with the microposts through biotin-avidin binding. The reaction of a biotinylated protein (B) with immobilized avidin (A) is governed by:

$$A+B \leftrightarrow AB \tag{1}$$

where *AB* is the avidin-biotin-protein complex, i.e., the captured protein. The rate of this encounter is balanced by the following equation:[49]

$$\frac{\mathrm{d[AB]}}{\mathrm{dt}} = \mathrm{k_{on}[A]_s([B]_{max}\text{-}[AB])\text{-}k_{off}[AB]} \tag{2}$$

The rate constants in Eq. (2) have been quantitated by surface plasmon resonance imaging, where k_{on} and k_{off} were found to be $8.7 \pm 0.3 \cdot 10^4$ M^{-1} s^{-1} and $7.2 \pm 0.5 \cdot 10^{-2}$ s^{-1}, respectively. These parameters reflect the entropic considerations of surface reactions; they favor the reactant state more than free solution kinetics.[50] Furthermore, we approximated the maximum surface density of extracted biotinylated membrane protein, $[B]_{max}$, as 6.85 pmol cm^{-2}. This is a one to one ratio with a theoretical monolayer of NeutrAvidin proteins and appropriately neglects the multivalency of avidin proteins due to steric effects between membrane proteins, which are of similar size to NeutrAvidin molecules.[51]

These constants and the rate expression in Eq. (2) were used in conjunction with the velocity fields and time-dependent protein transport to provide the time-lapse images in

Figure 2.16A-D. Line plots of the surface density of captured protein are also shown in Figure 2.16. This data indicates that for geometry I, less protein is initially captured on the rear surface area of the large, circular posts. However, this phenomenon is reduced after several seconds and the coverage of captured protein becomes more homogenous as it is for the other geometries. This is likely due to the reaction kinetics shown in Eq. (2).

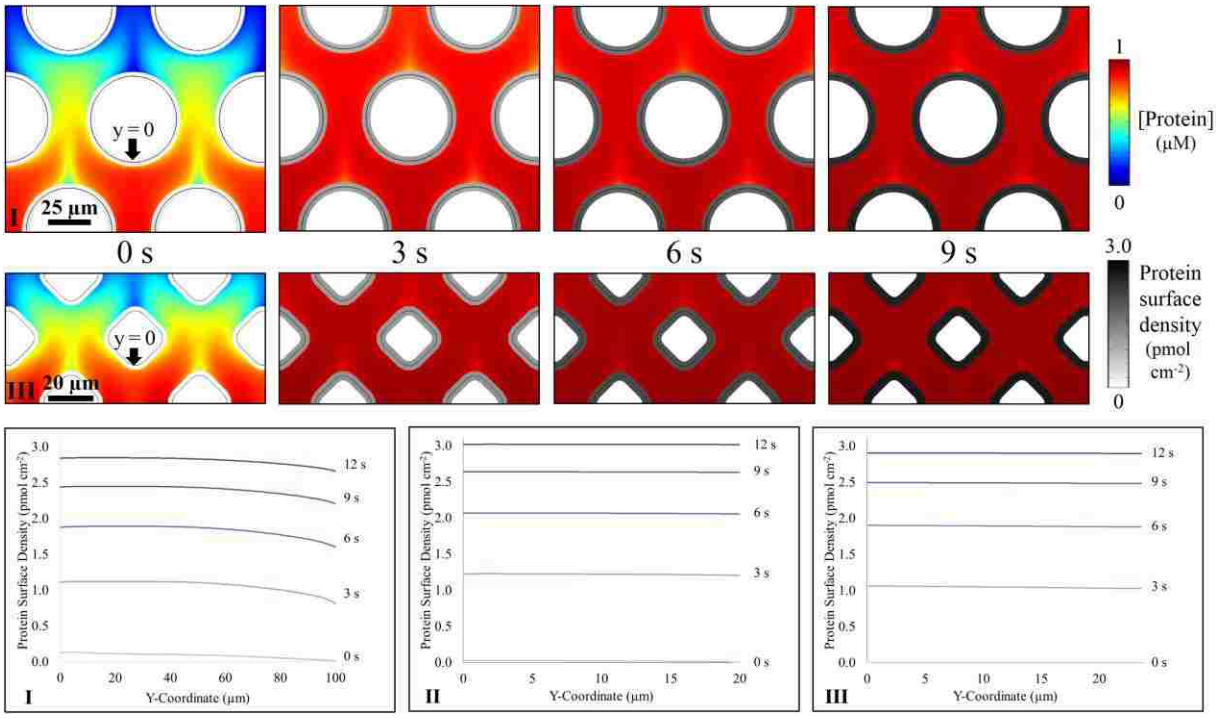

Figure 2.16 Time-dependent (with the first set of images arbitrarily assigned as 0 s) protein concentration profiles (A, rainbow scale), and surface densities of captured protein (B-D, grey scale along post borders) for SPE bed geometries III and I. Line plots of surface densities are presented for all three geometries against the spatial y-coordinate (illustrated in 0 s images).

Only protein flowing in laminar flow streams passing directly over the post surface has the potential to be affinity captured. Initially, protein in these flow streams may be depleted by the front of the posts before they reach the rear surface area of the post. But, over time the higher surface density of affinity captured protein on the front of the posts disfavors protein capture by Eq. (2), leaving more protein for capture on the rear of the posts. This would likely not be visible on the smaller posts in geometry II and III. However, they too

exhibited reduced reaction kinetics at longer times in the line plots in Figure 2.16. Because biotinylated protein were infused over the course of an hour, it is not likely that heterogeneous protein immobilization on the posts of geometry I would be experimentally observable nor were they (see Figure 2.9) or bear any consequence on the µSPE bed's performance for capturing biotinylated proteins from the whole cell lysate.

2.3.4.2 Diffusion Model for Approximating the Effects of Post Geometry on the Effective Bed Length

Due to computational limits, COMSOL was incapable of modeling an entire µSPE bed, but it is wise to assess how protein diffusion propagates throughout the µSPE bed's entire length (L = 24 mm). In general, diffusion of a protein is governed by Fick's 2nd law, where the probability (P) of occupying the axial position (x) at time (t) is dictated by its diffusion coefficient (D):

$$\frac{\partial \mathrm{P}}{\partial \mathrm{t}} = \mathrm{D}\frac{\partial^2 \mathrm{P}}{\partial \mathrm{x}^2} \tag{3}$$

An analytic solution to this differential equation is:

$$\mathrm{P}(\mathrm{x},\mathrm{t}) = \frac{1}{\sqrt{2\pi\sigma^2}}\mathrm{e}^{\left(-\frac{\mathrm{x}^2}{2\sigma^2}\right)} \tag{4}$$

where $P(x,t)$ is a Gaussian packet with standard deviation ($\sigma = \sqrt{2\mathrm{Dt}} = \sqrt{2\mathrm{DL}/\bar{\mathrm{v}}}$), where $\bar{\mathrm{v}}$ is the protein's average velocity throughout the µSPE bed. The probability packet $P(x,t)$ spreads in time, indicating that a protein molecule is more likely to occupy axial positions farther from its initial position.

However, the protein does not travel linearly through the bed, instead it will travel around the posts and effectively travel a distance of $\mathrm{L}_{\mathrm{eff}} = \mathrm{C}\cdot\mathrm{L}$, where C is a geometric correction factor intimately tied to the post shape. For circular posts, the protein will travel

about a half perimeter of the circle yielding $C = \pi/2 \approx 1.57$; for diamond posts, the protein travels about a triangle, yielding $C = \sqrt{2} \approx 1.41$; these assignments can be shown to be independent of the post size and are geometrically illustrated in Figure 2.17. Consequently, the effective path length of proteins in an SPE bed with circular posts is roughly twice that of one with diamond posts permitting twice the time for diffusion to increase the probability that proteins interact with the posts.

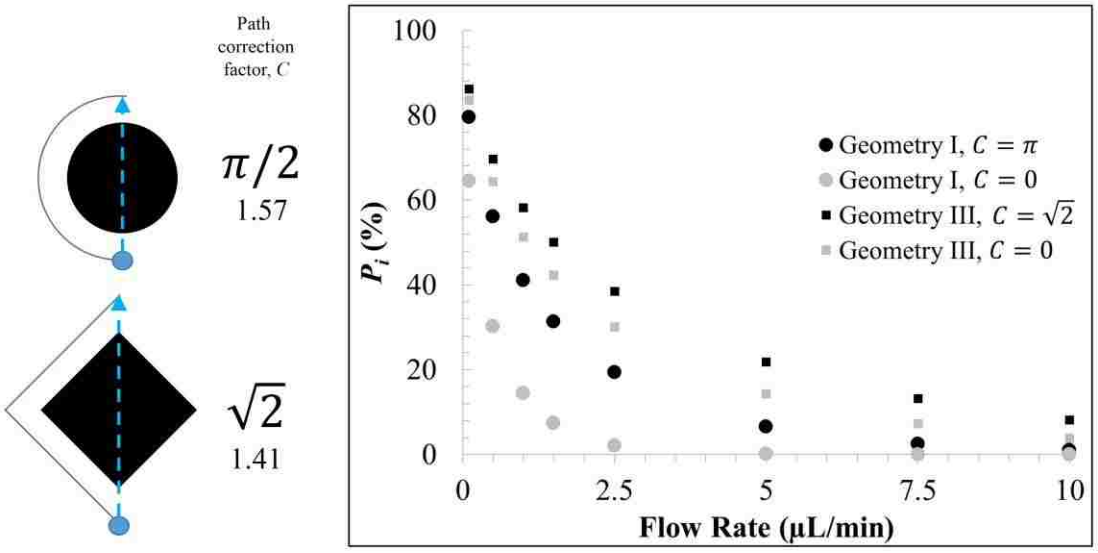

Figure 2.17 Schematic illustration of the path correction factor (C) for both circular and diamond posts. The probability of protein-post interaction (P_i) for geometries I and III, both with (solid black, where $C = \pi/2$ or $\sqrt{2}$) and without (solid grey, where $C = 0$) the path correction factor applied to the μSPE bed's length.

If we consider a worst case scenario, where a protein has the initial position exactly centered ($x = 0$) between two posts with spacing W_s (boundary conditions of $\pm W_s/2$), we can approximate that after the protein has passed through the μSPE bed, the probability that it has diffused to and interacted with the posts (P_i) is given by integration of the following equation:

$$P_i(t = C \cdot L/\bar{v}) = 2\int_{|x|=W_s/2}^{\infty} P(x, t = C \cdot L/\bar{v})dx \qquad (5)$$

The standard statistical method (shown in Figure 2.18) to perform this integration uses z-scores associated with the Gaussian packet, where $z(x) = x/\sigma$ and $P_{z(x)}$ is the normalized area of the Gaussian packet from -∞ to z(x). Thus, Eq. (5) can be simplified to:

$$P_i(t = C \cdot L/\bar{v}) = 1\text{-}\left[P_{z\left(x=\frac{W}{2}\right)}\text{-}P_{z\left(x=\frac{-W}{2}\right)}\right] \qquad (6)$$

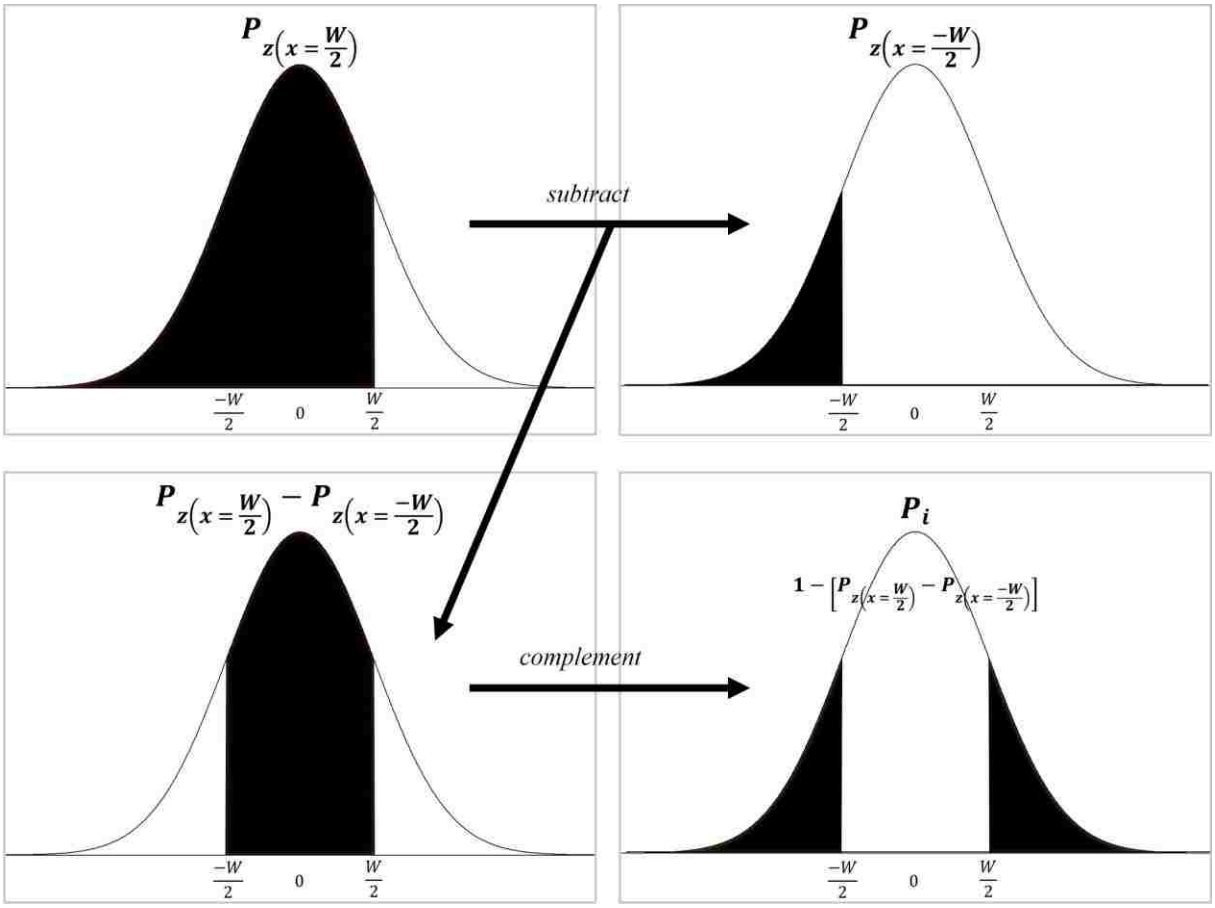

Figure 2.18 Schematic for extracting the probability of a protein interacting with SPE bed posts (P_i) from the Gaussian probability packets in the analytic solution of Fick's 2nd law.

Equation (6) can then be solved with a standard Excel spreadsheet by calculating $\sigma = \sqrt{2D \cdot C \cdot L/\bar{v}}$ then solving for $z\left(x = \pm\frac{W}{2}\right)$ and P_z using the NORMSDIST function in a standard Excel worksheet. In Figure 2.18, we show the solutions for geometries I and III. Here, we used the average velocities through the μSPE beds I and III that were obtained via

the simulation results in Figure 2.15 and scaled these velocities proportionally for higher flow rates. Also, we tested both geometries for the effect of applying the path correction factors. Note that this model approximates the protein's velocity as $\bar{v}$ irrespective of its axial position *x*, thereby ignoring Poiseuelle flow and under approximating diffusion effects.

In all cases, higher flow rates restrict protein diffusion and increase the probability that proteins will never contact the microposts and thus, not be recovered. Regardless of the path correction factor, geometry III outperforms geometry I in this model, predominately because the smaller spacing between posts in geometry III necessitates the protein to diffuse a shorter distance to contact a post. If the path correction factor is not applied, geometry I has a 20% higher probability of capturing the protein flowing at 0.1 μL $min,^{-1}$ and even with the path correction factor, which slightly enhances the performance of geometry I with respect to elongated protein path length for increased axial diffusion, geometry III remains optimal due to the small interpost spacing. In future developments of the μSPE geometry, circular posts with post spacing on the order of 10 μm (likened to geometry II) may enable increased throughput without detracting from the assay's efficiency.

2.4 Conclusion

A polymer microfluidic chip was designed, fabricated, and evaluated for the solid-phase extraction and purification of membrane proteins from a cell lysate generated from MCF-7 cells that were subjected to a biotinylation step prior to lysis. The μSPE assay was shown to produce significantly lower levels of cytosolic protein contamination compared to a commercially-available detergent method, which is based on liquid-liquid extraction. Furthermore, the surface activation protocol via UV-exposure was simple in execution and the production of bed containing polymer micropillars formed via hot embossing did not require

extensive post-fabrication steps to create the selection bed, such as the addition of functionalized beads or the formation of chemically modified polymer or monolithic supports. We were able to recover ~83% of the biotinylated protein fraction using 100 µm diameter circular posts that were spaced by 50 µm. The total load of protein for this bed geometry was determined to be 6.85 pmol cm^{-2}. While the total load is modest, this can be increased by reducing the post diameter and spacing.

The results secured using this novel µSPE device and assay for the extraction and purification of membrane proteins will provide a very attractive platform for future studies requiring the analysis of these proteins to determine potential therapeutic targets or selection agents for various cell types due to the higher purity fractions isolated and the ability to process small numbers of cells with high enrichment factors. For example, when the µSPE device is integrated to devices for multidimensional electrophoresis, solid-phase proteolytic digestion and mass spectrometry, top-down proteomic analysis of membrane proteins from rare cells can be undertaken, such as circulating tumor cells.

2.5 References

(1) Wu, C. C.; Yates, J. R., 3rd *Nat Biotechnol* **2003**, *21*, 262.

(2) Cooper, E. C.; Jan, L. Y. *Proc Natl Acad Sci U S A* **1999**, *96*, 4759.

(3) Almen, M. S.; Nordstrom, K. J.; Fredriksson, R.; Schioth, H. B. *BMC biology* **2009**, *7*, 50.

(4) Wallin, E.; von Heijne, G. *Protein science : a publication of the Protein Society* **1998**, *7*, 1029.

(5) Macher, B. A.; Yen, T. Y. *Molecular bioSystems* **2007**, *3*, 705.

(6) Brekke, O. H.; Sandlie, I. *Nature reviews. Drug discovery* **2003**, *2*, 52.

(7) Zheng, Y. Z.; Foster, L. J. *J Proteomics* **2009**, *72*, 12.

(8) Tan, S.; Tan, H. T.; Chung, M. C. *Proteomics* **2008**, *8*, 3924.

(9) Castle, J. D. *Current protocols in immunology / edited by John E. Coligan ... [et al.]* **2003**, *Chapter 8*, Unit 8 1B.

(10) Huber, L. A.; Pfaller, K.; Vietor, I. *Circ Res* **2003**, *92*, 962.

(11) Lawson, E. L.; Clifton, J. G.; Huang, F.; Li, X.; Hixson, D. C.; Josic, D. *Electrophoresis* **2006**, *27*, 2747.

(12) Ghosh, D.; Krokhin, O.; Antonovici, M.; Ens, W.; Standing, K. G.; Beavis, R. C.; Wilkins, J. A. *Journal of proteome research* **2004**, *3*, 841.

(13) Schindler, J.; Lewandrowski, U.; Sickmann, A.; Friauf, E.; Nothwang, H. G. *Molecular & cellular proteomics : MCP* **2006**, *5*, 390.

(14) Schindler, J.; Nothwang, H. G. *Proteomics* **2006**, *6*, 5409.

(15) McCarthy, F. M.; Cooksey, A. M.; Burgess, S. C. *Methods Mol Biol* **2009**, *528*, 110.

(16) McCarthy, F. M.; Burgess, S. C.; van den Berg, B. H.; Koter, M. D.; Pharr, G. T. *Journal of proteome research* **2005**, *4*, 316.

(17) Elia, G. *Methods Mol Biol* **2012**, *869*, 361.

(18) Wollscheid, B.; Bausch-Fluck, D.; Henderson, C.; O'Brien, R.; Bibel, M.; Schiess, R.; Aebersold, R.; Watts, J. D. *Nat Biotechnol* **2009**, *27*, 378.

(19) Robinson, J. M.; Ackerman, W. E. t.; Tewari, A. K.; Kniss, D. A.; Vandre, D. D. *Analytical biochemistry* **2009**, *387*, 87.

(20) Simonson, A. B.; Schnitzer, J. E. *J Thromb Haemost* **2007**, *5 Suppl 1*, 183.

(21) Rybak, J. N.; Ettorre, A.; Kaissling, B.; Giavazzi, R.; Neri, D.; Elia, G. *Nature methods* **2005**, *2*, 291.

(22) Scheurer, S. B.; Roesli, C.; Neri, D.; Elia, G. *Proteomics* **2005**, *5*, 3035.

(23) Scheurer, S. B.; Rybak, J. N.; Roesli, C.; Brunisholz, R. A.; Potthast, F.; Schlapbach, R.; Neri, D.; Elia, G. *Proteomics* **2005**, *5*, 2718.

(24) du Vigneaud, V., Hofmann, K., Melville, D. B., Rachele, J. R., *Journal of Biological Chemistry* **1941**, *140*, 763.

(25) du Vigneaud, V., Melville, D. B., Folkers, K., Wolf, D. E., et al. *Journal of Biological Chemistry* **1942**, *146*, 475.

(26) Melville, D. B., Moyer, A. W., Hofmann, K., du Vigneaud, V. *Journal of Biological Chemistry* **1942**, *146*, 487.

(27) Harris, S. A.; Wolf, D. E.; Mozingo, R.; Folkers, K. *Science* **1943**, *97*, 447.

(28) Trotter, J.; Hamilton, J. A. *Biochemistry* **1966**, *5*, 713.

(29) Livnah, O.; Bayer, E. A.; Wilchek, M.; Sussman, J. L. *Proc Natl Acad Sci U S A* **1993**, *90*, 5076.

(30) Weber, P. C.; Ohlendorf, D. H.; Wendoloski, J. J.; Salemme, F. R. *Science* **1989**, *243*, 85.

(31) Sabarth, N.; Lamer, S.; Zimny-Arndt, U.; Jungblut, P. R.; Meyer, T. F.; Bumann, D. *The Journal of biological chemistry* **2002**, *277*, 27896.

(32) Shin, B. K.; Wang, H.; Yim, A. M.; Le Naour, F.; Brichory, F.; Jang, J. H.; Zhao, R.; Puravs, E.; Tra, J.; Michael, C. W.; Misek, D. E.; Hanash, S. M. *The Journal of biological chemistry* **2003**, *278*, 7607.

(33) Tang, X.; Yi, W.; Munske, G. R.; Adhikari, D. P.; Zakharova, N. L.; Bruce, J. E. *Journal of proteome research* **2007**, *6*, 724.

(34) Zhang, W.; Zhou, G.; Zhao, Y.; White, M. A.; Zhao, Y. *Electrophoresis* **2003**, *24*, 2855.

(35) Zhao, Y.; Zhang, W.; Kho, Y.; Zhao, Y. *Anal Chem* **2004**, *76*, 1817.

(36) Elia, G. *Proteomics* **2008**, *8*, 4012.

(37) Wei, S.; Vaidya, B.; Patel, A. B.; Soper, S. A.; McCarley, R. L. *The journal of physical chemistry. B* **2005**, *109*, 16988.

(38) Figeys. D., D., A. and Aebersold, R. *Journal of Chromatography A* **1997**, *763*, 295.

(39) Jemere, A. B.; Oleschuk, R. D.; Ouchen, F.; Fajuyigbe, F.; Harrison, D. J. *Electrophoresis* **2002**, *23*, 3537.

(40) Witek, M. A.; Hupert, M. L.; Park, D. S. W.; Fears, K.; Murphy, M. C.; Soper, S. A. *Analytical Chemistry* **2008**, *80*, 3483.

(41) Lahiri, J.; Isaacs, L.; Tien, J. and Whitesides, G. *Analytical Chemistry* **1999**, *71*, 777.

(42) Green, N. M. *The Biochemical journal* **1965**, *94*, 23C.

(43) Vuong, G. L., Weiss, S.M., Kammer, W., Priemer, M., Vingron, M., Nordheim, A. and Cahill, M.A. *Electrophoresis* **2000**, *21*, 2594.

(44) Gygi, S. P., Rist, B., Gerber, S.A., Turecek, F., Gelb, M.H. and Aebersold, R. *Nature Biotechnology* **1999**, *17*, 994.

(45) Lion, N., Gellon, J.O., Jensen, H. and Girault, H.H. *Journal of Chromatography A* **2003**, *1003*, 11.

(46) Shigdarm S.; Qian, C.; Li, L..; Pu, C.; Li, Y.; Li, L.;, Marappan, M.; Lin, J.; Wang, L.; Duan, Wei. *PLoS One* **2013**, *8*, e57613.

(47) Prang, N.; Preithner, S.; Brischwein, K.; Göster, P.; Wöppel, A.; Müller, J.; Steiger, C.; Peters, M.; Baeuerle, P. A. and da Silva, A. J. *British Journal of Cancer* **2005**, *92*, 342.

(48) Raj, T.; Flygare, W. H. *Biochemistry* **1974**, *13*, 3336.

(49) Duan, X.; Li, Y.; Rajan, N. K.; Routenberg, D. A.; Modis, Y.; Reed, M. A. *Nature nanotechnology* **2012**, *7*, 401.

(50) D'Agata, R., Grasso, G., Spoto, G. *The Open Spectroscopy Journal* **2008**, *2*, 1.

(51) Kossek, S.; Padeste, C.; Tiefenauer, L. *Journal of molecular recognition : JMR* **1996**, *9*, 485.

3 Microchip Two-dimensional Membrane Protein Expression Profiling Using Laser-Induced Fluorescence

3.1 Introduction

A common method for protein analysis involves the use of two-dimensional electrophoresis that commonly employs an isoelectric focusing (IEF) dimension, which separates the proteins based upon differences in their isoelectric point (pI) using immobilized pH gradient strips (IPG), followed by sodium dodecyl sulfate polyacrylamide gel electrophoresis (SDS-PAGE), which sorts proteins through differences in their molecular weights (Figure 3.1). To determine the identity of the various proteins comprising these 2D maps, the spots can be subjected to high resolution MS/MS analysis (top-down proteomics) or digested via proteolytic enzymes followed by MS analysis (bottom-up proteomics).[27] Complex biological samples, such as blood serum and cell lysates, hold great promise for clinical diagnostics. The wide range of protein components that can potentially exist in complex biological samples makes it difficult to analyze these types of materials using one-dimensional (1D) separations due to the limited peak capacity provided by these separation platforms.

As noted by Giddings,[2] the combination of two *different* separation techniques can provide a significantly higher peak capacity, P, than the individual 1D mechanisms as long as the dimensions compromising the multi-dimensional separation are orthogonal, which means that the selected dimensions possess different, but compatible, separation mechanisms. Furthermore, the subsequent dimension in any multi-dimensional separation should not destroy the resolution achieved by the previous one. If the separation mechanisms of the multi-dimensional separation are orthogonal, the product of the peak capacity contained within the individual separation dimensions gives the number of resolved components.[3] Although IEF/SDS-PAGE continues to be the main separation method for many proteomic

studies, there are still drawbacks associated with utilizing the technique. IEF/SDS-PAGE is a time-consuming and laborious process involving extensive gel pouring and pH gradient formation as well as long operational times (>24 h) to generate the required 2D map. Moreover, after the separation, protein bands require staining for visualization and subsequent band excision from the gel for follow-up identification purposes, which can result in sample loss.[4,5] In addition, membrane proteins tend to be excluded when using IEF/SDS-PAGE due to their poor solubility in the buffering system utilized,[6,7] and the staining and visualization techniques associated with IEF/SDS-PAGE often do not detect proteins that are typically low in abundance due to limitations in the mass detection limits.[8]

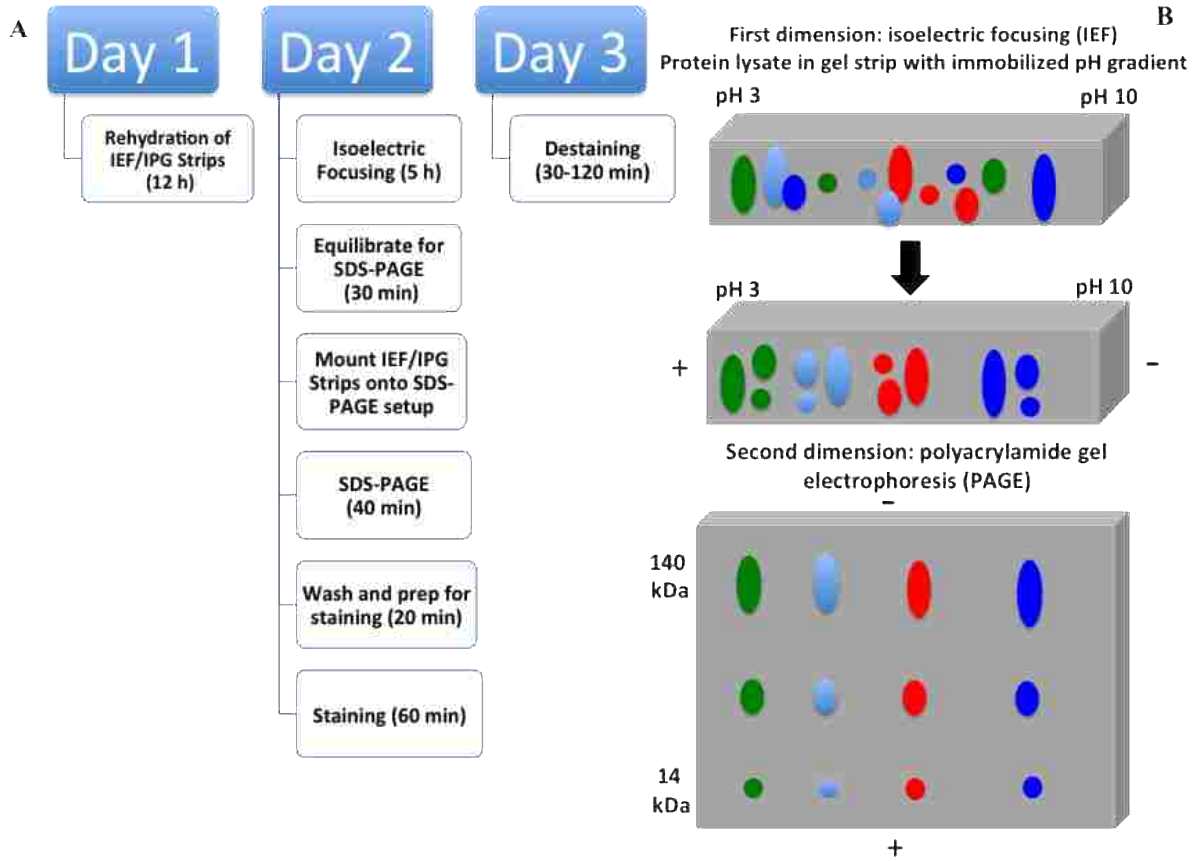

Figure 3.1 Workflow of traditional 2D IEF/SDS-PAGE and a schematic of the two separation mechanisms.

Because of the drawbacks of 2D IEF/SDS-PAGE, researchers focused their efforts toward the use of capillary-based 2D separations using various combinations of electrophoresis or chromatography methods. Examples of these types of 2D platforms include capillary sieving electrophoresis coupled to micellar electrokinetic capillary chromatography,[9-11] nano-reverse phase liquid chromatography coupled to strong cation exchange chromatography,[12] and size-exclusion liquid chromatography coupled to reverse phase liquid chromatography[13] have all been used for the analysis of proteins by researchers.

While capillary-based multi-dimensional separation reports have shown success in eliminating tedious tasks such as gel pouring and reducing the development time of electrophoresis, the increasing demands on proteomic studies have compelled the need to further reduce development times, process smaller sample volumes, generate higher throughput by performing multiple separations in parallel, and integrate front-end processing to the 2D separation. Therefore, the techniques encompassing microchip capillary electrophoresis (μ-CE) have been considered as attractive alternatives to their traditional capillary counterparts.

3.1.1 2D Separations on Microfluidic Chips

Microchip 2D separations offer automation capabilities and rapid separations with high resolving power as opposed to the conventional slab gel techniques (IEF/SDS-PAGE). They can also provide viable interfaces between the separation dimensions to minimize unswept volumes between separation dimensions preserving plate numbers. The separation efficiencies are high in μ-CE due to effective heat dissipation, the ability to use higher electric field strengths, minimal sample consumption due to smaller footprints, and faster times because of shorter column lengths. Li *et al.*[14] integrated IEF with parallel sodium dodecyl

sulfate micro-capillary gel electrophoresis (SDS μ-CGE) for a comprehensive 2D separation of five model proteins and generated a peak capacity of ~1,700 in 10 min. Chen *et al.*[15] described a microfabricated 2D IEF/SDS-PAGE system that separated three model proteins a little under 2 min.; however, the peak capacity was not reported. Yang and collaborators[16] reported a 2D IEF/SDS-PAGE separation of whole cell *E. coli* protein lysate with an estimated peak capacity of 2,880 that was obtained within 12 min.

All of the abovementioned examples of microchip 2D employed IEF in the first dimension. Regrettably, IEF requires an equilibration step before the focusing step,[16] which in turn increases the overall development times of the entire 2D separation. Additionally, IEF is not compatible with highly hydrophobic proteins (membrane proteins) as they are not compatible with the aqueous buffers required for IEF. To avoid some of the issues associated with using IEF, alternative techniques such as CZE or micellar electrokinetic chromatography (MEKC) have been employed.

Ramsey and co-workers[17] separated peptides with a 2D microchip system that combined open-channel electrochromatography (OCEC) with CZE in which they reported a peak capacity of 150 that was obtained in 13 min. The same group also utilized glass microfluidic devices to perform 2D separations of bovine serum albumin tryptic digest.[18] A MEKC separation was performed in 19.6 cm-long serpentine channel with the peptides rapidly sampled into a 1.3 cm long second dimension channel where they were separated by CE. Figure 3.2 shows the device employed for the separations. The turns in the serpentine channels were asymmetrically tapered to minimize geometrical contributions to band broadening and they provided ample channel length for high-efficiency chromatographic separations.

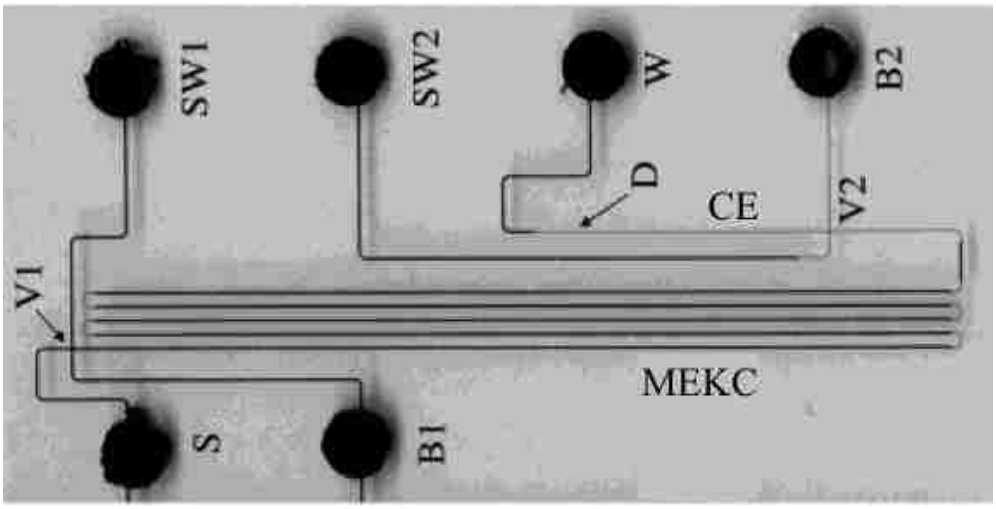

Figure 3.2 Image of the microchip used by Ramsey *et al*. Injections were made at valve 1 (V1) for the first dimension MEKC separation and at valve 2 (V2) for the second dimension CE separation. Detection of the sample was done at 1 cm downstream from V2 at point D using laser-induced fluorescence. The reservoirs are labeled sample (S), buffer 1 (B1), sample waste 1 (SW1), buffer 2 (B2), sample waste 2 (SW2), and waste (W). (Reproduced from Ramsey, J. D.; Jacobson, S. C.; Culbertson, C. T.; Ramsey, J. M. *Anal Chem* **2003**, *75*, 3758.[18] with permission, Copyright 2013, American Chemical Society).

The electric field strengths were 200 V/cm for MEKC and 2,400 V/cm for CE. A peak capacity of 4,200 (110 in the first dimension and 38 in the second dimension) was reported for the 2D separation of bovine serum albumin tryptic digest with an analysis time of less than 15 min.

The use of microemulsions in microemulsion electrokinetic chromatography (MEEKC) has also emerged as an attractive alternative to MEKC. It was first introduced by Watarai *et al*.[19] in 1991 for the separation of fluorescent aromatic compounds and has been widely applied for the separation of various analytes including proteins.[20-23] The separation medium in MEEKC is a microemulsion, which is a transparent solution consisting of an oil (*i.e*., n-heptane), a surfactant (*i.e*., SDS), a co-surfactant (*i.e*., n-butanol), and water. The structure of oil in a water emulsion is similar to that of micelles in MEKC except the microemulsion has an oil droplet as a core.[23]

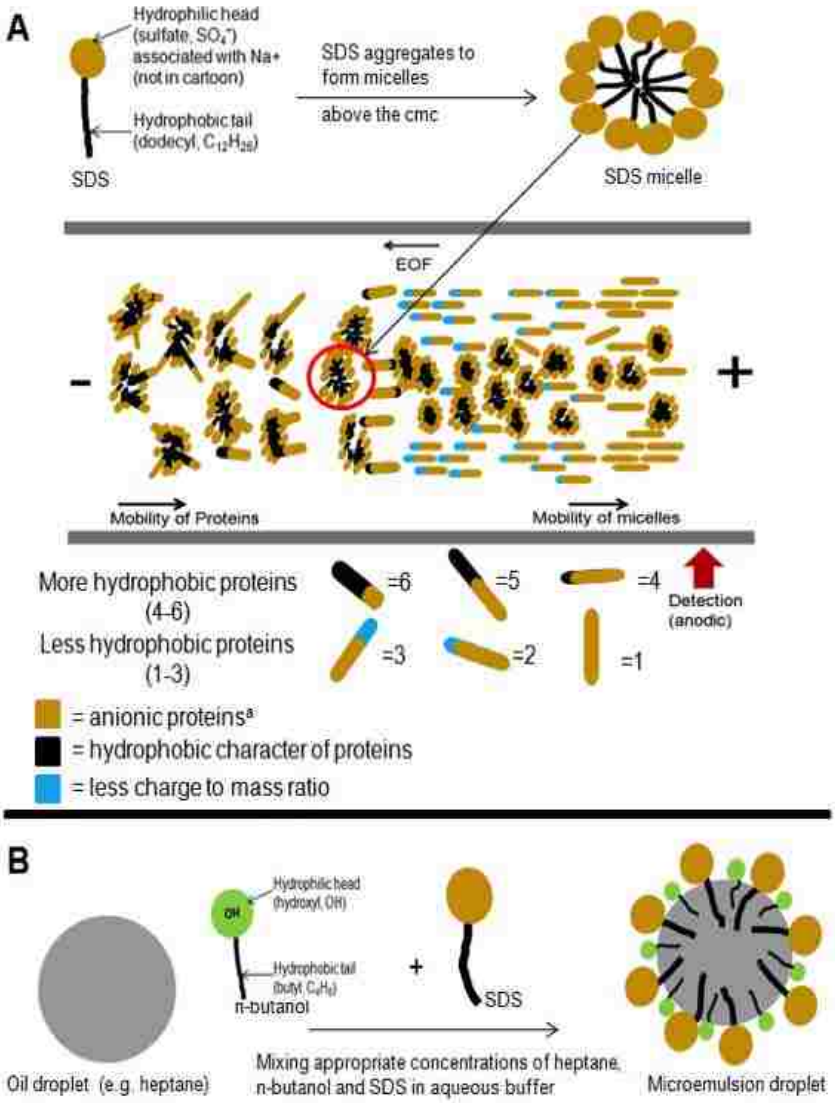

Figure 3.3 (A) Depiction of micelle formation in aqueous buffer and its utilization in the second dimensional phase have a microchip 2D SDS µ-CGE and MEKC protein separation. (B) Depiction of microemulsion formation in aqueous buffer and its utilization in the second dimensional phase of a microchip 2D SDS µ-CGE and MEEKC protein separation. *a = anionic proteins acquire their charge in two ways: (1) because the pH conditions for the separation is above their pKa and (2) because SDS imparts a negative charge on the proteins during sample prep and during the first dimension separation.* (Reproduced from Osiri, J. K.; Shadpour, H.; Soper, S. A. *Anal Bioanal Chem* **2010**, *398*, 489 with permission, Copyright 2013, Springer Science and Business Media).

Figure 3.3 depicts the formation of micelles in aqueous buffer, its employment in the second dimensional phase of 2D SDS µ-CGE and MEKC protein separation, and how microemulsions are formed. The SDS micelles form in buffer above the SDS cmc, critical micellar concentration (0.24% w/v). The aggregate number for SDS is about 62 molecules

forming a core diameter of ~17Å. In a reverse polarity mode (detection is anodic), SDS micelles migrate towards the anode due to their ionized sulfate group, which is negatively charged, whereas the direction of EOF is towards the cathode. Separation in the MEKC is based on the differences in the partition coefficient of proteins within the micelles and the aqueous phase and according to the mass-to-charge ratio of proteins when they are in the aqueous medium.

More hydrophobic domains within a protein result in stronger hydrophobic character and the more hydrophobic proteins have a tendency to interact more with the micellar core. On the other hand, anionic proteins experience columbic repulsion and may not interact with the micelles. This is especially true when their hydrophobic domains are masked by SDS (see rods that are gold only or gold/blue without any black color). These proteins are separated based on their electrophoretic mobility in the aqueous medium with the proteins possessing the highest charge-to-mass ratio migrating the fastest.

Overall, the migration of proteins is in the order of 1-6 with protein 1 migrating the fastest and protein 6 migrating the slowest. In MEEKC, SDS surfactants impart a net negative charge to the oil emulsions, and the co-surfactant (n-butanol) reduces the surface tension between the oil and the aqueous phase, which results in a miscible oil/water system. The hydrophobic core diameter for the microemulsion is ~100Å.

3.1.2 Previously Reported Work Employing SDS µ-CGE with MEKC for 2D Separations

The Soper research group has reported 2D microchip separations using SDS µ-CGE with both MEKC and MEEKC. In 2006, Shadpour and Soper described two-dimensional electrophoretic separations of proteins in a PMMA-based microchip. SDS µ-CGE (SDS 14-200 sieving matrix with 12 mM Tris-HCl, 0.1% w/v (3.5 mM) SDS, pH 8.5, containing

0.05% MHEC, methyl hydroxyl ethyl cellulose) and MEKC (12 mM Tris-HCl, 0.4 % w/v (14 mM) SDS, pH 8.5, containing 0.05% MHEC) were used as the separation modes in the first and second dimension of the electrophoresis, respectively. The use of MHEC aids in the suppression of the electroosmotic flow (EOF) while preserving the selectivity of the separation. The electrophoretic separations were carried out at ambient temperature in reverse mode (detection end anodic).

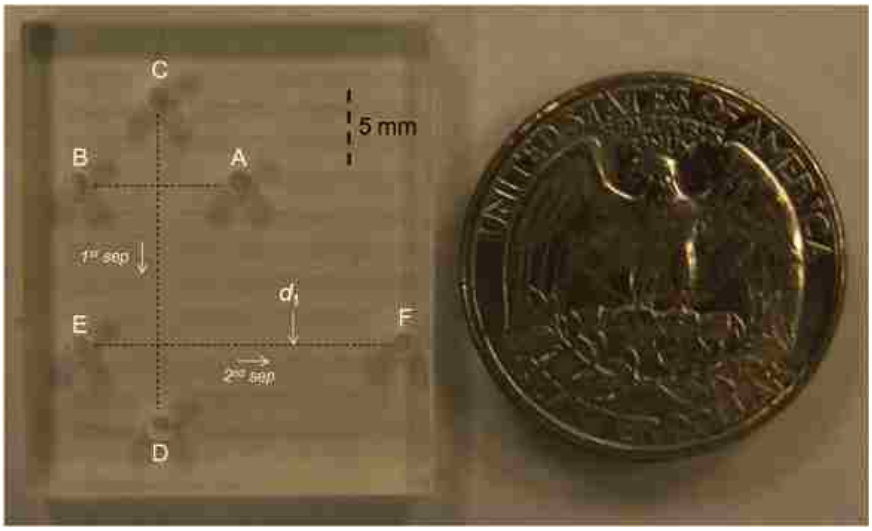

Figure 3.4 Photograph of the PMMA µ-capillary electrophoresis chip used for the 2D separations. The channel width in all cases was 15 µm with a channel depth of ~30 µm. The solution reservoirs were; (A) sample reservoir; (B) sample waste reservoir; (C) SDS µ-CGE buffer reservoir; (D) SDS µ-CGE buffer waste reservoir; (E) MEKC or MEEKC buffer reservoir; (F) MEKC or MEEKC buffer waste reservoir. d_1 represents the LIF detection position for the 2D separations. (Reproduced from Shadpour, H.; Soper, S. A. *Anal Chem* **2006**, *78*, 3519.[24] with permission, Copyright 2013, American Chemical Society).

The PMMA microchip (Figure 3.4) incorporated a 30-mm SDS µ-CGE and a 10-mm MEKC dimension length and electrokinetic injection and separation were used with field strengths of up to 400 V/cm. Platinum wires were used to apply high voltages to the reservoirs. For the SDS µ-CGE dimension, the injection and effective separation lengths were each 10 mm. The total separation channel length for a complete 2D separation was 20 mm (*i.e.*, 10 mm for both the 1st and 2nd dimensions). The 30 nM protein mixture consisted of 10

Alexa Fluor 633 conjugated proteins (wheat germ agglutinin (WG), actin (AC), ovalbumin (OV), protein A (PA), streptavidin (ST), bovine serum albumin (BSA), *Helix pomatia* (HPA), transferrin (TR), concanavalin A (CO), and lectin peanut agglutinin (PNA), ranging in size from 38 to 110 kDa, detected using laser-induced fluorescence with excitation/emission at 633/652 nm. They reported plate numbers (N) of 4.8×10^4 and 1.2×10^4 in the SDS µ-CGE and MEKC separation dimensions, respectively, for the proteins corresponding to plate heights (H) of 0.62 and 0.87 µm.

Both the SDS µ -CGE (1D separation) and MEKC (1D separation) are shown in Figure 3.5. The electropherograms suggest that the proteins that are closer in MW comigrate and are not resolved from one another indicating the need for a 2D separation that can provide improved resolution. The time to start the second dimension (MEKC) depends on the migration time (MT) of the smallest protein or co-migrated proteins in the SDS µ-CGE dimension. The migration time can be estimated by using Eq 1. for the smallest component (lowest MW) in any given mixture. For this work, the estimated MT was ~71 s for WG, which was the smallest protein (38,000 Da) in the mixture. Therefore, the first MEKC cycle was set to start at 70 s.

$$\log (MW) = 1.59 \times 10^{-2} MT + 3.45 \quad (1)$$

The MEKC cycles were performed by proper switching of the high voltage applied to points E and F (see Figure 3.4). The word "cycle" refers to a complete MEKC electrophoretic run that was used for the second dimension.

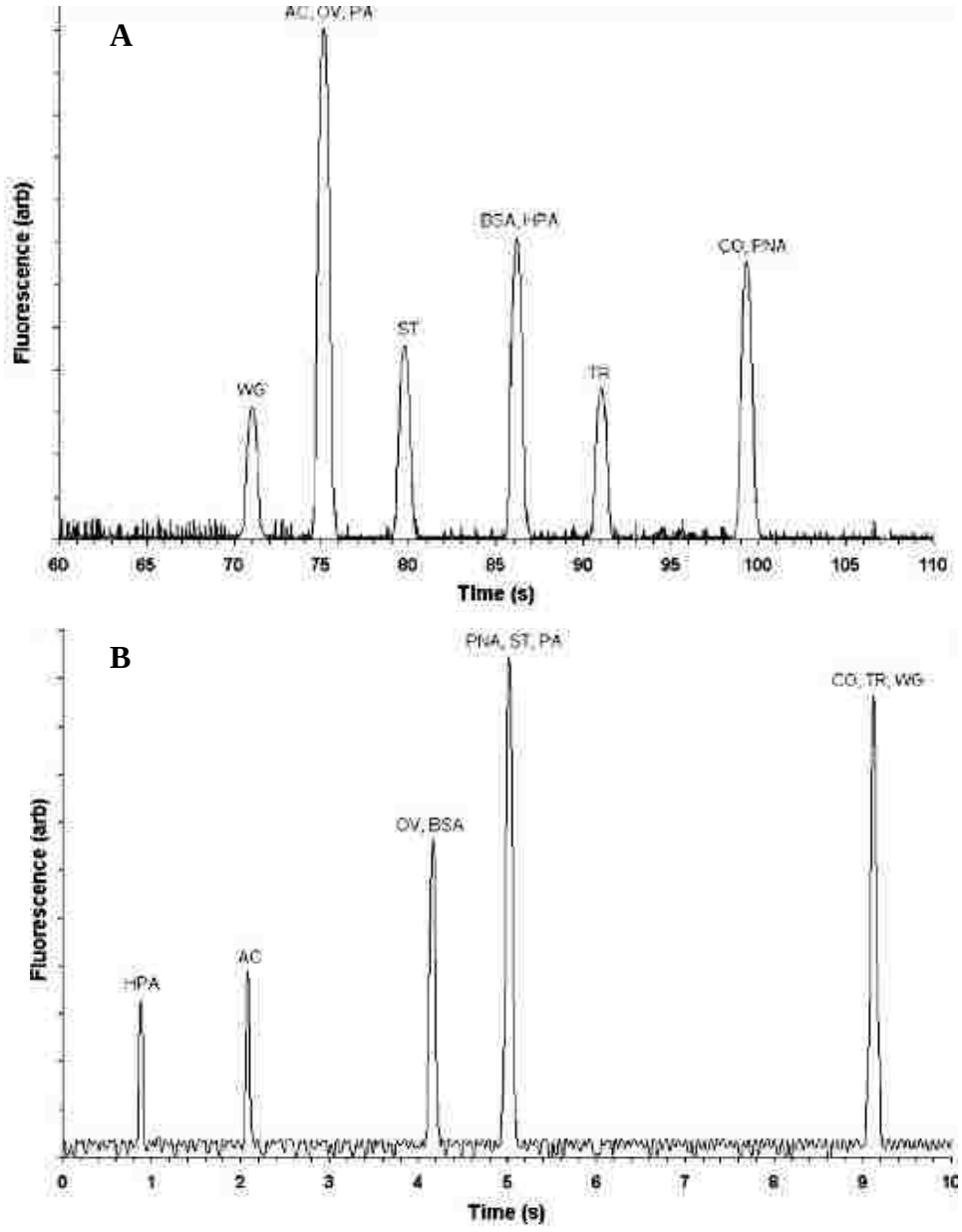

Figure 3.5 (A) SDS µ-CGE analysis (1D separation of a 30 nM protein mixture using the PMMA microchip. (B) The MEKC separation (1D) of a 30 nM protein mixture using the PMMA microchip. (Reproduced from Shadpour, H.; Soper, S. A. *Anal Chem* **2006**, *78*, 3519.[24] with permission, Copyright 2013, American Chemical Society).

Based on all proteins eluting from the MEKC channel within a 10 s separation window, the MEKC cycles were then fixed at 10 s. For different protein mixtures, longer separation windows could be selected at the expense of longer 2D development times. The linear output of the detector from 2D analysis and three-dimensional images of the 2D µ-CE

separation are shown in Figure 3.6. It can be seen that the 2D analysis was able to resolve all 10 proteins in the mixture, including those species that could not be separated using individual 1D separations under similar experimental conditions.

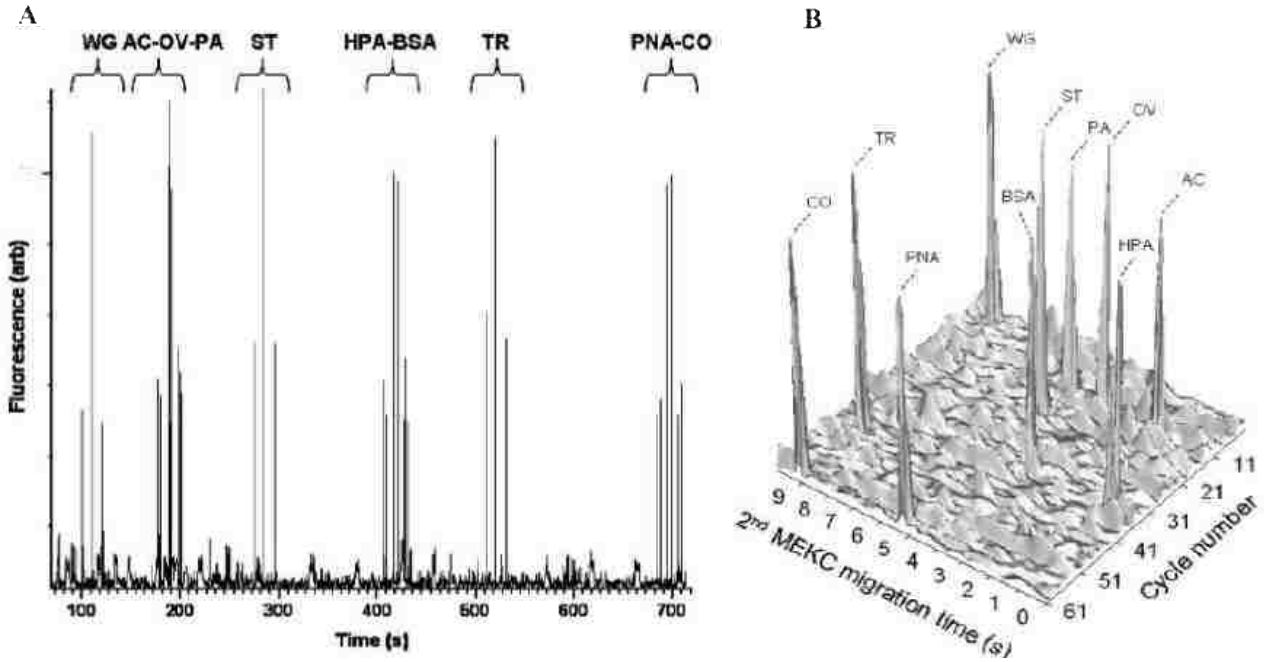

Figure 3.6 2D μ-CE separation of a 30 nM protein mixture in the PMMA microchip. (A) Linear output of the LIF 632.8 nm detector system from the 2D analysis of the protein sample (B) A three-dimensional image of the data shown in A with the cycle number plotted versus the MEKC migration time. (Reproduced from Shadpour, H.; Soper, S. A. *Anal Chem* **2006**, *78*, 3519.[24] with permission, Copyright 2013, American Chemical Society).

For some time, most of the μ-CE examples were focused on demonstrating proof-of-concept of the multidimensional separation using model systems, which can limit the number of components analyzed with the constituents present in similar concentrations, both of which do not represent "true" biological samples. Therefore, Osiri and co-workers[25] also reported 2D profiling of fetal calf serum (FCS) proteins within 30 min using SDS μ-CGE in the first dimension and μ-MEKC in the second dimension. The FCS proteins were covalently labeled with a thiol-reactive AlexaFluor 633 dye prior to the μ-CE 2D separation and detected using laser-induced fluorescence (LIF). The sample was electrokinetically injected into the

separation channel at 200 V/cm with the 2D SDS µ-CGE × MEKC separations in the first and second dimensions performed at 300 V/cm and 400 V/cm respectively.

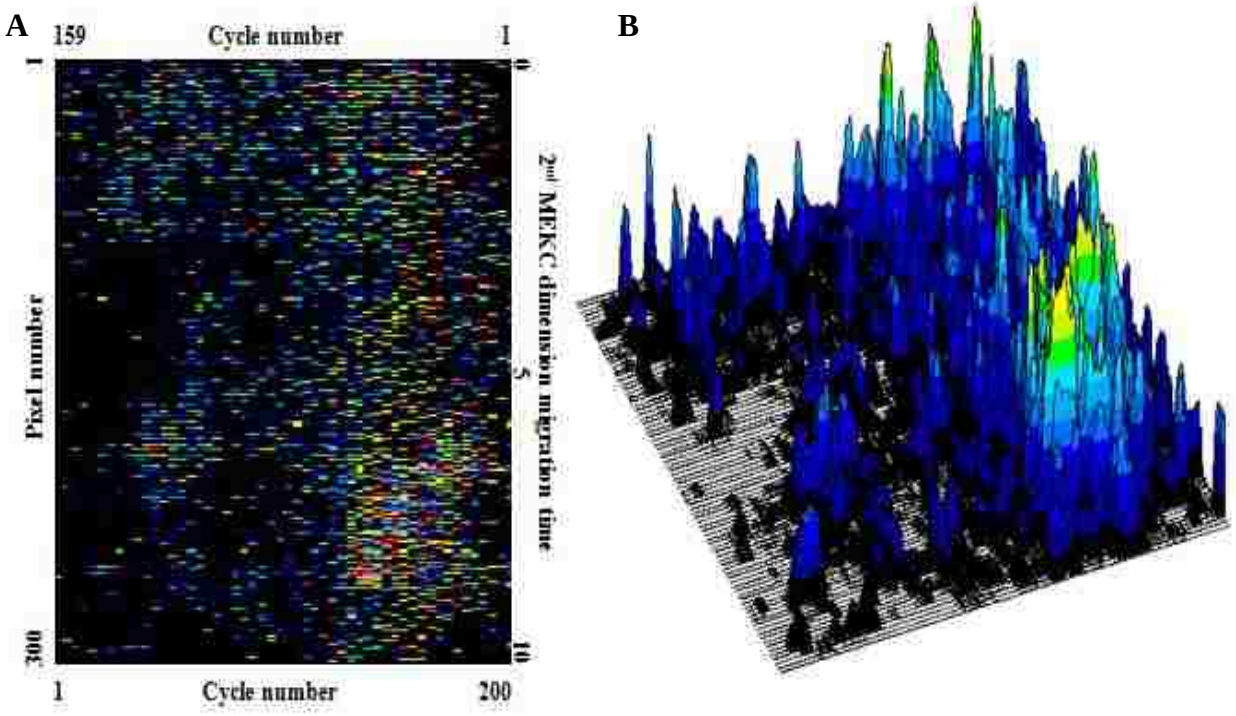

Figure 3.7 SDS µ-CGE/µ-MEKC 2D separation of a FCS protein mixture. The 2D SDS µ-CGE × MEKC were performed at 300 V/cm and 400 V/cm, respectively. (A) 2D image of the microchip FCS map. (B) 3D landscape of the FCS proteins. Reproduced from Osiri, J. K.; Shadpour, H.; Park, S.; Snowden, B. C.; Chen, Z. Y.; Soper, S. A. *Electrophoresis* **2008**, *29*, 4984.[25] with permission, Copyright 2013, John Wiley & Sons).

The SDS µ-CGE was performed utilizing an effective length, the length used for the separation, L_{eff} = 60 mm while the µ-MEKC separation employed L_{eff} = 50 mm. The results of the 2D separation are shown in Figure 3.7. The authors reported a peak capacity for the 2D separation of 2,600 (±149).

Separations on microfluidic platforms have garnered much appeal for the analysis of complex biological samples because they can easily lend themselves to performance characteristics that rival their macroscale counterparts using a much shorter operational time, but still generating much improved data production rates. In addition, these formats, due to

their small footprint and lithographic fabrication techniques, will permit the development of multi-channel formats that can significantly improve the production rate of data. In the aforementioned report, our lab has demonstrated the ability to generate peak capacities of 2,600 (±149) for a biological serum sample using an 11 cm effective separation length in both dimensions. Although the peak capacity is well below the number of protein components typically found in a serum proteome, it is still attractive for the analysis of a complex sample such as serum. In addition, the isolation of sub-populations of protein types, such as membrane proteins, is also appealing for this peak capacity and the analysis of a sample of cell lysate.

Therefore, in this work, we report the use of a polymer-based microchip for 2D profiling of the membrane protein fraction of MCF-7 cell lysates with sufficient peak capacities using SDS μ-CGE in the first dimension and μ-MEKC in the second dimension. The readout strategy relied upon the employment of laser-induced fluorescence (LIF), which was accomplished by covalently labeling the MCF-7 membrane proteins with an amine-reactive DyLight NHS Ester 550 dye prior to the μ-CE 2D separation. The SDS μ-CGE was performed using L_{eff} = 30 mm while the μ-MEKC separation utilized L_{eff} = 40 mm. We then compared our μ-CE separation results with results reported in literature on the conventional 2D IEF/SDS-PAGE of MCF-7 cell lysate.

3.2 Materials and Methods

3.2.1 Microchip Fabrication

PMMA was selected as the μ-CE substrate because of its suitable physiochemical properties for this application, such as minimal non-specific adsorption artifacts and low levels of autofluorescence, improving the detection limits for ultra-sensitive fluorescence

detection. Microchips were made according to procedures described previously. In brief, microstructures were micromilled into a brass plate (0.25" thick alloy 353 engravers brass, McMaster-Carr, Atlanta, GA, USA) using a Kern MMP 2522 micromilling machine (KERN Mikro-und Feinwerktechnik GmbH & Co., Germany).

Once fabricated, the mold master produced PMMA replicates using hot-embossing. Hot-embossing required heating the molding tool to 155°C and pressed into the PMMA plate with a pressure of 1,100 psi for 4 min using a PHI Precision Press (PHI-Tulip, City of Industry, CA, USA). Following embossing, the PMMA substrate was cooled to room temperature and removed from the molding die. The embossed PMMA substrate was cleaned with 50% isopropanol in ultrapure water. Finally, a PMMA cover plate (0.250 mm) was thermal fusion bonded to the substrate by heating in a temperature programmable furnace to 107°C, slightly above the Tg of PMMA. Figure 3.8A shows the topographical layout of the microdevice used for this work. All channels were 50 µm deep and 50 µm wide. Buffer, sample, or waste reservoirs are shown in Figure 3.8A, in which letters A to F are representative of the 1.5 mm diameter solution reservoirs on the PMMA microchip.

3.2.2 Laser-induced Fluorescence (LIF) Detection, Power Supply and Data Analysis

Fluorescence detection was accomplished using an in-house constructed LIF system. A schematic diagram of this detection system is shown in Figure 3.8B. The excitation source consisted of a laser diode with a lasing wavelength of 532 nm (LBS-532-TD-5, Laserglow Technologies, Toronto, ON, Canada). The diode laser light was filtered using a laser line filter (LLF1, CWL = 532 nm, XL08, Omega Optical, Brattleboro, VT, USA).

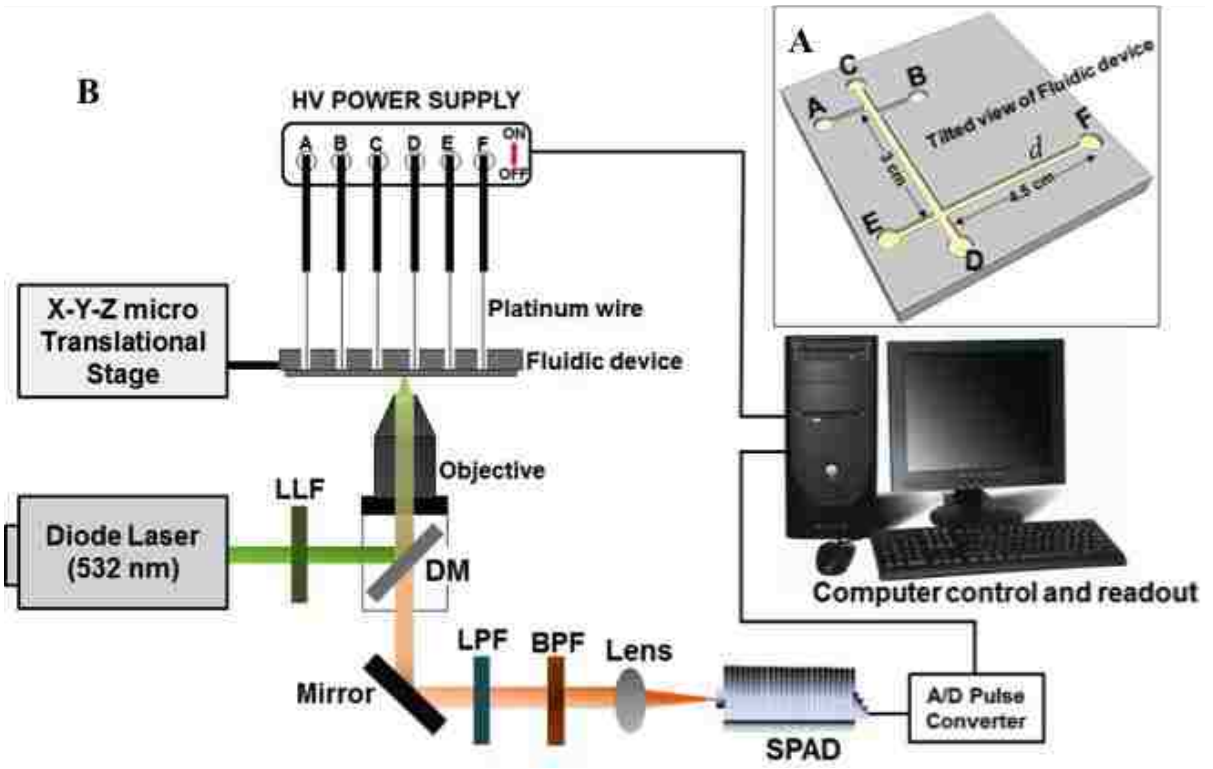

Figure 3.8 (A) Schematic of the 2D microchip electrophoresis device used for these studies. The channels were 50 µm deep and 50 µm wide in all cases. The 1st and 2nd dimension channels were 4 cm (filled with gel media) and 5 cm (filled with MEKC buffer), respectively, in terms of their total column lengths. The effective column lengths for the 1st and 2nd dimensions were 3 cm and 4 cm, respectively. (B) Diagram of the in-house constructed LIF system used for the µ-CE separation. The system was configured in an epi-illumination format and was equipped with a 40x microscope objective (NA = 0.65) used to focus the laser excitation radiation into the micro-separation channel and collect the resulting fluorescence as well (epi-illumination). An x-y-z micro-translational was used to position the chip above the objective. A 532 nm diode laser served as the excitation source.

A dichroic mirror (XF2018, Omega Optical) reflected the 532 nm and the laser light beam was directed into a focusing objective using a second dichroic mirror (XF2055, Omega Optical). The excitation beam was focused utilizing a 40x microscope objective (Nikon, Natick, MA, USA) into the separation channel of the microchip, which was situated on an *x, y, z* micro-translational stage (Newport, Irvine, CA, USA). The fluorescence emission resulting from the DyLight 550 labeled membrane proteins was collected by the same objective and transmitted through the dichroic, reflected onto another dichroic mirror (DMLP605, Thorlabs, Newton, NJ, USA) and finally filtered through a filter stack containing

a long pass filter (CWL = 550 nm, 3RD550LP, Omega Optical) and a band pass filter (CWL = 570 nm, XB99, Omega Optical).

The resulting photons were transduced employing a single photon avalanche diode (SPAD; SPCM 200B, PicoQuant, Berlin, Germany). Programmed high-voltage was applied to the reservoirs of the microchip with six independently controlled power supplies (EMCO, Sutter Creek, CA, USA). Electrical contact between the solution in the fluid reservoirs and the high-voltage leads was achieved utilizing platinum wires (Scientific Instrument Services, Ringoes, NJ, USA). The LIF signals were acquired on a personal computer equipped with an I/O interface board (CB-68LP, National Instruments, Austin, TX, USA) and a pulse converter (TB-01, IBH, Glasgow, UK). The software for data acquisition and control of the power supply was created using LabView. The LabView program interface is shown in Figure 3.9. Dye-labeled protein samples were first electrokinetically injected into the injection cross (A-B, Figure 3.8A) by applying a positive potential at waste reservoir (B) while grounding the sample reservoir (A). Data were collected continuously from the start of the initial SDS µ-CGE after the injection step. SDS µ-CGE was initiated by applying a positive potential at the waste reservoir (D) and grounding reservoir C.

In this particular case, proteins were sampled into the second dimension from the onset of the first dimension; therefore, proteins were allowed to separate in the second dimension after a 3 s electrophoretic run in the first dimension by applying a positive potential to reservoir E while grounding D. This 3 s separation in the first dimension transferred proteins into the second dimension for further separation. LIF was monitored on E-F at 40 mm (*d*, see Figure 3.8A) from the intersection of C-D and E-F (see Figure 3.8A).

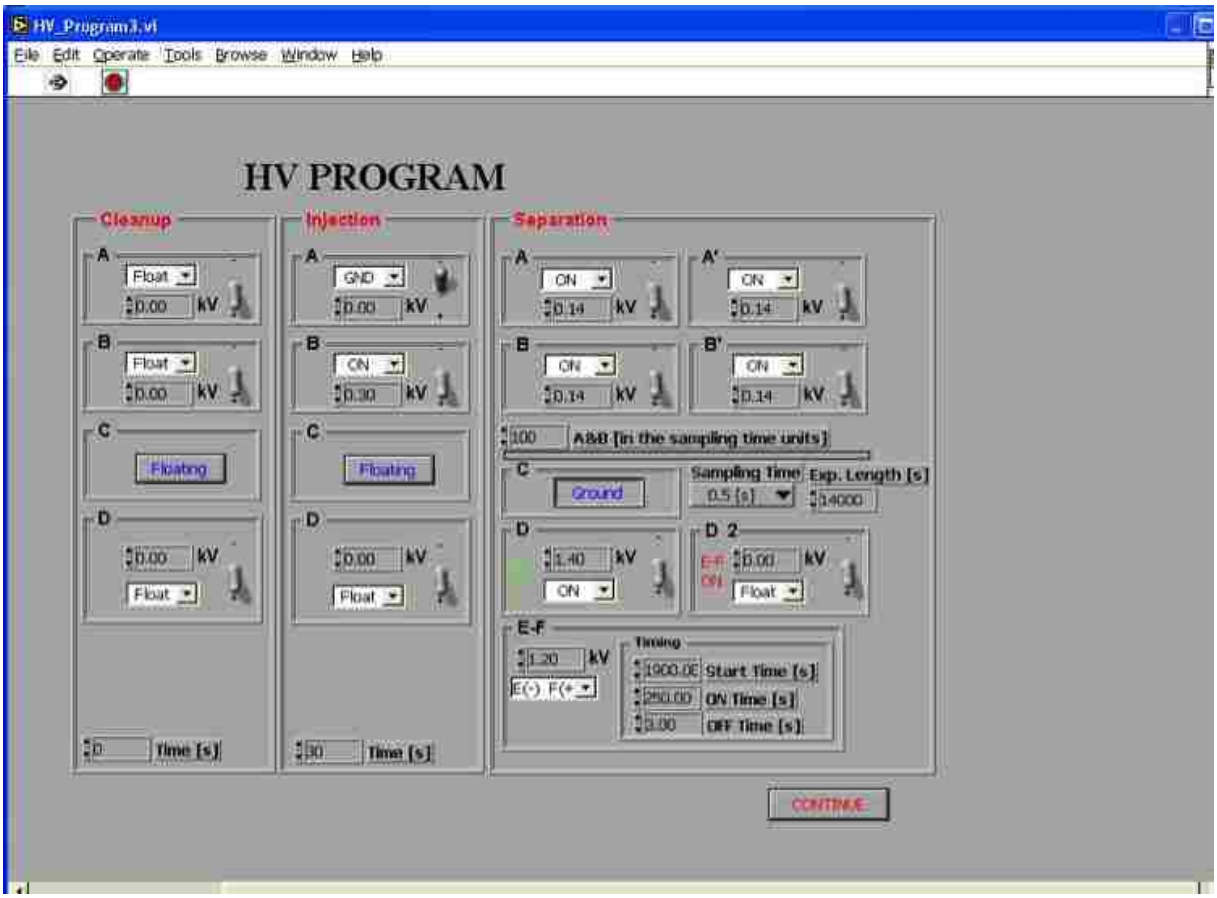

Figure 3.9 Computer screen-shot of the LabView program used to control the power supply that applies voltage to the reservoirs during the electrophoretic separations of the MCF-7 membrane proteins. The total separation time and the time to start the sampling into the second dimension is also set using this program.

Raw 2D electropherograms were converted to 2D images and then to three-dimensional (3D) landscape representations (see Results and Discussion) by taking the LIF signals from successive runs for each MEKC cycle and plotting the electropherogram at the corresponding cycle on the SDS µ-CGE axis. This procedure was performed using OriginLab software (Northampton, MA, USA) and ImageJ software (National Institutes of Health, Bethesda, MD).

3.2.3 Fluorescence Labeling of the MCF-7 Membrane Protein Fraction

Prior to fluorescence labeling and separation, the MCF-7 membrane proteins were extracted as described previously in Section 2.2.4 using the Mem-PER™ Plus Membrane Protein Extraction Reagent Kit available through Pierce Biotechnology (Rockford, IL). The

membrane proteins were covalently labeled with DyLight 550 (excitation/emission = 562/576 nm), an amine-reactive dye (Pierce Biotechnology, Rockford, IL, USA) following the manufacturer's guidelines. Briefly, after extraction, the membrane proteins were reacted with the DyLight 550 in an approximate 1:10 molar ratio for 1 h. The excess dye was removed using a Zeba Spin column (Pierce Biotechnology, Rockford, IL, USA). The amine reactive dye contained *N*-hydroxysuccinimide (NHS) esters that reacted with primary amines on the membrane proteins, forming a stable, covalent amide bond. The DyLight 550-conjugated proteins of the membrane protein fraction were then diluted in the μ-CE run buffer in a 1:5 volume ratio (membrane protein sample: run buffer) along with 2-mercaptoethanol and heated to 95°C for 5 min. Prior to use in the microchip, all solutions were filtered with a 0.2 μm Nylon-66 membrane syringe filter (Cole-Parmer Instrument Co., Vernon Hills, IL, USA) except for membrane protein solutions, which were centrifuged (~6,000 rpm, 5 min) to remove any particulates.

3.2.4 2D Electrophoretic Separations with 2D SDS-PAGE/MEKC Microfluidic Device

Before the electrophoretic separation, a solution of 2 mg/mL of methyl hydroxyethyl cellulose (MHEC) (Fluka BioChemika, Switzerland) was dissolved in 1X PBS (pH = 7.2, Sigma-Aldrich, St. Louis, MO, USA) and flushed through the fluidic channels through reservoir A (see Figure 3.8A) while applying vacuum to reservoir F. This process aids in the suppression of the electroosmotic flow (EOF). The EOF in PMMA channels with buffer containing MHEC (0.05% w/v) as a dynamic coating agent has been measured to be ~1.20 ± 0.07 x 10^{-5} cm^2/Vs.[243] It should also be noted that no sieving properties are provided by buffers containing methylcellulose derivatives (e.g., MHEC) when the concentration is below 0.1%.[311] All electrophoretic separations were carried out at ambient temperature in reverse

mode (detection end anodic) for both SDS µ-CGE and the MEKC dimensions. Prior to the µ-CE 2D separation, the first dimension channel (see Figure 3.8A) was filled with a sieving matrix, which consisted of SDS 14-200 linear polyacrylamide gel (Beckman Coulter Inc., Fullerton, CA, USA) containing 0.05% w/v MHEC. The gel filling was monitored using brightfield microscopy to make sure the gel was filled exactly at the intersection of the 1st and 2nd dimensions. The second dimension channel was then filled with the MEKC buffer, which consisted of 12 mM Tris-HCl, 0.4% w/v SDS, and 0.05% w/v MHEC (pH = 8.5).

For the injection/separation scheme, shown in Figure 3.10, 2D separations were performed in channels A-B, C-D, and E-F serving as injection, 1st dimension SDS µ-CGE and 2nd dimension MEKC channels, respectively, and setting the detection point at *d* (see Figure 3.8A). After the gel and run buffers were pressure filled into the channels, reservoir A was emptied and subsequently filled with 2 µL of the dye-labeled membrane protein sample. The sample was injected into the sampling channel (see A-B channel, Figure 3.8A) at 200 V/cm. The injection was initiated by grounding the voltage to the sample reservoir (A, Figure 3.8A) and applying +0.30 kV to the waste reservoir (B, Figure 3.8A) to fill the cross channel (points C-F were floated during the injection).

Following injection, a high positive voltage was switched to point D and point C was grounded (Figure 3.8A). Then, pull back voltages (~10% of applied voltage to point D) were applied to the sample and waste reservoirs (A and B, see Figure 3.8A). The electric fields (*E*) employed for the SDS µ-CGE and the MEKC separations were 350 V/cm and 400 V/cm, respectively.

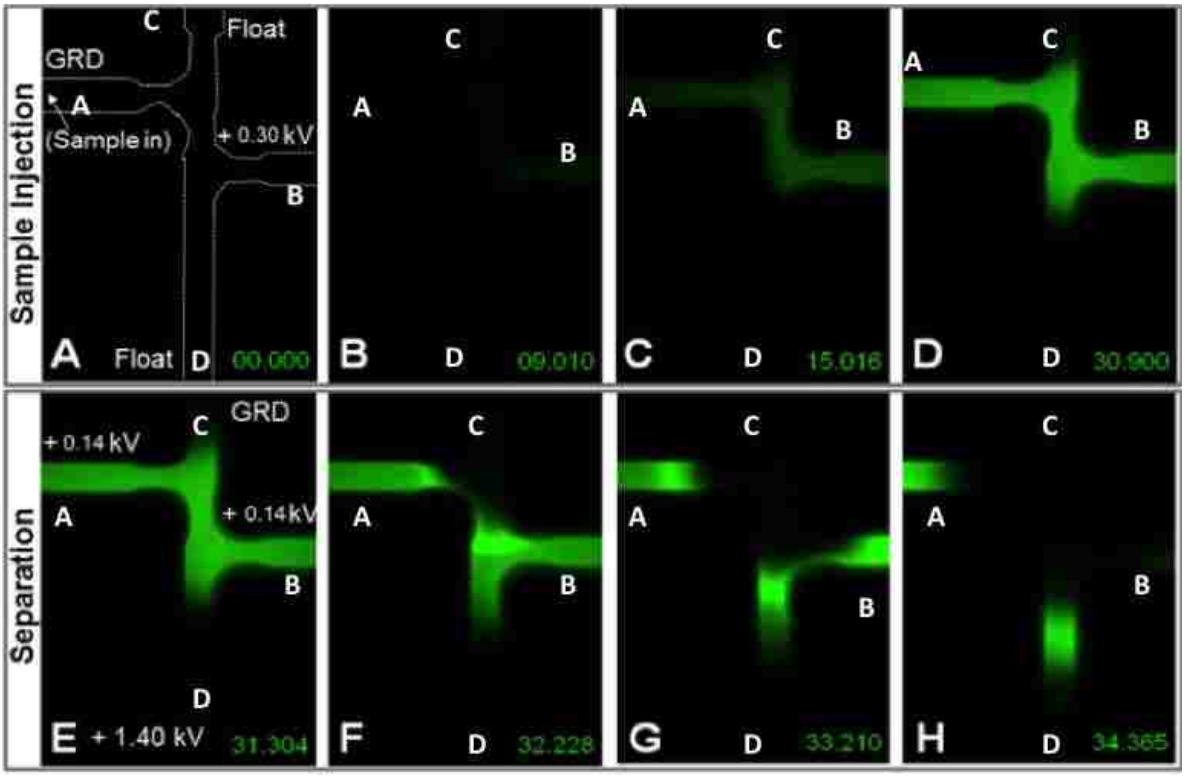

Figure 3.10 The injection/separation scheme depicting the formation of the protein plug when voltages are applied during injection and separation, respectively.

Table 3.1 represents the high-voltage protocol adopted for the 2D separation. As shown in this Table, the injection and run steps were the same as discussed previously. The SDS μ-CGE separation was carried out at 350 V/cm using L_{eff} = 30 mm (see C-D channel, Figure 3.8A). The 2nd dimension MEKC separations were programmed to begin after a 30 min electrophoretic run time in the 1st dimension (SDS μ-CGE). Each 2nd dimension MEKC cycle consisted of a 250 s run cycle (MEKC development time) and operated at a field strength of 400 V/cm, which was found to be sufficient time to assure that all of the components injected into the 2nd dimension reached the LIF detection zone (L_{eff} = 40 mm).

Table 3.1. High-voltage protocol for 2D separations using the PMMA microchip. Letters A – F refer to reservoirs on the 2D platform as shown in Figure 3.7A. [1]G: Grounded, F: Floating.

	Applied voltages (kV)[1]					
Step	A	B	C	D	E	F
Injection	G	+ 0.30	F	F	F	F
SDS μ-CGE	+ 0.14	+ 0.14	G	+ 1.40	F	F
Second MEKC cycle	+ 0.14	+ 0.14	F	F	G	+ 2.00
First to second sample transfer	+ 0.14	+ 0.14	G	+ 1.40	F	F

Sample eluting from the 1st dimension was injected into the 2nd dimension after a 3 s run period in the 1st dimension. During the MEKC cycle, the applied field in the 1st dimension was stopped, parking the components in the 1st dimension during the 2nd dimension run.

3.2.5 2D Slab Gel Separation of MCF-7 Proteins Using IEF/SDS-PAGE

The results of the traditional 2D gel electrophoresis from the work of Pionneau and co-workers[27,28] was used as a comparison of traditional 2DE gel separations of MCF-7 proteins utilizing IEF with SDS-PAGE. IPG strips from pH 5 to 8 were used in the first dimension. The strips were rehydrated with 150 μg of protein until a total of 195,000 V/h was reached. After focusing, the strips were then placed on 18 cm x 20 cm x 1 mm 8–18.5% polyacrylamide linear gradient gel for the separation in the second dimension. SDS-PAGE was carried out at 40 V for 1 h, and 100 V for 21 h and stained with silver nitrate for visualization.

3.2.6 Software Analysis of 2D Data

In order to obtain a 3D image of the electrophoretic data from the microchip, a text file of the raw 2D run formatted into a 3D matrix was input into OriginLab (Northampton, MA, USA). The matrix was constructed such that each column represented one MEKC cycle. The

matrix was then plotted as a 3D surface plot. A 2D image plot was also done in ImageJ (National Institutes of Health, Bethesda, MD) to resemble a 2D gel.

3.3 Results and Discussion

3.3.1 Results of 2D Slab Gel Separation of MCF-7 Membrane Proteins Using IEF/SDS-PAGE

As it is shown in Figure 3.11, the whole cell extract gel has many more protein spots, which is expected due to the IEF buffer incompatibility with the MCF-7 membrane proteins.

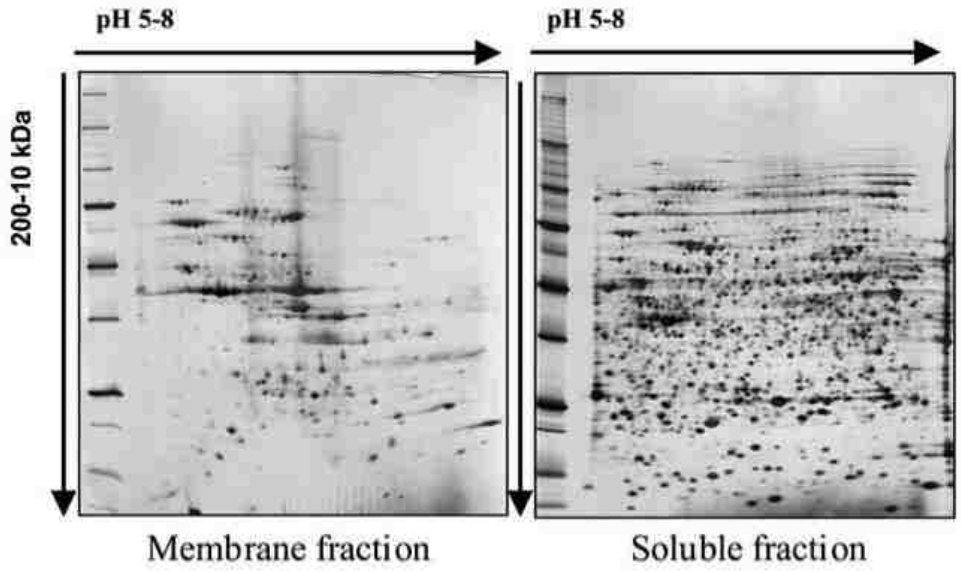

Figure 3.11 2D protein patterns from MCF-7 cell membrane extract and whole-cell extract. The 150 µg of protein was separated first on the IPG strips and then on an 8-18.5% gradient gel followed by silver staining. (Reproduced from Pionneau, C., Canelle, L., Bousquet, J., Hardouin, J., Bigeard, J., Caron, M., Joubert-Caron, R. *Cancer Genomics & Proteomics* **2005**, *2*, 199 with permission, Copyright 2013).

This confirms that it is highly possible that some membrane proteins could have been missed and/or not separated because they never entered the gel from the IPG strips because the proteins are hydrophobic and the buffers are aqueous (hydrophilic). There is also more band smearing in the membrane protein gel as opposed to the whole cell extract that could also be due to the native characteristics of the hydrophobic membrane proteins and their insolubility, post-translational modifications, and/or nucleic acid contamination. The average

spot size was determined to be ~200 (±4.6) pixel^2, a peak area of 117,924 pixel^2, and a peak capacity of 589 (±5.1) pixel^2.

3.3.2 1D μ-CGE of MCF-7 Membrane Protein Fraction Employing SDS-PAGE

The use of a highly viscous gel can alter a separation to become a size-based separation, minimize the diffusion of solutes, prevent analyte adsorption onto the microchip walls, and aid in EOF suppression.[29] Separating proteins in their native state (non-denatured) can result in band smears, poor migration time, poor reproducibility, and less distinct protein spots.[30] In addition, the electrophoretic mobilities of native proteins are dependent upon the mass-to-charge ratios rather than their molecular weight solely;[31] therefore, the formation of SDS-protein complexes after denaturing establishes the foundation for performing electrokinetic protein transfer due to the overall negative charge of the proteins but also prepares the proteins for a size-based separation.[14]

We were interested in analyzing the peak capacity for a 1D μ-CGE separation of the MCF-7 membrane proteins using L_{eff} = 30 mm with SDS as the denaturing and complexing agent and polyacrylamide gel electrophoresis sizing matrix. The results of the SDS μ-CGE analysis using the PMMA microchip are shown in Figure 3.12. As seen in the electropherogram, approximately 22 bands could be observed with varying degrees of resolution and widths due to potential peak overlap arising from proteins with similar molecular weights. From the data, (see bands marked with an asterisk in Figure 3.12), we determined the average peak width was estimated to be 3.1 ±2.3 s, producing a plate number of 4.8 x 10^5 ±1.6. From these values and a separation window of ~25 min (defined by the migration time difference between the last and first migrating components), we estimated a peak capacity for the 1D separation to be 55 ±3.3 (n = 3).

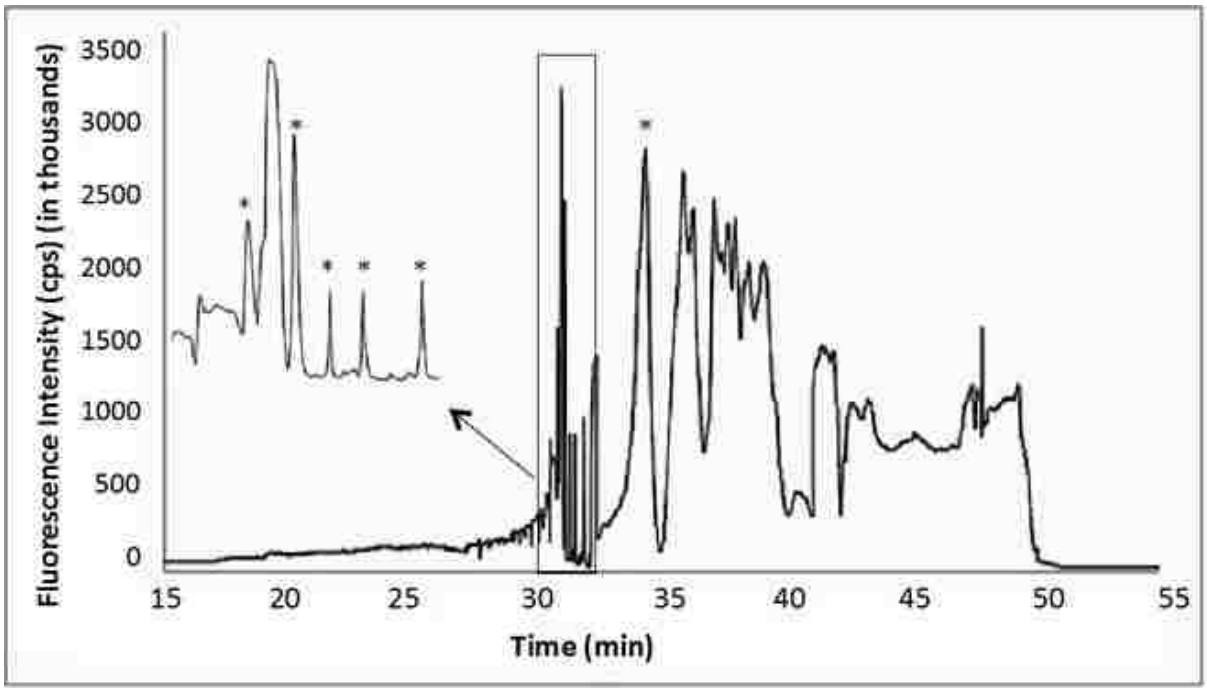

Figure 3.12 SDS µ-CGE 1D separation of MCF-7 membrane proteins from whole cell lysate. The protein sample, which was labeled with an amine-reactive fluorescent dye, DyLight 550, was placed into reservoir A of the microchip (see Figure 3.7A) and electrokinetically injected into the separation channel at 200 V/cm. The 1D SDS µ-CGE was performed at E = 350 V/cm. The total separation length was 4 cm with an effective length of 3 cm.

Obviously, this is well below the level necessary to analyze a sample as complex as that projected for a mammalian proteome. The average peak width determined above from the SDS-PAGE dimension was then used to select the appropriate sampling time into the second dimension, which was set at 3 s.

3.3.3 2D µ-SDS-PAGE/ µ-MEKC Separation of MCF-7 Membrane Proteins

In the 2D electrophoretic separation, SDS-PAGE was used as the first dimension and MEKC as the second dimension. SDS forms complexes with proteins, which are subsequently electrophoresed through a sieving matrix allowing for the separation of species primarily based on differences in the molecular weights. MEKC utilizes micelles as a pseudo-stationary phase with separation based upon selective partitioning of solutes to the micelles. In the case here, we are employing SDS micelles as a pseudo-stationary phase, which provides an attractive interface to SDS-PAGE due to the fact that both dimensions use SDS. Shadpour *et*

al.[24] from our group has previously demonstrated the orthogonality of SDS-MEKC to SDS μ-CGE, making it an elegant format for producing high peak capacities for multi-dimensional electrophoretic analysis of intact proteins. Using the migration order and migration times of 10 model proteins, the degree of orthogonality was evaluated and a plot of the normalized migration time for a SDS-PAGE 1D separation versus that of the SDS MEKC 1D separation produced a scatter plot with minimal data points occurring along the diagonal (slope = 1.0, intercept = 0.0) providing an orthogonality value between the two separation mechanisms of 77%.

In the 2D format utilized for this work, electrophoretic zones are "parked" in the first dimension while the second dimension is affected in a serial fashion. Therefore, issues with zonal dispersion due to longitudinal diffusion should be considered because it can have a significant impact on the peak capacity of the separation for the 2D analysis. This was achieved by calculating the height equivalent to a theoretical plate for longitudinal diffusion only (H_D) of the 1D SDS μ-CGE dimension and comparing that value to H_{TOT} secured from the complete 2D separation. A representative diffusion coefficient for proteins in a sieving matrix as used herein was taken as ~10^{-8} cm^2 s^{-1}, which is the measured diffusion coefficient of cytochrome C in polyacrylamides,[32] resulting in H_D = 3.24 x 10^{-6} cm (H_D = 2Dt/L; t = time; L = column length, cm). The number of plates for a typical band migrating from the 2D separation (see Figure 3.12) was 3.47 x 10^5, resulting in H_{TOT} = 1.15 x 10^{-5} cm. Therefore, the diffusional component to H_{TOT} was calculated to be approximately 28%.

For 47 10 s MEKC cycles, which represents the parking time (470 s; time that is allocated to performing the MEKC separations) and a total separation time of 3,300 s, the percent contribution of diffusional spreading during the parking phases of the separation to

H_D is roughly 85%. Reductions in the development time for the MEKC cycles can reduce H_D stemming from the parking phases of the separation, potentially producing higher peak capacities. However, due the inherent nature of these proteins being very hydrophobic (*i.e.* membrane proteins), shorter development times for the MEKC dimension is inadvisable because the proteins need time to separate in the pseudo-stationary phase. Higher field strengths could be utilized but issues of bubble formation from Joule heating could arise.

In order to sample all components migrating from the 1st dimension to the 2nd dimension, 47 MEKC cycles were required with each cycle run for 10 s (E = 400V/cm). The development time for the full 2D separation was estimated to be ~55 min. Although the analysis time is long from a capillary electrophoresis standpoint, this is a significant improvement compared to the 24+ h required for a conventional 2D IEF/SDS-PAGE analysis. A typical 2D image of the MCF-7 membrane protein separation and the corresponding 3D landscape image are shown in Figure 3.13A. The image secured from Figure 3.13A was imported into ImageJ for analysis. From the input data to ImageJ, the average size of each protein spot for the μ-CE run was determined to be 133 (±7) pixel^2, which yielded a peak capacity for the 2D separation of 1,768 (±9), which was obtained by dividing the total pixel area in the image of 235,200 pixel^2 by the average spot size.

In order to ensure that the electrophoresis of membrane proteins was working properly, we chose 3 known proteins (bovine serum albumin 66 kDa, transferrin 80 kDa, and concanavalin A 104 kDa) to separate using the same microfluidic device. Each protein had a concentration of 5 μM and was labeled as described in Section 3.2.3.

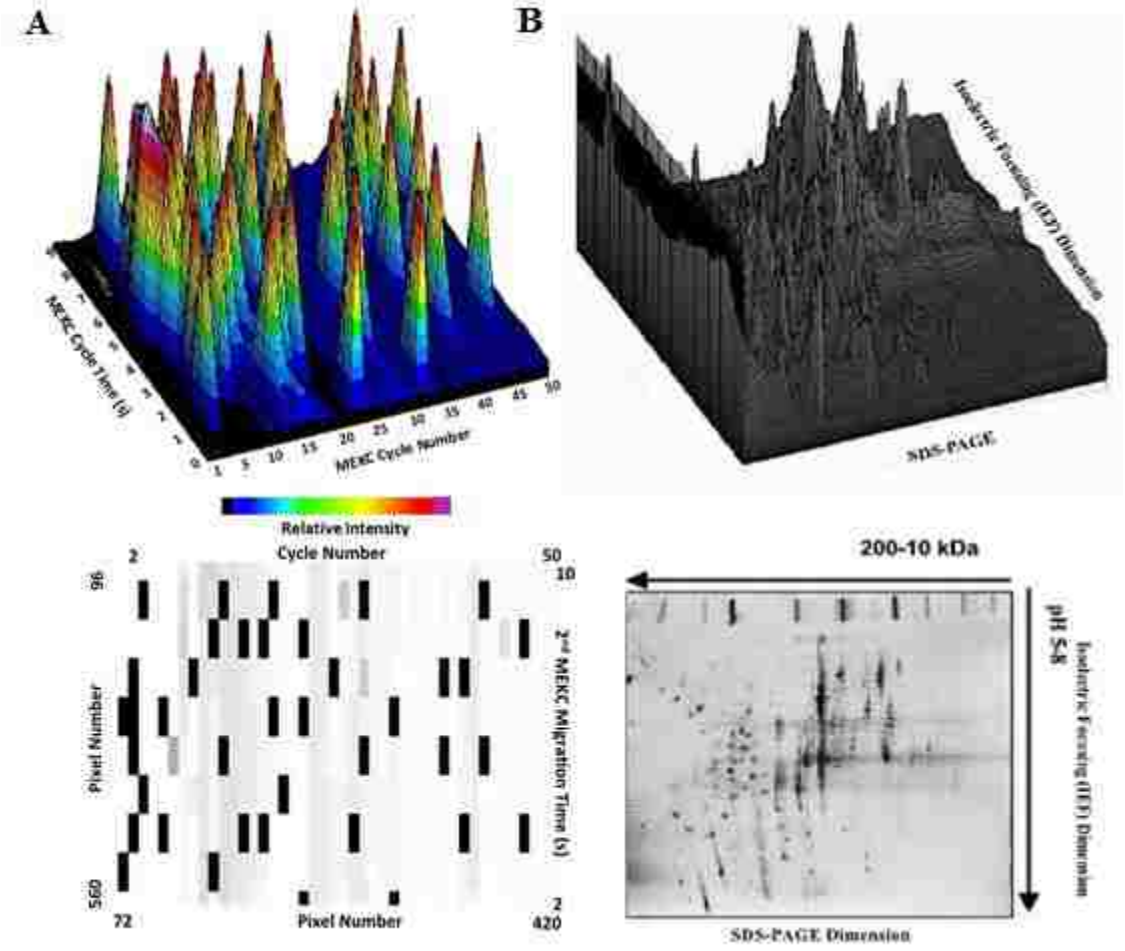

Figure 3.13 (A) SDS μCGE/μ-MEKC 2D separation of a MCF-7 membrane protein fraction. The protein sample was placed into reservoir A (see Figure 3.7A) and electrokinetically injected into the separation channel at 200 V/cm. The 2D SDS μ-CGE × MEKC were performed at 350 V/cm and 400 V/cm, respectively. Serial 10 s MEKC cycles were performed with a total of 47 MEKC cycles and a 3 s transfer time from the 1st to 2nd dimension. The bottom panel shows a 2D image of the microchip MCF-7 map, while the top panel shows a 3D landscape image of the MCF-7 membrane protein map. (B) 2D image of a conventional IEF/2D PAGE separation of the MCF-7 membrane protein sample (bottom panel) and the corresponding 3D landscape (top panel). Separation conditions are provided in the Materials and Methods section.

Figure 3.14 shows the results of the SDS μCGE/μ-MEKC 2D separation of the 3 known proteins. We utilized conditions described previously in work by Shadpour *et al.*[24] The 2D separation required a total of 71 MEKC cycles with a MEKC cycle run time of 10 s. The total separation time was ~750 s (12.5 min).

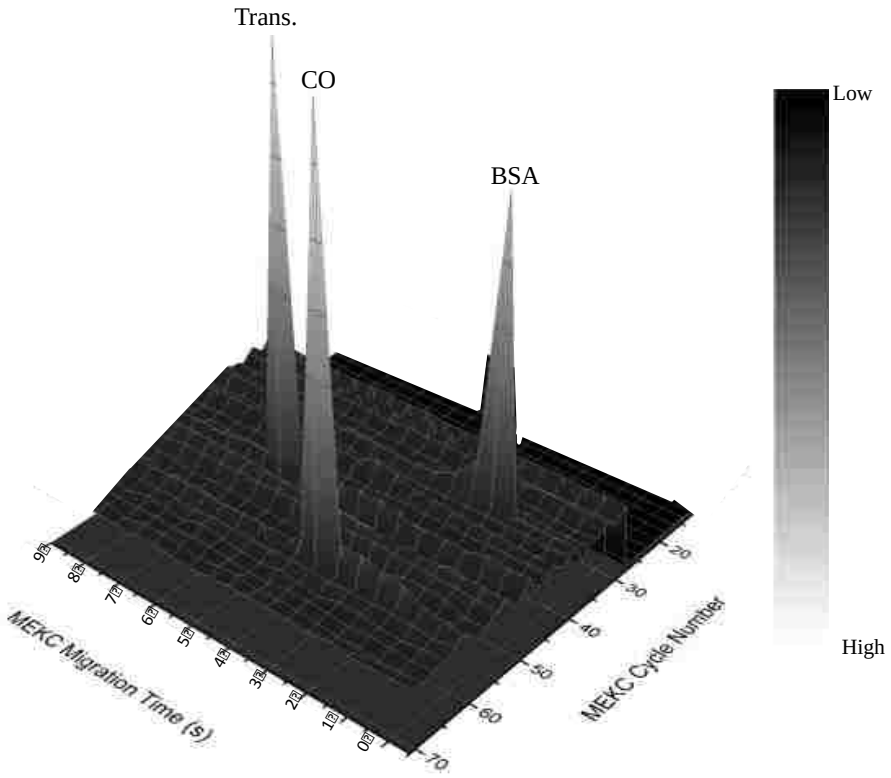

Figure 3.14 3-D landscape of SDS μCGE/μ-MEKC 2D separation of 3 proteins (bovine serum albumin, transferrin, concanavilin A) of known molecular weight. The 2-D SDS μ-CGE × MEKC were performed at 350 V/cm and 400 V/cm, respectively. Serial 10 s MEKC cycles were performed and a total of 71 MEKC cycles were used with a 1 s transfer time from the 1st to 2nd dimension.

The separation had a peak capacity of 926 (±3.4) and an average plate number of 1.01 x 10^3 (±2.3). The data shows that the proteins are well resolved and suggests that there are not any issues with the electrophoretic conditions and that any peak broadening is likely a factor of the membrane proteins aggregating and not remaining solubilized in the buffer solution after the extraction and labeling processes.

3.4 Conclusion

Separations on microfluidic platforms have been attractive for years and are garnering more appeal for the analysis of complex biological samples because they can easily lend themselves to performance characteristics that rival techniques and instrumentation used on the macro-scale, but using shorter operational times without significantly sacrificing separation efficiency and thus, generating data production rates that are notable. In addition,

these formats, due to their small footprint and lithographic fabrication techniques, will permit the development of multi-channel formats that can significantly improve the production rate of data. In the present report, we were able to demonstrate the ability to generate peak capacities of 1,768 (±9) for a biological membrane protein sample using a 7 cm effective separation length in both dimensions. The 2D separation platform is very attractive for interfacing to mass spectrometry (MS) for discovery-based applications. The 2D separation has band broadening which is likely due to the membrane proteins not being well solubilized. In order to overcome the issue of broadening, we can perform a 2D separation on the biotinylated MCF-7 membrane proteins that we extracted using the μ-SPE device, which we have already shown to be well solubilized and purified from the membrane of the cell and other contaminating species (*i.e.* cytosolic proteins).

As stated previously, the goal of this work is to develop an integrated system for the analysis of proteins from a top-down perspective. We have already shown the separation of intact proteins and now we must discuss how we plan to integrate the extraction and separation platforms with the remaining processing steps in the proteomic pipeline for this analysis. The next chapter will discuss our approach to how we will select cells and biotinylate the cell surface membrane proteins on-chip before moving the membrane proteins to the extraction bed to be purified, which we discussed in Chapter 2. After the separation of the extracted membrane proteins, we will need to digest the proteins before the MS analysis; therefore, we will discuss the fabrication of an on-chip bioreactor for digestion. In Chapter 4, we will examine our approach to perform cell selection, biotinylation, and lysis. Additionally, we will also consider how we plan to integrate each processing step into a modular platform.

3.5 References

(1) Lion, N.; Rohner, T. C.; Dayon, L.; Arnaud, I. L.; Damoc, E.; Youhnovski, N.; Wu, Z. Y.; Roussel, C.; Josserand, J.; Jensen, H.; Rossier, J. S.; Przybylski, M.; Girault, H. H. *Electrophoresis* **2003**, *24*, 3533.

(2) Giddings, J. C. *Unified Separation Science*; Wiley: New York, NY, 1991.

(3) Liu, H.; Yang, C.; Yang, Q.; Zhang, W.; Zhang, Y. *Journal of chromatography. B, Analytical technologies in the biomedical and life sciences* **2005**, *817*, 119.

(4) Anderson, L.; Anderson, N. G. *Proc Natl Acad Sci U S A* **1977**, *74*, 5421.

(5) O'Farrell, P. H. *The Journal of biological chemistry* **1975**, *250*, 4007.

(6) Righetti, P. G. *Journal of biochemical and biophysical methods* **1988**, *16*, 99.

(7) Santoni, V., Malloy, M. and Rabilloud, T. *Electrophoresis* **2000**, *21*, 1054.

(8) Gygi, S. P.; Corthals, G. L.; Zhang, Y.; Rochon, Y.; Aebersold, R. *Proc Natl Acad Sci U S A* **2000**, *97*, 9390.

(9) Michels, D. A.; Hu, S.; Dambrowitz, K. A.; Eggertson, M. J.; Lauterbach, K.; Dovichi, N. J. *Electrophoresis* **2004**, *25*, 3098.

(10) Kraly, J. R.; Jones, M. R.; Gomez, D. G.; Dickerson, J. A.; Harwood, M. M.; Eggertson, M.; Paulson, T. G.; Sanchez, C. A.; Odze, R.; Feng, Z.; Reid, B. J.; Dovichi, N. J. *Anal Chem* **2006**, *78*, 5977.

(11) Hu, S.; Michels, D. A.; Fazal, M. A.; Ratisoontorn, C.; Cunningham, M. L.; Dovichi, N. J. *Anal Chem* **2004**, *76*, 4044.

(12) Shen, Y.; Jacobs, J. M.; Camp, D. G., 2nd; Fang, R.; Moore, R. J.; Smith, R. D.; Xiao, W.; Davis, R. W.; Tompkins, R. G. *Anal Chem* **2004**, *76*, 1134.

(13) Opiteck, G. J.; Ramirez, S. M.; Jorgenson, J. W.; Moseley, M. A., 3rd *Analytical biochemistry* **1998**, *258*, 349.

(14) Li, Y.; Buch, J. S.; Rosenberger, F.; DeVoe, D. L.; Lee, C. S. *Anal Chem* **2004**, *76*, 742.

(15) Chen, X.; Wu, H.; Mao, C.; Whitesides, G. M. *Anal Chem* **2002**, *74*, 1772.

(16) Yang, S.; Liu, J.; Lee, C. S.; Devoe, D. L. *Lab on a chip* **2009**, *9*, 592.

(17) Rocklin, R. D.; Ramsey, R. S.; Ramsey, J. M. *Anal Chem* **2000**, *72*, 5244.

(18) Ramsey, J. D.; Jacobson, S. C.; Culbertson, C. T.; Ramsey, J. M. *Anal Chem* **2003**, *75*, 3758.

(19) Watarai, H. *Chem Lett* **1991**, 391.

(20) Hansen, S. H. *Electrophoresis* **2003**, *24*, 3900.

(21) Timerbaev, A. R.; Vasylenko, O. O.; Foteeva, L. S.; Rudnev, A. V.; Semenova, O.; Keppler, B. K. *Journal of separation science* **2007**, *30*, 399.

(22) Xie, J. P.; Chen, X. F.; Zhang, J. Y.; Liu, J. Q.; Tian, J. N.; Chen, X. G.; Hu, Z. D. *Journal of pharmaceutical and biomedical analysis* **2004**, *36*, 1.

(23) Zhou, G. H.; Luo, G. A.; Zhang, X. D. *Journal of Chromatography A* **1999**, *853*, 277.

(24) Shadpour, H.; Soper, S. A. *Anal Chem* **2006**, *78*, 3519.

(25) Osiri, J. K.; Shadpour, H.; Park, S.; Snowden, B. C.; Chen, Z. Y.; Soper, S. A. *Electrophoresis* **2008**, *29*, 4984.

(26) Strege, M. A., Lagu, A. L. *Journal of Chromatography A* **1993**, *630*, 337.

(27) Pionneau, C., Canelle, L., Bousquet, J., Hardouin, J., Bigeard, J., Caron, M., Joubert-Caron, R. *Cancer Genomics & Proteomics* **2005**, *2*, 199.

(28) Canelle, L.; Bousquet, J.; Pionneau, C.; Hardouin, J.; Choquet-Kastylevsky, G.; Joubert-Caron, R.; Caron, M. *Electrophoresis* **2006**, *27*, 1609.

(29) Liu, Y. M.; Sweedler, J. V. *Anal Chem* **1996**, *68*, 3928.

(30) Jungblut, P.; Thiede, B.; Zimny-Arndt, U.; Muller, E. C.; Scheler, C.; Wittmann-Liebold, B.; Otto, A. *Electrophoresis* **1996**, *17*, 839.

(31) Wang, Y. C.; Choi, M. H.; Han, J. *Anal Chem* **2004**, *76*, 4426.

(32) Lewus, R. K.; Carta, G. *Ind Eng Chem Res* **2001**, *40*, 1548.

(33) Osiri, J. K.; Shadpour, H.; Soper, S. A. *Anal Bioanal Chem* **2010**, *398*, 489.

4 Summary and On-going Developments

4.1 Summary

Many researchers have been attempting to integrate various proteomic processing steps onto a single microfluidic platform to build an autonomously operating system. However, the ultimate goal of integrating several proteomic analysis units into one system for building such a multifunctional system has not been realized to-date. As previously discussed in Chapter 1, the overall goal of this work is to assemble a fully integrated fluidic system using a novel design approach; task-specific modules will be interconnected to a fluidic motherboard to provide full process automation for mass-limited samples using circulating tumor cells (CTCs) as a demonstrator of the technology. The integrated system will be directly interfaced to nanostructure-assisted laser desorption ionization MS (NALDI-MS) to provide the ability to identify isolated protein components with little or no operator intervention. The design strategy will employ a novel modular format with the system using 4 modules; (1) cell biotinylation and lysis module; (2) affinity selection module of a particular sub-population of the proteome (*i.e.,* those that have been biotinylated); (3) microchip electrophoresis module; and (4) solid-phase bioreactor for proteolytic digestion with subsequent deposition onto the NALDI plate for reading results via MS analysis. To reduce sample complexity and improve the identification efficiency of the various components (*i.e.*, proteins) comprising the sample via mass spectrometry (MS), we will select a particular organelle for the analysis; in this case the sub-population we propose to focus on is membrane proteins from the isolated cells.

Multidimensional protein separation is regarded as the workhorse of many proteomic studies; therefore, careful attention must be paid toward the development and implementation

of multidimensional microelectrophoresis platforms both as an independent proteomic unit and as an integral part of a multifunctional system. We demonstrated the ability to generate peak capacities around 1,768 (±9) within 1 h for a biological sample of membrane proteins from an MCF-7 cell lysate using a microchip separation platform, whose effective separation length was 7 cm. While this peak capacity is still far below the total number of protein components found in a sample of a cell lysate, the technique remains attractive due to the fact that a sample of membrane proteins (representing a complex biological sample) has not been separated on a microfluidic platform to date. We were also able to perform a solid-phase extraction of biotinylated membrane proteins from MCF-7 cell lysate.

4.2 On-going Developments and Future Work

4.2.1 Background

In Chapters 2 and 3, our efforts were focused on the extraction and separation of membrane proteins from CTC surrogates (MCF-7; a breast cancer cell line) and the separation of membrane proteins from CTCs, respectively. There is a wealth of literature on the development of microfluidic devices (*device* in this context being units that have only one processing step) for the analysis of proteins, including those for solid-phase extractions[1,2] 2D separations,[3-11] and proteolytic solid-phase bioreactions.[12-17] Because complex protein samples can require the transfer of sample from one processing step to the next and be a source of material loss and/or contamination, it is advantageous to consider the use of a fully integrated fluidic system (*systems* are defined here as units that have various devices integrated to them). In these systems, the sample is moved hydrodynamically or electrokinetically through the entire processing pipeline without requiring operator intervention. This allows for the reduction of analysis time, the ability to improve result

reproducibility, and eliminate sample handling by the operator, which can be problematic especially for mass-limited samples or those containing proteins that have a tendency to adhere with high propensities to surfaces, such as membrane proteins.

A schematic of the proposed integrated fluidic system we are pursuing is shown in Figure 4.1. The system will accommodate all of the necessary processing steps of the analysis pipeline using task-specific modules fabricated in thermoplastics with the material selected for each module based upon the application needed to produce optimal performance. Micro-replication from a metal mold master will be utilized to fabricate the modules.

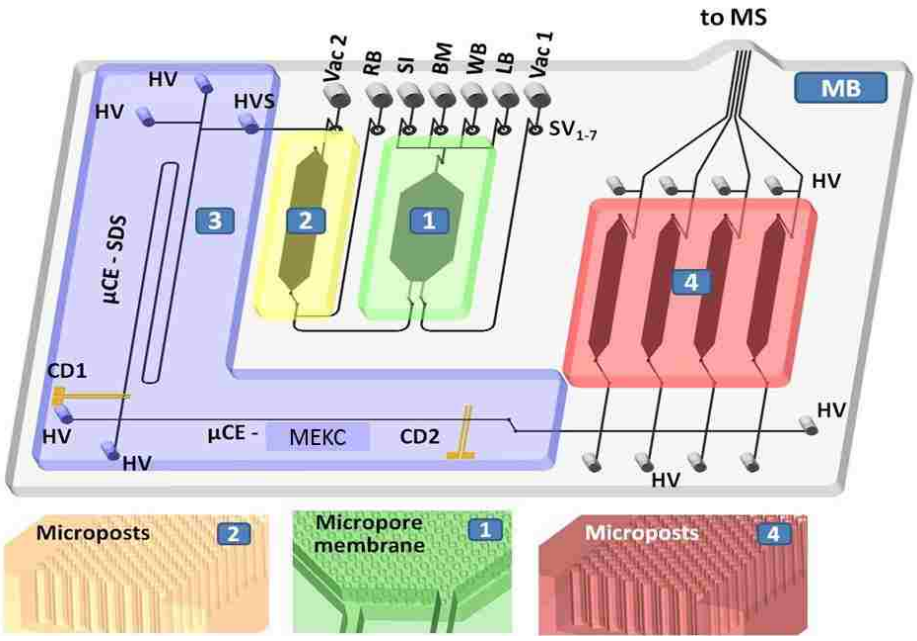

Figure 4.1 Integrated and modular fluidic system for processing a sub-population of a cell proteome that is selected via affinity techniques. The fluidic motherboard (MB) is populated with 4 modules: (1) Cell retention, biotinylation reactor and lysis module made from PC due to its compatibility with the PC membrane; (2) solid-phase affinity module made from PMMA due to its high surface load of functional groups when UV-treated; (3) 2D µCE module made from PMMA due to its propensity to generate high electrophoretic plate numbers; and (4) solid-phase bioreactor for proteolytic digestion of protein components sorted via 2D µCE that is also made from PMMA. The modules are interconnected to a PC-based motherboard; selected here based on its ability to form membrane values due to its high elongation at break threshold. Other components consist of: HV – high voltage power supplies; CD – conductivity detectors; Vac – vacuum; SI – sample inlet; RB – release buffer; SV – solenoid valves; LB – lysis buffer; BM – biotin reaction mixture; WB – wash buffer.

We will integrate an affinity selection module to the protein processing system to select CTCs directly from whole blood with high purity (no-preprocessing required). In order to accommodate the capability to process large input volumes to select sufficient numbers of CTCs, a series of high aspect ratio fluidic channels (narrow and deep) will be utilized in the CTC selection module. While we have already fabricated modules for the extraction of the biotinylated cell surface proteins and the separation of membrane proteins from MCF-7 cells, we still need to explore how to accomplish the on-chip cell lysis of the CTCs, the label-free detection of the proteins, protein digestion, and the mass spectrometry interface.

4.2.2 Cell Selection Module

4.2.2.1 Cell Selection, Biotinylation, and Lysis Module Design

The design of the cell selection module builds from previous experiences in the affinity capture of rare cells from samples such as blood.[18-21] The previous worked described a platform consisting of 51 channels (width = 30 μm; depth = 150 μm) with the walls being covalently decorated with anti-EpCAM antibodies. This module could process 1 mL of blood in ~40 min with CTC recoveries of 98%.[18] However, we anticipate the need to process larger input volumes to increase the yield of CTCs needed to accommodate the NALDI-MS detection/identification phases of the assay. The module design is shown in Figure 4.2.

For this module, 500 sinusoidal channels will be used so that large input volumes can be processed within reasonable timeframes using an optimized linear flow velocity (in terms of recovery) of 2.0 mm/s for the EpCAM antigen/antibody pair.[18] Each channel of the selection bed will be 30 μm wide, which is close to the diameter of a CTC and will improve recovery, and 250 μm deep, which will improve throughput.

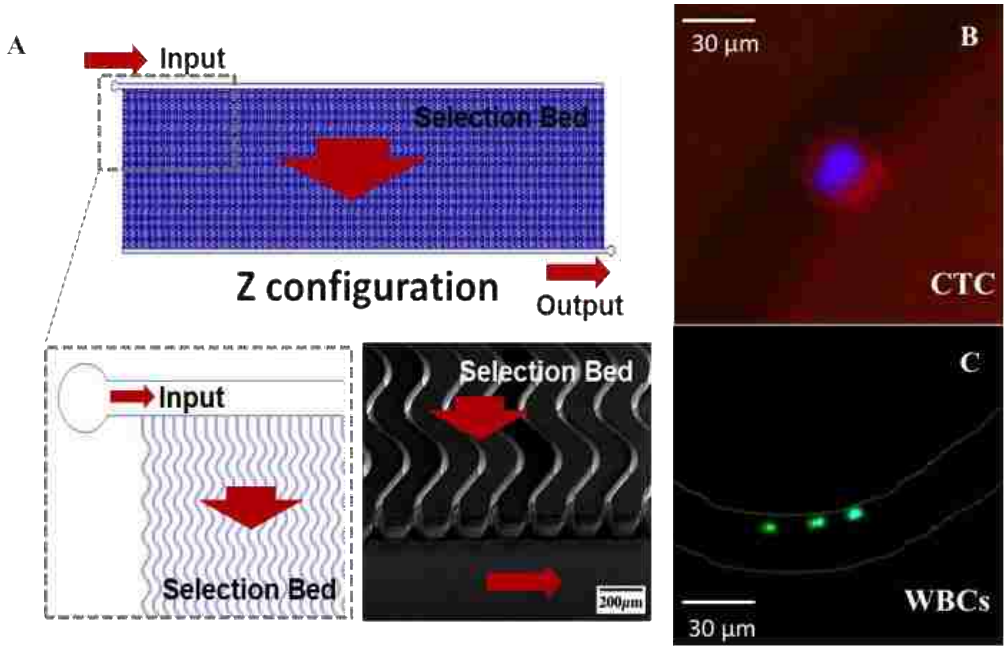

Figure 4.2 (A) Schematic of rare cell selection module that can process large input samples (~10 mL) with high throughput (<40 min) and a SEM of the molded module, which is made from PMMA, is shown in the bottom right. The input/output channels are much larger than the cell selection channels, and thus there is a lower pressure drop in these channels; the input channel fills before the selection channels. (B&C) Images of cells captured in selection channels.

Channels (feed and selection channels) are arranged in a Z-configuration to provide the single-channel inlet and outlet. This configuration has been found to minimize bubble formation compared to the previous designs that were used during blood filling.[18-21] A volumetric flow rate of 0.45 mL/min will be utilized to generate the linear velocity that is needed in each channel (2 mm/s) for CTC recoveries >90%.[18]

Once the rare cells have been selected, they are essentially "attached" to the channel walls of the selection bed. In this state, we will seek to biotinylate the membrane proteins of the selected cells. We will covalently attach biotin to the extracellular primary amine groups of the membrane proteins, but other functionalities, such as sulfhydryls, can be tagged as well. Membrane protein biotinylation provides an anchoring group for the affinity SPE of this sub-population (as discussed in Chapter 2). Following biotinylation, cells will be washed and then lysed with the membrane proteins delipidized and solubilized. Biological membranes are

composed of ~50 lipid molecules per protein molecule.[22] Therefore, the removal of the lipids is vital because it can assist in the solubilization of the membrane proteins. The lysis, delipidization, and solubilization of the cells will be done using a buffer containing 4% CHAPS, Tris, 7M urea, 2M thiourea, and magnesium acetate. Because the SPE of the membrane proteins is affinity-based, the buffer will not be carried downstream and will not interfere with subsequent processing steps.

4.2.3 Detection of Proteins Employing Contact Conductivity Detection

4.2.3.1 Electrochemical Detection (ECD)

The readout strategy that is most commonly used for detection methods in microfluidic devices is laser-induced fluorescence (LIF) due to the fact that it provides superb sensitivity with detection limits approaching the single-molecule level.[23-26] Regrettably, most LIF systems do not lend themselves to developing miniaturized systems with the detector components often times requiring much larger footprints compared to those of microfluidic devices and also, in most cases the proteins are themselves not fluorescent. As such, fluorescent dyes must be appended to the proteins to make them detectable. There have been attempts to fabricate miniaturized LIF detectors with integrated capabilities;[27,28] however, LIF requires analytes that either show intrinsic fluorescence or can be readily associated with (either covalently or non-covalently) labeling chromophores as noted above; this can complicate sample processing.

Another strategy that has shown promise in microfluidic applications is the use of electrochemical detection (ECD), such as amperometric or potentiometric detection systems.[29-39] Some of the features that make ECD attractive are the simple instrumentation that is needed to perform the detection and the favorable sensitivity and limits of detection it

offers. However, the target analyte must be intrinsically electroactive or have an electroactive species appended to it in order to carry out detection with amperometric or potentiometric methods. Conductivity detection can also be considered an electrochemical technique as well. It has the ability to detect any analyte irrespective of whether it contains an electroactive species or not. The only requirement is that the migrating analyte zones possess a conductivity that is different from that of the carrier electrolyte. An additional advantage of conductivity is that the performance improves with reduced detection volumes, making it an appealing detector for microelectrophoretic separations. There have been reports of detection limits ~10^{-7} M using an integrated conductivity detector for a volume of ~30 pL.[40,41]

Galloway and co-workers[42] from our group have demonstrated the use of a simple, bipolar-pulse, contact conductivity detector that was integrated directly into a PMMA microfluidic device performing electrophoresis for the detection of various mono- or polyanionic molecules (*i.e.,* amino acids, peptides, proteins or oligonucleotides) was achieved. In this format, voltage pulses of equal amplitude and duration but opposite polarity were applied to the conductivity electrodes with the current passing between the electrodes measured at the end of the second pulse. The Faradaic reactions that occur at the electrodes could be minimized because the pulse frequency was appropriately chosen with respect to the cell constant (the time to charge the double layer) and the electrical double layer does not have sufficient time to form. The layout of the PMMA device employed for the studies is shown in Figure 4.3.

Several different electrophoresis formats such as MEKC (proteins), free-solution zone electrophoresis (FSE) (amino acids and peptides), and reverse-phase ion-pair open channel capillary electrochromatography (RP-IPOCCEC) (oligonucleotides) were utilized to separate

ionic materials in a 3 cm effective length fluidic channel within the configured PMMA device.

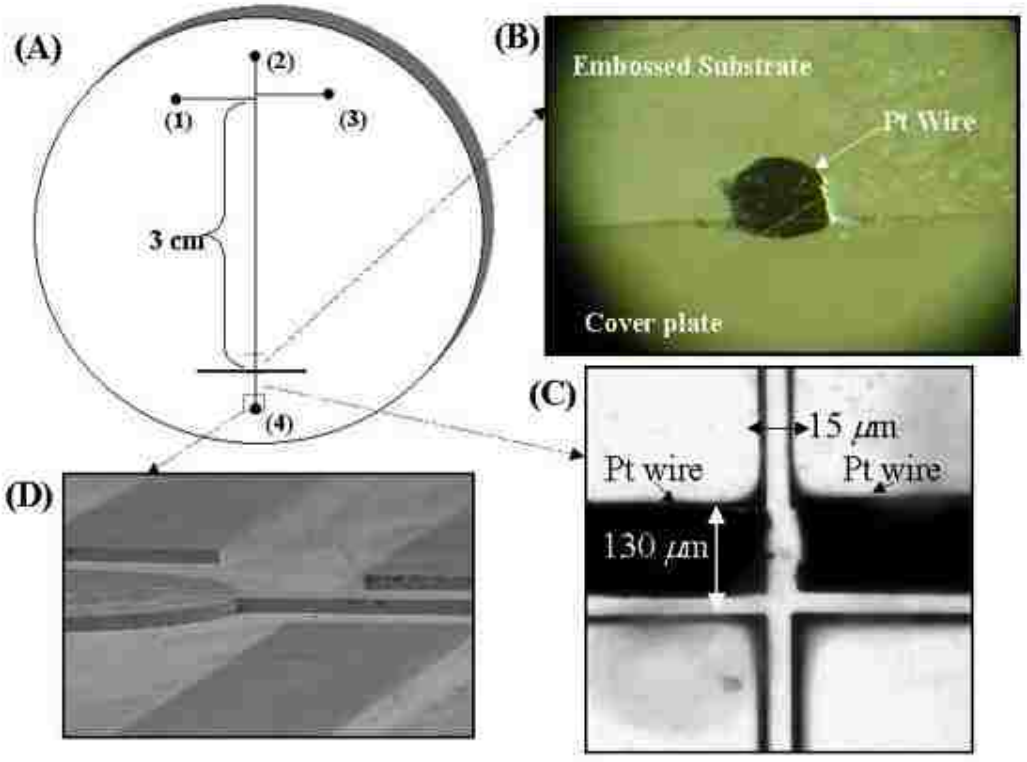

Figure 4.3 (A) Topographical layout of an assembled microfluidic device with an integrated conductivity detector. Injection channel length was 1.0 cm; separation channel was 4.0 cm (L_{eff} = 3.0 cm). The separation channel was 15 μm wide and 85 μm deep. The solution reservoirs are: (1) sample reservoir; (2) electrolyte reservoir; (3) waste reservoir; and (4) receiving reservoir. (B) Optical micrograph of the assembled device cut near the conductivity cell using microtoming. (C) Optical micrograph of the integrated conductivity detector (T-cell, electrode gap ~20 μm). In this micrograph, the cover plate was not assembled to the fluidic device. Working and reference electrodes were 127 μm in diameter and were placed 0.5 cm upstream from the receiving reservoir. (D) SEM of Ni electroform embossing tool taken near the receiving electrode. (Reproduced from Galloway, M.; Stryjewski, W.; Henry, A.; Ford, S. M.; Llopis, S.; McCarley, R. L.; Soper, S. A. *Anal. Chem.* **2002**, *74*, 2407 with permission, Copyright 2013).

Figure 4.4 shows the results from a separation of nine peptides using the PMMA microdevice for FSE. The solid line represents the 3rd electrophoretic run and the dotted line is the 35th electrophoretic run on the same chip. The electrophoretic conditions were as

follows: carrier electrolyte was 100 μM phosphate (pH 5.0) with a 3 s electrokinetic injection time and field strength 150 V/cm for the electrophoresis.

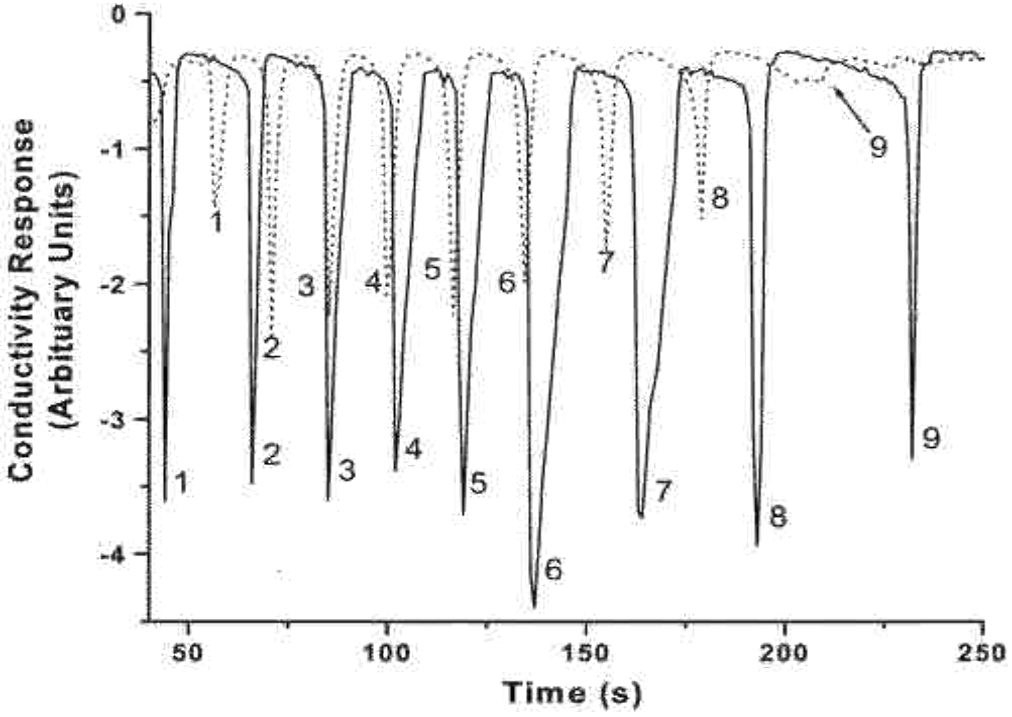

Figure 4.4 FSE separation of a peptide mixture (~0.23 μM total peptide concentration) consisting of (1) bradykinin, (2) bradykinin fragment 1-5, (3) substance P, (4) [Arg^8]-vasopressin, (5) luteinizing hormone, (6) bombesin, (7) leucine enkephalin, (8) methionine enkephalin, and (9) oxytocin in a PMMA device using contact conductivity detection. (Reproduced from Galloway, M.; Stryjewski, W.; Henry, A.; Ford, S. M.; Llopis, S.; McCarley, R. L.; Soper, S. A. *Anal. Chem.* **2002**, *74*, 2407 with permission, Copyright 2013).

The detector was operated at 5.0 kHz with bipolar pulse amplitude of ± 0.5 V. Baseline separation of all 9 peptides was achieved in the 3 cm length channel with the separation requiring <250 s. The sensing system we will use consists of a pair of electrodes to measure the change in the bulk solution conductance created by an electrophoretic band migrating through the electrodes.

We have shown that conductivity sensing can provide a label-less readout modality for a variety of materials, including proteins and peptides,[42,43] but with a limit-of-detection (LOD) somewhat inferior to laser-induced fluorescence. To optimize the LOD by increasing the

sampling efficiency generated by an electrode pair whose field extends across the entire fluidic channel,[42] we will investigate two approaches, labeled Type I and II (see Figure 4.5). We will employ Pt wires placed orthogonal to the output channel in the Type I configuration (see Figure 4.5A). This will provide high signal-to-noise ratios, but it also requires the placement of the microelectrodes into guide channels by hand using microscopic inspection and thus, is not conducive to simple production.

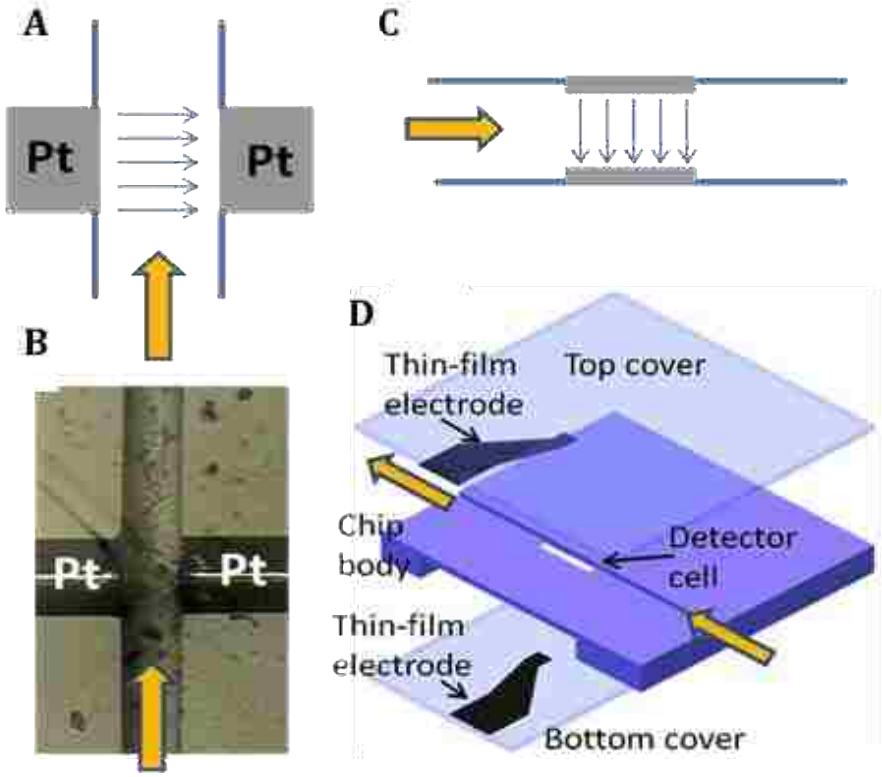

Figure 4.5 Conductivity detectors consisting of Type I (A, B) and Type II (C, D). The Type I detector is constructed with Pt wires inserted into guide channels embossed into the fluidic structure. The Type II detector use thin-film electrodes lithographically patterned on the cover and bottom plates. In both cases, the sampling efficiency is 100%.

Our initial studies have used this conductivity format for rapid system evaluation. The Type II configuration is more amenable to simple production through the lithographic patterning of thin film metal electrodes and consists of placing electrodes on the top and bottom faces of a fluidic channel (see Figure 4.5C). Thin film electrodes can be produced via

deposition (sputtering or evaporation) through a shadow mask, lithographically through selective etching of a deposited metal layer, or electroplated onto UV modified polymers.[44,45] Figure 4.5D schematically shows the assembly process of the Type II detector. The detector cell is an integral part of the fluidic module and is replicated during the same embossing step used to create the fluid channels by double-sided hot embossing.[46] In the next step, the bottom of the detector cell will be cut through using, for example, laser ablation or high precision micromilling. This two-step process can be done in a single step with the use of double-sided micro-injection molding, which is capable of making through-holes directly and will be used in future efforts.[47] During module assembly, the detector cell is covered on the top and the bottom with polymer films pre-patterned with platinum or other noble metal thin-film electrodes.

Highly sensitive electronic circuitry for conductivity measurements developed by our group will be used for this application.[18] The conductivity measurement circuit has been specially designed for applications in micro-environments and uses a gyrator sub-circuit to reduce the effects of parasitic capacitance due to wiring and the electrode configuration, which otherwise would dominate changes in electrical properties of the solution and degrade the LOD of the conductivity measurement. The dimensions of the conductivity detector cell and the electrodes will be optimized to provide favorable LODs and sampling efficiencies without degrading plate number through zonal dispersion induced by the finite detection volume.

In general, the LOD of conductivity detection is inversely proportional to the detector cell constant (K) defined as $K = L/A$, where L is the distance between the electrodes and A is the sensing area of the electrodes. Thus, better LODs are generated by closely spaced

electrodes with large surface area. For initial studies, we will use 50 μm electrodes placed over 50 μm wide and 50 μm deep microchannels at the sensing area with a gap of 50 μm, but these can be reduced to further optimize the LOD for conductivity sensing. Specifically, we will also look at various buffer compositions, separation channel lengths and field strengths to optimize separation performance (*i.e.*, resolution) and at the same time, reduce development time. The effects of these separation conditions on the conductivity detection limit will be evaluated as well.

4.2.3.2 Heart-cut 2D Separation of Membrane Proteins

In a heart-cut transfer protocol securing readout results from the first dimension of the 2D electrophoresis process of the membrane proteins prior to inserting into the second dimension would be particularly attractive because it would permit more efficient injection of material from the first dimension into the second dimension. For example, using the methods described in Chapter 3, <1% of the total electrophoresis band is inevitably injected into the second dimension. With heart cutting and online detection in both the first and second dimensions, the injection efficiency can conceivably be improved to near 100%.

Also in Chapter 3, a 1D separation was required to determine when the first peak was expected at the end of the first dimension. In those separations, which employed "blinded" injection of material from the first dimension into the second dimension, one peak may be sampled multiple times into the second dimension, and the transfer efficiency can deteriorate as well. Also, prolonged development times are apparent with the blinded injection protocol. Figure 4.6 shows the schematic of our approach to heart cutting 2D analysis. In our heart-cut protocol, electrode sensors are placed around the end of the first dimension and as a protein plug transverses the electrode sensors, the signal generated by the plug above baseline (or

background buffer) would, after a preset time, initiate protein movement from the first dimension into the second dimension.

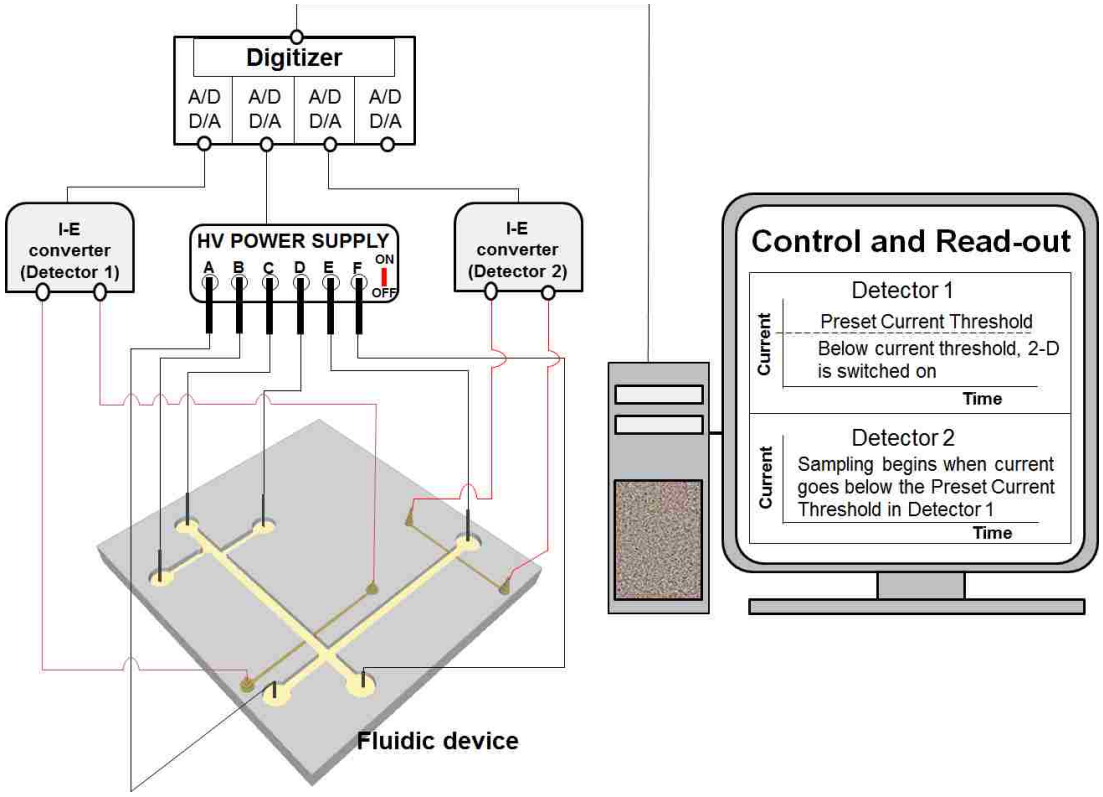

Figure 4.6 Schematic of the 2D heart-cut separation layout. Conductivity detectors are placed at the end of each separation dimension with preset modes to determine the on and off times.

Therefore, a dual detection process is required. Conductivity sensing would be particularly attractive for this due to the simple instrumentation required for the detection process and the fact that labeling of the proteins are not required, simplifying sample pre-processing.

4.2.4 Proteolytic Digestion of Separated Membrane Proteins

4.2.4.1 Solid-phase Proteolytic Digestion

Solid-phase bioreactors are being utilized more frequently instead of solution-phase digestion in-part because in-soluiton digestion can result in autodigestion of the proteolytic

enzyme forming peptides, which can complicate identification of the target proteins. While this can be minimized using low concentrations of the enzyme, it results in longer reaction times (>24 h). Solid-phase bioreactors can eliminate this artifact as well as provide the ability to: (*i*) Reuse the enzyme for subsequent analysis;[48-50] (*ii*) enhance the stability and activity of the enzyme;[16,51,52] and (*iii*) simplify on-line processing in addition to allowing easier separation of the reaction products from the enzyme.

Researchers have adopted various approaches for designing proteolytic reactors integrated into microfluidic devices, for example the use of trypsin-coated microparticles loaded into microchannels. Our group has generated an interesting approach for performing solid-phase bioreactions.[15,53] The solid-phase bioreactor consists of a channel populated with microposts that contain a functional scaffold from which the proteolytic enzyme can be covalently linked.[15,53] We have also shown the use of a solid-phase bioreactor (see Figure 4.7) that allowed for continuous deposition onto a MALDI plate, a reaction time of ~24 s, and no noticeable loss of enzyme activity throughout the depositions.[15]

The attractive nature of this approach is that the fluidic module and solid support are fabricated in a single step using micro-replication of a thermoplastic.[54] Following molding of the bioreactor and fluidic network, the solid support is exposed to UV radiation to create carboxylic acids that can be linked through an amide bond using EDC/NHS coupling chemistry to the proteolytic enzyme.[15]

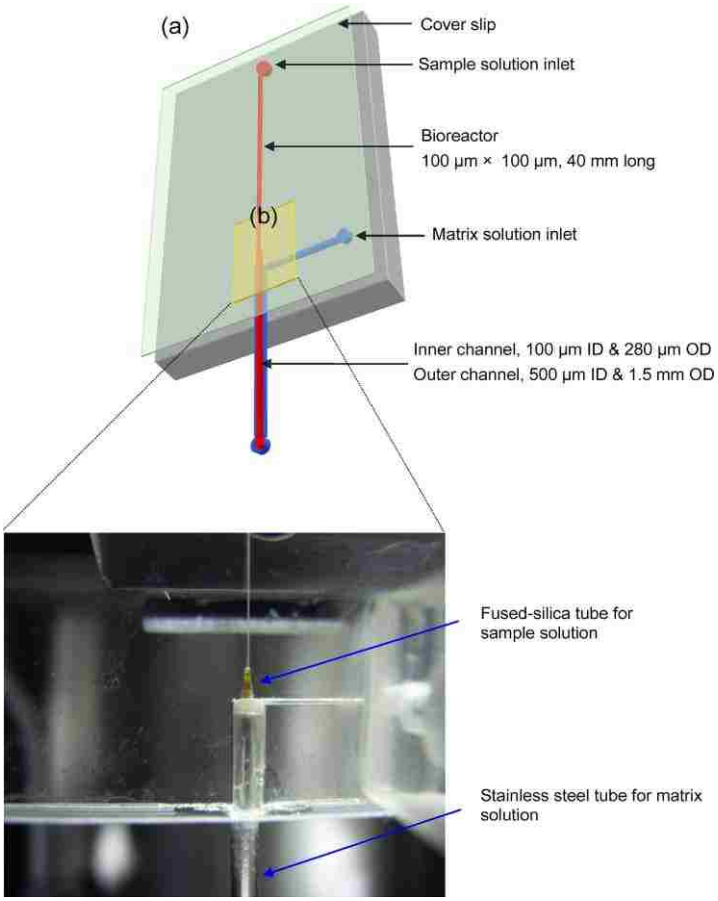

Figure 4.7 (a) Schematic of the bioreactor. (b) The assembled tryptic digest microfluidic chip that includes: PMMA chip and cover slip, inlet and outlet connectors, capillary and stainless steel tubing. At the end of the bioreactor are coaxial tubes that were sealed to mix digests with a matrix solution and to deposit onto the MALDI target plate (Reproduced from Lee, J.; Musyimi, H. K.; Soper, S. A.; Murray, K. K. *J Am Soc Mass Spectrom* **2008**, *19*, 964 with permission, Copyright 2013, Springer Science and Business Media).

We have shown that by using this arrangement, proteolytic reactions can be carried out in ~20 s using either hydrodynamic or electrokinetic pumping.[15,55]

4.2.4.2 Micropost Arrays for Solid-phase Bioreactor

Shortcomings associated with many solid-phase bioreactors are twofold. First, diffusional kinetic barriers produced by immobilizing the reagents to the solid support can be significant. Reducing the channel dimensions can have a profound impact on the efficiency of conversion of the chemical reactant to product during travel through the bioreactor. The second shortcoming associated with solid-phase bioreactors is the limited load of chemical

reagent to the surface, especially for non-porous materials. The load level of reagent in the bioreactor is determined by the size of the immobilized reagent and the surface area of the bioreactor. For example, assuming an open-bed reactor with a rectangular geometry of 5 x 5 μm, the effective surface area is only (l = 1.0 cm) 2.0 x 10^{-3} cm^2. For a molecule with a cross sectional area of 100 $Å^2$, this would amount to ~2.0 x 10^{11} molecules attached to the surface of the reactor (0.3 pmol). In order to keep an enzymatic reaction pseudo first order, only ~0.003 pmol of material could be analyzed.

To address these issues, researchers have adopted 3D architectures in open microfluidic channels employing either polymer monoliths[53,56-63] or hydrogels.[49,64-71] The challenge with these techniques is that many of the reagents required to prepare the hydrogel or monolith are incompatible with the material used to fabricate the fluidic chip when polymers are the substrate.[57] Another consideration is the porosities of these materials, which can create large pressure drops for material driven through the reactor hydrostatically or exclusion effects prohibiting the entrance of large molecules into the reactor bed. Finally, the chemical preparation of hydrogels or monoliths adds additional processing time and labor to the chip fabrication.

We will use micropost arrays as the solid-phase bioreactors, which can provide greatly increased surface area so that the efficiency of a chemical reaction between the solid and fluidized materials can be improved, but do so with minimal amounts of time and labor needed to prepare the reactor bed. These reactors consist of microchannels populated with microposts generated using hot embossing in a single fabrication step.[15] Moreover, it has been found that micropost arrays can also be utilized to promote mixing or enhance reaction rates.

We will use computational fluid dynamics to futher study the flow patterns around the posts within the microchannels. We will initiate our studies using posts of 20 μm diameter and an interpost spacing of 20 μm. The channel dimensions for these bioreactors will be 50 μm in depth, 1 mm in width, and 7 mm in length. With these dimensions, the bioreactor surface area is approximately 28 mm^2 with a surface area to volume ratio of 103 mm^{-1}. We have successfully immobilized trypsin onto PMMA surfaces using microfluidic channels populated with microposts. Results for the digestion of *cytochrome c* using trypsin showed that with a residence time of ~20 s, the sequence coverage (ratio of the identified amino acid residues to the total number of amino acid residues in the protein) was 98% compared to only 9% for an open channel reactor of the same size. We will investigate different post geometries (*e.g.* squares, diamonds, circles), post sizes (lateral dimensions) and interpost spacing to produce high loads of enzyme and attempt to further reduce the reaction time and efficiency. If we desire smaller posts and interpost spacing, we can use UV *LiGA* to manufacture the master for replicating the desired parts using hot embossing.[72]

We will carefully evaluate the ability of obtaining peptides from a variety of membrane proteins using trypsin; however, trypsin cleavage is less frequent for integral membrane proteins,[73] because lysine and arginine residues are not uniformly distributed along the protein sequence.[74] Therefore, trypsin may be used in conjunction with chymotrypsin to aid in the sequence coverage and identification of integral membrane proteins. Chymotrypsin, although less specific than trypsin, effectively cleaves peptide bonds consisting of amino acids with aromatic or large hydrophobic side chains.[75] This will require the formation of mixed-monolayers of enzymes or the sequential patterning of trypsin and chymotrypsin reactor beds by masking.

4.2.5 NALDI-MS Platform for the Analysis of Mass-limited Samples

The samples from the digestion module will be continuously depostied from the microfluidic system onto a MALDI target for off-line analysis. To improve the mass LOD required to further accommodate the microfluidic outputs, we will utilize engineered plates comprised of Si nanowires grown via chemical vapor deposition (CVD) techniques onto Si substrates (NALDI), which have been shown to improve the LOD by approximately 10-fold compared to conventional MALDI.[76-79] NALDI does not require a matrix, which also results in less interference in the low mass range. Also, a NALDI target plate is built on a hydrophobic surface that will create narrow lines of aqueous solvent when the chip effluent is deposited onto the plate via direct deposition.[80,81]

Continous deposition from the fluidic system to the target plate will be utilized for the NALDI analysis. The fluidic system will be fit into a stationary mount, a guide channel will be embossed into the fluidic motherboard, and used for transporting samples onto the target. The NALDI plate will be placed on another mount operated using linear actuators and a motion controller interfaced to a computer running LabView. During deposition, the fluidic system outlet will be brought into contact with the target for depositing the effluent. The rate of target motion will be matched to the (off-line) MS readout rate. After sample deposition, the target will be loaded into the MS and spectra acquired. We will also investigate the effects of co-deposition of SDS onto MALDI/NALDI plates and its effects on the integrity of the MS.

Recent studies have shown that SDS concentrations ranging from 0.3% to 1.0% (w/v) can improve the sequence coverage for proteins analyzed via MALDI-MS,[82-84] whereas concentrations above 1% lead to loss of spectral quality due to excess Na^+ and also, formation

of SDS cluster peaks in the MS. As noted above, for our MEKC dimension of the 2D μCE, we will be using SDS concentrations near the CMC (>0.23%), so we will be below the critical 1% level to maintain MS integrity. In all of the cited work, however, the effects of SDS were evaluated for MALDI-MS, in which a matrix was used; the effects of co-deposition of SDS with NALDI have not been evaluated. Therefore, we will investigate the effects of SDS concentration on the integrity of NALDI.

4.2.6 Integration of Modules for Membrane Protein Analysis

The overall goal of this work is to integrate the previously discussed modules to a motherboard that possesses a fluidic bus, interconnects and valves for controlling reagent/sample flow direction that is driven hydrodynamically through the use of off-chip pumps. The proposed integrated system is based on a modular format (see Figure 4.1) and consists of four modules. Fluidic modules will be interconnected to the modules using the design concept shown in Figure 4.6. An excimer laser will be employed to drill holes of the appropriate shape and size into the fluidic motherboard and module. Then, a Tefzel tube will be inserted into the laser-drilled holes.

Exerting pressure on the assembly allows the proper leak-free interconnection (up to ~600 psi). As can be seen from the micrograph depicted in Figure 4.6, this interconnection produces minimal unswept or dead volumes, which is a critical performance metric when analyzing mass-limited samples. We will use a combination of electrokinetic and hydrodynamic pumping. For example, the cell biotinylation and SPE modules will use hydrodynamic pumping with off-chip pumps.

Electrokinetic fluid drive will be used for the µ-CE with subsequent deposition onto the MALDI plate. We have already discussed the use of COMSOL to investigate the flow patterns around microposts for the SPE work (see Chapter 2). COMSOL and/or computational fluid dynamics will be employed to study flow patterns around various posted architectures, which will include the packing geometry (hexagonal, equilateral or square array), post spacing or post diameter.

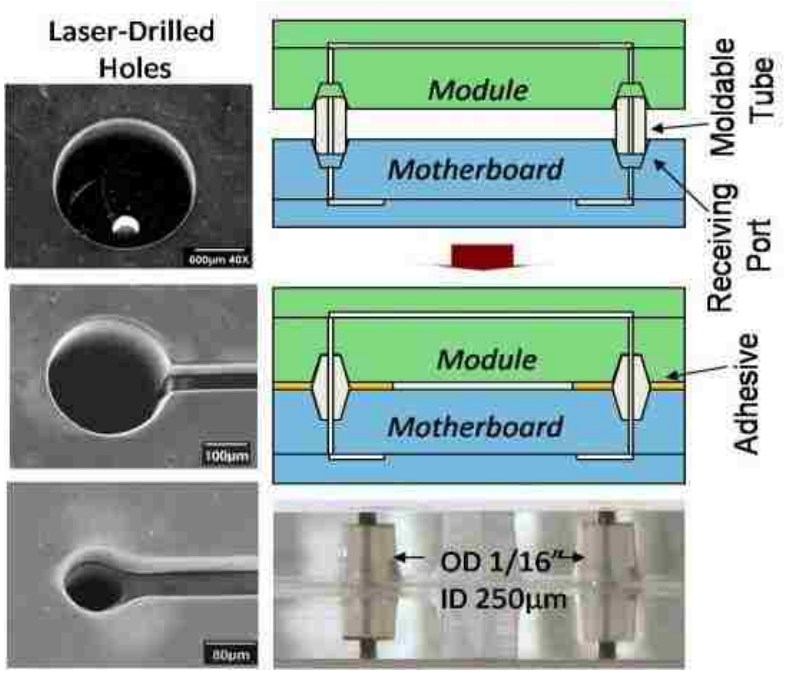

Figure 4.8 Micrographs on the left show laser drilled holes using an ArF excimer laser into a thermoplastic (PC). The schematics on the right show the interconnect technology that will be used to provide leak-free connections of modules to the fluidic motherboard. The micrograph (bottom right) shows a connection between two polymer pieces with dye filling the fluidic via, showing near zero dead volume.

We will also analyze the flow distribution[85,86] within and between the module and motherboard. The transport velocity through posted beds will be optimized with respect to balancing the encounter and reaction rates.[87,88] For electrokinetic driving, we will analyze material discontinuities (motherboard/module interfaces and interconnects) to evaluate the

effects of material dependent electroosmotic flows (EOFs) that may generate laminar flow profiles and consequently, degrade plate numbers for the µ-CE phases of the processing.[89]

We will employ several on-chip valves (see Figure 4.1, SV1-7) poised on the fluidic motherboard. Figure 4.9 shows drawings of the design and operation of these valves, which consist of a two-layered structure (fluidic substrate and cover plate) as opposed to three-layered structures typically employed for PDMS-based membrane values. Valves will be actuated with solenoids. Simplicity of fabrication, and the use of a single material differentiates these fluid control elements from other on-chip valves, which are typically hybrid devices consisting of glass and PDMS.[90-94]

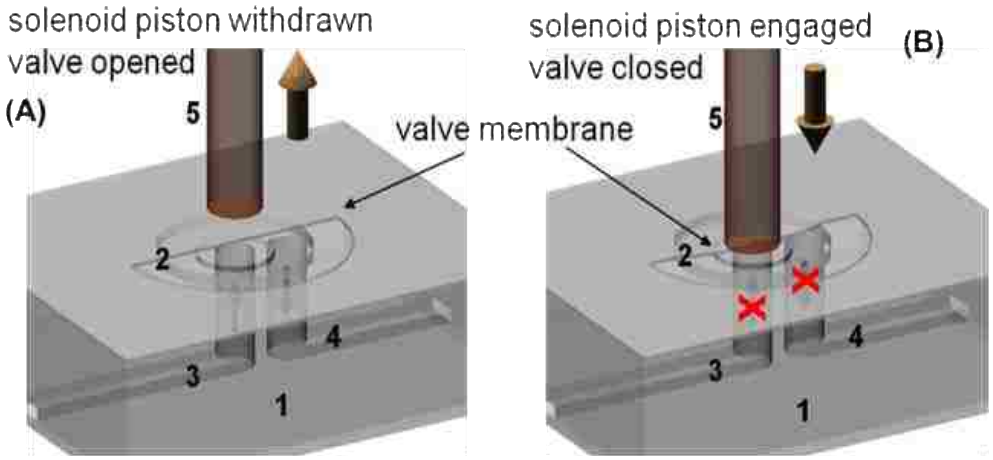

Figure 4.9 Physical operation of the on-chip valve. **A** – valve in open position, **B** – valve in closed position; **1** – PC chip body; **2** – PC membrane; **3** – inlet; **4** – outlet; **5** – solenoid actuated plunger. Half-circle cutouts in the membrane were used for clarity of the pictures.

We have successfully tested these micro-valves with head pressures up to 105 psi with no leakage; these valves can take more than an order of magnitude higher pressure load than hybrid thermoplastic/elastomeric valves.[95] The valving membrane (motherboard cover plate) used here is PC, with the substrate also made from PC to allow simple thermal fusion bonding of these materials.

4.3 References

(1) Yang, W.; Sun, X.; Pan, T.; Woolley, A. T. *Electrophoresis* **2008**, *29*, 3429.

(2) Zhao, Y.; Zhang, W.; Kho, Y.; Zhao, Y. *Anal Chem* **2004**, *76*, 1817.

(3) Chen, H.; Fan, Z. H. *Electrophoresis* **2009**, *30*, 758.

(4) Chen, X.; Wu, H.; Mao, C.; Whitesides, G. M. *Anal Chem* **2002**, *74*, 1772.

(5) Erickson, D., Li, D. *Analytica chimica acta* **2004**, *507*, 11.

(6) Molloy, M. P.; Brzezinski, E. E.; Hang, J.; McDowell, M. T.; VanBogelen, R. A. *Proteomics* **2003**, *3*, 1912.

(7) Osiri, J. K.; Shadpour, H.; Park, S.; Snowden, B. C.; Chen, Z. Y.; Soper, S. A. *Electrophoresis* **2008**, *29*, 4984.

(8) Service, R. F. *Science* **2001**, *294*, 2074.

(9) Shadpour, H.; Soper, S. A. *Anal Chem* **2006**, *78*, 3519.

(10) Smith, R. D. *Nat Biotechnol* **2000**, *18*, 1041.

(11) Wang, H.; Hanash, S. *Journal of chromatography. B, Analytical technologies in the biomedical and life sciences* **2003**, *787*, 11.

(12) Brivio, M.; Fokkens, R. H.; Verboom, W.; Reinhoudt, D. N.; Tas, N. R.; Goedbloed, M.; van den Berg, A. *Anal Chem* **2002**, *74*, 3972.

(13) Duan, J.; Sun, L.; Liang, Z.; Zhang, J.; Wang, H.; Zhang, L.; Zhang, W.; Zhang, Y. *Journal of chromatography. A* **2006**, *1106*, 165.

(14) Jin, L. J.; Ferrance, J.; Sanders, J. C.; Landers, J. P. *Lab on a chip* **2003**, *3*, 11.

(15) Lee, J.; Musyimi, H. K.; Soper, S. A.; Murray, K. K. *J Am Soc Mass Spectrom* **2008**, *19*, 964.

(16) Letant, S. E.; Hart, B. R.; Kane, S. R.; Hadi, M. Z.; Shields, S. J.; Reynolds, J. G. *Adv Mater* **2004**, *16*, 689.

(17) Peterson, D. S.; Rohr, T.; Svec, F.; Frechet, J. M. *Anal Chem* **2002**, *74*, 4081.

(18) Adams, A. A.; Okagbare, P. I.; Feng, J.; Hupert, M. L.; Patterson, D.; Gottert, J.; McCarley, R. L.; Nikitopoulos, D.; Murphy, M. C.; Soper, S. A. *J Am Chem Soc* **2008**, *130*, 8633.

(19) Dharmasiri, U.; Balamurugan, S.; Adams, A. A.; Okagbare, P. I.; Obubuafo, A.; Soper, S. A. *Electrophoresis* **2009**, *30*, 3289.

(20) Dharmasiri, U.; Njoroge, S. K.; Witek, M. A.; Adebiyi, M. G.; Kamande, J. W.; Hupert, M. L.; Barany, F.; Soper, S. A. *Anal Chem* **2011**, *83*, 2301.

(21) Dharmasiri, U.; Witek, M. A.; Adams, A. A.; Osiri, J. K.; Hupert, M. L.; Bianchi, T. S.; Roelke, D. L.; Soper, S. A. *Anal Chem* **2010**, *82*, 2844.

(22) Yates, J. R.; Ruse, C. I.; Nakorchevsky, A. *Annual Review of Biomedical Engineering* **2009**, *11*, 49.

(23) Wabuyele, M. B.; Ford, S. M.; Stryjewski, W.; Barrow, J.; Soper, S. A. *Electrophoresis* **2001**, *22*, 3939.

(24) Effenhauser, C. S.; Bruin, G. J.; Paulus, A.; Ehrat, M. *Anal Chem* **1997**, *69*, 3451.

(25) Fister, J. C.; Jacobson, S. C.; Davis, L. M.; Ramsey, J. M. *Anal Chem* **1998**, *70*, 431.

(26) Haab, B. B.; Mathies, R. A. *Anal Chem* **1999**, *71*, 5137.

(27) Webster, J. R.; Burns, M. A.; Burke, D. T.; Mastrangelo, C. H. *Anal Chem* **2001**, *73*, 1622.

(28) Burns, M. A.; Johnson, B. N.; Brahmasandra, S. N.; Handique, K.; Webster, J. R.; Krishnan, M.; Sammarco, T. S.; Man, P. M.; Jones, D.; Heldsinger, D.; Mastrangelo, C. H.; Burke, D. T. *Science* **1998**, *282*, 484.

(29) Baba, Y. *Electrochemistry* **2000**, *68*, 197.

(30) Martin, R. S.; Gawron, A. J.; Lunte, S. M. *Anal Chem* **2000**, *72*, 3196.

(31) Rossier, J. S.; Roberts, M. A.; Ferrigno, R.; Girault, H. H. *Anal Chem* **1999**, *71*, 4294.

(32) Suzuki, H.; Arakawa, H.; Sasaki, S.; Karube, I. *Anal Chem* **1999**, *71*, 1737.

(33) Tantra, R.; Manz, A. *Anal Chem* **2000**, *72*, 2875.

(34) Wang, J.; Chatrathi, M. P.; Tian, B. *Anal Chem* **2000**, *72*, 5774.

(35) Wang, J.; Tian, B.; Sahlin, E. *Anal Chem* **1999**, *71*, 5436.

(36) Woolley, A. T.; Lao, K.; Glazer, A. N.; Mathies, R. A. *Anal Chem* **1998**, *70*, 684.

(37) Gawron, A. J.; Martin, R. S.; Lunte, S. M. *Electrophoresis* **2001**, *22*, 242.

(38) Martin, R. S.; Gawron, A. J.; Fogarty, B. A.; Regan, F. B.; Dempsey, E.; Lunte, S. M. *The Analyst* **2001**, *126*, 277.

(39) Lacher, N. A.; Garrison, K. E.; Martin, R. S.; Lunte, S. M. *Electrophoresis* **2001**, *22*, 2526.

(40) Huang, X. H.; Pang, T. K. J.; Gordon, M. J.; Zare, R. N. *Analytical Chemistry* **1987**, *59*, 2747.

(41) Huang, X. H.; Luckey, J. A.; Gordon, M. J.; Zare, R. N. *Analytical Chemistry* **1989**, *61*, 766.

(42) Galloway, M.; Stryjewski, W.; Henry, A.; Ford, S. M.; Llopis, S.; McCarley, R. L.; Soper, S. A. *Anal. Chem.* **2002**, *74*, 2407.

(43) Shadpour, H.; Hupert, M. L.; Patterson, D.; Liu, C. G.; Galloway, M.; Stryjewski, W.; Goettert, J.; Soper, S. A. *Anal. Chem.* **2007**, *79*, 870.

(44) Henry, A. C.; Tutt, T. J.; Galloway, M.; Davidson, Y. Y.; McWhorter, C. S.; Soper, S. A.; McCarley, R. L. *Anal Chem* **2000**, *72*, 5331.

(45) Vaidya, B.; Soper, S. A.; McCarley, R. L. *The Analyst* **2002**, *127*, 1289.

(46) Xu, F.; Datta, P.; Wang, H.; Gurung, S.; Hashimoto, M.; Wei, S.; Goettert, J.; McCarley, R. L.; Soper, S. A. *Anal Chem* **2007**, *79*, 9007.

(47) Yin, H., Qu, X. and Jia, C. *Journal of University of Science and Technology Beijing* **2008**, *15*, 480.

(48) Mao, H.; Yang, T.; Cremer, P. S. *Anal Chem* **2002**, *74*, 379.

(49) Seong, G. H.; Zhan, W.; Crooks, R. M. *Anal Chem* **2002**, *74*, 3372.

(50) Davidson, Y. Y., Soper, S. A., Margolis, S., Sander, L. C. *Journal of separation science* **2001**, *24*, 10.

(51) Laurell, T., Drott, J. Rosengren, L., Lindstrom, K. *Sensors and Actuators B: Chemical* **1996**, *31*, 161.

(52) Manjón, A., Obón, J. M., Casanova, P., Fernández, V. M., Ilborra, J. L. *Biotechnology letters* **2002**, *24*, 1227.

(53) Hasselbrink, E. F., Jr.; Shepodd, T. J.; Rehm, J. E. *Anal Chem* **2002**, *74*, 4913.

(54) Hupert, M. L., Guy, W. J., Llopis, S. D., Shadpour, H., Sudheer, R., Nikitopoulos, D. E., Soper, S. A. *Microfluidics and Nanofluidics* **2007**, *3*, 1.

(55) Lee, C. S.; Lee, S. H.; Kim, Y. G.; Lee, J. H.; Kim, Y. K.; Kim, B. G. *Biosensors & bioelectronics* **2007**, *22*, 891.

(56) Peters, E. C., Svec, F., Fréchet, J. M. *Adv Mater* **1999**, *11*, 1169.

(57) Stachowiak, T. B.; Rohr, T.; Hilder, E. F.; Peterson, D. S.; Yi, M.; Svec, F.; Frechet, J. M. *Electrophoresis* **2003**, *24*, 3689.

(58) Svec, F., Fréchet, J. M. *Ind Eng Chem Res* **1999**, *38*, 34.

(59) Yu, C., Svec, F., Fréchet, J. M. *Abstr Pap Am Chem S* **2001**, *222*, U84.

(60) Yu, C., Xu, M., Svec, F., Fréchet, J. M. *Journal of Polymer Science Part A-Polymer Chemistry* **2002**, *40*, 755.

(61) Yu, C.; Davey, M. H.; Svec, F.; Frechet, J. M. *Anal Chem* **2001**, *73*, 5088.

(62) Yu, C.; Svec, F.; Frechet, J. M. *Electrophoresis* **2000**, *21*, 120.

(63) Xie, S., Svec, F., Fréchet, J. M. J. *Biotechnology & Bioengineering* **1999**, *62*, 30.

(64) Burdick, J. A.; Khademhosseini, A.; Langer, R. *Langmuir : the ACS journal of surfaces and colloids* **2004**, *20*, 5153.

(65) Harmon, M. E., Tang, M., Frank, C. W. *Polymer* **2003**, *44*, 4547.

(66) Neidhart, M., Rethage, J., Kuchen, S., Künzler, P., Crowl, R., Billingham, M., Gay, R., Gay, S. *Arthritis & Rheumatism* **2000**, *43*, 2634.

(67) Hoffmann, J., Plötner, M., Kuckling, D., Fischer, W. J. *Sens. Actuator A-Phys.* **1999**, *77*, 139.

(68) Khoury, C., Adalsteinsson, T., Johnson, B., Crone, W. C., Beebe, D. J. *Biomedical Microdevices* **2003**, *5*, 35.

(69) Siegal, R. A., Gu, Y. D., Baldi, A., Ziaie, B. *Macromolecular Symposia* **2004**, *207*, 249.

(70) Campbell, T. D., Washington, R. P., Ginn, B. T., Blakemore, L. J., Trombley, P. Q., and Steinbock,O. *Abstr Pap Am Chem S* **2003**, *225*, U512.

(71) Lesho, M. J., Sheppard, N. F. *Abstr Pap Am Chem S* **1994**, *208*, 423.

(72) Witek, M. A.; Hupert, M. L.; Park, D. S. W.; Fears, K.; Murphy, M. C.; Soper, S. A. *Analytical Chemistry* **2008**, *80*, 3483.

(73) Kyte, J.; Doolittle, R. F. *Journal of molecular biology* **1982**, *157*, 105.

(74) Sipos, L.; von Heijne, G. *European journal of biochemistry / FEBS* **1993**, *213*, 1333.

(75) Lu, B.; McClatchy, D. B.; Kim, J. Y.; Yates, J. R., 3rd *Proteomics* **2008**, *8*, 3947.

(76) Daniels, R. H.; Dikler, S.; Li, E.; Stacey, C. *JALA* **2008**, 314.

(77) Go, E. P.; Apon, J. V.; Saghatelian, A.; Daniels, R. H.; Sahi, V.; Dubrow, R.; Cravatt, B. F.; Vertes, A.; Siuzdak, G. *Anal. Chem.* **2005**, *77*, 1641.

(78) Kang, M.-J.; Pyun, J.-C.; Lee, J.-C.; Park, J.-H.; Park, J.-G.; Lee, J.-G.; Choi, H.-J. *Rapid Commun. Mass Spectrom.* **2005**, *19*, 3166.

(79) Vidova, V.; Novak, P.; Strohalm, M.; Pol, J.; Havlicek, V.; Volny, M. *Anal Chem* **2010**, *82*, 4994.

(80) Lee, J.; Musyimi, H. K.; Soper, S. A.; Murray, K. K. *J. Am. Soc. Mass Spectrom.* **2008**, *19*, 964.

(81) Lee, J.; Soper, S. A.; Murray, K. K. *Analyst* **2009**, *134*, 2426.

(82) Zhang, N.; Li, L. *Rapid Commun. Mass Spectrom.* **2004**, *18*, 889.

(83) Tummala, R.; Green-Church, K. B.; Limbach, P. A. *American Society for Mass Spectrometry* **2005**, *16*, 1438.

(84) Tummala, R.; Limbach, P. A. *Rapid Commun. Mass Spectrom.* **2004**, *18*, 2031.

(85) Drummond, J. E.; Tahir, M. I. *International Journal of Multiphase Flow* **1984**, *10*, 515.

(86) Gordon, D. *Computational Fluids* **1978**, *6*, 1.

(87) Adams, A. A.; Okagbare, P. I.; Feng, J.; Hupert, M. L.; Patterson, D.; Gottert, J.; McCarley, R. L.; Nikitopoulos, D.; Murphy, M. C.; Soper, S. A. *J. Am. Chem. Soc.* **2008**, *130*, 8633.

(88) Chang, K. C.; Hammer, D. A. *BIophysical Journal* **1999**, *76*, 1280.

(89) Shadpour, H.; Musyimi, H.; Chen, J.; Soper, S. A. *J. Chromatogr. A* **2006**, *1111*, 238.

(90) Lagally, E. T.; Sintegral membrane proteinson, P. C.; Mathies, R. A. *Sens. Actuator B-Chem.* **2000**, *63*, 138.

(91) Grover, W. H.; Skelley, A. M.; Liu, C. N.; Lagally, E. T.; Mathies, R. A. *Sens. Actuator B-Chem.* **2003**, *89*, 315.

(92) Lagally, E. T.; Scherer, J. R.; Blazej, R. G.; Toriello, N. M.; Diep, B. A.; Ramchandani, M.; Sensabaugh, G. F.; Riley, L. W.; Mathies, R. A. *Analytical Chemistry* **2004**, *76*, 3162.

(93) Skelley, A. M.; Scherer, J. R.; Aubrey, A. D.; Grover, W. H.; Ivester, R. H. C.; Ehrenfreund, P.; Grunthaner, F. J.; Bada, J. L.; Mathies, R. A. *Proc. Natl. Acad. Sci. U. S. A.* **2005**, *102*, 1041.

(94) Grover, W. H.; Ivester, R. H. C.; Jensen, E. C.; Mathies, R. A. *Lab On A Chip* **2006**, *6*, 623.

(95) Zhang, W.; Lin, S.; Wang, C.; Hu, J.; Li, C.; Zhuang, Z.; Zhou, Y.; Mathies, R. A.; Yang, C. J. *Lab Chip* **2009**, *9*, 3088.

Appendix: Permissions

JOHN WILEY AND SONS LICENSE TERMS AND CONDITIONS

Aug 28, 2013

This is a License Agreement between Katrina N Battle ("You") and John Wiley and Sons ("John Wiley and Sons") provided by Copyright Clearance Center ("CCC"). The license consists of your order details, the terms and conditions provided by John Wiley and Sons, and the payment terms and conditions.
All payments must be made in full to CCC. For payment instructions, please see information listed at the bottom of this form.
License Number 3217821263929
License date Aug 28, 2013
Licensed content publisher John Wiley and Sons
Licensed content publication Proteomics
Licensed content title Technologies for plasma membrane proteomics
Licensed copyright line Copyright © 2010 WILEY-VCH Verlag GmbH & Co. KGaA, Weinheim
Licensed content author Stuart J. Cordwell,Tine E. Thingholm
Licensed content date Oct 15, 2009
Start page 611
End page 627
Type of use Dissertation/Thesis
Requestor type University/Academic
Format Print and electronic
Portion Figure/table
Number of figures/tables 2
Original Wiley figure/table number(s) Figure1, Figure 3
Will you be translating? No
Total 0.00 USD

AMERICAN CHEMICAL SOCIETY LICENSE TERMS AND CONDITIONS

Title: Protein Digestion: An Overview of the Available Techniques and Recent Developments
Author: Linda Switzar, Martin Giera, and Wilfried M. A. Niessen
Publication: Journal of Proteome Research
Publisher: American Chemical Society
Date: Mar 1, 2013 Copyright © 2013, American Chemical Society
PERMISSION/LICENSE IS GRANTED FOR YOUR ORDER AT NO CHARGE
This type of permission/license, instead of the standard Terms & Conditions, is sent to you because no fee is being charged for your order. Please note the following:
Permission is granted for your request in both print and electronic formats, and translations.
If figures and/or tables were requested, they may be adapted or used in part.
Please print this page for your records and send a copy of it to your publisher/graduate school.
Appropriate credit for the requested material should be given as follows: "Reprinted (adapted)

with permission from (COMPLETE REFERENCE CITATION). Copyright (YEAR) American Chemical Society." Insert appropriate information in place of the capitalized words. One-time permission is granted only for the use specified in your request. No additional uses are granted (such as derivative works or other editions). For any other uses, please submit a new request. If credit is given to another source for the material you requested, permission must be obtained from that source.

ELSEVIER LICENSE TERMS AND CONDITIONS

Aug 28, 2013
This is a License Agreement between Katrina N Battle ("You") and Elsevier ("Elsevier") provided by Copyright Clearance Center ("CCC"). The license consists of your order details, the terms and conditions provided by Elsevier, and the payment terms and conditions.
All payments must be made in full to CCC. For payment instructions, please see information listed at the bottom of this form.
Supplier Elsevier Limited The Boulevard,Langford Lane Kidlington,Oxford,OX5 1GB,UK
Registered Company Number 1982084
Customer name Katrina N Battle
Customer address 116 Manning Drive CHAPEL HILL, NC 27599
License number 3217930781023
License date Aug 28, 2013
Licensed content publisher Elsevier
Licensed content publication Current Opinion in Chemical Biology
Licensed content title Mass spectrometry for proteomics
Licensed content author Xuemei Han,Aaron Aslanian,John R Yates
Licensed content date October 2008
Licensed content volume number 12
Licensed content issue number 5
Number of pages 8
Start Page 483
End Page 490
Type of Use reuse in a thesis/dissertation
Intended publisher of new work other
Portion figures/tables/illustrations
Number of figures/tables/illustrations 1
Format both print and electronic
Are you the author of this Elsevier article? No
Will you be translating? No
Order reference number
Title of your thesis/dissertation Microfluidics for the Analysis of Integral Membrane Proteins: A Top-down Approach
Expected completion date Dec 2013
Estimated size (number of pages) 157
Elsevier VAT number GB 494 6272 12
Permissions price 0.00 USD
VAT/Local Sales Tax 0.0 USD / 0.0 GBP

AMERICAN CHEMICAL SOCIETY LICENSE TERMS AND CONDITIONS

Title: Proteomics on Full-Length Membrane Proteins Using Mass Spectrometry
Author: Johannes le Coutre et al.
Publication: Biochemistry
Publisher: American Chemical Society
Date: Apr 1, 2000 Copyright © 2000, American Chemical Society
PERMISSION/LICENSE IS GRANTED FOR YOUR ORDER AT NO CHARGE
This type of permission/license, instead of the standard Terms & Conditions, is sent to you because no fee is being charged for your order. Please note the following:
Permission is granted for your request in both print and electronic formats, and translations.
If figures and/or tables were requested, they may be adapted or used in part. Please print this page for your records and send a copy of it to your publisher/graduate school. Appropriate credit for the requested material should be given as follows: "Reprinted (adapted) with permission from (COMPLETE REFERENCE CITATION). Copyright (YEAR) American Chemical Society." Insert appropriate information in place of the capitalized words. One-time permission is granted only for the use specified in your request. No additional uses are granted (such as derivative works or other editions). For any other uses, please submit a new request. If credit is given to another source for the material you requested, permission must be obtained from that source.

AMERICAN CHEMICAL SOCIETY LICENSE TERMS AND CONDITIONS

Title: Preconcentration of Proteins on Microfluidic Devices Using Porous Silica Membranes
Author: Robert S. Foote,*, Julia Khandurina,†, Stephen C. Jacobson,‡ and, and J. Michael Ramsey§
Publication: Analytical Chemistry
Publisher: American Chemical Society
Date: Jan 1, 2005 Copyright © 2005, American Chemical Society
PERMISSION/LICENSE IS GRANTED FOR YOUR ORDER AT NO CHARGE
This type of permission/license, instead of the standard Terms & Conditions, is sent to you because no fee is being charged for your order. Please note the following: Permission is granted for your request in both print and electronic formats, and translations. If figures and/or tables were requested, they may be adapted or used in part. Please print this page for your records and send a copy of it to your publisher/graduate school. Appropriate credit for the requested material should be given as follows: "Reprinted (adapted) with permission from (COMPLETE REFERENCE CITATION). Copyright (YEAR) American Chemical Society." Insert appropriate information in place of the capitalized words. One-time permission is granted only for the use specified in your request. No additional uses are granted (such as derivative works or other editions). For any other uses, please submit a new request. If credit is given to another source for the material you requested, permission must be obtained from that source.

ELSEVIER LICENSE TERMS AND CONDITIONS

Aug 28, 2013

This is a License Agreement between Katrina N Battle ("You") and Elsevier ("Elsevier") provided by Copyright Clearance Center ("CCC"). The license consists of your order details, the terms and conditions provided by Elsevier, and the payment terms and conditions.

All payments must be made in full to CCC. For payment instructions, please see information listed at the bottom of this form.

Supplier Elsevier Limited The Boulevard,Langford Lane Kidlington,Oxford,OX5 1GB,UK
Registered Company
Customer name Katrina N Battle
Customer address 116 Manning Drive CHAPEL HILL, NC 27599
License number 3217921349499
License date Aug 28, 2013
Licensed content publisher Elsevier
Licensed content publication Analytica Chimica Acta
Licensed content title Protein digestion and phosphopeptide enrichment on a glass microchip
Licensed content author Guihua Eileen Yue, Michael G. Roper, Catherine Balchunas, Abigail Pulsipher, Joshua J. Coon, Jeffery Shabanowitz, Donald F. Hunt, James P. Landers, Jerome P. Ferrance
Licensed content date 30 March 2006
Licensed content volume number 564
Licensed content issue number 1
Number of pages 7
Start Page 116
End Page 122
Type of Use reuse in a thesis/dissertation
Intended publisher of new work other
Portion figures/tables/illustrations
Number of figures/tables/illustrations 1
Format both print and electronic
Are you the author of this Elsevier article? No
Will you be translating? No
Order reference number
Title of your thesis/dissertation
Microfluidics for the Analysis of Integral Membrane Proteins: A Top-down Approach
Expected completion date Dec 2013
Estimated size (number of pages) 157
Elsevier VAT number GB 494 6272 12
Permissions price 0.00 USD
VAT/Local Sales Tax 0.0 USD / 0.0 GBP
Total 0.00 USD

JOHN WILEY AND SONS LICENSE TERMS AND CONDITIONS

Aug 28, 2013
This is a License Agreement between Katrina N Battle ("You") and John Wiley and Sons ("John Wiley and Sons") provided by Copyright Clearance Center ("CCC"). The license consists of your order details, the terms and conditions provided by John Wiley and Sons, and the payment terms and conditions. All payments must be made in full to CCC. For payment instructions, please see information listed at the bottom of this form.
License Number 3217920921415
License date Aug 28, 2013
Licensed content publisher John Wiley and Sons
Licensed content publication Proteomics
Licensed content title Analysis of outer membrane proteome of Escherichia coli related to resistance to ampicillin and tetracycline
Licensed copyright line Copyright © 2006 WILEY-VCH Verlag GmbH & Co. KGaA, Weinheim
Licensed content author Changxin Xu,Xiangmin Lin,Haixia Ren,Yueling Zhang,Sanying Wang,Xuanxian Peng
Licensed content date Dec 21, 2005
Start page 462
End page 473
Type of use Dissertation/Thesis
Requestor type University/Academic
Format Print and electronic
Portion Figure/table
Number of figures/tables 1
Original Wiley figure/table number(s) Figure 4
Will you be translating? No
Total 0.00 USD

JOHN WILEY AND SONS LICENSE TERMS AND CONDITIONS

Aug 29, 2013
This is a License Agreement between Katrina N Battle ("You") and John Wiley and Sons ("John Wiley and Sons") provided by Copyright Clearance Center ("CCC"). The license consists of your order details, the terms and conditions provided by John Wiley and Sons, and the payment terms and conditions. All payments must be made in full to CCC. For payment instructions, please see information listed at the bottom of this form.
License Number 3218551499370
License date Aug 29, 2013
Licensed content publisher John Wiley and Sons
Licensed content publication Electrophoresis
Licensed content title A proteomic approach to investigate potential biomarkers directed against membrane-associated breast cancer proteins
Licensed copyright line Copyright © 2006 WILEY-VCH Verlag GmbH & Co. KGaA, Weinheim

Licensed content author Ludovic Canelle,Jordane Bousquet,Cedric Pionneau,Julie Hardouin,Genevieve Choquet-Kastylevsky,Raymonde Joubert-Caron,Michel Caron
Licensed content date Mar 20, 2006
Start page 1609
End page 1616
Type of use Dissertation/Thesis
Requestor type University/Academic
Format Print and electronic
Portion Figure/table
Number of figures/tables 1
Original Wiley figure/table number(s) Figure 2
Will you be translating? No
Total 0.00 USD

JOHN WILEY AND SONS LICENSE TERMS AND CONDITIONS

Aug 29, 2013
This is a License Agreement between Katrina N Battle ("You") and John Wiley and Sons ("John Wiley and Sons") provided by Copyright Clearance Center ("CCC"). The license consists of your order details, the terms and conditions provided by John Wiley and Sons, and the payment terms and conditions. All payments must be made in full to CCC. For payment instructions, please see information listed at the bottom of this form.
License Number 3218541268418
License date Aug 29, 2013
Licensed content publisher John Wiley and Sons
Licensed content publication Electrophoresis
Licensed content title Generating high peak capacity 2-D maps of complex proteomes using PMMA microchip electrophoresis
Licensed copyright line Copyright © 2008 WILEY-VCH Verlag GmbH & Co. KGaA, Weinheim
Licensed content author John K. Osiri, Hamed Shadpour, Sunjung Park, Brandy C. Snowden, Zhi Yuan Chen, Steven A. Soper
Licensed content date Jan 7, 2009
Start page 4984
End page 4992
Type of use Dissertation/Thesis
Requestor type University/Academic
Format Print and electronic
Portion Figure/table
Number of figures/tables 1
Original Wiley figure/table number(s) Figure 3
Will you be translating? No
Total 0.00 USD

SPRINGER LICENSE TERMS AND CONDITIONS

Sep 02, 2013

This is a License Agreement between Katrina N Battle ("You") and Springer ("Springer") provided by Copyright Clearance Center ("CCC"). The license consists of your order details, the terms and conditions provided by Springer, and the payment terms and conditions. All payments must be made in full to CCC. For payment instructions, please see information listed at the bottom of this form.

License Number 3221020531492
License date Sep 02, 2013
Licensed content publisher Springer
Licensed content publication Analytical and Bioanalytical Chemistry
Licensed content title Ultra-fast two-dimensional microchip electrophoresis using SDS μ-CGE and microemulsion electrokinetic chromatography for protein separations
Licensed content author John K. Osiri
Licensed content date Jan 1, 2010
Volume number 398
Issue number 1
Type of Use Thesis/Dissertation
Portion Figures
Author of this Springer article No
Order reference number
Title of your thesis /dissertation Microfluidics for the Analysis of Integral Membrane Proteins: A Top-down Approach
Expected completion date Dec 2013
Estimated size (pages) 157
Total 0.00 USD

Limited License

With reference to your request to reprint in your thesis material on which Springer Science and Business Media control the copyright, permission is granted, free of charge, for the use indicated in your enquiry. Licenses are for one-time use only with a maximum distribution equal to the number that you identified in the licensing process. This License includes use in an electronic form, provided its password protected or on the university's intranet or repository, including UMI (according to the definition at the Sherpa website: http://www.sherpa.ac.uk/romeo/). For any other electronic use, please contact Springer at (permissions.dordrecht@springer.com or permissions.heidelberg@springer.com). The material can only be used for the purpose of defending your thesis, and with a maximum of 100 extra copies in paper. Although Springer holds copyright to the material and is entitled to negotiate on rights, this license is only valid, subject to a courtesy information to the author (address is given with the article/chapter) and provided it concerns original material which does not carry references to other sources (if material in question appears with credit to another source, authorization from that source is required as well). Permission free of charge on this occasion does not prejudice any rights we might have to charge for reproduction of our copyrighted material in the future.

Copyright Permission Request

TO WHOM IT MAY CONCERN:

I am not an author of the Science article entitled, Structural origins of high-affinity biotin binding to streptavidin by Weber P. C., Ohlendorf D. H., Wendoloski J. J., Salemme F. R. (Science, 1989, 243, 85), but I would like to obtain permission to incorporate a figure presented in the article (shown below) in my dissertation entitled, Microfluidics for the Analysis of Integral Membrane Proteins: A Top-down Approach.
Thanks,
Katrina Battle

Dear Katrina: Re: 1 fig from "Structural origins of high-affinity biotin binding to streptavidin" *Science* 6 January 1989: Vol. 243 no. 4887 pp. 85-88, DOI: 10.1126/science.2911722

Thank you very much for your request and for your interest in our content.
Please feel free to include the figure in your thesis or dissertation subject to the guidelines listed on our website. Permission covers the distribution of your dissertation or thesis on demand by a third party distributor (e.g. ProQuest/UMI), provided the AAAS material covered by this permission remains *in situ* and is not distributed by that third party outside of the context of your Thesis/Dissertation. Permission does not apply to figures/photos/artwork or any other content or materials included in your work that are credited to non-AAAS sources. If the requested material is sourced to or references non-AAAS sources, you must obtain authorization from that source as well before using that material. You agree to hold harmless and indemnify AAAS against any claims arising from your use of any content in your work that is credited to non-AAAS sources. By using the AAAS Material identified in your request, you agree to abide by all the terms and conditions herein. AAAS makes no representations or warranties as to the accuracy of any information contained in the AAAS material covered by this permission, including any warranties of merchantability or fitness for a particular purpose. If how you wish to use our content falls outside of these guidelines or if you have any questions please just let me know.

Best regards,
Liz Sandler (Ms) Elizabeth Sandler
Rights and Permissions The American Association for the Advancement of Science 1200 New York Ave., NW Washington, DC 20005
+1-202-326-6765 (tel) esandler@aaas.org

SPRINGER LICENSE TERMS AND CONDITIONS

Sep 03, 2013
This is a License Agreement between Katrina N Battle ("You") and Springer ("Springer") provided by Copyright Clearance Center ("CCC"). The license consists of your order details, the terms and conditions provided by Springer, and the payment terms and conditions. All payments must be made in full to CCC. For payment instructions, please see information listed at the bottom of this form.

License Number 3221461465685
License date Sep 03, 2013
Licensed content publisher Springer
Licensed content publication Journal of The American Society for Mass Spectrometry
Licensed content title Development of an automated digestion and droplet deposition microfluidic chip for MALDI-TOF MS
Licensed content author Jeonghoon Lee
Licensed content date Jan 1, 2008
Volume number 19
Issue number 7
Type of Use Thesis/Dissertation
Portion Figures
Author of this Springer article No
Order reference number
Title of your thesis/dissertation Microfluidics for the Analysis of Integral Membrane Proteins: A Top-down Approach
Expected completion date Dec 2013
Estimated size(pages) 157
Total 0.00 USD
Terms and Conditions

and the original publisher /journal title, volume, year of publication, page, chapter/article title, name(s) of author(s), figure number(s), original copyright notice) is given to the publication in which the material was originally published, by adding; with kind permission from Springer Science and Business Media"

Title: Contact Conductivity Detection in Poly(methyl methacylate)-Based Microfluidic Devices for Analysis of Mono- and Polyanionic Molecules
Author: Michelle Galloway et al.
Publication: Analytical Chemistry
Publisher: American Chemical Society
Date: May 1, 2002

PERMISSION/LICENSE IS GRANTED FOR YOUR ORDER AT NO CHARGE
This type of permission/license, instead of the standard Terms & Conditions, is sent to you because no fee is being charged for your order. Please note the following: Permission is granted for your request in both print and electronic formats, and translations. If figures and/or tables were requested, they may be adapted or used in part. Please print this page for your records and send a copy of it to your publisher/graduate school. Appropriate credit for the requested material should be given as follows: "Reprinted (adapted) with permission from (COMPLETE REFERENCE CITATION). Copyright (YEAR) American Chemical Society." Insert appropriate information in place of the capitalized words. One-time permission is granted only for the use specified in your request. No additional uses are granted (such as derivative works or other editions). For any other uses, please submit a new request. If credit is given to another source for the material you requested, permission must be obtained from that source.

DATE: 29/08/2013
Full name: Katrina Battle
Comments: Hello! I would like to use a Figure from an article published in your journal in my dissertation in both electronic and print formats. The figure is Figure 3 from the article titled: Proteomic Analysis of Membrane-associated Proteins from the Breast Cancer Cell Line MCF7 from CANCER GENOMICS & PROTEOMICS 2: 199-208 (2005).

Dear Mrs. Battle:

Following your request we are pleased to permit reproduction of Figure 3 of the paper entitled: **“Proteomic Analysis of Membrane-associated Proteins from the Breast Cancer Cell Line MCF7”** by C. Pionneau *et al.* which was published in CANCER GENOMICS & PROTEOMICS Volume 2, No. 4, pp. 199-208 (July-August 2005), provided that you mention the source of information.

With best regards,

Yours sincerely,

John G. Delinasios

Managing Editor
International Institute of Anticancer Research (IIAR)
Editorial Office of ANTICANCER RESEARCH, IN VIVO and CANCER GENOMICS & PROTEOMICS
1st km Kapandritiou-Kalamou Road P.O. Box 22, GR-19014 Kapandriti, Attiki Greece
Tel: +30-22950-52945 Tel/Fax:+30-22950-53389
e-mail: iiar@iiar-anticancer.org
web: www.iiar-anticancer.org / http://iiarjournals.org
From: editor@cgp-journal.com [mailto:editor@cgp-journal.com] **Sent:** Friday, August 30, 2013 6:25 AM **To:** editor@cgp-journal.com **Subject:** Contact e-mail from www.cgp-journal.com

JOHN WILEY AND SONS LICENSE
TERMS AND CONDITIONS
Nov 09, 2013
This is a License Agreement between Katrina N Battle ("You") and John Wiley and Sons ("John Wiley and Sons") provided by Copyright Clearance Center ("CCC"). The license consists of your order details, the terms and conditions provided by John Wiley and Sons, and the payment terms and conditions. All payments must be made in full to CCC. For payment instructions, please see information listed at the bottom of this form.
License Number 3264830399756
License date Nov 09, 2013
Licensed content publisher John Wiley and Sons
Licensed content publication Proteomics
Licensed content title Digital microfluidic hydrogel microreactors for proteomics
Licensed copyright line © 2012 WILEY-VCH Verlag GmbH & Co. KGaA, Weinheim
Licensed content author Vivienne N. Luk, Lindsey K. Fiddes,Victoria M. Luk, Eugenia Kumacheva, Aaron R. Wheeler
Licensed content date May 16, 2012
Start page 1310
End page 1318
Type of use Journal
Requestor type University/Academic
Is the reuse sponsored by or associated with a pharmaceutical or medical no
Format Print and electronic
Portion Figure/table
Number of figures/tables 1
Original Wiley figure/table number(s) Figure 2
Will you be translating? No
Title of new article Microfluidic Analysis of Integral Membrane Proteins: How do we get there?
Publication the new article is in Electrophoresis
Publisher of new article John Wiley and Sons
Author of new article Katrina Battle, Franklin Uba, and Steve A. Soper
Expected publication date of new article Mar 2014
Estimated size of new article (pages) 8
Total 0.00 USD

Terms and Conditions

TERMS AND CONDITIONS

This copyrighted material is owned by or exclusively licensed to John Wiley & Sons, Inc. or one of its group companies (each a "Wiley Company") or a society for whom a Wiley Company has exclusive publishing rights in relation to a particular journal (collectively "WILEY"). By clicking "accept" in connection with completing this licensing transaction, you agree that the following terms and conditions apply to this transaction (along with the billing and payment terms and conditions established by the Copyright Clearance Center Inc., ("CCC's Billing and Payment terms and conditions"), at the time that you opened your RightsLink account (these are available at any time at http://myaccount.copyright.com).

Terms and Conditions

1. The materials you have requested permission to reproduce (the "Materials") are protected by copyright.

2.You are hereby granted a personal, non-exclusive, non-sublicensable, non-transferable, worldwide, limited license to reproduce the Materials for the purpose specified in the licensing process. This license is for a one-time use only with a maximum distribution equal to the number that you identified in the licensing process. Any form of republication granted by this license must be completed within two years of the date of the grant of this license (although copies prepared before may be distributed thereafter). The Materials shall not be used in any other manner or for any other purpose. Permission is granted subject to an appropriate acknowledgement given to the author, title of the material/book/journal and the publisher. You shall also duplicate the copyright notice that appears in the Wiley publication in your use of the Material. Permission is also granted on the understanding that nowhere in the text is a previously published source acknowledged for all or part of this Material. Any third party material is expressly excluded from this permission.

NATURE PUBLISHING GROUP LICENSE

TERMS AND CONDITIONS

Nov 09, 2013

This is a License Agreement between Katrina N Battle ("You") and Nature Publishing Group ("Nature Publishing Group") provided by Copyright Clearance Center ("CCC"). The license consists of your order details, the terms and conditions provided by Nature Publishing Group, and the payment terms and conditions. All payments must be made in full to CCC. For payment instructions, please see information listed at the bottom of this form.

License Number 3264830553161

License date Nov 09, 2013

Licensed content publisher Nature Publishing Group

Licensed content publication Nature Medicine

Licensed content title Clinical microfluidics for neutrophil genomics and proteomics

Licensed content author Kenneth T Kotz, Wenzong Xiao, Carol Miller-Graziano, Wei-Jun Qian, Aman Russom, Elizabeth A Warner

Licensed content date Aug 29, 2010

Volume number 16

Issue number 9

Type of Use reuse in a journal/magazine

Requestor type academic/university or research institute

Format print and electronic
Portion figures/tables/illustrations
Number of figures/tables/illustrations 1
High-res required no
Figures a and b from Figure 1
Author of this NPG article no
Your reference number
Title of the article Microfluidic Analysis of Integral Membrane Proteins: How do we get there?
Publication the new article is in Electrophoresis
Publisher of your article John Wiley and Sons
Author of the article Katrina Battle, Franklin Uba, and Steve A. Soper
Expected publication date Mar 2014
Estimated size of new article (number of pages) 8
Total 0.00 USD
Terms and Conditions
Terms and Conditions for Permissions
Nature Publishing Group hereby grants you a non-exclusive license to reproduce this material for this purpose, and for no other use, subject to the conditions below:
1. NPG warrants that it has, to the best of its knowledge, the rights to license reuse of this material. However, you should ensure that the material you are requesting is original to
Nature Publishing Group and does not carry the copyright of another entity (as credited in the published version). If the credit line on any part of the material you have requested indicates that it was reprinted or adapted by NPG with permission from another source, then you should also seek permission from that source to reuse the material.
2. Permission granted free of charge for material in print is also usually granted for any electronic version of that work, provided that the material is incidental to the work as a whole and that the electronic version is essentially equivalent to, or substitutes for, the print version. Where print permission has been granted for a fee, separate permission must be obtained for any additional, electronic re-use (unless, as in the case of a full paper, this has already been accounted for during your initial request in the calculation of a print run).NB: In all cases, web-based use of full-text articles must be authorized separately through the 'Use on a Web Site' option when requesting permission.
Once you receive your invoice for this order, you may pay your invoice by credit card.
Please follow instructions provided at that time.
Make Payment To:
Copyright Clearance Center
Dept 001
P.O. Box 843006
Boston, MA 02284-3006
For suggestions or comments regarding this order, contact RightsLink Customer
Support: customercare@copyright.com or +1-877-622-5543 (toll free in the US) or +1-978-646-2777.
Gratis licenses (referencing $0 in the Total field) are free. Please retain this printable license for your reference. No payment is required.

JOHN WILEY AND SONS LICENSE
TERMS AND CONDITIONS
Nov 09, 2013
This is a License Agreement between Katrina N Battle ("You") and John Wiley and Sons ("John Wiley and Sons") provided by Copyright Clearance Center ("CCC"). The license consists of your order details, the terms and conditions provided by John Wiley and Sons, and the payment terms and conditions.
All payments must be made in full to CCC. For payment instructions, please see information listed at the bottom of this form.
License Number 3264820629885
License date Nov 09, 2013
Licensed content publisher John Wiley and Sons
Licensed content publication Electrophoresis
Licensed content title Integrated electrokinetic sample fractionation and solid-phase extraction in microfluidic devices
Licensed copyright line © 2012 WILEY-VCH Verlag GmbH & Co. KGaA, Weinheim
Licensed content author Zhen Wang, Abebaw B. Jemere, D. Jed Harrison
Licensed content date Sep 5, 2012
Start page 3151
End page 3158
Type of use Journal
Requestor type University/Academic
Is the reuse sponsored by or associated with a pharmaceutical or medical products company? no
Format Print and electronic
Portion Figure/table
Number of figures/tables 2
Original Wiley figure/table number(s) Figure 5, Figure 6
Will you be translating? No
Title of new article Microfluidic Analysis of Integral Membrane Proteins: How do we get there?
Publication the new article is in Electrophoresis
Publisher of new article John Wiley and Sons
Author of new article Katrina Battle, Franklin Uba, and Steve A. Soper
Expected publication date of new article Mar 2014
Estimated size of new article (pages) 8
Total 0.00 USD
Terms and Conditions
TERMS AND CONDITIONS
This copyrighted material is owned by or exclusively licensed to John Wiley & Sons, Inc. or one of its group companies (each a "Wiley Company") or a society for whom a Wiley Company has exclusive publishing rights in relation to a particular journal (collectively "WILEY"). By clicking "accept" in connection with completing this licensing transaction, you agree that the following terms and conditions apply to this transaction (along with the billing and payment terms and conditions established by the Copyright Clearance Center Inc., ("CCC's Billing and Payment terms and conditions"), at the time that you opened your

RightsLink account (these are available at any time at http://myaccount.copyright.com).
Terms and Conditions
1. The materials you have requested permission to reproduce (the "Materials") are protected by copyright.
2.You are hereby granted a personal, non-exclusive, non-sublicensable, non-transferable, worldwide, limited license to reproduce the Materials for the purpose specified in the licensing process. This license is for a one-time use only with a maximum distribution equal to the number that you identified in the licensing process. Any form of republication granted by this license must be completed within two years of the date of the grant of this license (although copies prepared before may be distributed thereafter). The Materials shall not be used in any other manner or for any other purpose. Permission is granted subject to an appropriate acknowledgement given to the author, title of the material/book/journal and the publisher. You shall also duplicate the copyright notice that appears in the Wiley publication in your use of the Material. Permission is also granted on the understanding that nowhere in the text is a previously published source acknowledged for all or part of this Material. Any third party material is expressly excluded from this permission.
Once you receive your invoice for this order, you may pay your invoice by credit card.
Please follow instructions provided at that time.
Make Payment To:
Copyright Clearance Center
Dept 001
P.O. Box 843006
Boston, MA 02284-3006
For suggestions or comments regarding this order, contact RightsLink Customer
Support: customercare@copyright.com or +1-877-622-5543 (toll free in the US) or +1-978-646-2777.
Gratis licenses (referencing $0 in the Total field) are free. Please retain this printable license for your reference. No payment is required.

AMERICAN CHEMICAL SOCIETY LICENSE TERMS AND CONDITIONS

Title: Fabrication of High-Quality Microfluidic Solid-Phase Chromatography Columns
Author: Jens Huft, Charles A. Haynes, and Carl L. Hansen
Publication: Analytical Chemistry
Publisher: American Chemical Society
Date: Feb 1, 2013
Copyright © 2013, American Chemical Society
PERMISSION/LICENSE IS GRANTED FOR YOUR ORDER AT NO CHARGE
This type of permission/license, instead of the standard Terms & Conditions, is sent to you because no fee is being charged for your order. Please note the following:
Permission is granted for your request in both print and electronic formats, and translations.
If figures and/or tables were requested, they may be adapted or used in part. Please print this page for your records and send a copy of it to your publisher/graduate school.
Appropriate credit for the requested material should be given as follows: "Reprinted (adapted) with permission from (COMPLETE REFERENCE CITATION). Copyright
(YEAR) American Chemical Society." Insert appropriate information in place of the

AMERICAN CHEMICAL SOCIETY LICENSE TERMS AND CONDITIONS

Title: A Digital Microfluidic Approach to Proteomic Sample Processing
Author: Vivienne N. Luk and Aaron R. Wheeler
Publication: Analytical Chemistry
Publisher: American Chemical Society
Date: Jun 1, 2009

PERMISSION/LICENSE IS GRANTED FOR YOUR ORDER AT NO CHARGE
This type of permission/license, instead of the standard Terms & Conditions, is sent to you because no fee is being charged for your order. Please note the following:
Permission is granted for your request in both print and electronic formats, and translations.
If figures and/or tables were requested, they may be adapted or used in part.
Please print this page for your records and send a copy of it to your publisher/graduate school.
Appropriate credit for the requested material should be given as follows: "Reprinted (adapted) with permission from (COMPLETE REFERENCE CITATION). Copyright (YEAR) American Chemical Society." Insert appropriate information in place of the capitalized words. One-time permission is granted only for the use specified in your request. No additional uses are granted (such as derivative works or other editions). For any other uses, please submit a new request.

Vita

Katrina Nychole Battle was born in Macon, Georgia to Leonard and Sherrye Battle. She began her early education at Hubbard Elementary School, Monroe County Middle School, and graduated with honors from Mary Persons High School in 2004. After high school, she chose to attend Jackson State University in Jackson, MS for her undergraduate studies in chemistry. While at Jackson State, Katrina remained active in her studies as well as the surrounding community. She was an active participant in the Student Government Association, the NOBCChE Chapter on Campus, and also became a member of Alpha Kappa Alpha Sorority, Inc. As a junior at Jackson State, Katrina was chosen to be an intern at the National Crime Lab in Qunatico, VA through participation in the Federal Bureau of Investigation's Summer Honor's Internship Program (SHIP). Following graduation from Jackson State, she enrolled at Lousiana State University in Baton Rouge in the fall of 2008 where she was mentored in the Soper Research Group by Professor Steven A. Soper. She has co-authored two publications and has presented her research at national conferences. Her dissertation is entitled "Microfluidics for the Analysis of Integral Membrane Proteins: A Top-down Approach." The degree of Doctor of Philosophy will be conferred at the December 2013 commencement ceremony.